

DIURNAL VARIATION IN EXCITATION-CONTRACTION  
COUPLING IN RAT VENTRICULAR MYOCYTES

Thesis submitted for the degree of

Doctor of Philosophy

at the University of Leicester

by

Helen Elizabeth Collins BSc. Hons (Leicester)

Department of Cardiovascular sciences

University of Leicester

September 2010

UMI Number: U594485

All rights reserved

INFORMATION TO ALL USERS

The quality of this reproduction is dependent upon the quality of the copy submitted.

In the unlikely event that the author did not send a complete manuscript and there are missing pages, these will be noted. Also, if material had to be removed, a note will indicate the deletion.



UMI U594485

Published by ProQuest LLC 2013. Copyright in the Dissertation held by the Author.  
Microform Edition © ProQuest LLC.

All rights reserved. This work is protected against  
unauthorized copying under Title 17, United States Code.



ProQuest LLC  
789 East Eisenhower Parkway  
P.O. Box 1346  
Ann Arbor, MI 48106-1346

# Diurnal variation in excitation-contraction coupling in rat ventricular myocytes

Helen E Collins

Diurnal variation has been reported in many cardiovascular haemodynamics parameters such as heart rate and blood pressure and the cardiac action potential. This variation may result from the diurnal variation in sympathetic activity or in cardiac gene expression. However, it is unknown whether these time-of-day dependent changes impact on excitation-contraction (EC) coupling. There is also a morning peak in the onset of ventricular arrhythmias and associated sudden cardiac death in man, which appear linked to the increase in sympathetic activity. Therefore, the aims of this investigation were to determine whether there was a time-of-day dependent variation in EC-coupling and its modulation by sympathetic stimulation.

Left ventricular myocytes were isolated during either the resting period (ZT3) or the active period (ZT15) of the adult Wistar rat.  $[Ca^{2+}]_i$  was determined using Fura-2 and contraction strength was determined using cell-edge detection in response to electrical field stimulation, and gene expression was determined using quantitative real-time RT-PCR. To determine the effects of hypertension-induced hypertrophy, myocytes were isolated from pre- and post-hypertensive spontaneously hypertensive rats (SHR).

The basal  $Ca^{2+}$  transient, contraction strength and SR  $Ca^{2+}$  content were significantly greater in resting period (ZT3) myocytes than active period (ZT15) myocytes. Systolic  $[Ca^{2+}]_i$ , amplitude of  $Ca^{2+}$  transient and SR  $Ca^{2+}$  content in response to isoproterenol ( $> 3nM$ ) were significantly greater in resting period (ZT3) myocytes. The percentage of myocytes developing arrhythmic activity in response to isoproterenol was greater in resting period (ZT3) myocytes. Nitric oxide synthase (NOS) inhibition using L-NNA significantly increased systolic  $[Ca^{2+}]_i$ , amplitude of  $Ca^{2+}$  transient, SR  $Ca^{2+}$  content and the percentage of myocytes developing arrhythmic activity in active period (ZT15) myocytes thereby depressing time-of-day dependent variation in these parameters. In addition, expression of NOS1 was significantly greater in active period (ZT15) myocytes. Diurnal variation in the  $Ca^{2+}$  transient and its responsiveness to isoproterenol were depressed in adult SHR, however, this did not reflect a depression of diurnal cycling in NOS1 expression.

This shows for the first time a time-of-day dependent variation in the  $Ca^{2+}$ -transient and resulting contraction strength, reflecting levels of SR  $Ca^{2+}$ -loading, due to a NOS-signalling pathway. There was also a reduction in sympathetic-induced arrhythmic activity in active period (ZT15) myocytes which was associated with increased NOS activity. Therefore, variation in NOS may be a means of protecting against arrhythmias during severe sympathetic stimulation. Loss of protection through disruption to the circadian clock resulting from cardiomyopathies such as hypertension-induced hypertrophy may result in a decreased threshold for sympathetic-induced arrhythmias, however; this requires further work to elucidate the underlying molecular mechanisms.

## Acknowledgements

I would like to thank, first and foremost, my PhD supervisor, Dr Glenn Rodrigo, firstly for the opportunity to undertake a PhD with him inspite of my legendary CV and most importantly, for all of the guidance, advice and technical assistance he has given me throughout the duration of the project. Secondly, for putting up with my erratic personality, endless talking, generally being annoying and also for making me laugh. I would like to thank the members of staff at the division of Biomedical services based at the University of Leicester, especially Ken White and Debbie Bursnall for the assistance provided during tissue retrieval, and training and assistance with schedule one procedures. I would like to thank Professor Nilesh Samani for the kind donation of adolescent/ adult SHR and WKY rats and the department of Cardiovascular sciences based at the University of Leicester for funding my PhD. I would like to thank Professor Nick Standen, Dr Maciej Tomaszewski and Dr Bob Norman for providing additional advice and guidance throughout the duration of my PhD. I would like to thank the following people who have helped my understanding in molecular biology based techniques in the department of cardiovascular sciences, they are: Dr Andy Bingham, Jasbir moore, Dr Kieran Brack, Dr Andrea Koekemoer, Dr Danny Chan, Dr Joanne Singletary, Dr Veryan Codd and Dr Timothy Barnes. With particular thanks going to Andrea, Jasbir, Kieran, Sadat and James for being exceptional colleagues as well as friends throughout. Most importantly, I would like to thank my boyfriend and general partner in crime, Colin, for all of his love, support, kindness and encouragement throughout the duration of my PhD also for making me laugh everyday and for putting up with me. Lastly, I would like to thank my mum; dad, Sister Debbie, niece Casey for being the backbone to my life and for their love, support and encouragement throughout my PhD.

## **Publications**

Collins, H.E., Rodrigo, G.C. (2010). Inotropic response of cardiac ventricular myocytes to beta-adrenergic stimulation with isoproterenol exhibits diurnal variation: involvement of nitric oxide. *Circulation Research* 106 (7), 1244-1252.

## **Abstracts**

Rodrigo, G.C., Collins, H.E. The role of nitric oxide in the diurnal variation in excitation-contraction coupling in ventricular myocytes. The Annual Physiological Society meeting, Dublin, July 2009. Poster presentation.

Collins, H.E., Rodrigo, G.C. Diurnal variation in excitation-contraction coupling in rat ventricular myocytes: sensitivity to  $\beta$ -adrenergic stimulation. The Annual Physiological Society meeting, Dublin, July 2009. Oral presentation.

Collins, H.E., Rodrigo, G.C. Diurnal variation in the response of cardiac ventricular myocytes to  $\beta$ -adrenergic stimulation: Involvement of endogenous nitric oxide. European society of Cardiology congress meeting, Barcelona, August 2009. Poster presentation.

## Abbreviations

|                           |                                                     |
|---------------------------|-----------------------------------------------------|
| <b>AM</b>                 | Acetoxymethyl                                       |
| <b>Ach</b>                | Acetylcholine                                       |
| <b>K<sub>Ach</sub></b>    | Acetylcholine-activated K <sup>+</sup> channel      |
| <b>AP</b>                 | Action potential                                    |
| <b>APD</b>                | Action potential duration                           |
| <b>AMP</b>                | Adenosine monophosphate                             |
| <b>ATP</b>                | Adenosine triphosphate                              |
| <b>AC</b>                 | Adenylate cyclase                                   |
| <b>ANOVA</b>              | Analysis of variance                                |
| <b>K<sub>ATP</sub></b>    | ATP-sensitive K <sup>+</sup> channel                |
| <b>AV-node</b>            | Atrioventricular node                               |
| <b>ANS</b>                | Autonomic nervous system                            |
| <b>β-ARK1</b>             | β-adrenergic receptor kinase 1 (GRK)                |
| <b>BSA</b>                | Bovine serum albumin                                |
| <b>BP</b>                 | Blood pressure                                      |
| <b>I<sub>Cl(ca)</sub></b> | Ca <sup>2+</sup> -activated Cl <sup>-</sup> current |
| <b>CaCl<sub>2</sub></b>   | Calcium chloride                                    |
| <b>I<sub>Ca</sub></b>     | Calcium current                                     |
| <b>CICR</b>               | Calcium-induced calcium release                     |
| <b>CAST</b>               | Cardiac arrhythmia suppression trial                |
| <b>CO</b>                 | Cardiac output                                      |
| <b>CCM</b>                | Cardiomyocyte-specific circadian clock mutant       |
| <b>CVS</b>                | Cardiovascular system                               |
| <b>CVP</b>                | Central venous pressure                             |
| <b>CCD</b>                | Charge coupled device                               |
| <b>cDNA</b>               | Complementary DNA                                   |
| <b>CT</b>                 | Crossing threshold                                  |

|                      |                                                                   |
|----------------------|-------------------------------------------------------------------|
| <b>cAMP</b>          | Cyclic AMP                                                        |
| <b>cGMP</b>          | Cyclic GMP                                                        |
| <b>DAD</b>           | Delayed after-depolarisation                                      |
| <b>dNTPS</b>         | Deoxynucleoside triphosphates                                     |
| <b>DNA</b>           | Deoxyribonucleic acid                                             |
| <b>DMSO</b>          | Dimethyl sulfoxide                                                |
| <b>K<sub>d</sub></b> | Dissociation constant                                             |
| <b>EAD</b>           | Early after-depolarisation                                        |
| <b>ECG</b>           | Electrocardiogram                                                 |
| <b>eNOS/NOS3</b>     | Endothelial nitric oxide synthase                                 |
| <b>E<sub>K</sub></b> | Equilibrium potential for potassium                               |
| <b>EDTA</b>          | Ethylenediamine tetraacetic acid                                  |
| <b>EGTA</b>          | Ethylene glycol-bis(2-aminoethylether)-N,N,N',N'-tetraacetic acid |
| <b>EC-coupling</b>   | Excitation-contraction coupling                                   |
| <b>FCS</b>           | Foetal calf serum                                                 |
| <b>FFR</b>           | Force-frequency relationship                                      |
| <b>I<sub>f</sub></b> | Funny current                                                     |
| <b>gDNA</b>          | Genomic DNA                                                       |
| <b>GAPDH</b>         | Glyceraldehyde-3-phosphate dehydrogenase                          |
| <b>GHK</b>           | Goldman-Hodgkin-Katz                                              |
| <b>GPCR</b>          | G-protein coupled receptor                                        |
| <b>GRK</b>           | G-protein coupled receptor kinase ( $\beta$ ARK1)                 |
| <b>GC</b>            | Guanylate cyclase                                                 |
| <b>HF</b>            | Heart failure                                                     |
| <b>HR</b>            | Heart rate                                                        |
| <b>HRV</b>           | Heart rate variability                                            |
| <b>HF</b>            | High frequency                                                    |
| <b>HCl</b>           | Hydrochloric acid                                                 |
| <b>HCN</b>           | Hyperpolarisation-activated cyclic nucleotide-gated channels      |

|                         |                                                            |
|-------------------------|------------------------------------------------------------|
| <b>iNOS/NOS2</b>        | Inducible Nitric oxide synthase                            |
| <b>IMS</b>              | Industrial methylated spirit                               |
| <b>G<sub>i</sub></b>    | Inhibitory GTP binding protein                             |
| <b>IP<sub>3</sub></b>   | Inositol 1, 4, 5-trisphosphate                             |
| <b>I<sub>K1</sub></b>   | Inward rectifier K <sup>+</sup> current                    |
| <b>IP<sub>3</sub>R</b>  | Inositol 1, 4, 5-trisphosphate (IP <sub>3</sub> ) receptor |
| <b>I/R</b>              | Ischaemia/reperfusion                                      |
| <b>ISO</b>              | Isoproterenol                                              |
| <b>KO</b>               | Knock out                                                  |
| <b>LV</b>               | Left ventricular                                           |
| <b>L/D</b>              | Light/dark                                                 |
| <b>LF</b>               | Low frequency                                              |
| <b>LQTS</b>             | Long QT syndrome                                           |
| <b>LTCC</b>             | L-type Ca <sup>2+</sup> channel                            |
| <b>MgCl<sub>2</sub></b> | Magnesium chloride                                         |
| <b>MAP</b>              | Mean arterial pressure                                     |
| <b>mRNA</b>             | Messenger RNA                                              |
| <b>mNOS</b>             | Mitochondrial nitric oxide synthase                        |
| <b>MI</b>               | Myocardial infarction                                      |
| <b>MHC</b>              | Myosin heavy chain                                         |
| <b>nNOS/NOS1</b>        | Neuronal Nitric oxide synthase                             |
| <b>NO</b>               | Nitric oxide                                               |
| <b>NOS</b>              | Nitric oxide synthase                                      |
| <b>NOS1AP</b>           | Nitric oxide synthase 1 adaptor protein (CAPON)            |
| <b>I<sub>nsc</sub></b>  | Non-specific cationic current                              |
| <b>NT</b>               | Normal Tyrode                                              |
| <b>L-NNA</b>            | N-ω-nitro-L-arginine                                       |
| <b>ONOO<sup>-</sup></b> | Peroxynitrite                                              |
| <b>PIP<sub>2</sub></b>  | Phosphatidylinositol 4,5-bisphosphate                      |

|                                            |                                                   |
|--------------------------------------------|---------------------------------------------------|
| <b>PDE</b>                                 | Phosphodiesterase                                 |
| <b>PLB</b>                                 | Phospholamban                                     |
| <b>PP1</b>                                 | Protein phosphatase type 1                        |
| <b>PP2A</b>                                | Protein phosphatase type 2a                       |
| <b>PKA</b>                                 | Protein kinase A                                  |
| <b>PKC</b>                                 | Protein kinase C                                  |
| <b>PKG</b>                                 | Protein kinase G                                  |
| <b>KCl</b>                                 | Potassium chloride                                |
| <b>PCR</b>                                 | Polymerase chain reaction                         |
| <b>I<sub>Kr</sub></b>                      | Rapid delayed rectifier K <sup>+</sup> current    |
| <b>ROS</b>                                 | Reactive oxygen species                           |
| <b>RMP</b>                                 | Resting membrane potential                        |
| <b>RT</b>                                  | Reverse transcription                             |
| <b>RT-PCR</b>                              | Reverse transcription polymerase chain reaction   |
| <b>RNA</b>                                 | Ribonucleic acid                                  |
| <b>RyR</b>                                 | Ryanodine receptor                                |
| <b>PCMA</b>                                | Sarcolemmal Ca <sup>2+</sup> ATPase               |
| <b>SERCA</b>                               | Sarcoplasmic/endoplasmic reticulum calcium ATPase |
| <b>SR</b>                                  | Sarcoplasmic reticulum                            |
| <b>G<sub>s</sub></b>                       | Stimulatory GTP binding protein                   |
| <b>SA-node</b>                             | Sino-atrial node                                  |
| <b>I<sub>Ks</sub></b>                      | Slow delayed rectifier K <sup>+</sup> current     |
| <b>NCX 1</b>                               | Sodium/ Calcium exchanger                         |
| <b>NaCl</b>                                | Sodium chloride                                   |
| <b>I<sub>Na</sub></b>                      | Sodium current                                    |
| <b>NHE 1</b>                               | Sodium/ Hydrogen exchanger                        |
| <b>NaOH</b>                                | Sodium hydroxide                                  |
| <b>NaH<sub>2</sub>PO<sub>4</sub></b>       | Sodium phosphate monobasic                        |
| <b>Na<sup>+</sup>/K<sup>+</sup> ATPase</b> | Sodium/potassium ATPase                           |

|                        |                                                                                          |
|------------------------|------------------------------------------------------------------------------------------|
| <b>Na-pyruvate</b>     | Sodium pyruvate                                                                          |
| <b>SHR</b>             | Spontaneously hypertensive rat                                                           |
| <b>SEM</b>             | Standard error of the mean                                                               |
| <b>SV</b>              | Stroke volume                                                                            |
| <b>SCD</b>             | Sudden cardiac death                                                                     |
| <b>SO</b>              | Superoxide                                                                               |
| <b>SOD</b>             | Superoxide dismutase                                                                     |
| <b>SCN</b>             | Suprachiasmatic nucleus                                                                  |
| <b>TTX</b>             | Tetrodotoxin                                                                             |
| <b>I<sub>ti</sub></b>  | Transient inward current                                                                 |
| <b>I<sub>to</sub></b>  | Transient outward K <sup>+</sup> current                                                 |
| <b>T-tubules</b>       | Transverse tubules                                                                       |
| <b>TPR</b>             | Total peripheral resistance                                                              |
| <b>Tdp</b>             | <i>Torsades de pointes</i>                                                               |
| <b>TBE</b>             | Tris-borate-EDTA                                                                         |
| <b>TTCC</b>            | T-type Ca <sup>2+</sup> channel                                                          |
| <b>I<sub>Kur</sub></b> | Ultra rapid delayed rectifier K <sup>+</sup> current                                     |
| <b>UCP2</b>            | Uncoupling protein 2                                                                     |
| <b>UCP3</b>            | Uncoupling protein 3                                                                     |
| <b>WKY</b>             | Wistar-kyoto                                                                             |
| <b>XOR</b>             | Xanthine oxidoreductase                                                                  |
| <b>ZT</b>              | Zeitgeber time                                                                           |
| <b>BAPTA</b>           | 1,2-bis(2-aminophenoxy)ethane- <i>N,N,N',N'</i> -tetraacetic acid                        |
| <b>DEANO</b>           | 2-(N, N-diethylamino)-diazolate-2-oxide                                                  |
| <b>HEPES</b>           | 4-(2-Hydroxyethyl)piperazine-1-ethanesulfonic acid                                       |
| <b>4-AAPNT</b>         | N-[(4S)-4-amino-5-[(2-aminoethyl)amino]pentyl]-N'-nitroguanidine tris(trifluoroacetate). |

# Table of Contents

|                                                                                                                              |    |
|------------------------------------------------------------------------------------------------------------------------------|----|
| Chapter 1: Introduction .....                                                                                                | 6  |
| 1.1 Introduction to investigation .....                                                                                      | 6  |
| 1.2 Diurnal variations in cardiac function .....                                                                             | 7  |
| 1.2.1 Diurnal variations in metabolic genes .....                                                                            | 9  |
| 1.2.2 Diurnal variations in haemodynamic parameters .....                                                                    | 9  |
| 1.2.3 Diurnal variations in cardiac electrophysiology .....                                                                  | 14 |
| 1.2.4 Diurnal variations in sympathetic stimulation .....                                                                    | 16 |
| 1.2.5 Diurnal variations in cardiovascular events .....                                                                      | 18 |
| 1.3 Cardiac excitation-contraction coupling .....                                                                            | 21 |
| 1.3.1 Excitation (electrical component) .....                                                                                | 21 |
| 1.3.2 Calcium cycling and contraction .....                                                                                  | 28 |
| 1.3.3 Decline in $\text{Ca}^{2+}$ transient (relaxation) .....                                                               | 31 |
| 1.4 The effect of $\beta$ -adrenergic stimulation on excitation-contraction coupling .....                                   | 33 |
| 1.4.1 $\beta$ -adrenergic receptor introduction .....                                                                        | 33 |
| 1.4.2 Additional effects of $\beta$ -adrenergic stimulation .....                                                            | 35 |
| 1.4.3 $\beta_1$ -adrenergic stimulation .....                                                                                | 36 |
| 1.4.4 $\beta_2$ -adrenergic stimulation .....                                                                                | 38 |
| 1.4.5 $\beta_3$ -adrenergic stimulation .....                                                                                | 40 |
| 1.5 Consequences of prolonged $\beta$ -stimulation .....                                                                     | 46 |
| 1.5.1 Early after-depolarisations (EADs) .....                                                                               | 47 |
| 1.5.2 Delayed after-depolarisations (DADS) .....                                                                             | 48 |
| 1.6 Consequences of hypertension and hypertrophy on cardiac excitation-contraction coupling and diurnal cycling .....        | 49 |
| 1.6.1 Altered $\text{Ca}^{2+}$ homeostasis in left-ventricular hypertrophy and resultant heart failure .....                 | 50 |
| 1.6.2 $\beta$ -adrenergic signalling in ventricular hypertrophy and heart failure .....                                      | 54 |
| 1.6.3 Changes in NOS signalling in hypertension, left-ventricular hypertrophy and heart failure .....                        | 56 |
| 1.6.4 The development of several cardiomyopathies results in disruption to circadian clock and altered diurnal cycling ..... | 58 |

|                                                                                              |    |
|----------------------------------------------------------------------------------------------|----|
| 1.7 Aims and objectives .....                                                                | 59 |
| Chapter 2: Materials and methods .....                                                       | 62 |
| 2.1 Experimental Animals and time-points.....                                                | 62 |
| 2.1.1 Animals.....                                                                           | 62 |
| 2.1.2 Time-points.....                                                                       | 63 |
| 2.2 Isolation of single rat ventricular myocytes .....                                       | 64 |
| 2.3 Superfusion of ventricular myocytes .....                                                | 65 |
| 2.3.1 Contraction studies .....                                                              | 65 |
| 2.3.2 Fluorescence studies.....                                                              | 67 |
| 2.4 Fluorescence microscopy .....                                                            | 67 |
| 2.4.1 Measurement of intracellular calcium .....                                             | 68 |
| 2.4.2 <i>In-vivo</i> Calibration of Fura-2 signal .....                                      | 69 |
| 2.5 Molecular biology .....                                                                  | 70 |
| 2.5.1 Tissue retrieval .....                                                                 | 70 |
| 2.5.2 RNA extraction.....                                                                    | 70 |
| 2.5.3 Spectrophotometric assessment of RNA yield and quality .....                           | 74 |
| 2.5.4 RNA cleanup .....                                                                      | 75 |
| 2.5.5 Denaturing agarose gel electrophoresis of RNA .....                                    | 76 |
| 2.5.6 Semi-quantitative PCR of 18S.....                                                      | 77 |
| 2.5.7 Additional DNase treatment of RNA for the analysis of single exon spanning genes ..... | 79 |
| 2.5.8 Reverse transcription.....                                                             | 79 |
| 2.5.9 Quantitative real-time reverse transcription PCR.....                                  | 81 |
| <i>Choice of Taqman endogenous control gene (housekeeping gene)</i> .....                    | 81 |
| <i>Taqman gene expression assays (Taqman Probes)</i> .....                                   | 82 |
| <i>Standard curves</i> .....                                                                 | 82 |
| <i>Quantitative real-time RT-PCR of genes of interest</i> .....                              | 85 |
| 2.6 Experimental solutions.....                                                              | 87 |
| 2.6.1 Myocyte isolation and superfusion.....                                                 | 87 |
| 2.6.2 Experimental drugs.....                                                                | 87 |
| 2.6.3 Fluorescent dyes .....                                                                 | 88 |
| 2.6.4 Molecular biology .....                                                                | 88 |
| 2.7 Data acquisition and statistics .....                                                    | 89 |

|                                                                                                                                                                       |     |
|-----------------------------------------------------------------------------------------------------------------------------------------------------------------------|-----|
| Chapter 3: Diurnal variation in excitation-contraction coupling in rat ventricular myocytes .....                                                                     | 91  |
| 3.1 Introduction.....                                                                                                                                                 | 91  |
| 3.2 Results .....                                                                                                                                                     | 93  |
| 3.2.1 Diurnal variation in the basal Ca <sup>2+</sup> transient .....                                                                                                 | 93  |
| 3.2.2 Diurnal variation in basal contraction .....                                                                                                                    | 94  |
| 3.2.3 Diurnal variation in basal SR Ca <sup>2+</sup> content .....                                                                                                    | 95  |
| 3.2.4 Diurnal variation in circadian clock and metabolic genes.....                                                                                                   | 97  |
| 3.2.5 Diurnal variation in EC-coupling genes .....                                                                                                                    | 100 |
| 3.3 Discussion .....                                                                                                                                                  | 101 |
| 3.3.1 Is the isolated ventricular myocyte an appropriate model to study diurnal cycling in ventricular function?.....                                                 | 102 |
| 3.3.2 Diurnal variation in cardiac EC-coupling.....                                                                                                                   | 106 |
| 3.3.3 Diurnal variation in contraction.....                                                                                                                           | 115 |
| 3.3.4 What are the physiological implications of the reduced Ca <sup>2+</sup> transient during the active period?.....                                                | 115 |
| Chapter 4: Diurnal variation in the response of ventricular myocytes to β-adrenergic stimulation with isoproterenol .....                                             | 118 |
| 4.1 Introduction.....                                                                                                                                                 | 118 |
| 4.2 Results .....                                                                                                                                                     | 121 |
| 4.2.1 Diurnal variation in the response of the Ca <sup>2+</sup> transient to β-adrenergic stimulation with isoproterenol .....                                        | 121 |
| 4.2.2 The effects of stimulation frequency on diurnal variation in the response of the Ca <sup>2+</sup> transient to β-adrenergic stimulation with isoproterenol..... | 124 |
| 4.2.3 Diurnal variation in the response of contraction strength to β-adrenergic stimulation with isoproterenol.....                                                   | 127 |
| 4.2.4 Diurnal variation in SR Ca <sup>2+</sup> content in response to β-adrenergic stimulation with isoproterenol.....                                                | 129 |
| 4.2.5 Diurnal variation in the development of arrhythmic activity in ventricular myocytes in response to β-adrenergic stimulation with isoproterenol .....            | 131 |
| 4.3 Discussion .....                                                                                                                                                  | 133 |
| 4.3.1 Diurnal variation in the responsiveness of the Ca <sup>2+</sup> transient to isoproterenol .....                                                                | 134 |
| 4.3.2 Diurnal variation in the generation of arrhythmic activity .....                                                                                                | 138 |
| 4.3.3 The time-of-day dependent decrease in the responsiveness of the Ca <sup>2+</sup> transient to isoproterenol in active period myocytes is paradoxical.....       | 143 |

|                                                                                                                                                                                                                         |     |
|-------------------------------------------------------------------------------------------------------------------------------------------------------------------------------------------------------------------------|-----|
| 4.3.4 Possible mechanisms for diurnal variation in $\beta$ -adrenergic responsiveness                                                                                                                                   | 145 |
| Chapter 5: The role of nitric oxide synthase in the diurnal variation in responsiveness of ventricular myocytes to $\beta$ -adrenergic stimulation with isoproterenol                                                   | 146 |
| 5.1 Introduction                                                                                                                                                                                                        | 146 |
| 5.2 Results                                                                                                                                                                                                             | 148 |
| 5.2.1 The effect of NOS inhibition on the diurnal variation in the response of the $\text{Ca}^{2+}$ transient to $\beta$ -adrenergic stimulation with isoproterenol                                                     | 148 |
| 5.2.2 The effect of NOS inhibition on the diurnal variation in SR $\text{Ca}^{2+}$ content in response to $\beta$ -adrenergic stimulation with isoproterenol                                                            | 151 |
| 5.2.3 The effect of NOS inhibition on the development of arrhythmic activity in ventricular myocytes in response to $\beta$ -adrenergic stimulation with isoproterenol                                                  | 153 |
| 5.2.4 Diurnal variation in the $\beta_1$ -adrenergic receptor and the $\beta_3$ -adrenergic receptor mRNA expression in the adult Wistar                                                                                | 155 |
| 5.2.5 Diurnal variation in neuronal nitric oxide synthase, nitric oxide synthase 1 adaptor protein and endothelial nitric oxide synthase mRNA expression in adult Wistar                                                | 157 |
| 5.3 Discussion                                                                                                                                                                                                          | 159 |
| 5.3.1 Is the relative contribution of $\beta_1$ and $\beta_3$ -adrenergic receptors responsible for the diurnal variation in the responsiveness to ISO?                                                                 | 160 |
| 5.3.2 The role of NOS-signalling in the time-of-day dependent variation in the responsiveness of the $\text{Ca}^{2+}$ transient to $\beta$ -adrenergic stimulation                                                      | 163 |
| 5.3.3 Additional mechanisms for the reduced responsiveness of active period myocytes to isoproterenol                                                                                                                   | 167 |
| 5.3.4 The protective role of NOS in preventing arrhythmogenesis                                                                                                                                                         | 169 |
| 5.3.5 Limitations of our model and study                                                                                                                                                                                | 172 |
| Chapter 6: Effects of hypertension on the diurnal variation in excitation-contraction coupling in left ventricular myocytes                                                                                             | 176 |
| 6.1 Introduction                                                                                                                                                                                                        | 176 |
| 6.2 Results                                                                                                                                                                                                             | 178 |
| 6.2.1 Loss of diurnal variation in the basal $\text{Ca}^{2+}$ transient in adult SHR                                                                                                                                    | 178 |
| 6.2.2 Diurnal variation in the response of the $\text{Ca}^{2+}$ transient to $\beta$ -adrenergic stimulation with isoproterenol is lost in the adult SHR                                                                | 180 |
| 6.2.3 Diurnal changes in mRNA expression in hypertension                                                                                                                                                                | 182 |
| 6.2.4 Developmental differences in the basal $\text{Ca}^{2+}$ transient and the responsiveness of the $\text{Ca}^{2+}$ transient to $\beta$ -adrenergic stimulation with isoproterenol between adolescent and adult WKY | 189 |
| 6.3 Discussion                                                                                                                                                                                                          | 190 |

|                                                                                                                                                                     |     |
|---------------------------------------------------------------------------------------------------------------------------------------------------------------------|-----|
| 6.3.1 Why is the time-of-day dependent variation in the Ca <sup>2+</sup> transient and its responsiveness to isoproterenol depressed in the hypertensive SHR? ..... | 191 |
| 6.3.2 Study limitations.....                                                                                                                                        | 200 |
| Chapter 7: Physiological and clinical implications of diurnal cycling in EC-coupling                                                                                | 204 |
| 7.1 What is the physiological role of diurnal variation in EC-coupling and NOS-signalling in the healthy individual? .....                                          | 205 |
| 7.2 What is the physiological role of diurnal variation in EC-coupling and NOS-signalling in the diseased myocardium? .....                                         | 207 |
| 7.3 Is the β <sub>3</sub> -adrenergic-NOS-cGMP pathway a possible target for the prevention of ventricular arrhythmias that occur in cardiomyopathies? .....        | 209 |
| 7.4 Possible future work arising from present investigation.....                                                                                                    | 211 |
| Appendix 1.....                                                                                                                                                     | 214 |
| Appendix 2 .....                                                                                                                                                    | 218 |
| Appendix 3 .....                                                                                                                                                    | 222 |
| Appendix 4 .....                                                                                                                                                    | 224 |
| Bibliography .....                                                                                                                                                  | 227 |

# **Chapter 1: Introduction**

## ***1.1 Introduction to investigation***

It has been shown that many fatal cardiovascular events occur early in the morning, in the hours after waking and resuming activity (Guo and Stein, 2003, Hastings et al., 2003). These cardiovascular events include the onset of myocardial infarction (MI), ventricular arrhythmias, and sudden cardiac death (SCD), all of which contribute to a large proportion of deaths in the UK each year (Guo and Stein, 2003). This morning peak in fatal cardiovascular events may be due to changes in the underlying physiology of the myocardium, resulting in the heart being more sensitive to ischaemic injury during an MI or more electrically unstable leading to the generation of arrhythmias at this time. The case for a change in the underlying physiology of the cardiovascular system (CVS) and myocardium is suggested by the findings that, diurnal variations have been reported in cardiovascular haemodynamics parameters such as heart rate (HR) and blood pressure (BP), the cardiac action potential (AP), sympathetic stimulation, cardiac metabolic genes and fibrinolysis (Young et al., 2001a, Guo and Stein, 2003), all of which may contribute to the morning sensitivity of the myocardium to fatal cardiovascular events in both human and animal models. This morning peak in fatal cardiovascular events is more pronounced in patients with existing cardiomyopathies, such as left-ventricular (LV) hypertrophy and heart failure (HF). Therefore, an understanding of the physiological mechanisms underlying this morning peak in fatal cardiovascular events will potentially facilitate better management and treatment strategies in patients with these cardiomyopathies.

## ***1.2 Diurnal variations in cardiac function***

During the course of a 24 hour day, environmental and physical conditions faced by an animal will constantly change and is most obvious in terms of the transition between the resting “passive” period and active “foraging” period, which are both dictated to by changes in the 24 hour light/dark (L/D) cycle.

To anticipate changes in activity, the animal has an innate circadian clock, located in the suprachiasmatic nucleus (SCN) that allows the animal to pre-empt the changes in its normal cycling and to prepare for its active period and its resting period (Young, 2006, Young and Bray, 2007). The mammalian circadian clock consists of a network of proteins that form dynamic transcriptionally-based feedback loops which interact with each another and oscillate over the course of 24 hours. Of these, the most defined feedback loop of the circadian clock involves the dimerisation of the CLOCK and brain and muscle aryl hydrocarbon receptor nuclear translocator (BMAL1) proteins, which both peak in expression during the light phase of the L/D cycle (~ZT0). Following dimerisation, CLOCK/BMAL1 interacts with E-box elements in the promoter regions of the period genes (Per 1, 2, 3) and the cryptochrome genes (CRY 1 and CRY2), promoting their transcription. The Per and CRY genes, which both peak in expression during the dark phase of the L/D cycle (> ZT12), also form a heterodimer following translation and this heterodimer is responsible for the subsequent inhibition of CLOCK/BMAL1.

In recent years the existence of cell specific, peripheral circadian clocks have also been identified (Young and Bray, 2007), and as the CVS is central to the operation of the animal it is therefore not surprising that amongst these is the cardiomyocyte-specific circadian clock (Durgan et al., 2005, Durgan and Young, 2010). However, the circadian clock located in the SCN is often referred to as the “central clock” as in cases of SCN removal and SCN ablation there is significant global loss of diurnal variation in

circadian clock gene expression (Akhtar et al., 2002) and depressed cycling of cardiovascular haemodynamic parameters (Sei et al., 2008).

The central circadian clock can be reset in the presence of a Zeitgeber (or time-giver). Zeitgebers are external cues that are capable of synchronising or resetting the central circadian clock of the SCN with the environment i.e. the L/D cycle (Durgan et al., 2005, Young, 2006, Young and Bray, 2007). Light is a strong Zeitgeber and therefore has a strong impact in setting/re-setting the central circadian clock and will also impact on the cycling of peripheral clocks which are under the control of the central clock (Durgan et al., 2005, Young, 2006, Young and Bray, 2007). The central circadian clock is thought to regulate these peripheral circadian clocks through the release of neurohumoral factors for example melatonin (Durgan et al., 2005, Young, 2006, Young and Bray, 2007). Other common Zeitgebers include glucocorticoids, glucose, epinephrine, norepinephrine and angiotensin II (Durgan et al., 2005, Young, 2006, Young and Bray, 2007).

Over the years, many significant cardiovascular variables have been shown to exhibit patterns of diurnal variation, these include: cardiac metabolic gene expression (see section 1.2.1), cardiac haemodynamic parameters (see section 1.2.2), cardiac electrophysiology (see section 1.2.3), sympathetic nervous system (see section 1.2.4) and the onset of SCD and fatal arrhythmias (see section 1.2.5). Some of these CVS variables and events may be regulated by the peripheral circadian clock rather than the central clock, for example the peripheral circadian clock located in the cardiomyocyte is believed to control cardiac metabolic gene expression (see section 1.2.1 of introduction), as in cardiomyocyte-specific circadian clock mutant (CCM) mice there is significant loss of diurnal variation in these genes (Bray et al., 2008, Durgan and Young, 2010).

### **1.2.1 Diurnal variations in metabolic genes**

In recent years, it has been documented that ~10-15% of rodent myocardial genes exhibit diurnal patterns of expression (Storch et al., 2002, Martino et al., 2004). Of these myocardial genes, Young and colleagues have shown a strong diurnal pattern of expression in genes regulating cardiac carbohydrate, fatty acid and mitochondrial metabolic activity in adult male Wistar rats (Young et al., 2001a). The carbohydrate, fatty acid and mitochondrial metabolic genes all showed peak expression levels in the middle of the period of darkness corresponding to ZT15-18, which represents the active period in the rat (Young et al., 2001a). The authors linked the changes in metabolic gene expression to similar increases in cardiac power, carbohydrate oxidation and oxygen consumption during the active period of the rat (ZT18) (Young et al., 2001a).

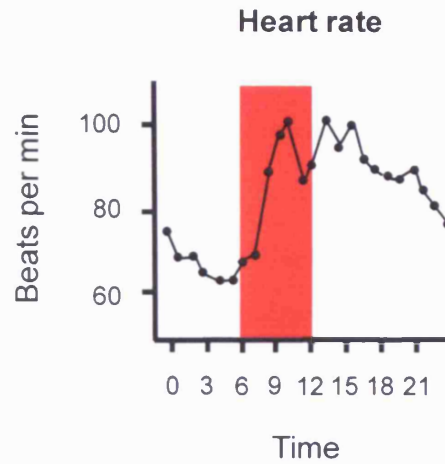
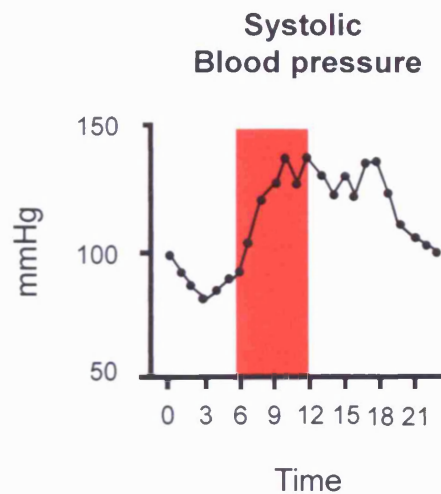
### **1.2.2 Diurnal variations in haemodynamic parameters**

Periods of inactivity, like those seen during periods of rest and sleep are not metabolically demanding, which is evident from decreased metabolic rate, oxygen demand and cardiac workload. However, upon waking, metabolic rate, oxygen demand and cardiac workload all increase in order to allow the individual to resume normal physical activity. In order to enhance cardiac workload upon waking, various haemodynamic parameters must also increase. At present, many cardiovascular haemodynamic parameters have been shown to exhibit diurnal variation in man and these include the following: heart rate (HR) (Degaute et al., 1991, Veerman et al., 1995), stroke volume (SV) (Veerman et al., 1995), (also cardiac output, CO), total peripheral resistance (TPR) (Veerman et al., 1995), blood pressure (BP) (Richards et al., 1986, Degaute et al., 1991, Veerman et al., 1995), mean arterial pressure (MAP) (Veerman et al., 1995) and central venous pressure (CVP) (Engel and Talan, 1991). The majority of these are increased in the morning upon arousal from sleep and changing

from a supine position to a standing, active position (with the exception of TPR which has reverse pattern) (Smith et al., 1987, Engel and Talan, 1991, Veerman et al., 1995). Diurnal variation in all of these haemodynamic parameters is important physiologically for the active animal as they permit an increase in blood flow to active muscles and blood flow the back to the lungs thereby increasing cardiac performance. The diurnal variation in these haemodynamic variables has been suggested to be due the well documented morning increase in the activity of the sympathetic nervous system (Narkiewicz et al., 2002, Sherwood et al., 2002, Scheer et al., 2004) (see section 1.2.4 of introduction). More recently, Young and colleagues, amongst others, have shown that the peripheral cardiomyocyte circadian clock contributes to diurnal variation in haemodynamic parameters such as HR, as *in vivo* telemetry measurements of HR, BP and MAP in wild type and CCM mice, showed diurnal variation in HR was depressed in CCM mice (Bray et al., 2008, Durgan and Young, 2010).

### ***Heart rate and stroke volume***

In order to increase physical activity upon arousal from sleep, CO must increase to cope with the increased demand from working muscle. The increase in CO is facilitated by increasing HR and/or SV (Levick, 2003); therefore, it is not surprising that diurnal variation has been documented in HR, SV and consequentially CO in virtually all species (Guo and Stein, 2003) and this diurnal variation in HR is documented in figure 1.1A. Smith *et al* (1987) looked at haemodynamic parameters in un-anaesthetised free-moving rats by means of implanted probes and catheters monitoring HR, SV and CO. They found that HR and CO were decreased during the resting period of the rat and increased when the rat resumed activity at night, however, they found that SV did not exhibit diurnal variation. Engel & Talan (1991) examined beat-to-beat analysis of HR and SV in monkeys, which are diurnal species, and reported that HR and CO were

**A****B**

**Figure 1.1- Diurnal variation in cardiovascular haemodynamic parameters in man (adapted from Hastings *et al*, 2003).**

- A. This figure shows a typical average 24 hour profile of heart rate (HR) and shows that HR is increased in the early morning between 6am and 12pm (highlighted in red) peaking at ~9am.
- B. This figure shows a typical average 24 hour profile of systolic blood pressure (SBP) and shows similar to HR (figure 1.1A), SBP is also increased in the early morning between 6am and 12pm (highlighted in red) peaking at ~9am.

decreased when the animal was resting and conversely increased when the animal resumed activity following rest. However, in accordance with data presented by Smith *et al* (1987), they also reported that SV did not vary in a diurnal manner. Moreover, diurnal variation in HR and CO present in monkeys has also been reported in the diurnal human. In male subjects undergoing 24 hour ambulatory BP monitoring, HR has been reported to rise in the morning, peaking at 10am and decreases by half during the night time trough (Degaute et al., 1991). In a similar study in healthy male human subjects, 24 hour intra-arterial ambulatory BP measurements were obtained in which HR, SV and CO were all significantly increased in the morning corresponding to a peak between 9am and midday with a fall in all of these parameters at night, with CO decreasing by ~30% (Veerman et al., 1995).

### ***Total peripheral resistance***

Total peripheral resistance (TPR) refers to the resistance to blood flow provided by the systemic vasculature and resistance vessels as a result of vascular tone generated by vasoconstriction of the vascular smooth muscle, and can be calculated from both MAP and CO (Levick, 2003, Klabunde, 2005), in the following equation:

$$TPR = \frac{MAP}{CO}$$

Diurnal variation in TPR has been documented in numerous studies. In diurnal species such as humans, TPR has been shown to peak at night with the trough occurring in the early morning, in the hours prior to and slightly after waking. Veerman *et al* (1995) found that TPR was increased by 22% in the night in 8 healthy volunteers and Engel and Talan (1991) examined TPR in 7 monkeys and also observed a night time increase in TPR (Engel and Talan, 1991, Veerman et al., 1995). However, in nocturnal species such as rats, i.e. those active during darkness, the relationship is inverse as TPR peaks during the daylight corresponding to the onset of the inactive period of the rat. Smith *et*

*al* (1987) measured various haemodynamic parameters in free-moving male rats and found that TPR peaked during daylight and was decreased during night time.

### ***Blood pressure and mean arterial pressure***

It is well established that diastolic and systolic blood pressure (BP) and mean arterial pressure (MAP) fluctuate with time of day as significant diurnal variations in BP and MAP have been identified in various animal species and in humans (Guo and Stein, 2003). An element of the variation in BP will result from changes in physical activity (Kario et al., 1999, O'Shea and Murphy, 2000); however, this has also been shown to occur independent of activity as diurnal variation is still present in sedated patients and elderly patients with limited activity (Ohya et al., 2001, Rachmani et al., 2004). This time-of-day dependent variation in systolic BP is shown in figure 1.1B. Diurnal changes in BP in man are suggested to reflect changes in autonomic control of the heart and vasculature, as the morning increase in BP is similar to the morning surge in the activity of the sympathetic nervous system (Pickering, 1990, Narkiewicz et al., 2002, Sherwood et al., 2002). This morning surge in the activity of the sympathetic nervous system will also impact on TPR, as sympathetic stimulation will promote vasoconstriction in the arterioles which will increase TPR and as a result this increase in TPR will also increase BP (Levick, 2003, Klabunde, 2005). BP is dependent on SV, TPR and also changes in sympathetic activity therefore the diurnal fluctuation in BP could result from the sympathetic-mediated and independent changes to SV and/or TPR which impact on BP (Levick, 2003, Klabunde, 2005). During 24 hour ambulatory BP measurements in healthy men, Degaute *et al* (1991) have shown that BP exhibits a large peak in the morning corresponding to 10am and a smaller peak at 8pm, with troughs at 3pm and 3am. In addition, this ambulatory data was confirmed by Veerman *et al* (1995) who examined various haemodynamic parameters in normotensive patients, through invasive intra-arterial ambulatory 24 hour BP measurements. Veerman and colleagues

found that BP and MAP were highest in the early morning when the patients arose from sleep, peaking between 7 and 9am and both parameters were decreased during the night time resting period. The authors also correlated the daylight increase in BP and MAP with similar increases in CO, HR, SV and a decrease in TPR, all of which may contribute to increased morning workload of heart upon waking (Veerman et al., 1995). In addition, the time-of-day dependent increase in cardiovascular haemodynamic parameters (BP, MAP, HR, & SV) reported by Veerman and colleagues have been reported to reflect the morning surge in sympathetic activity in man (Veerman et al., 1995).

Time-of-day dependent variations in BP and MAP have also been reported in rat. However, due to the nocturnal nature of the rat, BP peaks during the evening and decreases in daylight, the inverse of that seen in diurnal humans (van den Buuse, 1999). Moreover, the diurnal relationship seen in MAP is also inverse in the rat, as it was shown to be decreased during daylight between 5am-4pm (inactive period of rat) and increased during night time (active period of rat) (Smith et al., 1987).

### *Central venous pressure*

Central venous pressure (CVP) is another cardiovascular haemodynamic parameter shown to exhibit diurnal variation, decreasing during night time and increased during the early hours of the day in monkeys (Engel and Talan, 1991). This increase in CVP may reflect the morning peak in sympathetic activity, as the circulating catecholamines, norepinephrine and epinephrine, have been reported to increase CVP through a decrease in venous compliance (Klabunde, 2005). However, the evening decrease in CVP in monkeys has been suggested to occur due a decrease in CO rather than a decrease in sympathetic activity at this time, as Engel and Talan (1991) shown that adrenergic receptor antagonists ( $\alpha$  &  $\beta$ ) failed to attenuate the night time decrease in CVP.

### 1.2.3 Diurnal variations in cardiac electrophysiology

The increased morning predominance of SCD linked to the development of ventricular arrhythmias is believed to be associated with the morning increase in sympathetic activity (Arntz et al., 1993, Goldstein et al., 1996, Guo and Stein, 2003, Piepoli and Capucci, 2007). Ventricular arrhythmias can be triggered by changes in AP configuration through changes in ion channel activity and/or  $\text{Ca}^{2+}$  homeostasis. Sympathetic stimulation is known to modulate a number of ion channels and pumps within the ventricular myocyte, which have also been shown to be involved in ventricular arrhythmias (Tristani-Firouzi et al., 2001). Therefore, the morning predominance of ventricular arrhythmias and SCD may be due to diurnal variation in ion channels resulting in a pro-arrhythmic configuration of the cardiac AP which is emphasised by the increase in sympathetic activity.

Indeed, Yamashita *et al* (2003) have shown diurnal variation exists in the expression of Kv1.5 and Kv4.2 potassium channels. Both of these Kv channels affect the cardiac AP differently, forming the transient outward current,  $I_{to}$  (encoded by Kv4.2) which is responsible for early partial repolarisation and development of the “notch” in the cardiac AP and the ultra-rapid  $\text{K}^+$  current,  $I_{Kur}$  (encoded by Kv1.5) which contributes to the AP plateau by regulating AP repolarisation. They found that expression of Kv1.5 mRNA is increased during periods of darkness when the rat is active, whereas expression of Kv4.2 mRNA is increased during the resting period (period of light). This diurnal variation in the expressions of Kv1.5 and Kv4.2 may impact on AP duration (APD), as increased Kv1.5 expression is associated with APD shortening (Brunner et al., 2003, Tanabe et al., 2006). Therefore, as diurnal variation in Kv1.5 and Kv4.2 may modulate the APD, this may reflect an increased incidence of ventricular arrhythmias in particular those associated with short APDs.

Circadian rhythms in the cardiac electrophysiology of humans have also been identified, with an increase in the rate of the sinoatrial (SA) node, the QT interval and the refractory period of the conduction system between midnight and 7am (Cinca et al.,

1986). The prolongation of the cardiac QT interval is known to be potentially pro-arrhythmic and this may explain the morning dominance in arrhythmias and SCD (Day et al., 1990, Vincent et al., 1992). Hayano *et al* (1998) also found that atrioventricular (AV) node conduction and refractoriness show significant circadian rhythms in man, with an increase in AV node conduction and shorter refractory period in the morning hours. In an earlier study of 9 patients with cardiac electrophysiological conduction problems, Kong *et al* (1995) have also shown that the refractory period is shortest in the morning which the authors suggest contributes to the morning onset of ventricular arrhythmias as a long refractory period typically protects the myocardium from re-excitation and the generation of ventricular arrhythmias. As HR shows diurnal variation, peaking in the early morning, it may be that HR may be driving the diurnal changes in QT interval and refractoriness, however, in these papers measurements of QT interval and refractoriness have not been corrected for changes in HR, therefore, diurnal variation in these parameters cannot be ruled out.

The predominance of ventricular arrhythmias and SCD may also be due to alterations in the activity of the sympathetic nervous system which directly impacts on cardiac electrophysiology. It has been suggested that the diurnal variation in cardiac conduction and QT interval result from the activity of the sympathetic nervous system (Bexton et al., 1986, Guo and Stein, 2003). Diurnal variation in QT interval is thought to be due to sympathetic innervation as Bexton *et al* (1986) have reported that diurnal variation in QT interval is depressed in patients following a recent heart transplant and absent in patients with diabetic autonomic neuropathy, which in both instances have decreased sympathetic innervation in comparison to control patients. This abnormal diurnal cycling is also present in BP and CO in recent heart transplant patients (Idema et al., 1994). However, the diurnal variation in QT interval may be only depressed rather than absent following heart transplant due to the presence of circulating catecholamines. Reinnervation of sympathetic nerve fibres has been shown to frequently occur and therefore the depressed diurnal cycling in QT interval may be temporary (Fagard et al., 1995, Murphy et al., 2000, Bengel et al., 2001).

#### 1.2.4 Diurnal variations in sympathetic stimulation

The morning increase in the onset of fatal cardiovascular events and the underlying haemodynamic parameters, cardiac electrophysiology and cardiac function correlate with the known documented morning surge in sympathetic activity (Guo and Stein, 2003). In support of the notion that sympathetic-induced ventricular arrhythmias contribute to the morning peak in SCD,  $\beta$ -blockers have been shown to decrease the onset of many cardiovascular events such as SCD (Dorian, 2005) and MI (Quyyumi, 1990).  $\beta$ -blockers may have either an acute effect, mediated through blocking  $\beta_1/\beta_2$ -adrenergic receptors or a chronic effect, reducing the response of the cells to sympathetic stimulation through changes in gene transcription, with respect to decreasing the morning onset of SCD. Sympathetic stimulation is also believed to affect many of the cardiovascular parameters which exhibit diurnal variation, for example, SV and HR are enhanced by sympathetic stimulation (Veerman et al., 1995, Scheer et al., 2004). Sympathetic activity is also believed to affect diurnal variation in BP (more specifically, BP dipping) as  $\beta$ -blocker administration has been shown to promote BP dipping in patients classed as non-dippers (Lemmer, 2006). In addition, changes in sympathetic activity are believed to underlie the documented diurnal variation in the expression of the  $K^+$  channel, Kv1.5 ( $I_{K_{ur}}$ ) in the rat, as Yamashita *et al* (2003) reported that upon addition of propranolol, a  $\beta$ -blocker, diurnal variation in Kv1.5 expression was attenuated, suggesting that diurnal cycling of sympathetic activity was responsible for controlling Kv1.5 gene transcription.

In man, the levels of the circulating catecholamines, norepinephrine and epinephrine, and sympathetic activity have been shown to be increased in the early morning, when moving from a supine to upright position upon waking and resuming physical activity (Prinz et al., 1979, Linsell et al., 1985, Richards et al., 1986, Dodt et al., 1997). Conversely, the activity of the parasympathetic nervous system is increased during the night and decreased during daytime in man.

Diurnal variation in the activity of the autonomic nervous system (ANS) has also been identified by power spectral analysis of heart rate variation (HRV) in many species, as HRV can be used as an index of the activity of the ANS. Yamasaki *et al* (1996) performed power spectral analysis on HRV data obtained from 24 hour ambulatory ECG measurements in healthy male and female subjects. The authors identified the existence of a low frequency (LF) component and a high frequency (HF) component, corresponding to sympathetic and parasympathetic activity, respectively, and found that sympathetic activity was highest between 08:00-12:00 and that parasympathetic activity was highest between 00:00-06:00 (Yamasaki *et al.*, 1996). In an earlier study, Lombardi *et al* (1992) have also shown through analysis of HRV, that sympathetic activity is highest during the day and that parasympathetic activity is highest during night in control subjects. However, in the same study in post-MI patients, sympathetic activity was increased during the day and night and parasympathetic activity was decreased at night, indicating loss of normal ANS activity following MI (Lombardi *et al.*, 1992). Analysis of HRV in miniature swine has also been shown to mirror that of human subjects (Kuwahara *et al.*, 1999). Interestingly, in the guinea pig, analysis of HRV has shown that sympathetic and parasympathetic activity does not exhibit diurnal variation (Akita *et al.*, 2002).

In the nocturnal rat, sympathetic activity and the circulating catecholamines, norepinephrine and epinephrine, are highest during the active period and conversely, parasympathetic activity is increased during the resting period and decreased during the active period in the nocturnal rat. Indeed, Hashimoto *et al* (1999) performed power spectral analysis of HRV in male Wistar rats and found that sympathetic activity was greatest during the night (dark phase), which marks the active period of the rat and conversely, parasympathetic activity was greatest during the daytime (light phase), which marks the inactive period of the rat.

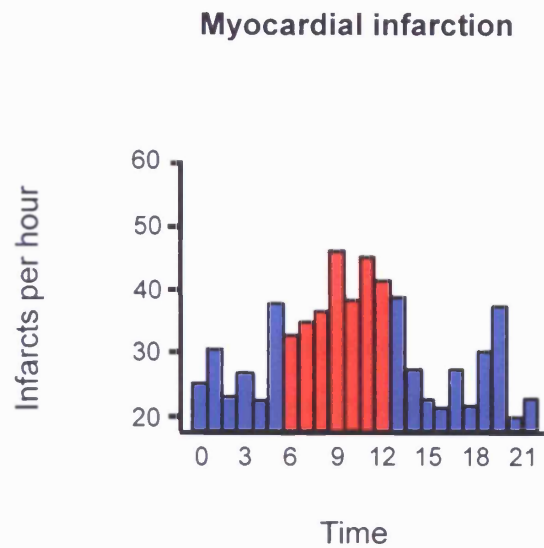
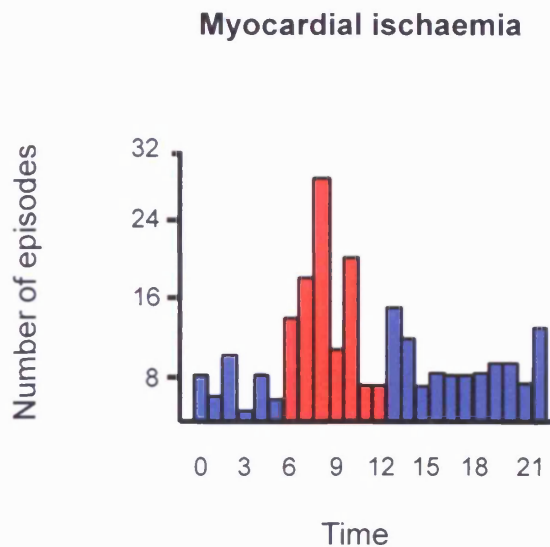
### **1.2.5 Diurnal variations in cardiovascular events**

It is well documented that the onset of many fatal cardiovascular events like MI (Peckova et al., 1998, Hastings et al., 2003), ventricular arrhythmias (Tofler et al., 1995) and SCD (Arntz et al., 1993, Guo and Stein, 2003) are most common in the morning in man, which coincides with arousal from sleep and the onset of physical activity. Diurnal variation in the onset of these events is also correlated with morning increases in the activity of the sympathetic nervous system (increased catecholamine levels), haemodynamic parameters (BP, HR, CO, SV) and cardiac electrophysiology.

#### ***Myocardial infarction***

Significant circadian and diurnal variations have been reported in the onset of MI, with the onset of MI being increased in the early hours of the morning in man (Hastings et al., 2003), which is illustrated in figure 1.2. Peckova *et al* (1998) looked at data pertaining to ~6600 MIs in non-hospitalised patients and found that the incidence of MI was lowest during the night, and increased to peak during the early morning between 8 and 11am. The authors suggested that the increased morning onset of MI is related to the onset of physical activity following sleep. This circadian variation in the onset of MI has also been reported in patients suffering from HF, as the peak incidence was also highest in the morning between 6am and midday (Aronow and Ahn, 2003).

Recent data suggests that diurnal variation also exists in the sensitivity of the myocardium to oxidative stress and tolerance to ischaemia/reperfusion (I/R) injury. Indeed, Durgan *et al* (2010) have shown that following coronary artery occlusion to induce I/R injury, wild-type mice had larger infarct sizes and decreased contractile function, during the active period (ZT12) than resting period (ZT0) and also one month following reperfusion, these ischaemic active period (ZT12) animals had a greater degree of fibrosis and ventricular remodelling than their resting period (ZT0)

**A****B**

**Figure 1.2- Diurnal variation in the onset of fatal cardiovascular events in man (adapted from Hastings *et al*, 2003).**

- A. This figure shows the number of incidences of myocardial infarction occurring during 24 hours and shows that the incidence of myocardial infarction is increased during the early morning, between the hours of 6am and 12pm (highlighted in red).
- B. This figure shows the number of episodes of myocardial ischaemia occurring during 24 hours and shows that, similar to the incidence of myocardial infarction (figure 1.2A), the number of episodes of myocardial ischaemia are increased in the early morning between 6 and 12pm (highlighted in red).

counterparts . In addition, the authors showed that diurnal variation in the tolerance to I/R injury was abolished in CCM mice, suggesting that the cardiomyocyte circadian clock controls tolerance to I/R injury (Durgan et al., 2010). In man, the diurnal variation in the sensitivity of the myocardium to injury is important in terms of treatment, as De luca *et al* (2005) have shown that in patients undergoing angioplasty that post-operative survival was highest when patients were treated during the afternoon and evening from 1pm to midnight, however, patients treated in the early morning (4-8am) had reduced post-operative health and survival rates. In addition, this diurnal variation in the sensitivity of the myocardium to injury is important in terms of the development of cardiovascular pathology, as Mukamal *et al* (2000) have documented an increased risk of HF in post MI patients if the preceding MI occurred during the evening.

### ***Ventricular arrhythmias***

Diurnal variation has been reported in the onset of ventricular arrhythmias in various species including man and is believed to reflect the time-of-day dependent increase in sympathetic activity (Guo and Stein, 2003). The onset of ventricular arrhythmias has been reported to peak in the early hours of the morning and reach a trough in the evening in man. Indeed, Tofler *et al* (1995) looked at the onset of ventricular arrhythmias in patients with implantable cardioverter-defibrillators and found that the greatest proportion of ventricular arrhythmias occurred in the morning, as illustrated in figure 1.3A, which may contribute to the increased SCD seen at this time. In support of the findings of Tofler and colleagues, Mallavarapu *et al* (1995) looked at the incidence of ventricular arrhythmias in post-MI patients with implanted cardioverter-defibrillators and found that a large number of ventricular arrhythmias occurred between 10-11am and the lowest incidence between 2-3am. In addition, the cardiac arrhythmia suppression trial (CAST) has also shown that ventricular arrhythmias are most

prominent in the early morning between the hours of 6 & 10am, in which a greater amount of ventricular premature depolarisations were seen (Goldstein et al., 1996).

### ***Sudden cardiac death (SCD)***

As there is a strong link between the incidence of ventricular arrhythmias and SCD in both animals and humans, it is not too surprising that diurnal variation has also been reported in the occurrence of SCD (Guo and Stein, 2003). Indeed, Arntz *et al* (1993) used ECG measurements obtained as printouts from external defibrillators from patients during resuscitation attempts, to determine whether circadian variation exists in SCD. The authors showed that the onset of SCD largely peaked between 6am and midday, although there was a secondary smaller peak between 3-7pm, as illustrated in figure 1.3B (Arntz et al., 1993). In addition, the authors correlated the morning onset of SCD with the increased incidence of ventricular fibrillation rather than asystole and bradycardia-related arrhythmias (Arntz et al., 1993). Moreover, circadian variations in SCD have also been shown in 2 large population based studies. The first being, The Framingham heart study, which examined 5209 patients over > 30 years, found that SCD exhibited a strong circadian variation as the onset of SCD peaked between 7 and 9am (Willich et al., 1987). The second population based study investigating the onset of SCD was performed by Muller *et al* (1987) and they analysed ~2200 death certificates and found that there was an increased incidence of SCD in the morning between 7 and 11am and a lower incidence during night time hours.

As changes in parameters underlying cardiac excitation-contraction (EC) coupling, namely the cardiac AP and calcium ( $Ca^{2+}$ ) regulation, are factors likely to impact on the diurnal variation seen in the onsets of MI, ventricular arrhythmias and SCD, EC-coupling will be discussed in the following section (section 1.3 of introduction).

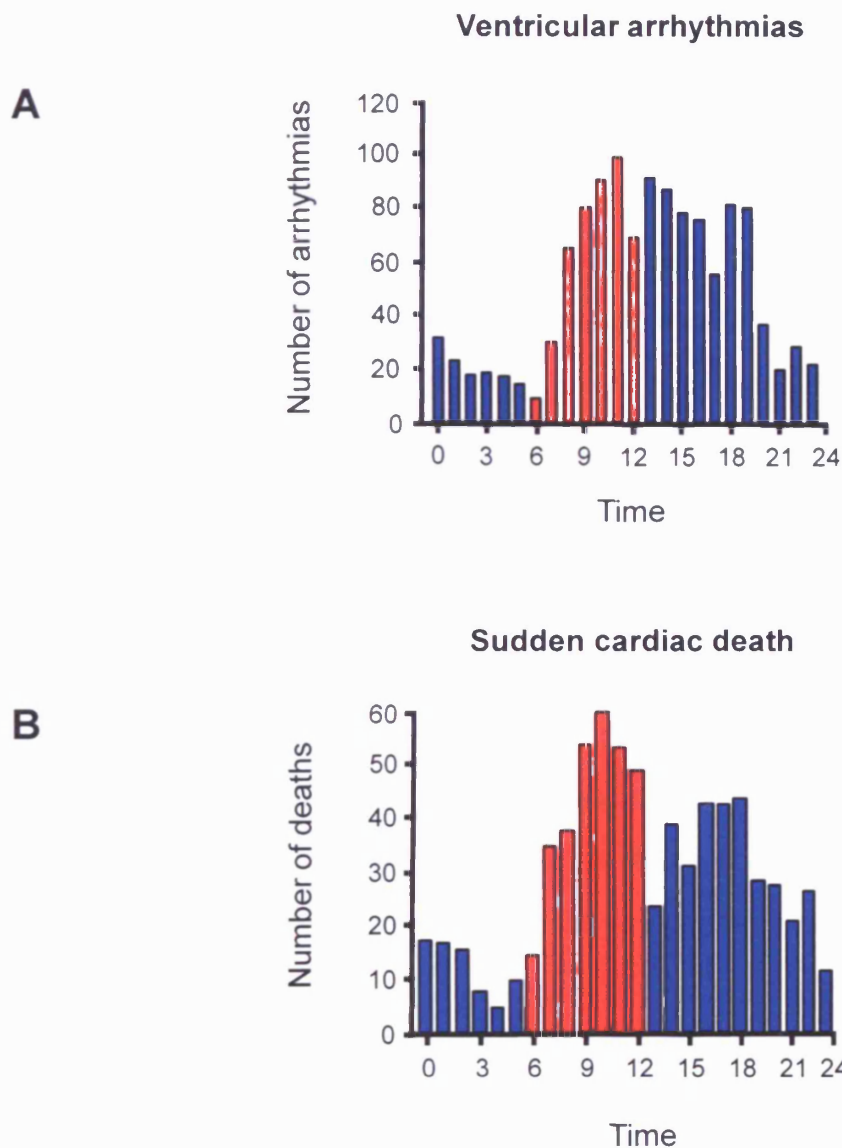


**Figure 1.3- Diurnal variation in the onset of ventricular arrhythmias and sudden cardiac death in man (adapted from Tofler *et al*, 1995 and Arntz *et al*, 1993).**

A. This figure shows the number of ventricular arrhythmias occurring during 24 hours and shows that the incidence of ventricular arrhythmias is increased during the early morning, between the hours of 6am and 12pm (highlighted in red), adapted from Tofler *et al* (1995).

B. This figure shows the number of incidences of sudden cardiac death occurring during 24 hours and shows that the incidence of sudden cardiac death is increased during the early morning, between the hours of 6am and 12pm (highlighted in red), adapted from Arntz *et al* (1993).

### ***1.3 Cardiac excitation-contraction coupling***

Mammalian cardiac EC-coupling is comprised of three main components which are: electrical, chemical and mechanical, all of which must occur during cardiac contraction. Diurnal variations observed in K<sup>+</sup> channel expression (Kv4.2 and Kv1.5), QT interval, cardiac conduction, cardiac refractoriness, contractile performance and sympathetic stimulation may impact directly on EC-coupling and therefore, all components of EC-coupling will be discussed below in detail.

#### **1.3.1 Excitation (electrical component)**

Generation of the cardiac ventricular AP marks the first stage in EC-coupling, in which the transduction of an electrical signal leads to the initiation of cardiac contraction and a mechanical output. The ventricular AP is shown in figure 1.4 and highlights the underlying ionic currents responsible for the various phases of the AP.

**Phase 4:** This phase represents the period of cardiac diastole where electrical and contractile activity of the ventricular myocyte is at rest and is the phase of the ventricular AP where the resting membrane potential (RMP) is restored and maintained prior to subsequent APs. The RMP of cardiac ventricular cells is between -70 and -90 mV, a figure close to the equilibrium potential for potassium ions (K<sup>+</sup>), which highlights the importance of K<sup>+</sup> as the major ionic component of RMP in cardiac cells (Tamargo et al., 2004, Grant, 2009). The equilibrium potential for K<sup>+</sup> can be described by the Nernst equation (Hille, 2001):

$$E_K = \frac{RT}{zF} \ln \frac{[K^+]_o}{[K^+]_i}$$

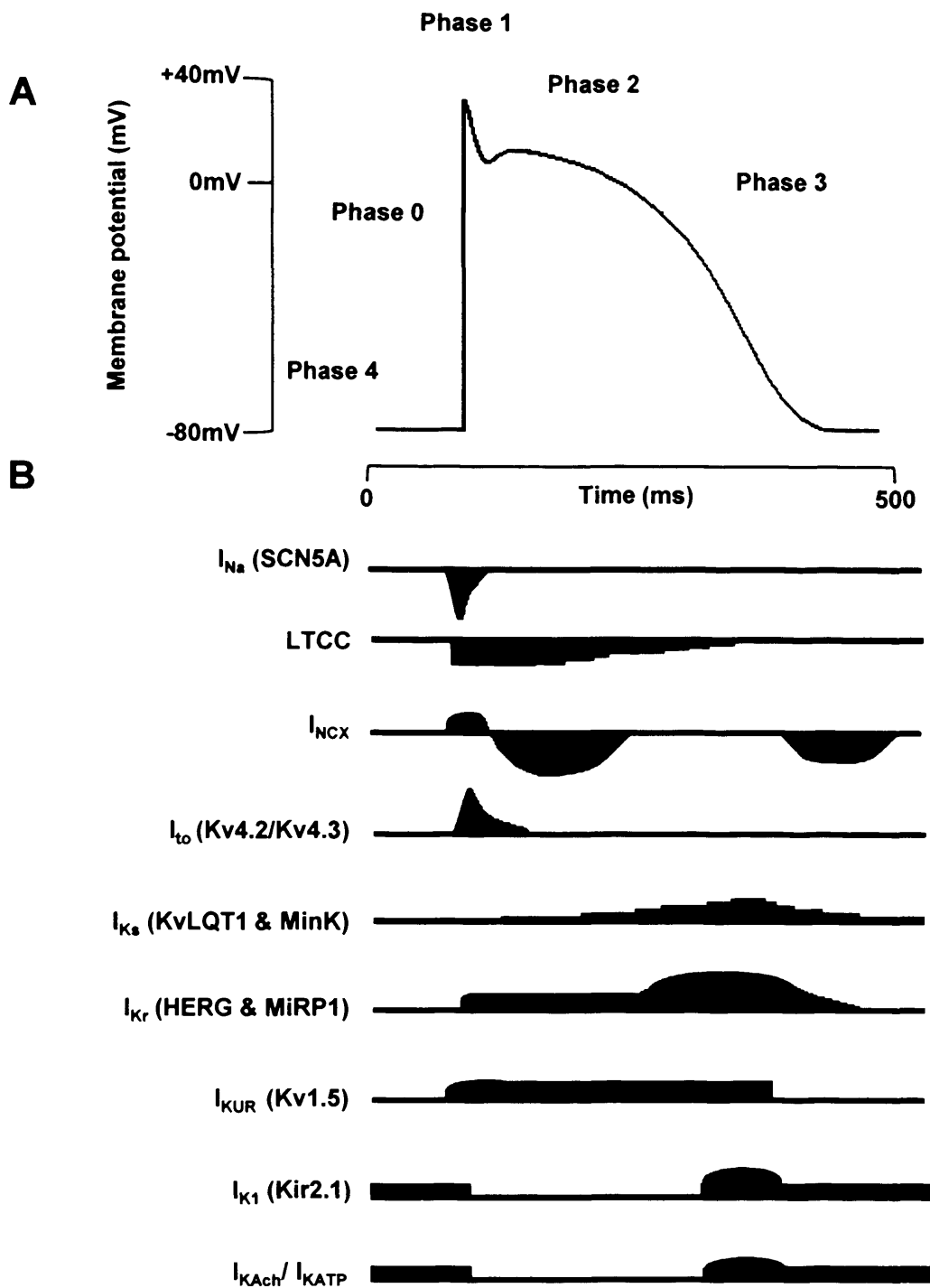


**Figure 1.4- The cardiac ventricular action potential (adapted from Tamargo *et al*, 2005).**

- A. This figure shows the human cardiac ventricular action potential (AP). The ventricular AP is defined by 5 separate phases (phases 0, 1, 2, 3, 4). Phase 4 is the resting phase of the AP, where the resting membrane potential (RMP) is restored and maintained by  $I_{K1}$ . Phase 0 corresponds to the rapid AP upstroke, which is governed by  $I_{Na}$ . Phase 1 is the notch phase of the AP and results from inactivation of  $I_{Na}$  and increases in  $I_{to}$  and  $I_{Kur}$ . Phase 2 is the plateau phase of the AP and also the longest phase. Phase 2 involves the opening of LTCC balanced by the opening of delayed rectifier  $K^+$  channels ( $I_{Kr}$ ,  $I_{Ks}$ ,  $I_{Kur}$ ). Phase 3 is the late repolarisation phase of the AP and occurs due to the inactivation of LTCC in the presence of sustained delayed rectifier currents and  $I_{K1}$ . NCX current also contributes to the AP plateau and repolarisation phases.
- B. The figure shows the underlying ionic currents that contribute to the cardiac ventricular AP and is for illustrative purposes to show the relative time courses of the currents and not the relative current amplitudes, which are not drawn to scale.

However, as the cell membrane is not exclusively permeable to  $K^+$  and is also permeable to other ions such as  $Na^+$  and  $Cl^-$ , the Goldman-Hodgkin-Katz (GHK) equation can be used, which takes into account membrane permeability of  $K^+$ ,  $Na^+$  and  $Cl^-$  in addition to electrochemical potential (Hille, 2001):

$$V_m = \frac{RT}{F} \log_{10} pK \frac{[K^+]_o}{[K^+]_i} + pNa \frac{[Na^+]_o}{[Na^+]_i} + pCl \frac{[Cl^-]_i}{[Cl^-]_o}$$

**R** = Gas constant ( $8.31 \text{ J} \cdot \text{K}^{-1}$ )

**T** = Absolute temperature

**Z** = Ionic valency

**F** = Faradays constant ( $9.65 \times 10^4 \text{ C mol}^{-1}$ )

**pNa** = Relative membrane permeability for Sodium

**pK** = Relative membrane permeability for Potassium

**pCl** = Relative membrane permeability for Chloride

**V<sub>m</sub>** = Membrane potential

**[K<sup>+</sup>]<sub>o</sub>** = Extracellular potassium concentration

**[K<sup>+</sup>]<sub>i</sub>** = Intracellular potassium concentration

**[Na<sup>+</sup>]<sub>o</sub>** = Extracellular sodium concentration

**[Na<sup>+</sup>]<sub>i</sub>** = Intracellular sodium concentration

**[Cl<sup>-</sup>]<sub>o</sub>** = Extracellular chloride concentration

**[Cl<sup>-</sup>]<sub>i</sub>** = Intracellular chloride concentration

Activation of the cardiac Kir 2.1/2.2 channel is responsible for the generation of  $I_{K1}$  current which is responsible for the maintenance of the RMP. The high permeability of the membrane to  $K^+$  is a property of the inward rectifier  $K^+$  channel, Kir 2.1/2.2, which due to its high conductance to  $K^+$  at negative membrane potentials, means that RMP is close to  $E_K$  (Tristani-Firouzi et al., 2001, Tamargo et al., 2004). The  $Na^+/K^+$  ATPase

also contributes to the maintenance of the RMP, by pumping  $\text{Na}^+$  out of the cell in exchange for  $\text{K}^+$  influx and the pump helps to maintain a large intracellular  $\text{K}^+$  concentration within the cell compared to outside, creating a large inwardly directed  $\text{K}^+$  concentration gradient. This  $\text{K}^+$  concentration gradient therefore provides a driving force for  $\text{K}^+$  ions to leave the cell through the  $\text{Kir 2.1/2.2}$  ( $\text{I}_{\text{K1}}$ ). The steady-state equation is an additional equation that takes the  $\text{Na}^+/\text{K}^+$  ATPase current into account when considering the RMP and is outlined below (Mullins and Noda, 1963, Robinson, 1975, Nicholls, 2001):

$$E_m = \frac{RT}{zF} \ln \left( \frac{[\text{K}^+]_o + ba [\text{Na}^+]_o}{[\text{K}^+]_i + ba [\text{Na}^+]_i} \right)$$

***b*** = Coupling ratio of the  $\text{Na}^+$  pump

***a*** = Ratio of permeability of  $\text{Na}^+$  and  $\text{K}^+$

***Phase 0:*** The upstroke of the ventricular AP occurs as a result of rapid depolarisation resulting from the brief opening of the cardiac  $\text{Na}^+$  channel ( $\text{Na}_v1.5$  channel). These voltage-dependent channels open in response to an initial depolarisation of the membrane potential, leading to further depolarisation and a large increase in  $\text{Na}^+$  conductance generating an inward  $\text{Na}^+$  current ( $\text{I}_{\text{Na}}$ ) (Nerbonne and Kass, 2005, Grant, 2009). The increase in  $\text{Na}^+$  conductance contributes to the overshoot of the AP as it drives the membrane potential of the cell towards the  $\text{Na}^+$  equilibrium potential, at which point  $\text{Na}^+$  channels rapidly inactivate due to voltage-dependent inactivation (Nerbonne and Kass, 2005, Grant, 2009). Inward rectification of the  $\text{I}_{\text{K1}}$  channel occurs due to a voltage-dependent block of the channel by endogenous polyamines and  $\text{Mg}^{2+}$  during positive membrane potentials (Vandenberg, 1987, Lee et al., 1999) and this reduces outward  $\text{K}^+$  current through the channel and  $\text{I}_{\text{K1}}$  channels remain closed until the

late stages of phase 3 of the AP, where they aid cardiac repolarisation (see phase 3) (Tristani-Firouzi et al., 2001, Tamargo et al., 2004).

**Phase 1:** This is termed the “notch” phase of the ventricular AP and is the result of partial membrane repolarisation due to the fast voltage-dependent N-type inactivation of  $\text{Na}^+$  channel in combination with increases in the transient outward  $\text{K}^+$  current,  $I_{\text{to1}}$  and also the ultra rapid delayed rectifier  $\text{K}^+$  current,  $I_{\text{Kur}}$  (Kv1.5) (Tamargo et al., 2004). The transient outward current is a combination of two ionic currents; they are composed of a  $\text{K}^+$  current ( $I_{\text{to1}}$ ) and a  $\text{Ca}^{2+}$  activated  $\text{Cl}^-$  current ( $I_{\text{to2}}$ ), however, as the existence of  $I_{\text{to2}}$  is controversial (Tristani-Firouzi et al., 2001, Tamargo et al., 2004), only  $I_{\text{to1}}$  will be discussed. The transient outward  $\text{K}^+$  current,  $I_{\text{to1}}$ , is composed of a fast and slow activating component, corresponding to  $I_{\text{tof}}$  (Kv4.2/4.3) and  $I_{\text{tos}}$  (Kv1.4), respectively (Tristani-Firouzi et al., 2001, Grant, 2009). The transient outward current,  $I_{\text{tof}}$ , (Kv4.2/4.3) activates rapidly during depolarised membrane potentials ( $\sim -30\text{mV}$ ), however, the current quickly undergoes voltage-dependent inactivation (Nerbonne and Kass, 2005).  $I_{\text{Kur}}$  (Kv1.5) activates rapidly in comparison to the fast and slow delayed rectifier  $\text{K}^+$  channels (see phase 2), and inactivates slowly during the AP due to voltage-dependent C-type inactivation of the Kv1.5 channel. Therefore, as a result  $I_{\text{Kur}}$  is believed to contribute to the early repolarisation (phase 1) in addition to plateau phase (phase 2) and repolarisation (phase 3) of the AP (Tamargo et al., 2004). However, Kv1.5 channels which give rise to  $I_{\text{Kur}}$  are predominately localised to the atria and their presence in the human ventricle has been disputed and therefore their role in human ventricular AP is also controversial (Tamargo et al., 2004).

The purpose of the “notch” phase is to partially repolarise the cell which is beneficial as it provides the driving force for  $\text{Ca}^{2+}$  entry during the plateau phase of the AP (phase 2) and contributes to the shape of the AP plateau (Bouchard et al., 1995, Tamargo et al., 2004). The rodent myocardium has a large density of Kv4.2 channels and therefore also a large  $I_{\text{to}}$  current (Fiset et al., 1997). This increase in  $I_{\text{to}}$  results in a decrease in the AP plateau as  $I_{\text{to}}$  is much greater than LTCC current and thereby limits  $\text{Ca}^{2+}$  influx and as a result also decreases the APD (Fiset et al., 1997, Nerbonne and Kass, 2005). However,

in the human myocardium the expression of Kv4.2 and therefore  $I_{to}$  current is much lower than in the rat, therefore, phase 1 repolarisation is slowed due to a greater  $Ca^{2+}$  influx mediated by LTCC and this prolongs APD (Nerbonne and Kass, 2005). In LV hypertrophy and HF, Kv4.2/Kv4.3 and the  $I_{to}$  current have been shown to be reduced, thereby prolonging the APD and increasing the risk of arrhythmic activity (Kaab et al., 1998, Nabauer and Kaab, 1998). Interestingly, the expression of the  $K^+$  channel (Kv4.2) which produces  $I_{to}$  was shown to exhibit patterns of diurnal cycling in the rat heart (Yamashita et al., 2003) (see section 1.2.3).

**Phase 2:** This is the plateau phase of the AP, which determines the length of the cardiac ventricular AP and in which  $Ca^{2+}$  plays an integral part. In the myocardium there are two different  $Ca^{2+}$  channels and these are the L-type  $Ca^{2+}$  channel (LTCC) and the T-type  $Ca^{2+}$  channel (TTCC). The early plateau is the result of an increase in the inward  $Ca^{2+}$  current generated by activation of the LTCC ( $Ca_v1.2$ ), encoded by the gene *Ca<sub>v</sub>1c*. The LTCC current rapidly activates during depolarised membrane potentials ( $\sim -40mV$ ) and is long lasting, as the channel inactivates slowly, therefore, slowing repolarisation (Nerbonne and Kass, 2005). The LTCC exhibits both  $Ca^{2+}$  dependent and voltage-dependent inactivation. This slow inactivation of LTCC maintains the APD which is important for controlling contraction and generating a long refractory period. This long refractory period is the predominant way the myocardium prevents and protects against re-excitation and the development of ventricular arrhythmias.

The entry of  $Ca^{2+}$  through the LTCC during the AP is the main trigger for SR  $Ca^{2+}$  release and therefore the initiation of cardiac EC-coupling (Bers, 2002). The TTCC is also believed to have a small contribution to the early plateau phase, as TTCC rapidly activates and inactivates at negative membrane potentials, however, as TTCC are predominately localised to cardiac pacemaker cells, the major role of TTCC is believed to be in generating pacemaker activity (Grant, 2009, Ono and Iijima, 2010).

The inward  $Ca^{2+}$  current (and some slowly inactivating  $Na^+$  currents) are balanced by outward  $K^+$  currents generated by the ultra rapid ( $I_{Kur}$ ), rapid ( $I_{Kr}$ ) (hERG & MiRP1) and slow ( $I_{Ks}$ ) (KvLQT1 & MinK) delayed rectifier  $K^+$  channels, resulting in a balance of

inward and outward currents. The Kv1.5 channel responsible for the  $I_{Kur}$  current activates rapidly during phase 1 and is responsible for the early plateau stage (phase 2) when the other delayed rectifier  $K^+$  channels are inactive (Tamargo et al., 2004, Nerbonne and Kass, 2005). During the plateau phase,  $I_{Kr}$  and  $I_{Ks}$  activate slowly in comparison to  $I_{Kur}$ , at a membrane potential of  $\sim -30\text{mV}$ , thereby allowing LTCC to maintain a depolarised membrane potential (Tristani-Firouzi et al., 2001, Nerbonne and Kass, 2005). Both  $I_{Kr}$  and  $I_{Ks}$  are believed to contribute to the late plateau and towards the end of the plateau phase, the LTCC inactivate, reducing the inward  $\text{Ca}^{2+}$  current, which in the presence of the increased delayed rectifier  $K^+$  currents ( $I_{Kr}$  and  $I_{Ks}$ ), promotes repolarisation (Tamargo et al., 2004, Nerbonne and Kass, 2005).

**Phase 3:** The late repolarisation phase of the ventricular AP occurs as the inward  $\text{Ca}^{2+}$  current declines due to the inactivation of LTCC in combination with the parallel increase in the conductance of the outward delayed rectifier  $K^+$  currents,  $I_{Kr}$  and  $I_{Ks}$ , and as the membrane potential repolarises the inward rectifier  $K^+$  current,  $I_{K1}$ , also increases (Tamargo et al., 2004, Grant, 2009). The increase in  $K^+$  conductance promotes repolarisation of the membrane potential towards  $E_K$ , restoring membrane potential to resting levels in phase 4 of the AP.

### ***Role of NCX1 in the cardiac action potential***

The sodium/calcium exchanger (NCX1) is an ion exchanger located on the sarcolemmal membrane of the ventricular myocardium, which is important in the AP and also cardiac EC-coupling (see section 1.3.3 of introduction). NCX1 has the following stoichiometry:  $3\text{Na}^+ : 1\text{Ca}^{2+}$  and therefore is considered to be electrogenic (Reeves and Hale, 1984). NCX1 can operate in either a “forward-mode”, in which  $\text{Ca}^{2+}$  is extruded in exchange for an influx of  $\text{Na}^+$ , or in a “reverse-mode”, in which  $\text{Ca}^{2+}$  is brought into the myocyte in exchange for  $\text{Na}^+$  efflux. (Bers, 2002, Sher et al., 2008). The activity of NCX1 is regulated by the transmembrane concentration gradients of both respective ions and also by changes in membrane potential. Physiologically, changes in

intracellular ions are likely to be the main ionic stimulus to changes to mode of action with an increased  $[Ca^{2+}]_i$  concentration favouring forward-mode NCX and increased  $[Na^+]_i$  promoting reverse-mode NCX, however, these modes are further modulated by the membrane potential during the AP (Weber et al., 2002).

NCX1 is thought to contribute to the upstroke, plateau and repolarisation phases of the ventricular AP. During positive membrane potentials, such as during phase 0 (upstroke), the membrane potential will exceed the reversal potential of NCX promoting  $Ca^{2+}$  influx through reverse-mode NCX (Sher et al., 2008). During the late plateau (phase 2) and terminal ventricular repolarisation (phase 3), the NCX is thought to contribute by extruding intracellular  $Ca^{2+}$ , which had accumulated within the myocyte during the plateau phase, in exchange for  $Na^+$  through forward-mode NCX (Armoundas et al., 2003, Sher et al., 2008). However, NCX is not believed to contribute to phase 4 of the cardiac AP as intracellular  $Ca^{2+}$  levels are low and membrane potential is very negative.

### ***Other currents involved in ventricular action potential***

The inward rectifying  $K^+$  currents, acetylcholine-activated  $K^+$  current ( $I_{KAch}$ ) and the ATP-sensitive  $K^+$  current ( $I_{KATP}$ ) can also influence the cardiac ventricular AP. The acetylcholine-activated  $K^+$  channel responsible for  $I_{KAch}$  is composed of Kir 3.1 and Kir 3.4  $\alpha$ -subunits (Tamargo et al., 2004, Grant, 2009). In order to generate the acetylcholine-activated  $K^+$  current ( $I_{KAch}$ ) acetylcholine must first bind to the muscarinic  $M_2$  receptor. The  $M_2$  receptor is a G-protein coupled receptor (GPCR) and the  $\beta$  subunit of the  $G_i$ -protein will activate  $I_{KAch}$ . Activation of  $I_{KAch}$  hyperpolarises the membrane potential and slows conduction through the SA and AV nodes (Tamargo et al., 2004, Grant, 2009). However, activation of  $I_{KAch}$  is most important in terms of vagal control of HR and will not be discussed further. The ATP-sensitive  $K^+$  channel ( $K_{ATP}$ ) is composed of Kir 6.2  $\alpha$ -subunits in addition to SUR2A  $\beta$ -subunits and is inhibited by ATP and activated by ADP and therefore the open probability of the channel is

dependent on the ratio of ATP: ADP (Seino and Miki, 2003, Tamargo et al., 2004). In this respect, the  $K_{ATP}$  channel is an energy sensing channel that couples the energy status of the myocytes to the electrical activity/ membrane potential. The opening of  $K_{ATP}$  channels increases repolarisation thereby shortening APD and prevents  $Ca^{2+}$  overload by decreasing  $Ca^{2+}$  influx during the AP, which is important during metabolic stress for example during MI (Seino and Miki, 2003, Rodrigo and Standen, 2005a).

### **1.3.2 Calcium cycling and contraction**

Increased cytoplasmic  $Ca^{2+}$  is responsible for the resultant mechanical aspect of EC-coupling, contraction. Under resting conditions, contraction is inhibited due to myosin binding site of actin being blocked by tropomyosin which is complexed to troponin C, Troponin I and Troponin T (Solaro and Rarick, 1998, Bers, 2001). For contraction to occur intracellular  $Ca^{2+}$  must first increase and this  $Ca^{2+}$  binds to Troponin C and results in a conformational change in Troponin I, exposing the myosin binding site (Solaro and Rarick, 1998, Bers, 2001). The exposure of this binding site allows the interaction of both myosin and actin which promotes cross-bridge formation and subsequent contraction. Contraction exhibited is graded and thought to be affected by the amount of  $Ca^{2+}$  triggering the contraction (Solaro and Rarick, 1998, Bers, 2001) and can also be affected by the desensitisation of the contractile proteins to  $Ca^{2+}$  for example during  $\beta$ -adrenergic stimulation (see section 1.4 of introduction).

During the cardiac AP, the wave of depolarisation spreads to the ventricular myocyte T-tubules, shown in figure 1.5. On depolarisation, LTCC are activated and open, which results in the entry of  $Ca^{2+}$  into the myocytes, resulting in the generation of an inward  $Ca^{2+}$  current, which is the main route of  $Ca^{2+}$  entry from the extracellular space into the myocytes during cardiac EC-coupling. Small amounts of  $Ca^{2+}$  may also enter the myocyte via alternative mechanisms, for example, through TTCC or reverse-mode NCX (Levesque et al., 1994, Sipido et al., 1998).  $Ca^{2+}$  entry during EC-coupling can

arise from the activity of the electrogenic NCX (see earlier, section 1.3 of introduction).  $\text{Ca}^{2+}$  entry through the NCX is complex as the reversal potential during phase 4 of AP, immediately prior to excitation and phase 0 is calculated from the  $\text{Na}^+$  and  $\text{Ca}^{2+}$  gradients during diastole with the cell at rest (Weber et al., 2002). However, during the initial depolarization and contraction,  $\text{Na}^+$  and  $\text{Ca}^{2+}$  concentrations will quickly change due to influx of  $\text{Na}$  and  $\text{Ca}^{2+}$  and liberation of  $\text{Ca}^{2+}$  from the SR and the function of the NCX will reflect this. During cardiac diastole i.e. phase 4 of the ventricular AP, the RMP is between  $\sim -70$  and  $-90\text{mV}$  (see section 1.3). The NCX has a reversal potential of  $-50\text{mV}$  and as during rest the reversal potential of NCX is greater than the RMP,  $\text{Ca}^{2+}$  is extruded from the myocyte through forward mode NCX (Bers, 2002). Early in the AP the RMP becomes depolarised (up to  $+20\text{mV}$ ) and becomes greater than the reversal potential of NCX and therefore, there is an immediate increase in  $\text{Ca}^{2+}$  due to  $\text{Ca}^{2+}$  influx being favoured through reverse mode NCX (Bers, 2002). However, due to the local build up of  $\text{Ca}^{2+}$  as a result of  $\text{Ca}^{2+}$  entry through the LTCC and SR  $\text{Ca}^{2+}$  release through RyR2, NCX is thought to rapidly switch to extrude  $\text{Ca}^{2+}$  from the cell through forward mode NCX and this is further modulated by  $\text{Na}^+$  which is altered by the  $\text{Na}$ -current (Weber et al., 2002, Armoundas et al., 2003). In addition, similar to conditions seen during cardiac diastole, during repolarisation of the cardiac AP, restoration of the negative RMP in addition to high  $[\text{Ca}^{2+}]_i$  promotes  $\text{Ca}^{2+}$  extrusion through forward mode NCX (Sher et al., 2008).

$\text{Ca}^{2+}$  entry through TTCC remains controversial due to the low density of TTCC in the ventricle and also due to fast voltage-dependent inactivation of the channel (Ono and Iijima, 2010).

The entry of  $\text{Ca}^{2+}$  through the LTCC triggers the release of  $\text{Ca}^{2+}$  from the sarcoplasmic reticulum (SR) through a process termed “calcium-induced calcium release” (CICR), through the opening of the  $\text{Ca}^{2+}$  release channels, ryanodine receptors (RyR2). RyR2 are located on the junctional SR in close proximity to the LTCC of the sarcolemma and open in response to a local increase in  $\text{Ca}^{2+}$ , resulting in the release of  $\text{Ca}^{2+}$  from the SR lumen (Scriven et al., 2000, Bers, 2002). However, the degree of subcellular

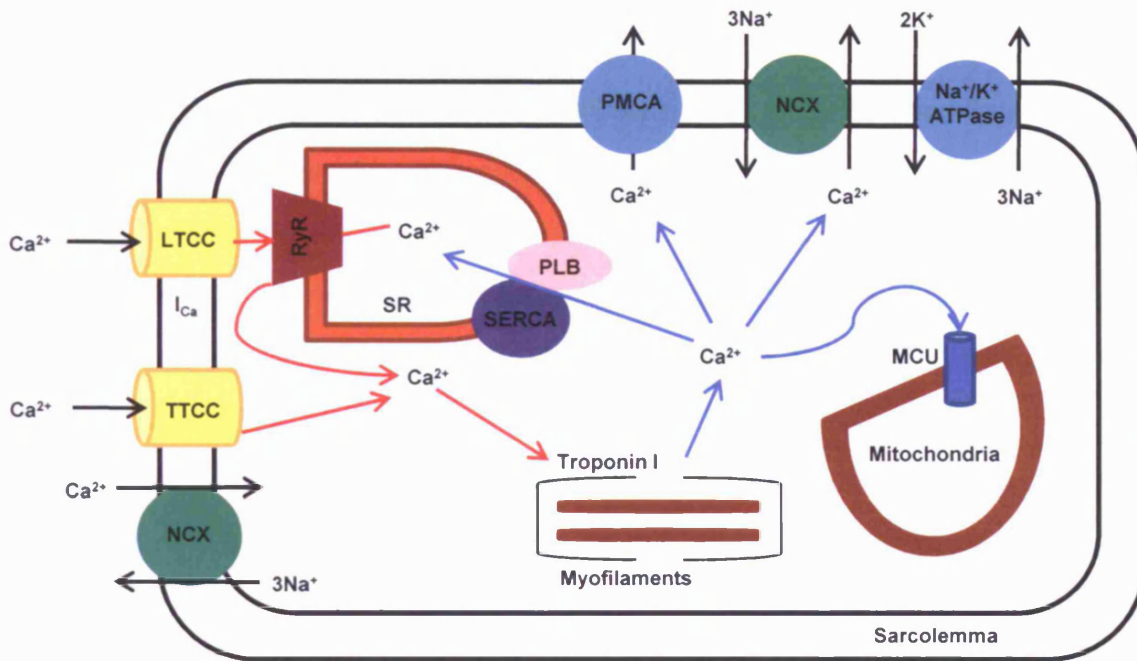


**Figure 1.5- The mechanism of cardiac excitation-contraction coupling (adapted from Bers, 2002).**

As an action potential arrives at the ventricular myocyte, LTCC are activated and open, promoting Ca<sup>2+</sup> entry into the myocyte. Ca<sup>+</sup> may also enter the myocyte through NCX and TTCC. Ca<sup>2+</sup> entry and accumulation in the vicinity of the sarcoplasmic reticulum Ca<sup>2+</sup> release channel, RyR2, will be detected by RyR2. When the Ca<sup>2+</sup> concentration reaches a critical level, it triggers calcium-induced calcium release (CICR) from the SR. Ca<sup>2+</sup> released from the SR interacts with the contractile myofilaments, promoting contraction. Myocyte relaxation is triggered by Ca<sup>2+</sup> dissociation from the myofilaments and reuptake into the SR through the action of SERCA2a or Ca<sup>2+</sup> is extruded from the myocyte through the action of NCX. Ca<sup>2+</sup> may also leave the cytosol through the action of plasma membrane Ca<sup>2+</sup> ATPase (PMCA) or through the action of the mitochondrial Ca<sup>2+</sup> uniporter (MCU).

organisation of RyR2 and LTCC is far more complex than this. In fact, at each junction of the SR, ~100 RyR2 are grouped in the region of each LTCC, forming a large,  $\text{Ca}^{2+}$  release unit often referred to as a “couplon” (Bers, 2001, Bers, 2002). The existence of these  $\text{Ca}^{2+}$  release units was first suggested from the presence of  $\text{Ca}^{2+}$  sparks (Cheng et al., 1993).  $\text{Ca}^{2+}$  sparks represent coordinated SR  $\text{Ca}^{2+}$  release events occurring as a result of the activation of ~10-25 RyR2 (Cheng et al., 1993, Wier and Balke, 1999). In addition,  $\text{Ca}^{2+}$  released at each couplon may also activate nearby RyR2 forming  $\text{Ca}^{2+}$  waves which spread throughout the cell. The existence and activation of RyR2-LTCC composed “couplons” and resultant generation of  $\text{Ca}^{2+}$  sparks is the basis of for the “local control theory” of cardiac EC-coupling (Cheng et al., 1993, Wier and Balke, 1999, Bers, 2002).

In addition, to their role as  $\text{Ca}^{2+}$  release channels, RyR2 are also scaffolding proteins which have been shown through coimmunoprecipitation and colocalisation experiments to be associated with the following proteins: calmodulin, FKBP12.6, PKA, protein phosphatases 1 (PP1) and 2A (PP2A), sorcin, triadin, junctin and calsequestrin (Bers, 2002). Of these RyR2-associated proteins, many have or have been suggested to have small, regulatory roles in cardiac EC-coupling (Terentyev et al., 2005, Beard et al., 2009).

The  $\text{Ca}^{2+}$  released via CICR accumulates in the cytoplasm and promotes contraction by binding to and activating the contractile myofilaments. CICR contributes to the reduction of the inward  $\text{Ca}^{2+}$  current through the LTCC via  $\text{Ca}^{2+}$ -dependent inactivation of the channel, acting as a feedback mechanism (Puglisi et al., 1999). The magnitude of CICR is dependent on SR  $\text{Ca}^{2+}$  content in addition to LTCC signal (Bassani et al., 1995). The contribution of the SR to  $\text{Ca}^{2+}$  release is thought to be species-dependent and varies from ~90% in the rat to ~65% in humans and interestingly this is believed to fall to ~50% in humans with HF (Bassani et al., 1994, Bers, 2001).

Aside from the LTCC triggering CICR, many other possible mechanisms have been proposed to contribute to CICR, these include: TTCC, NCX1, tetrodotoxin (TTX)-sensitive  $\text{Ca}^{2+}$  current,  $\text{Na}^+$  channels (slip-mode conductance), voltage-dependent  $\text{Ca}^{2+}$

release and inositol trisphosphate (IP<sub>3</sub>) receptor (Bers, 2001, Bers, 2002). However, as they are believed to have a negligible contribution in comparison to the role of the LTCC, which is considered the main trigger of CICR in cardiac EC-coupling, these will not be discussed further.

To permit further contraction, CICR through the RyR2 must be terminated in order to stop contraction and facilitate relaxation (see section 1.3.3 of introduction). In addition, SR Ca<sup>2+</sup> content must be restored through SR Ca<sup>2+</sup> reuptake prior to further contraction. CICR has been suggested to be terminated through RyR2 inactivation which helps to restore SR Ca<sup>2+</sup> by preventing RyR2 mediated SR Ca<sup>2+</sup> release (Sham et al., 1998, Bers, 2002). Another way in which CICR may be terminated is through a local decrease in SR Ca<sup>2+</sup> content (Lukyanenko et al., 1996). Failure to terminate SR Ca<sup>2+</sup> release through RyR2 can lead to diastolic SR Ca<sup>2+</sup> release and increased risk of Ca<sup>2+</sup> dependent after-depolarisations (see section 1.5 of introduction).

### **1.3.3 Decline in Ca<sup>2+</sup> transient (relaxation)**

To promote efficient contraction and pumping of the heart, relaxation of the myocyte must occur, as relaxation during diastole allows ventricular refilling prior to contraction during systole. In order for relaxation to occur bound Ca<sup>2+</sup> must first dissociate from the myofilament troponin C, which is facilitated by a reduction in intracellular Ca<sup>2+</sup>.

Relaxation is initiated by the inactivation of the LTCC, which promotes the repolarisation of the AP, as LTCC is a principal current in the plateau phase. This inactivation will also reduce the amount of Ca<sup>2+</sup> entering the myocyte and prevents further SR Ca<sup>2+</sup> release, allowing the SR Ca<sup>2+</sup> stores to be replenished. In addition, RyR2 inactivate which further contributes to the prevention of SR Ca<sup>2+</sup> release and store replenishment (Sham et al., 1998, Bers, 2002) (see earlier).

Cytosolic  $\text{Ca}^{2+}$  is either returned to the SR by the sarcoplasmic/ endoplasmic reticulum  $\text{Ca}^{2+}$  ATPase pump (SERCA 2a) or is removed from the myocyte by the NCX1; however, the relative contributions of SERCA 2a and NCX1 to removal of  $\text{Ca}^{2+}$  during relaxation differ between species (Bassani et al., 1994, Bers, 2002). In the rat, the majority of cytosolic  $\text{Ca}^{2+}$  is returned to the SR via the SERCA 2a pump (~90%) whereas, NCX1 has only a small contribution to  $\text{Ca}^{2+}$  extrusion (~7%) (Bassani et al., 1994, Bers, 2001). However, in humans, where SERCA 2a density is lower, the NCX1 contributes more to  $\text{Ca}^{2+}$  extrusion (~28%) (Bers, 2001).

The activity of SERCA 2a is regulated by an associated SR protein, Phospholamban (PLB), which inhibits SERCA 2a under basal conditions (Inui et al., 1986). During  $\beta$ -adrenergic stimulation, protein kinase A (PKA) phosphorylates PLB which relieves the inhibition on SERCA 2a allowing faster SR  $\text{Ca}^{2+}$  reuptake, which contributes to faster rate of relaxation (positive lusitropism) (Li et al., 2000) and, increases SR  $\text{Ca}^{2+}$  content and therefore subsequent  $\text{Ca}^{2+}$ -release (positive inotropism; see section 1.4 of introduction).

In addition, small amounts of  $\text{Ca}^{2+}$  can also leave the cytosol by means of the sarcolemmal  $\text{Ca}^{2+}$  ATPase (PMCA) and the mitochondrial  $\text{Ca}^{2+}$  uniporter, however, these two processes are believed to be slow and are therefore unlikely to significantly contribute to the decline of cytosolic  $\text{Ca}^{2+}$  during normal EC-coupling (Bassani et al., 1994, Bers, 2002).

However, to maintain steady state,  $\text{Ca}^{2+}$  influx must equal  $\text{Ca}^{2+}$  efflux and the concentration of  $\text{Ca}^{2+}$  released from the SR must equal SR  $\text{Ca}^{2+}$  uptake. It is important that an equal amount of  $\text{Ca}^{2+}$  released from the SR during EC-coupling is also removed from the cytosol (mainly by action of SERCA 2a) in order to maintain SR  $\text{Ca}^{2+}$  levels, maintain balanced  $\text{Ca}^{2+}$  levels within the myocyte and to prevent cytosolic, SR and mitochondrial  $\text{Ca}^{2+}$  overload. However, under some circumstances for example during  $\beta$ -adrenergic stimulation, the relative contributions of LTCC, RyR2 and SERCA 2a are altered resulting in changes to SR  $\text{Ca}^{2+}$  content which will affect resultant contraction strength and the amount of  $\text{Ca}^{2+}$  entering the SR or leaving the myocyte.

### ***Summary of EC-coupling***

In summary, the depolarization of the ventricular myocytes by the cardiac AP opens the voltage-dependent LTCC. Activation of LTCC will increase  $\text{Ca}^{2+}$  entry and this  $\text{Ca}^{2+}$  accumulates in the cytosol. A small amount of  $\text{Ca}^{2+}$  entry may also occur through NCX1 and TTCC. This local increase in  $\text{Ca}^{2+}$  concentration in the vicinity of RyR2 will be detected and result in CICR, which further increases the cytosolic  $\text{Ca}^{2+}$  levels. An increase in intracellular  $\text{Ca}^{2+}$  leads to  $\text{Ca}^{2+}$  binding to and activating contractile myofilaments resulting in the initiation of cellular contraction. For relaxation to occur, intracellular  $\text{Ca}^{2+}$  levels decline,  $\text{Ca}^{2+}$  dissociates from myofilaments and  $\text{Ca}^{2+}$  is removed from cytosol through SR  $\text{Ca}^{2+}$  reuptake (SERCA 2a) or  $\text{Ca}^{2+}$  is extruded from the myocyte (NCX1). The complex interaction of the various elements involved in EC-coupling and their modulation by sympathetic stimulation will be covered in more detail in the next section (section 1.4 of introduction).

## ***1.4 The effect of $\beta$ -adrenergic stimulation on excitation-contraction coupling***

### **1.4.1 $\beta$ -adrenergic receptor introduction**

The autonomic nervous system (ANS) consists of two separate branches, the sympathetic and parasympathetic branches, which have opposing effects on the mammalian myocardium. The sympathetic branch is best known for its contribution to the “fight or flight” response, where it acts to enhance CO through the release of catecholamines. Sympathetic stimulation increases HR (positive chronotropy), increases strength of contraction (positive inotropy), increases the rate of relaxation (positive lusitropy) and increases AV node conduction velocity (positive dromotropy) (Bers, 2002, Levick, 2003).

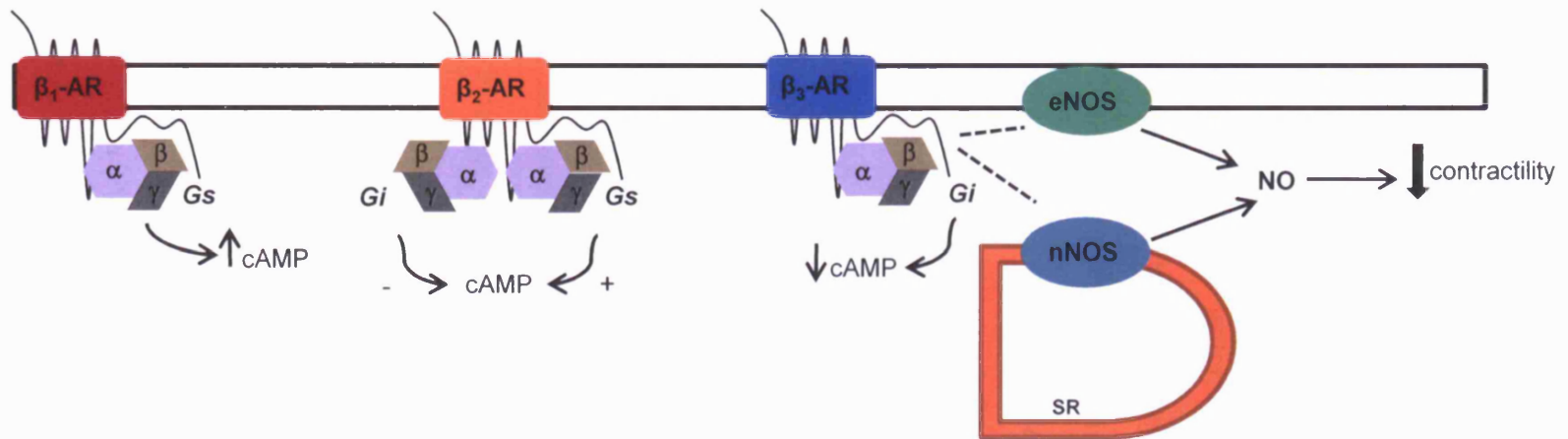


**Figure 1.6- The  $\beta$ -adrenergic receptors in the ventricular myocardium (adapted from Bers, 2001)**

This figure shows the coupling of the three isoforms of  $\beta$ -adrenergic receptor thought to be located in the mammalian ventricular myocardium. The  $\beta_1$ -adrenergic receptor is coupled to the stimulatory GTP binding protein,  $G_s$  which activates adenylate cyclase (AC) resulting in the production of cAMP and the activation of PKA, producing a global positive inotropic effect. The  $\beta_2$ -adrenergic receptor is coupled to the inhibitory ( $G_i$ ) GTP binding protein in addition to  $G_s$ . Activation of  $G_i$  reduces cAMP production and therefore PKA activation through inhibition of AC. The  $\beta_3$ -adrenergic receptor is coupled to the inhibitory ( $G_i$ ) GTP binding protein which reduces cAMP production through the inhibition of AC. In addition, the  $\beta_3$ -adrenergic receptor is coupled to both endothelial NOS (eNOS/NOS3) and neuronal NOS (nNOS/NOS1) which both produce nitric oxide (NO) which produces a negative inotropic effect.

Diurnal variation in sympathetic activity has been indicated through the morning increase in the circulating and neurally released catecholamines, epinephrine and norepinephrine (Linsell et al., 1985, Dodt et al., 1997) and also through diurnal changes in HRV (Hayano et al., 1990, Yamasaki et al., 1996), which may have an effect on cardiac EC-coupling. During sympathetic stimulation, epinephrine and norepinephrine, bind to sarcolemmal  $\beta$ -adrenergic receptors. In the mammalian myocardium these predominantly consist of the  $\beta_1$  isoform (~80%), however,  $\beta_2$  and  $\beta_3$ -adrenergic receptors are also expressed in the ventricular myocardium (Bristow et al., 1986, Bers, 2002, Wallukat, 2002). Sympathetic stimulation of cardiac  $\beta_1$ ,  $\beta_2$  and  $\beta_3$ -adrenergic receptors can be mimicked by the exogenous administration of the non-selective  $\beta$ -adrenergic receptor agonist, isoproterenol (ISO). All three isoforms of the cardiac  $\beta$ -adrenergic receptor and their downstream intracellular signalling cascades are shown in figure 1.6.

In addition,  $\alpha$ -adrenergic receptors are expressed in the ventricular myocardium, however, they are most abundant in the vasculature where they mediate vasoconstriction, through the activation of the  $G_q$  GTP binding protein and subsequent downstream activation of protein kinase C (PKC) (Rockman et al., 2002).  $\alpha$ -adrenergic receptors can be activated by norepinephrine and epinephrine mediating an albeit smaller positive inotropic effect than  $\beta$ -adrenergic receptor activation (Endoh et al., 1976). In addition, activation of cardiac  $\alpha$ -adrenergic receptors have been reported to be involved in both preconditioning (Tosaki et al., 1995) and the development of hypertrophy (Rockman et al., 2002). However,  $\alpha$ -adrenergic receptors will no longer be discussed in the context of the present investigation.

The  $\beta_1$ -adrenergic receptor is believed to be more sensitive to endogenous forms of sympathetic stimulation, for example norepinephrine and epinephrine, and exogenous forms of sympathetic stimulation, for example ISO, than the other  $\beta$ -adrenergic receptor isoforms (Hawthorn and Broadley, 1982, Brodde, 1993, Rodefeld et al., 1996). In terms of enhancing ventricular contraction and EC-coupling in the ventricular myocyte, both the positive inotropic and lusitropic effects mediated via  $\beta_1$ -adrenergic receptors are

important, as the inotropic response will increase SV thereby enhancing CO and contraction strength and the lusitropic response enhances ventricular filling during diastole resulting in efficient ventricular filling compensating for the reduction in filling time.

#### **1.4.2 Additional effects of $\beta$ -adrenergic stimulation**

In addition to the inotropic and lusitropic effects mediated by  $\beta$ -adrenergic stimulation, there is a strong chronotropic effect, which acts to increase HR. The positive chronotropic effect of sympathetic stimulation is due to the action on the sino-atrial node (SA node) mediated via alterations in pacemaker currents.  $\beta$ -adrenergic stimulation results in the activation of adenylate cyclase (AC) and production of cyclic AMP (cAMP). In addition to activating protein kinase A (PKA), cAMP will directly bind to and activate hyperpolarisation-activated cyclic nucleotide-gated channels (HCN) that underlie the funny current ( $I_f$ ) of the pacemaker (DiFrancesco, 1995, Biel et al., 2002). HCN channels are also gated by changes in membrane voltage (Biel et al., 2002). Moreover, cAMP is believed to increase the open probability of HCN channels by moving the  $I_f$  current activation curve to positive membrane voltages and also cAMP will affect the channel kinetics by enhancing channel activation and decreasing channel deactivation (DiFrancesco, 1995, Biel et al., 2002).

PKA can modulate a number of ionic currents associated with the ventricular AP. PKA phosphorylates LTCC, which contributes to the later phase of the pacemaker potential of the SA node cells, promoting faster depolarisation. In addition, PKA speeds up repolarisation and shortens the ventricular AP through phosphorylation of the delayed rectifier  $K^+$  channel,  $I_{Ks}$ , which helps to maintain diastolic interval at high HR (Tamargo et al., 2004, Terrenoire et al., 2005). PKA phosphorylation of the delayed rectifier  $K^+$  channel,  $I_{Kr}$ , decreases current amplitude and the voltage-dependent activation curve is shifted to more positive potentials (Tamargo et al., 2004). The cardiac  $Na^+$  channel possesses several sites for PKA dependent phosphorylation and Matsuda *et al* (1992)

have reported that  $I_{Na}$  is increased in response to the  $\beta$ -adrenergic receptor agonist, ISO in isolated rabbit cardiac myocytes, which enhances depolarisation, the upstroke of the AP and AP conduction velocity.  $\beta$ -adrenergic stimulation has also been shown to decrease  $I_{K1}$  through PKA dependent phosphorylation of Kir 2.1 channels, which depolarises the RMP of the AP (Tamargo et al., 2004). PKA also produces a positive dromotropic effect by increasing AV node conduction velocity (Levick, 2003). The positive chronotropic and dromotropic effects of  $\beta$ -adrenergic stimulation will not be discussed further.

PKA is believed to phosphorylate the inositol 1,4,5-trisphosphate receptor ( $IP_3R$ ), which is thought to increase the sensitivity of the receptor to its ligand,  $IP_3$  (Betzenhauser et al., 2009). As in section 1.3.2, activation of the  $IP_3R$  receptor has been implicated as a possible mechanism for triggering SR  $Ca^{2+}$  release and therefore,  $IP_3R$  activation may also enhance  $\beta$ -adrenergic stimulation by increasing trigger  $Ca^{2+}$ , as  $IP_3R$  activation itself is associated with  $Ca^{2+}$  release (Bers, 2001, Bers, 2002). However, the  $IP_3R$  receptor will only be discussed further in terms of its contribution to abnormal  $Ca^{2+}$  homeostasis occurring in the pathology of left-ventricular (LV) hypertrophy and heart failure (HF).

### **1.4.3 $\beta_1$ -adrenergic stimulation**

Activation of the  $\beta_1$ -adrenergic receptor produces positive inotropic, lusitropic and chronotropic effects in the heart.  $\beta_1$ -adrenergic receptors are G-protein coupled receptors (GPCRs) coupled to the stimulatory GTP binding protein,  $G_s$ . The  $G_s$  protein is composed of an  $\alpha$  subunit and a  $\beta\gamma$  subunit and upon activation  $G_s$  dissociates from  $\beta\gamma$  to activate membrane-bound adenylylate cyclase (AC, either type V or VI) (Ishikawa et al., 1994, Post et al., 1999). The activation of AC catalyses the conversion of ATP into cAMP, which is responsible for the activation of cAMP-dependent protein kinase or protein kinase A (PKA), as shown in figure 1.7.

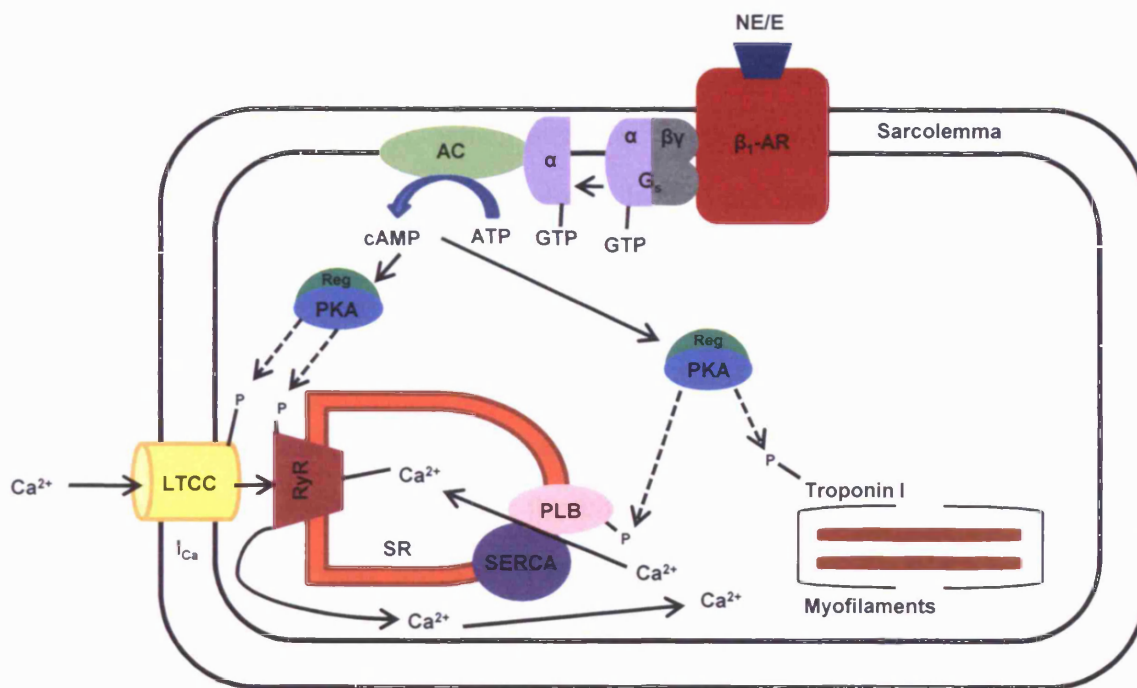


**Figure 1.7- The effect of  $\beta$ -adrenergic receptor stimulation on cardiac excitation-contraction coupling (adapted from Bers, 2002).**

Norepinephrine (NE) and epinephrine (E) will bind to and activate sarcolemmal  $\beta$ -adrenergic receptors.  $\beta$ -adrenergic receptors are GPCRs and activation of  $\beta_1$ -adrenergic receptors ( $\beta_1$ -AR) will result in the activation of the  $G_s\alpha$  GTP binding protein of the GPCR.  $G_s\alpha$  dissociates from its associated  $\beta\gamma$  subunit and activates adenylate cyclase (AC). Activation of AC will promote the conversion of ATP into the cyclic nucleotide, cAMP. cAMP binds to the regulatory subunit of PKA, resulting in its activation. PKA phosphorylates 4 key EC-coupling proteins; LTCC, RyR2, PLB and troponin I to mediate a positive inotropic effect.

Key EC-coupling proteins are phosphorylated by PKA to modulate contraction which results in positive inotropic and positive lusitropic effects in the ventricular myocardium. These key EC-coupling proteins are composed of the LTCC, RyR2, PLB and troponin I, all of which are indicated in figure 1.7, and the effects of PKA dependent phosphorylation of these proteins will now be discussed individually.

PKA phosphorylates LTCC which increases the open probability of the channels and lengthens the duration the channels remain in the open state (Tsien et al., 1986, Walsh et al., 1989, Bers, 2002). This promotes increased  $\text{Ca}^{2+}$  entry through the LTCC resulting in a larger  $\text{Ca}^{2+}$  influx (increased  $I_{\text{Ca}}$ ) and a larger  $\text{Ca}^{2+}$  signal for CICR, which increases the amplitude of the  $\text{Ca}^{2+}$  transient (Tsien et al., 1986, Bers, 2001). PKA also phosphorylates the  $\text{Ca}^{2+}$  release channel, RyR2 and its scaffolding proteins, which increases the open probability of the channel, lengthens the duration the channels remain in the open state and also enhances the sensitivity of the RyR2 to  $[\text{Ca}^{2+}]_i$  from LTCC and NCX1 (Marx et al., 2000, Bers, 2001). PKA mediated phosphorylation of RyR2 is thought to displace the RyR2-associated protein, FKBP12.6, which increases the open probability of RyR2 and can result in increased diastolic SR  $\text{Ca}^{2+}$  release (Wehrens et al., 2003, Gellen et al., 2008). PKA phosphorylates the SR protein, PLB. PLB is physically associated with and inhibits the activity of its fellow SR protein, SERCA 2a (Inui et al., 1986). Phosphorylation of PLB reduces its inhibition of SERCA, resulting in increased SERCA activity (Li et al., 2000, Bers, 2002). This has two beneficial actions, the first is to increase the rate of SR  $\text{Ca}^{2+}$  reuptake which enhances the rate of relaxation (positive lusitropic effect) and secondly, increases the SR  $\text{Ca}^{2+}$  content which increases the amplitude of subsequent  $\text{Ca}^{2+}$  transients (Endoh and Blinks, 1988, Li et al., 2000, Bers, 2002). PKA also phosphorylates troponin I, reducing the  $\text{Ca}^{2+}$  affinity of troponin C leading to faster dissociation of  $\text{Ca}^{2+}$  from contractile proteins which leads to increased relaxation rate (positive lusitropic effect) (Li et al., 2000, Kentish et al., 2001). The reduced affinity of the myofilaments to  $\text{Ca}^{2+}$  would on its own reduce contraction; however, this negative inotropic influence is less than the sum of the positive inotropic effects on the LTCC, PLB and RyR2 (Li et al.,

2000, Kentish et al., 2001). In summary, phosphorylation of PLB and troponin I by PKA both contribute to the positive lusitropic effects of sympathetic stimulation, namely through decreased SERCA 2a inhibition which increases SR  $\text{Ca}^{2+}$  reuptake and increased dissociation of  $\text{Ca}^{2+}$  from the contractile proteins, respectively (Li et al., 2000, Bers, 2001, Bers, 2002). This indirectly contributes to increased cardiac contraction and efficiency by permitting sufficient diastolic interval and rapid relaxation during high HRs which allows adequate ventricular filling. The positive lusitropic effects afforded by phosphorylation of PLB are believed to be the most important in terms of myocardial relaxation and decline of the  $\text{Ca}^{2+}$  transient (Li et al., 2000, Bers, 2001, Bers, 2002). In addition, phosphorylation of LTCC, which increases  $\text{Ca}^{2+}$  current and phosphorylation of PLB, which increases SR  $\text{Ca}^{2+}$  content, both contribute to the positive inotropic effect seen with sympathetic stimulation (Bers, 2001, Bers, 2002).

#### **1.4.4 $\beta_2$ -adrenergic stimulation**

As with the activation of  $\beta_1$ -adrenergic receptors, the activation of  $\beta_2$ -adrenergic receptors, which are also expressed in the ventricular myocardium, is associated with a positive inotropic effect (Bers, 2002, Wallukat, 2002). However, unlike  $\beta_1$ -adrenergic receptor activation which has a global effect throughout the cell, the effects of  $\beta_2$ -adrenergic receptor activation are localised within the cell, as the  $\beta_2$ -adrenergic receptor and components of its downstream signalling pathway are found predominately in the caveolae (Balijepalli et al., 2006, Calaghan et al., 2008). The  $\beta_2$ -adrenergic receptor has been shown to be present in the caveolae where it has been shown to co-immunoprecipitate with AC, PKA, LTCC and protein phosphatase 2A (PP2A) (Balijepalli et al., 2006). Activation of the  $\beta_2$ -adrenergic receptor produces a positive inotropic effect that is characteristically weaker than that produced through the activation of the  $\beta_1$ -adrenergic receptor, due to the increased  $\beta_1$ -adrenergic receptor

density v  $\beta_2$ -adrenergic receptor density in the ventricular myocardium and as the LTCC is the only effector protein targeted by  $\beta_2$ -adrenergic receptor signalling (see later).

$\beta_2$ -adrenergic receptors, like  $\beta_1$ -adrenergic receptors, are GPCRs, however, they are thought to be coupled to both the stimulatory GTP binding protein,  $G_s$ , and also the inhibitory GTP binding protein,  $G_i$ , shown in figure 1.8 (Xiao, 2001). Upon activation,  $G_s$  disassociates from  $\beta\gamma$  to activate AC which catalyses the production of cAMP activating PKA. The increase in cAMP and resultant PKA signalling observed during  $\beta_2$ -adrenergic receptor activation has been reported to be localised due to the compartmentalisation and restriction of the signalling pathway to the caveolae, where  $\beta_2$ -adrenergic receptors predominately exist (Balijepalli et al., 2006, Calaghan and White, 2006).  $\beta_2$ -adrenergic receptor signalling results in PKA phosphorylation of LTCC also localised to the caveolae (Chen-Izu et al., 2000, Balijepalli et al., 2006). Due to this localisation to the caveolae, PKA dependent inotropy associated with  $\beta_2$ -adrenergic receptor activation is not thought to include the phosphorylation of the SR proteins, PLB and RyR2, and also the myofilament protein, Troponin I as these components are not localised to the caveolae (Xiao et al., 1994, Calaghan et al., 2008). In addition, the restriction of  $\beta_2$ -adrenergic receptor mediated PKA signalling to the sarcolemmal LTCC is partly due to A-kinase anchoring protein (AKAP) which is a scaffold protein that binds PKA specifically to the  $\beta_2$ -adrenergic receptor and tethers PKA to the sarcolemmal membrane (Fink et al., 2001, Malbon et al., 2004).

The association of the  $G_i$  GTP binding protein with the  $\beta_2$ -adrenergic receptor is believed to contribute to the localised  $\beta$ -adrenergic signalling in the caveolae, by inhibiting  $G_s$  and AC (Taussig et al., 1993) and thereby decreasing the concentration of the local pool of cAMP, when it reaches critical levels, subsequently reducing PKA activation, see figure 1.8 (Jurevicius and Fischmeister, 1996). This local and reduced positive inotropic effect afforded by  $\beta_2$ -adrenergic receptor activation contributes to the differential responses of  $\beta_1$ -adrenergic receptor v  $\beta_2$ -adrenergic receptor.

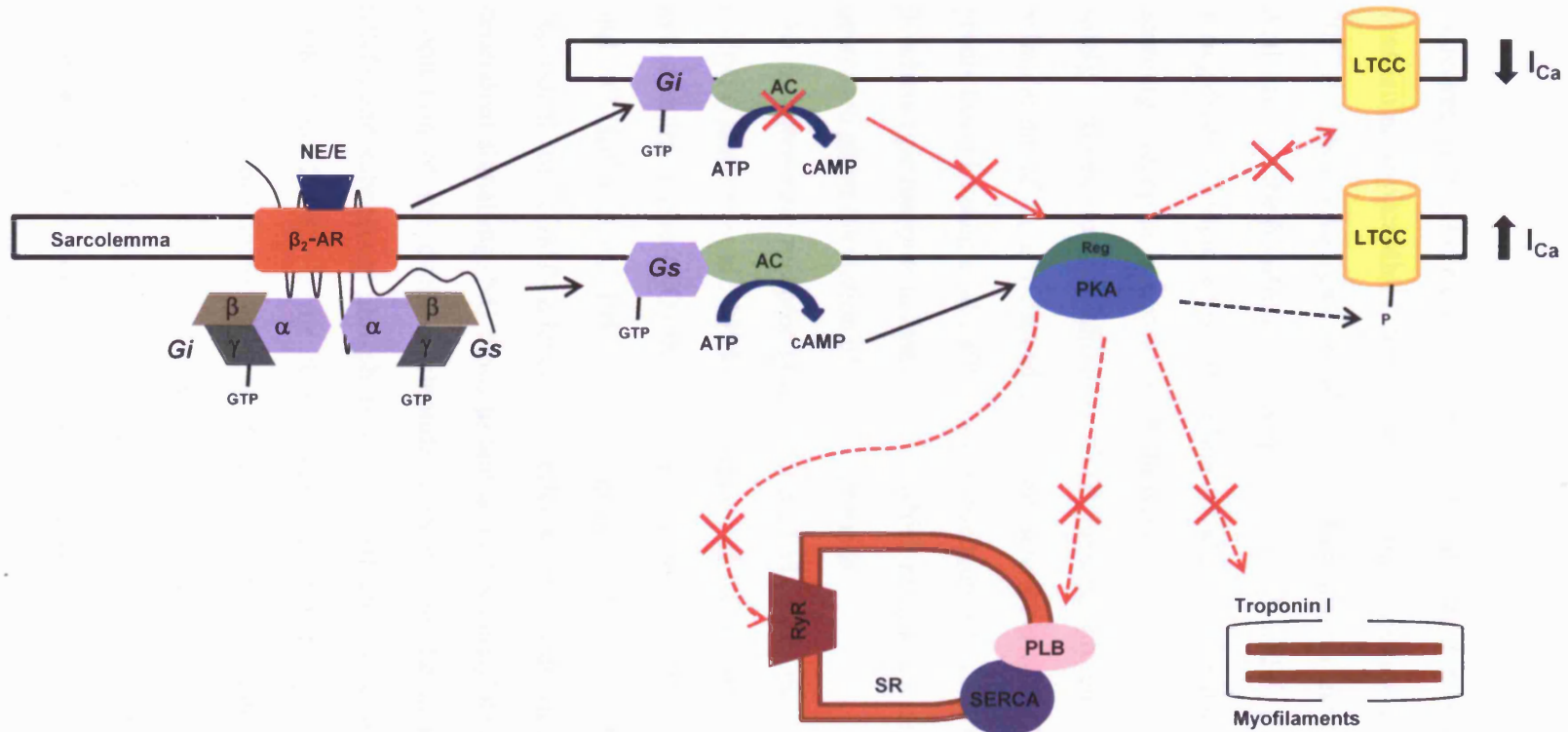


**Figure 1.8- Localised  $\beta_2$ -adrenergic receptor signalling in the mammalian ventricular myocardium.**

The cardiac  $\beta_2$ -adrenergic receptor is predominately located in sarcolemmal membrane and in caveolae. The cardiac  $\beta_2$ -adrenergic receptor is coupled to both the stimulatory ( $G_s$ ) and the inhibitory ( $G_i$ ) GTP binding protein. Activation of  $G_s$  activates adenylyl cyclase (AC) which increases production of cyclic AMP (cAMP) and activation of protein kinase A (PKA). PKA phosphorylates the L-type  $\text{Ca}^{2+}$  channel (LTCC) and increases ventricular contraction. Activation of  $G_i$  results in the inhibition of AC, which decreases cAMP production, PKA activation and subsequent phosphorylation of LTCC. Due to the location of the  $\beta_2$ -adrenergic receptor in the caveolae,  $\beta_2$ -adrenergic receptor signalling only targets the LTCC as it is not in close proximity to the other end effectors of EC-coupling such as RyR2, PLB and troponin I.

### 1.4.5 $\beta_3$ -adrenergic stimulation

In recent years the existence of the  $\beta_3$ -adrenergic receptor has been established in ventricular myocardium from various animal species including rat (Barbier et al., 2007a), rabbit (Audigane et al., 2009) and also in humans (Gauthier et al., 1996). Activation of the  $\beta_3$ -adrenergic receptor, unlike  $\beta_1$  and  $\beta_2$ -adrenergic receptors, results in a negative inotropic effect (Gauthier et al., 2000, Kitamura et al., 2000). The  $\beta_3$ -adrenergic receptor is also a GPCR; however, unlike  $\beta_1$  and  $\beta_2$ -adrenergic receptors, it is solely coupled to the inhibitory GTP binding protein,  $G_i$  (Gauthier et al., 1996). Stimulation of  $G_i$  is believed to inhibit activation of AC, thereby decreasing cAMP production (Taussig et al., 1993) and subsequent PKA activation in a similar manner as  $\beta_2$ -adrenergic receptor activation of  $G_i$  which results in a negative inotropic effect due to decreased phosphorylation of effector proteins.

The  $\beta_3$ -adrenergic receptor is also coupled via  $G_i$  to the enzyme nitric oxide synthase (NOS) (Gauthier et al., 1998). Activation of NOS results in the production of the free radical nitric oxide (NO) through the conversion of L-arginine and  $O_2$  to L-citrulline and NO (Kelly et al., 1996). NOS signalling has been shown to have either cGMP-dependent or cGMP-independent effects on cardiovascular function. In cGMP-dependent signalling, NO binds to and activates guanylate cyclase (GC), leading to the production of the cyclic nucleotide, cGMP, and the activation of protein kinase G (PKG) and subsequent phosphorylation of effector proteins, see figure 1.9 (Ziolo et al., 2008, Ziolo, 2008). In the cGMP-independent pathway, NO itself directly leads to S-nitrosylation of effector proteins (Ziolo et al., 2008). In addition, to the direct effects of  $G_i$  on AC activation and cAMP production in  $\beta_3$ -adrenergic receptor signalling, increased cGMP and NO concentrations associated with the activation of  $\beta_3$ -adrenergic receptor and NOS signalling are also believed to have an inhibitory effect on AC and cAMP thereby reducing PKA-dependent inotropy (Abi-Gerges et al., 2001).

In ventricular myocytes there are 3 isoforms of NOS and these are: neuronal nitric oxide synthase (nNOS/ NOS1), inducible nitric oxide synthase (iNOS/ NOS2) and endothelial

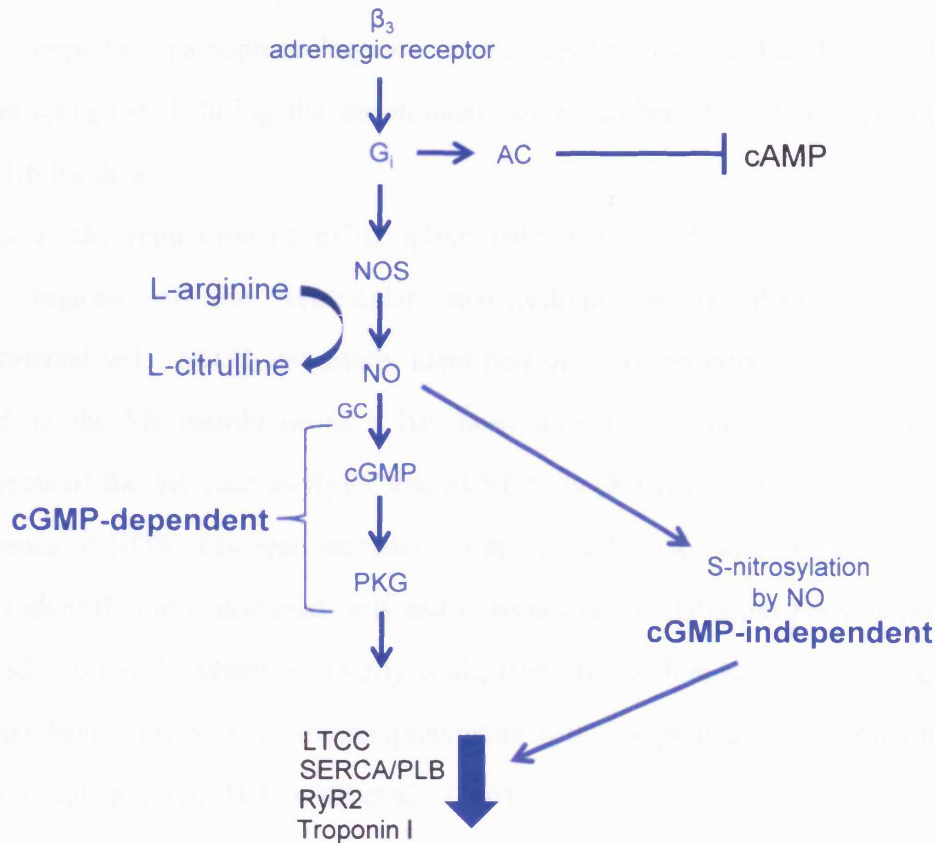


**Figure 1.9- Downstream signalling pathway activated upon  $\beta_3$ -adrenergic receptor activation.**

Activation of the cardiac  $\beta_3$ -adrenergic receptor results in a negative inotropic effect. The cardiac  $\beta_3$ -adrenergic receptor is coupled to the inhibitory ( $G_i$ ) GTP binding protein and activation of  $G_i$  results the inhibition of adenylate cyclase (AC), reduction in cAMP production and activation of PKA. In addition, the cardiac  $\beta_3$ -adrenergic receptor is coupled to nitric oxide synthase (NOS). NOS converts L-arginine to L-citrulline and nitric oxide (NO). NO mediates both cGMP-dependent and cGMP-independent signalling. cGMP-dependent signalling involves the activation of guanylate cyclase (GC), production of cyclic GMP (cGMP), activation of protein kinase G (PKG) which phosphorylates key EC-coupling genes. cGMP-independent signalling involves direct NO mediated S-nitrosylation of key EC-coupling genes.

nitric oxide synthase (eNOS/ NOS3) (Kelly et al., 1996, Ziolo et al., 2008). Recent research suggests that both NOS1 and NOS3 are important physiologically in the regulation of cardiac EC-coupling and ventricular function (Casadei, 2006). However, NOS2 is important pathophysiologically in the regulation of cardiac EC-coupling as NOS2 is upregulated during the development of a number of cardiomyopathies (see section 1.6 for detail).

In terms of the regulation of EC-coupling both NOS1 and NOS3 are localised to specific regions of the ventricular myocardium, where their signalling is compartmentalised. NOS1, originally identified in nerve terminals, is predominately localised to the SR membrane as it has been shown to co-immunoprecipitate with components of the SR such as RyR2 and SERCA 2a (Xu et al., 1999). More recently, the presence of NOS1 has been identified in mitochondria (Kanai et al., 2001). NOS3 was first identified in endothelial cells and in recent years NOS3 has been identified in atria in addition to the ventricles (Kelly et al., 1996, Barouch et al., 2002). In addition, NOS3 has been shown to co-immunoprecipitate with components of the sarcolemmal membrane and caveolae (Balijepalli et al., 2006).

NOS signalling shows a high degree of compartmentalisation due to the restriction of NOS1 in SR, which is believed to modulate the activities of RyR2, SERCA 2a and PLB (Xu et al., 1999, Barouch et al., 2002) and NOS3 in sarcolemmal membrane/ caveolae, which is thought to target LTCC (Wang et al., 2008b). There is evidence to suggest that compartmentalisation of NOS signalling is due to the close association of NOS isoforms with specific phosphodiesterases (PDE). PDE are responsible for the degradation of cyclic nucleotides such as cAMP and cGMP and this limits the response of signalling pathways downstream of these cyclic nucleotides. Wang *et al* (2009) have suggested that type 5 PDE, which is responsible for the breakdown of cGMP in cardiac myocytes, is responsible for the restriction of NOS3 signalling and the subsequent targeting of NOS3 signalling to the LTCC (Wang et al., 2009). To date it is unknown whether a similar mechanism exists in terms of specific PDE in the restriction of NOS1 signalling

to the SR, however, this remains a possibility that PDE may play a role in NOS1 signalling in the ventricular myocardium.

NOS1 and NOS3 are both  $\text{Ca}^{2+}$  dependent and expressed throughout the ventricle, whereas NOS2 is  $\text{Ca}^{2+}$  independent and is only expressed in response to inflammatory cytokines and during immune reactions and is of particular importance during LV hypertrophy and HF (Kelly et al., 1996, Ziolo et al., 2008). Therefore, NOS2 will only be discussed further in terms of its contribution to the pathology of these cardiomyopathies (see section 1.6 of introduction).

The overall negative inotropic response of  $\beta_3$ -adrenergic receptor stimulation is thought to result from a complex interaction of NO in cGMP-dependent and independent pathways targeting both the sarcolemmal and sarcoplasmic reticulum (SR)  $\text{Ca}^{2+}$ -fluxes. For example, NO-activated PKG contributes to the negative inotropic response to  $\beta$ -adrenergic stimulation, through PKG phosphorylation of troponin I (Layland et al., 2002), which reduces the myofilament  $\text{Ca}^{2+}$  sensitivity, and PKG phosphorylation of the LTCC subunits,  $\alpha 1c$  and  $\beta 2a$ , which reduce  $\text{Ca}^{2+}$  current (Yang et al., 2007). NO donors for example 2-(*N*, *N*-diethylamino)-diazene-2-oxide (DEANO) have been shown to inhibit the LTCC current in a cGMP-dependent manner (Abi-Gerges et al., 2001). NO can also result in the S-nitrosylation of the LTCC, also reducing current flow by inhibiting LTCC activity (Sun et al., 2006). NO is also believed to increase RyR2 open probability, increasing SR  $\text{Ca}^{2+}$  release, through S-nitrosylation of the RyR2 (Xu et al., 1998). PKG mediated phosphorylation (cGMP-dependent) and NO-mediated S-nitrosylation (cGMP-independent) of LTCC, RyR2, SERCA 2a/PLB and troponin are the result of both NOS1 and NOS3 activation and subsequent production of NO. All of the cGMP-dependent and cGMP-independent effects of NOS activation are illustrated in figure 1.10. Both NOS1 and NOS3 are located in the ventricular myocardium of many species in the SR and the sarcolemmal membrane, respectively, and are thought to contribute to the regulation of cardiac EC-coupling and ventricular contraction. Historically, research has concentrated on NOS3, suggesting a dominant role of this isoform in the regulation of EC-coupling. However, in recent years, the involvement of

NOS1 in EC-coupling and contraction has been established. Therefore, due to the complex nature of downstream signalling and effector functions associated with the activation of NOS1 and NOS3, the effects of each isoform will be discussed individually.

### ***Endothelial nitric oxide synthase***

As stated previously, NOS3 was originally identified in endothelial cells and later in the atria, ventricles, sarcolemmal membrane and caveolae (Kelly et al., 1996, Barouch et al., 2002), and has been reported to co-immunoprecipitate with components of the sarcolemma and caveolae, namely  $\beta_2$ -adrenergic receptors and LTCC (Balijepalli et al., 2006).

Activation of NOS3 in the face of severe sympathetic stimulation is believed to be cardioprotective. Firstly, NOS3 activation is said to be “anti-adrenergic”, by reducing the responsiveness of the LTCC and therefore contraction strength in response to  $\beta$ -adrenergic receptor activation. NOS3 gene knockout (KO) mice show larger  $\text{Ca}^{2+}$  transients as a result of increased LTCC current and increased contraction strength in response to  $\beta$ -adrenergic stimulation with ISO (Varghese et al., 2000, Barouch et al., 2002, Wang et al., 2008b). Secondly, NOS3 activation is thought to be “anti-arrhythmic” in addition to “anti-adrenergic”, as NOS3 KO mice exhibit a prolonged APD and a greater incidence of arrhythmias and early and delayed after-depolarisations (Kubota et al., 2000). Lastly, NOS3 activation is thought to be protective against aberrant ventricular remodelling associated with pressure-overload, as NOS3 KO mice show increased hypertrophy and fibrosis in response to ISO (Barouch et al., 2002). Further evidence supporting the “anti-adrenergic” and “anti-arrhythmic” roles of NOS3 and the role of NOS3 in preventing adverse LV-remodelling has come from transgenic mice studies. Mice with cardiac-specific over-expression of NOS3 exhibit a decreased response to  $\beta$ -adrenergic stimulation through decreased  $\text{Ca}^{2+}$  current and contraction

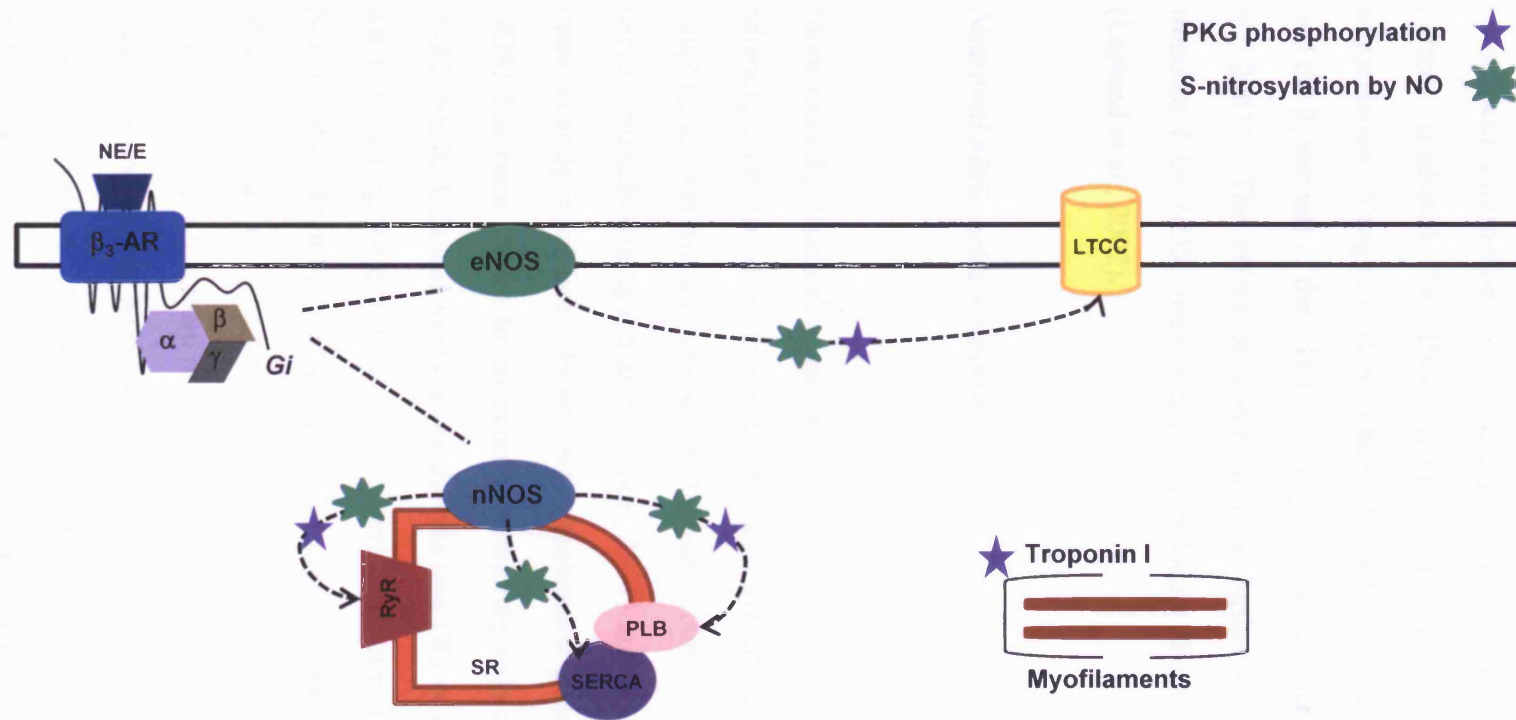


**Figure 1.10- Downstream signalling targets of endothelial nitric oxide synthase and neuronal nitric oxide synthase.** Activation of the cardiac  $\beta_3$ -adrenergic receptor is associated with the subsequent activation of nitric oxide synthase (NOS) isoforms. These isoforms consist of endothelial NOS (eNOS/NOS3) and neuronal NOS (nNOS/NOS1). In addition, inducible NOS (iNOS/NOS2) is located in the ventricular myocardium (not shown on diagram), however, it will not be discussed. The LTCC is the downstream signalling target of eNOS due to its localisation in the sarcolemmal membrane. Activation of eNOS has been reported to result in either direct S-nitrosylation of LTCC by NO or PKG mediated phosphorylation of the LTCC. nNOS is located in the SR and as a result nNOS downstream signalling is thought to target components of the SR; RyR2, SERCA 2a and PLB through either S-nitrosylation or PKG phosphorylation. In addition, troponin I has been shown to be phosphorylated by PKG.

(Brunner et al., 2001) and decreased LV hypertrophy in models of pressure-overload (Massion and Balligand, 2003). NOS3 limits the response of the  $\text{Ca}^{2+}$  transient and subsequent contraction to  $\beta$ -adrenergic stimulation, through the reduction of LTCC current mediated by PKG-dependent phosphorylation and NO-dependent S-nitrosylation. Yang *et al* (2007) have showed that PKG phosphorylates the  $\alpha_1c$  subunit and the  $\beta_2$  subunit of the LTCC, thereby mediating a decrease in LTCC current (Yang et al., 2007). The effect on contraction is further modulated by phosphorylation of troponin I by NOS3-mediated PKG, reducing the  $\text{Ca}^{2+}$  sensitivity of myofilaments (Layland et al., 2002).

### *Neuronal nitric oxide synthase*

More recently neuronal nitric oxide synthase (NOS1) has been implicated in the anti-adrenergic effects of  $\beta_3$ -adrenergic receptor signalling and regulation of cardiac EC-coupling and ventricular contraction (Casadei, 2006). NOS1 was originally identified in nerve terminals (Balligand and Cannon, 1997) and later in SR (Xu et al., 1999), and more recently it has been shown that mitochondria possess NOS1 (Kanai et al., 2001). NOS1 has been shown to co-immunoprecipitate with components of the SR, namely RyR2, SERCA 2a and xanthine oxidoreductase (Xu et al., 1999, Khan et al., 2004). In addition, during the development of several cardiomyopathies including LVH and HF, NOS1 is thought to be localised to the sarcolemmal membrane (Bendall et al., 2004). Much of the data implicating NOS in the regulation of EC-coupling and ventricular contraction originates from experiments performed in genetically modified mice such as those over-expressing NOS or those with genetic deletion/ pharmacological inhibition of NOS. However, a great deal of conflicting evidence pertaining to which NOS isoform modulates the responsiveness of the ventricular myocardium to sympathetic stimulation has arisen from data obtained using these mice. For example, Barouch *et al* (2002) have shown that the responsiveness of ventricular myocytes to  $\beta$ -adrenergic

stimulation with ISO is increased in NOS3 KO mice and decreased in NOS1 KO mice. Conversely, some studies have reported that NOS1 activation enhances responsiveness to  $\beta$ -adrenergic stimulation, as NOS1 KO mice have suppressed contraction,  $\text{Ca}^{2+}$  transient, slowed relaxation, decreased PLB phosphorylation and increased phosphatase activity in response to  $\beta$ -adrenergic stimulation (Wang et al., 2008a, Zhang et al., 2008). In addition, Martin *et al* (2006) have showed the responsiveness of the myocardium to  $\beta$ -adrenergic stimulation was increased in NOS1 KO mice rather than NOS3 KO mice. As NOS1 is predominately localised to the SR any modulating effects on EC-coupling are likely to involve cGMP-dependent and independent modulation of the following SR proteins: RyR2, SERCA 2a and PLB (Xu et al., 1999). Sears *et al* (2003) have shown that activation of NOS1 may be responsible for modulating SR function and resultant  $\text{Ca}^{2+}$  homeostasis as NOS1 KO mice have been shown to have increased  $\text{Ca}^{2+}$  transients and SR  $\text{Ca}^{2+}$  content. The authors also showed that SERCA 2a function was reduced in NOS1 KO mice, possibly indicating modulatory role for NOS1 on SERCA 2a in these mice. Indeed, modulation of SERCA by NOS1-signalling has been shown previously as NOS1-mediated PKG is believed to modulate the activity of SERCA/PLB resulting in reduced SR  $\text{Ca}^{2+}$  loading (Raeymaekers et al., 1988, Takasago et al., 1991). In addition, it has been reported that activation of NOS1 is responsible for the modulation of LTCC, RyR2 and SERCA 2a through NO-mediated S-nitrosylation as S-nitrosylation of these proteins is reduced in NOS1 KO mice (Burger et al., 2009).

NOS1-signalling may influence SR function through modulation of PLB activity. Indeed, it has been shown that NOS1 alters the phosphorylation status of PLB as NOS1 KO mice have reduced PLB phosphorylation (Wang et al., 2008a, Zhang et al., 2008, Garofalo et al., 2009). In addition, Wang *et al* (2008a) have suggested that PLB is a potential target of NOS1 signalling as NOS1 KO mice exhibit reduced contraction strength coupled to a reduction in the decline of the  $\text{Ca}^{2+}$  transient, indicative of reduced SERCA activity, and these differences were not observed in PLB KO mice which suggest a reduction in the function of PLB. This modulation of PLB by NOS1 will also

impact on SERCA 2a function as SERCA 2a activity is regulated by the phosphorylation status of PLB (Inui et al., 1986).

In addition, NOS1-derived NO is believed to contribute to cGMP-independent signalling through the S-nitrosylation of the RyR2, which increases the open probability of RyR2, as NOS1 KO mice showed decreased S-nitrosylation of RyR2 accompanied by decreased open probability of RyR2, suggesting a cGMP-independent signalling method for NOS on RyR2. (Gonzalez et al., 2007, Wang et al., 2010).

Mice over-expressing NOS1 also yield invaluable data on the role of NOS1 in the modulation of EC-coupling. Burkard *et al* (2007) have shown that mice with cardiac-specific NOS1 over-expression have a decreased  $Ca^{2+}$  transient, SR  $Ca^{2+}$  content, contraction strength, slowed kinetics of the  $Ca^{2+}$  transient and reduced LTCC current density. The authors suggest that the negative inotropic effect observed in mice over-expressing NOS1 is the result of NOS1 targeting LTCC resulting in a reduced LTCC current density and subsequently, a reduced  $Ca^{2+}$  transient (Burkard et al., 2007).

NOS1 has been shown to play a protective role in cellular survival and remodelling following MI, as Dawson *et al* (2005) have showed that NOS1 KO mice exhibit an increased mortality and development of LV hypertrophy after MI. In addition, NOS1 is thought to translocate from the SR to the sarcolemma during the development of pathological cardiomyopathies, which is likely to reduce this protective effect of NOS1 (Bendall et al., 2004) (see section 1.6 of introduction).

### ***1.5 Consequences of prolonged $\beta$ -stimulation***

There is a strong association between ventricular arrhythmias and SCD, which are shown to peak in the morning in man (Muller et al., 1987, Arntz et al., 1993, Goldstein et al., 1996). Prolonged or excessive  $\beta$ -adrenergic stimulation can result in the generation of after-depolarisations and the subsequent genesis of  $Ca^{2+}$  dependent

ventricular arrhythmias (Meredith et al., 1991, Anderson, 2003). These after-depolarisations consist of two types; early (EADs) and delayed after-depolarisations (DADs). Both EAD and DADs will be discussed individually below. As such it is interesting to speculate whether the morning onset of SCD may be associated with the morning peak ventricular arrhythmias driven by the increase in circulating catecholamine levels and the activity of the sympathetic nervous system (Piepoli and Capucci, 2007).

### **1.5.1 Early after-depolarisations (EADs)**

Early after-depolarisations (EADs), as illustrated in figure 1.11 A, arise on the “shoulder” of the cardiac AP located between the late plateau and repolarisation phases and are commonly associated with long APs, QT interval prolongation and slow HRs (Priori and Corr, 1990, Fozzard, 1992, Bers, 2001). EADs have been classified as either phase 2 EADs or phase 3 EADs (Charpentier et al., 1993).

Phase 2 EADs occur during the late plateau phase of the cardiac AP and are believed to arise due to reactivation of LTCC, due to the recovery of the channel from  $\text{Ca}^{2+}$ -dependent inactivation (January and Riddle, 1989, January et al., 1991, Charpentier et al., 1993). The recovery from inactivation and subsequent reactivation of the LTCC produces an inward depolarising “window current” through an increase in  $\text{Ca}^{2+}$  entry through LTCC which, if it occurs during the vulnerable period of the AP, can give rise to an extra-systole and the induction of ventricular arrhythmias (January et al., 1991, Charpentier et al., 1993, De Ferrari et al., 1995). Phase 3 EADs occur during the late repolarisation phase of the cardiac AP and, unlike phase 2 EADS, are not believed to be the result of the reactivation of LTCC, as the membrane potential is too negative (i.e. negative to  $-40\text{mV}$ ) to allow the activation of recovered LTCC and therefore, other ionic currents are believed to mediate phase 3 EADs (Charpentier et al., 1993). Background  $\text{Na}^+$  currents which occur during the AP plateau in addition to the AP

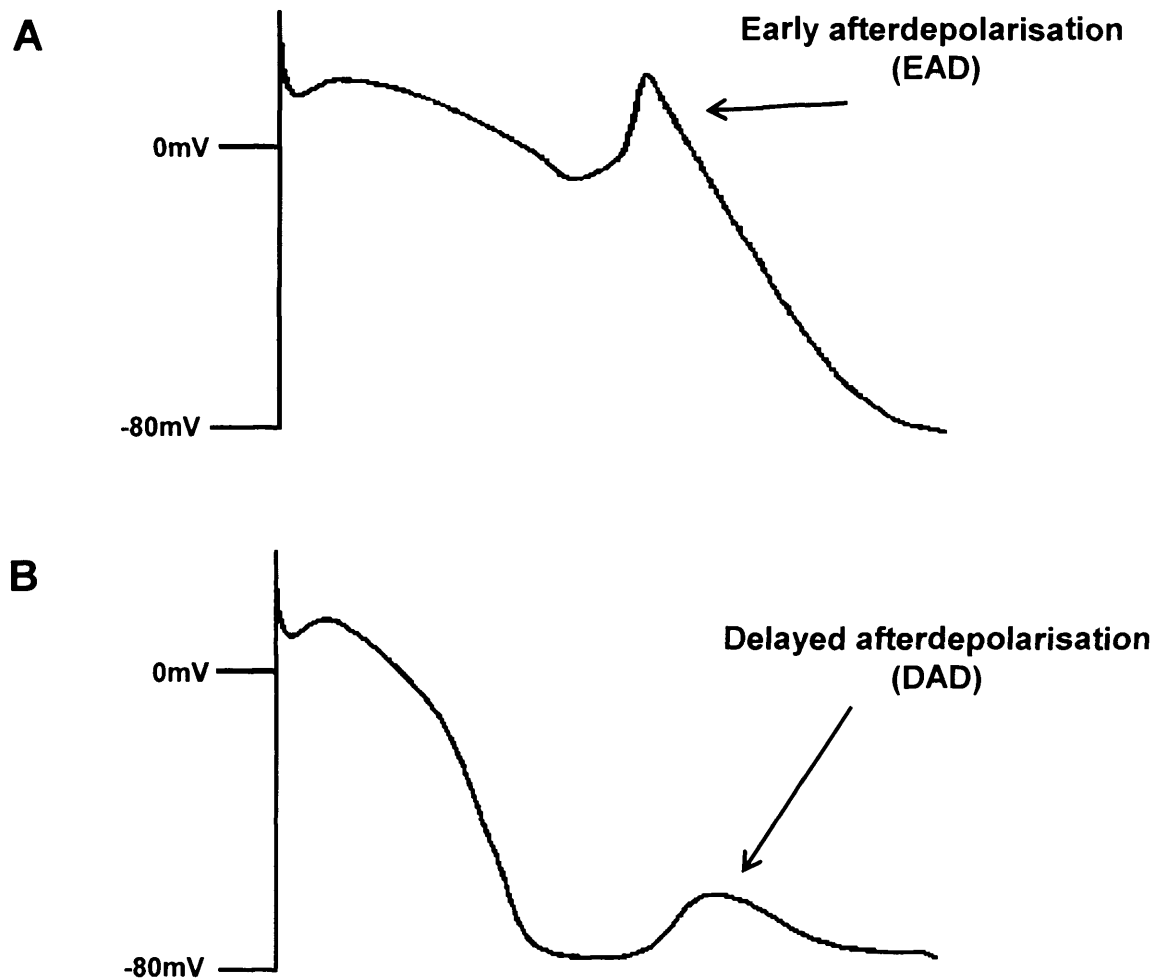


**Figure 1.11- Early and delayed After-depolarisations (adapted from Bers, 2001).**

- A. The figure shows a typical early after-depolarisation (EAD). EADs arise on the “shoulder” of the cardiac AP and are commonly associated with long APs, QT interval prolongation and slow HRs. EADs occur during the plateau phase of the cardiac AP and are believed to arise due to reactivation of LTCC, due to the recovery of the channel from  $\text{Ca}^{2+}$ -dependent inactivation.
- B. The figure shows a typical delayed after-depolarisation (DAD). DADs arise following full repolarisation of the cardiac AP and are associated with high  $[\text{Ca}^{2+}]_i$  and fast HRs. DADs occur as a result of SR  $\text{Ca}^{2+}$  overload and spontaneous SR  $\text{Ca}^{2+}$  release, which triggers the transient inward current through either  $I_{\text{NCX}}$ ,  $I_{\text{nsc}}$  or  $I_{\text{Ca(Cl)}}$ . In addition, if the magnitude of a DAD is large this can trigger an extrasystole.

upstroke are thought to contribute to the genesis of phase 3 EADS (January and Riddle, 1989, January et al., 1991). Hiraoka *et al* (1992) showed that the sodium channel activator, Veratridine, induced AP prolongation and the genesis of EADs in guinea pig ventricular myocytes and these were blocked upon addition of the sodium channel blocker, tetrodotoxin, thereby supporting the role of the  $\text{Na}^+$  current in the development of EADs. Both phase 2 and phase 3 EADs are linked to  $\beta$ -adrenergic stimulation and can lead to the generation of ventricular arrhythmias. In addition, as EADs are associated with prolonged QT interval they often lead to the generation ventricular arrhythmias in the form of *Torsades de Pointes*, which themselves are associated with long QT syndrome (January et al., 1991, Charpentier et al., 1993, De Ferrari et al., 1995).

### **1.5.2 Delayed after-depolarisations (DADS)**

Delayed after-depolarisations (DADs), as shown in figure 1.11 B, arise following full repolarisation of the cardiac AP and are referred to as phase 4 after-depolarisations (Priori and Corr, 1990, Fozzard, 1992, De Ferrari et al., 1995). DADs are favoured by high  $[\text{Ca}^{2+}]_i$  and fast HRs, two typical consequences of  $\beta$ -adrenergic stimulation (see section 1.4 of introduction) and as a result DADs are believed to contribute to the generation of the majority of sympathetic-induced ventricular arrhythmias (Priori and Corr, 1990, Fozzard, 1992, Bers, 2001).

$\text{Ca}^{2+}$ -overload that develops during sustained  $\beta_1$ -adrenergic stimulation can result in the spontaneous release of  $\text{Ca}^{2+}$  from the SR due to opening of the RyR2, which triggers the generation of a transient inward current ( $I_{ti}$ ), responsible for the after-depolarisation (January et al., 1991, Fozzard, 1992, De Ferrari et al., 1995, Bers, 2001). The NCX1 is thought to be the major contributor to the generation of the  $I_{ti}$ , as the spontaneous SR  $\text{Ca}^{2+}$  release, drives  $\text{Ca}^{2+}$  efflux and a coupled  $\text{Na}^+$  influx by forward-mode of the NCX resulting in the production of an inward depolarising  $\text{Na}^+$  current (January et al., 1991, Bers, 2001). The non-specific cationic current ( $I_{nsc}$ ) and the  $\text{Ca}^{2+}$ -activated  $\text{Cl}^-$  current

( $I_{Cl(ca)}$ ) have also been implicated in the generation of  $I_{ti}$ , however, in most species the predominant mechanism appears to be the NCX (Priori and Corr, 1990, January et al., 1991, Bers, 2001).

The magnitude of a DAD depends on both the amount of  $Ca^{2+}$  released from the SR and the density of NCX. The magnitude of a DAD can be further increased for a given  $Ca^{2+}$  release in HF (Bers, 2001, Bers, 2006) and this is in part due to SERCA2a/ PLB downregulation and upregulation of NCX1 in HF (Currie and Smith, 1999, Pogwizd et al., 1999). The likelihood for any given  $I_{ti}$  to give rise to an extrasystole will depend on the opposing effects of  $K^+$  channels. For example, in HF, the principal  $K^+$  current underlying the RMP,  $I_{K1}$ , is downregulated, which contributes to an unstable RMP and is pro-arrhythmic (Fauconnier et al., 2005). In addition, a reduction in  $I_{to}$  (Kaab et al., 1998) and the delayed rectifier  $K^+$  currents  $I_{Kr}$ ,  $I_{Ks}$ , and  $I_{Kur}$  (Janse, 2004), which reduce early repolarisation and increase APD, respectively, may also impact on the size of a DAD. Therefore, these changes in  $K^+$  currents, SERCA2a, PLB and NCX1 all render the failing heart more sensitive to ventricular arrhythmias and related SCD.

## ***1.6 Consequences of hypertension and hypertrophy on cardiac excitation-contraction coupling and diurnal cycling***

Hypertension and LV hypertrophy are conditions associated with an increased incidence of ventricular arrhythmias and after-depolarisations (McLenachan et al., 1987, Cleland et al., 2002). Hypertension is a common cause of LV hypertrophy, which is an adaptive response whereby the heart compensates to increased pressure-overload through an increase in ventricular mass (Rubin et al., 1983). LV hypertrophy may occur physiologically, for example in response to exercise, where the increase in ventricular mass permits an increase in SV (Lorell and Carabello, 2000, Olson and Schneider, 2003). Alternatively, it may be a pathophysiological response to impaired contractility,

for example, as a result of pressure-overload in hypertension or acute MI-induced necrotic cell death and fibrosis, where the heart responds by increasing ventricular mass to compensate (Lorell and Carabello, 2000, Olson and Schneider, 2003).

LV hypertrophy can be classified as either concentric, which corresponds to the increase in ventricular mass in response to pressure-overload and is deemed a compensated form of hypertrophy, or eccentric, in which the radius and thickness of the ventricular chamber both increase in size contributing to decreased contractile function, which is deemed a decompensated form of hypertrophy (Lorell and Carabello, 2000, Olson and Schneider, 2003). Compensated LV hypertrophy can progress to decompensated LV hypertrophy and subsequently HF (Lorell and Carabello, 2000).

Hypertension, LV hypertrophy and HF are all occurrences associated with an increased risk of SCD due to the increased incidence of  $\text{Ca}^{2+}$  dependent after-depolarisations and associated ventricular arrhythmias (McLenachan et al., 1987, Cleland et al., 2002). These arrhythmic events and related SCD appear to be triggered by increased sympathetic stimulation. Indeed, in HF patients treatment with  $\beta$ -blockers greatly reduces the incidence and risk of ventricular arrhythmias and subsequent SCD (Dorian, 2005).

### **1.6.1 Altered $\text{Ca}^{2+}$ homeostasis in left-ventricular hypertrophy and resultant heart failure**

There is an increased incidence of after-depolarisations (EADs and DADs) and ventricular arrhythmias in patients with hypertension-induced LV hypertrophy and HF, due to altered  $\text{Ca}^{2+}$  homeostasis. In addition, the morning preponderance of ventricular arrhythmias is more pronounced in patients with LV hypertrophy and HF (Maron et al., 1994). In the ventricular myocardium, diurnal variation has been documented in several ion channels and exchangers, namely  $\text{K}^+$  channels and NCX, and also in HR, all of which will impact EC-coupling, contraction strength and arrhythmogenesis (Veerman et

al., 1995, Yamashita et al., 2003, Shen et al., 2007). The  $K^+$  channels,  $I_{Kur}$  (Kv1.5) and  $I_{to}$  (Kv4.2) both exhibit a time-of-day dependent pattern of expression, as Kv4.2 expression is increased and Kv1.5 expression is decreased in the resting period (ZT6) (Yamashita et al., 2003). In addition, both of these  $K^+$  channels are integral components of the ventricular AP and therefore modulation of these currents through changes in APD and will impact arrhythmogenesis. In addition, during LV hypertrophy and HF, both  $I_{Kur}$  and  $I_{to}$  have been reported to be decreased, which results in AP prolongation (Kaab et al., 1998, Tamargo et al., 2004). The density of NCX in the sarcolemmal membrane also exhibits patterns of diurnal variation, as Shen *et al* (2007) found that surface expression of NCX was decreased in the resting period of the rats, which was correlated with an increased receptor internalisation and expression of phosphatidylinositol-(4,5)-bis-phosphate ( $PIP_2$ ).

Hypertension-induced LV hypertrophy and HF result in remodelling of  $Ca^{2+}$  handling and homeostatic mechanisms in addition to substantial gross pathological ventricular remodelling (Houser et al., 2000, Bers, 2006). Indeed, changes in the activity and/ or expression of NCX (Pogwizd et al., 1999), RyR2 (Marx et al., 2000), SERCA 2a (Currie and Smith, 1999) and  $K^+$  channels (Nabauer and Kaab, 1998) are associated with hypertension-induced LV hypertrophy and HF. These changes in  $Ca^{2+}$  handling proteins are pro-arrhythmic and predispose the ventricular myocardium to DADs, thereby contributing to the increased arrhythmic activity seen in patients with hypertension, LV hypertrophy and HF (Houser et al., 2000, Bers, 2006).

In animal and human models of hypertension-induced LV hypertrophy,  $Ca^{2+}$  homeostasis is subject to substantial remodelling, as during the onset of LV hypertrophy there is an initial compensatory increase in contraction strength and the systolic  $Ca^{2+}$  transient in order to maintain SV and CO. However, upon progression from compensated to decompensated LV hypertrophy there is a significant reduction of the systolic  $Ca^{2+}$  transient and consequentially, reduced contraction strength (Houser et al., 2000, Bers, 2006). In addition, diastolic  $Ca^{2+}$  levels increase as a result of increased SR  $Ca^{2+}$  release and abnormal  $Ca^{2+}$  handling (Houser et al., 2000, Bers, 2006). The

reduction in contraction strength in hypertension-induced LV hypertrophy occurs as the result of alterations in the key EC-coupling proteins, namely LTCC, RyR2, SERCA 2a and NCX1. In both LV-hypertrophy and HF, the activity of the LTCC is believed to be reduced (Chen et al., 2002), which results in a reduction in the “trigger”  $\text{Ca}^{2+}$  involved in promoting SR  $\text{Ca}^{2+}$  release and combined with the reduced activity of SERCA 2a and the subsequent reduction in SR  $\text{Ca}^{2+}$  content, EC-coupling gain is reduced (Houser et al., 2000, Bers, 2006).

RyR2 is typically hyperphosphorylated in cases of hypertension, LV-hypertrophy and also in HF (Marx et al., 2000). This hyperphosphorylation is detrimental as it increases the open probability of the channel and also reduces the association the FKBP12.6 protein with RyR2 (Marx et al., 2000, Wehrens et al., 2003). This is detrimental to myocyte survival in two ways, firstly, both instances result in an increase in spontaneous SR  $\text{Ca}^{2+}$  release, which decreases SR  $\text{Ca}^{2+}$  content and therefore the amount of releasable  $\text{Ca}^{2+}$ , thereby reducing contraction strength. Secondly, any increase in the tendency of spontaneous SR  $\text{Ca}^{2+}$  release will subsequently increase the risk of ventricular arrhythmias namely DAD-type arrhythmias. LV hypertrophy and HF are associated with reduced SERCA 2a expression and increased NCX1 expression, which may contribute to dysfunctional  $\text{Ca}^{2+}$  handling. Reduced SERCA 2a activity that occurs as a result of reduced expression will reduce SR  $\text{Ca}^{2+}$ -uptake and therefore SR  $\text{Ca}^{2+}$  content, which may contribute to the reduction in  $\text{Ca}^{2+}$  transient amplitude, contraction strength, and slowed rate of  $\text{Ca}^{2+}$  transient relaxation seen in LV hypertrophy and HF (Currie and Smith, 1999). SERCA 2a activity is further decreased in HF due to PLB hypophosphorylation. PLB is the endogenous inhibitor of SERCA 2a and this inhibition is relieved upon phosphorylation of PLB (Inui et al., 1986). Therefore, this reduction in PLB phosphorylation in HF will increase inhibition of SERCA 2a, which reduces SERCA 2a activity and thereby further reduces SR  $\text{Ca}^{2+}$  uptake and content (Currie and Smith, 1999). The reduction in SERCA 2a expression and activity in LV hypertrophy and HF may contribute to the increased incidence of ventricular arrhythmias in patients with these conditions (Houser et al., 2000, Bers,

2006). Indeed, SERCA 2a overexpression has been shown to improve myocyte survival, SR  $\text{Ca}^{2+}$  content and  $\text{Ca}^{2+}$  transient kinetics in addition to reducing the incidence of  $\text{Ca}^{2+}$  dependent afterdepolarisations in response to ISO (Davia et al., 2001). In addition, adenoviral transfer of SERCA 2a is thought to improve ventricular function in cases of LV hypertrophy and HF (Baartscheer, 2001).

As stated, LV hypertrophy and HF are conditions associated with an increase in the expression of NCX (Pogwizd et al., 1999). Increased NCX1 activity as a result of increased expression will result in enhanced  $\text{Ca}^{2+}$  removal from the myocyte, which further reduces SR  $\text{Ca}^{2+}$  content. The inward  $\text{Na}^+$  current generated by  $\text{Ca}^{2+}$  removal and the increased activity of NCX may contribute to the increased incidence of ventricular arrhythmias in LV hypertrophy and HF as NCX is associated with the development of DADS through the generation of the  $I_{\text{ti}}$  and in addition any increase in  $\text{Na}^+$  will increase the magnitude of the DAD (January et al., 1991, De Ferrari et al., 1995).

Ventricular myocytes are thought to express type 2 inositol 1,4,5-trisphosphate receptors ( $\text{IP}_3\text{R}$ ) and Bers (2002) has proposed that these  $\text{IP}_3\text{R}$  are possible alternative means of SR  $\text{Ca}^{2+}$  release, albeit negligible in comparison to  $\text{RyR}2$  (Bers, 2002, Harzheim et al., 2009). In addition to changes in LTCC,  $\text{RyR}2$ , SERCA 2a and NCX1 in hypertension, LV hypertrophy and also HF, there are thought to be changes in expression and activity of TTCC and  $\text{IP}_3\text{R}$ . The TTCC is believed to have a negligible contribution to normal EC-coupling due to its low expression level in the ventricle (Ono and Iijima, 2010). However, during LV hypertrophy, TTCC is believed to be re-expressed with other foetal genes (e.g. *mhc $\beta$* ) in the ventricle which could compensate for reduced LTCC by an increase in SR  $\text{Ca}^{2+}$  release mediated by the activation and opening of this receptor but conversely may contribute to abnormal  $\text{Ca}^{2+}$  homeostasis (Ono and Iijima, 2010). In addition, upregulation of  $\text{IP}_3\text{R}$  is believed to increase diastolic and systolic  $\text{Ca}^{2+}$  thereby contributing to the generation of ventricular arrhythmias in cases of LV hypertrophy and HF (Harzheim et al., 2009). However, as

IP<sub>3</sub>R are believed to play a negligible role in SR Ca<sup>2+</sup> release, IP<sub>3</sub>R will no longer be discussed in the context of the present investigation.

In summary, LV hypertrophy and HF are characterised by a reduction in contraction strength due to changes in the Ca<sup>2+</sup> transient and the Ca<sup>2+</sup> handling proteins; LTCC, RyR2, SERCA 2a, PLB and NCX1 (Houser et al., 2000, Bers, 2006). These changes in Ca<sup>2+</sup> handling proteins in addition to changes in K<sup>+</sup> channels can predispose the hypertrophic myocardium to the development of ventricular arrhythmias. This increase in ventricular arrhythmias coupled to diurnal changes in these Ca<sup>2+</sup> handling proteins may account for the morning peak in ventricular arrhythmias in LV hypertrophy and HF.

### **1.6.2 $\beta$ -adrenergic signalling in ventricular hypertrophy and heart failure**

LV hypertrophy and HF are conditions associated with enhanced sympathetic drive which results in excessive overstimulation of cardiac  $\beta$ -adrenergic receptors (Greenwood et al., 2001, Schlaich et al., 2003). Excessive  $\beta$ -adrenergic stimulation will result in an initial increase in  $\beta$ -adrenergic responsiveness, which can lead to the generation of ventricular arrhythmias and resultant SCD (Castellano and Bohm, 1997, Post et al., 1999). These ventricular arrhythmias are predominately due to the increased incidence of DADs (Priori and Corr, 1990, Fozzard, 1992, Schlotthauer and Bers, 2000, January et al., 1991). The threshold for the genesis of DADs is reduced in patients with LV hypertrophy and HF which is thought to contribute to the increased incidence of ventricular arrhythmias and SCD seen in these conditions (Bers, 2001, Bers, 2006). However, chronic exposure to  $\beta$ -adrenergic stimulation will result in the downregulation of  $\beta_1$  and  $\beta_2$ -adrenergic receptors, through phosphorylation by  $\beta$ -adrenergic receptor kinase 1 ( $\beta$ -ARK1), which targets the receptors for internalisation by  $\beta$ -arrestin thereby decreasing the  $\beta$ -adrenergic responsiveness of the myocardium, as illustrated in figure 1.12 (Post et al., 1999, Bers, 2001). Downregulation and internalisation of both  $\beta_1$  and

$\beta_2$ -adrenergic receptors decreases the effective receptor concentrations able to respond to  $\beta$ -stimulation, which will result in a decreased positive inotropic and lusitropic effects in response to sympathetic stimulation. It is believed that the progression from compensated hypertrophy to decompensated hypertrophy and HF involves a decrease in  $\beta$ -adrenergic responsiveness, in combination with altered  $\text{Ca}^{2+}$  handling (Olson and Schneider, 2003).

$\beta$ -adrenergic stimulation of the ventricular myocardium also results in the activation of  $\beta_3$ -adrenergic receptors, which upon activation produce negative inotropic effect through NO-cGMP dependent (PKG phosphorylation) and independent pathways (S-nitrosylation) (Ziolo, 2008). The  $\beta_3$ -adrenergic receptor has been reported to be upregulated in LV hypertrophy (Barbier et al., 2007b) and HF (Cheng et al., 2001), as unlike  $\beta_1$  and  $\beta_2$ -adrenergic receptors, the  $\beta_3$ -adrenergic receptor does not possess the  $\beta$ -ARK1 phosphorylation site and therefore cannot be downregulated like other  $\beta$ -adrenergic receptors (Skeberdis, 2004). Changing the ratio of  $\beta_3$ :  $\beta_1/\beta_2$ -adrenergic receptors will have an impact on the overall outcome and/or responsiveness of the diseased myocardium to sympathetic stimulation in terms of inotropy and arrhythmogenesis. Therefore, as the ratio of  $\beta_3$ : $\beta_1/\beta_2$ -adrenergic receptors increases, this may explain the reduced responsiveness of the failing heart to sympathetic stimulation. Indeed, changes in  $\beta_1/\beta_3$ -adrenergic receptor density in LV hypertrophy and HF, in addition to changes in LTCC, RyR2, SERCA 2a, PLB, NCX1 and the  $\text{K}^+$  channels,  $I_{\text{to}}$  and  $I_{\text{K1}}$  contribute to decreased  $\text{Ca}^{2+}$  transient, contraction strength and increased generation of ventricular arrhythmias and after-depolarisations associated with these conditions.

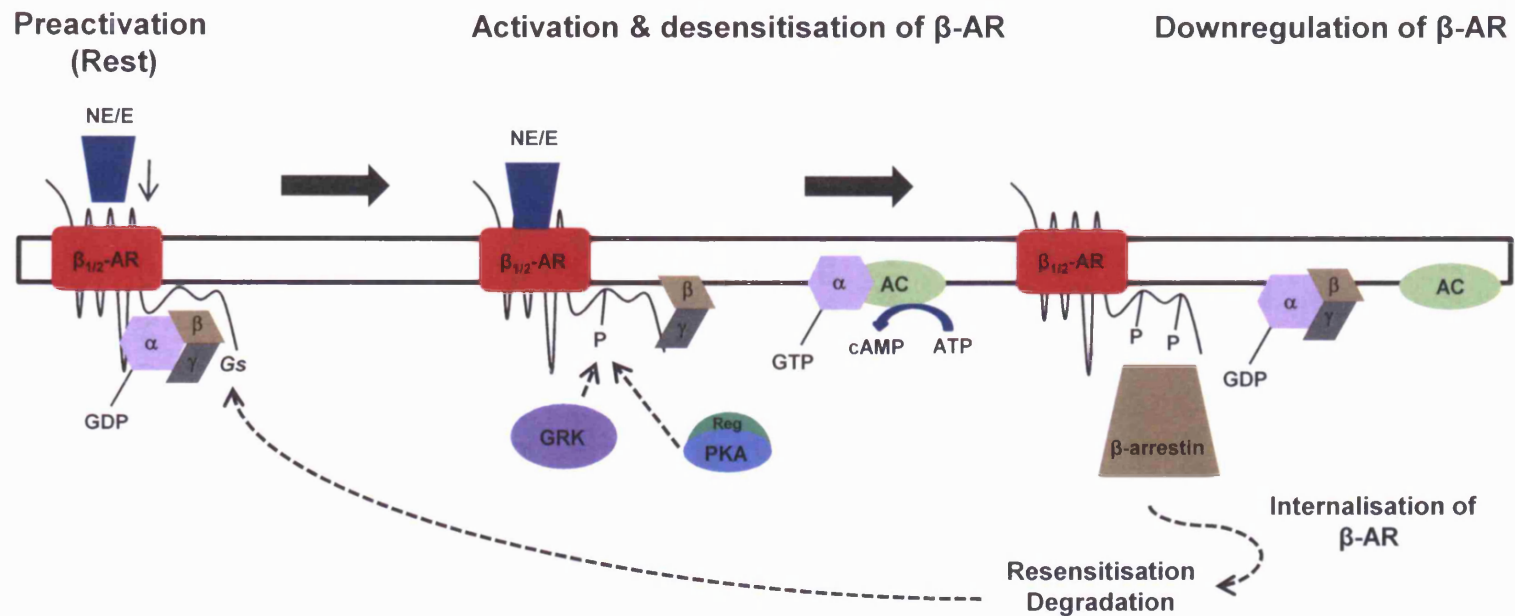


**Figure 1.12 – Desensitisation and downregulation of cardiac  $\beta_{1/2}$ -adrenergic receptors (adapted from Bers, 2001).** Prolonged or excessive  $\beta$ -adrenergic stimulation results in the desensitisation and subsequent downregulation of cardiac  $\beta$ -adrenergic receptors. Desensitisation of  $\beta$ -adrenergic receptors occurs during excessive  $\beta$ -adrenergic stimulation in which the receptors are phosphorylated by the G-protein receptor kinase (GRK, also referred to as  $\beta$ ARK1). The phosphorylated  $\beta$ -adrenergic receptor is targeted by  $\beta$ -arrestin and internalised, which leads to either resensitisation or degradation of the receptor. Both the  $\beta_1$  and  $\beta_2$ -adrenergic receptors are targeted by GRK and  $\beta$ -arrestin, however, the  $\beta_3$ -adrenergic receptor does not possess the GRK target residues and therefore is not downregulated.

### **1.6.3 Changes in NOS signalling in hypertension, left-ventricular hypertrophy and heart failure**

In hypertension-induced LV hypertrophy and HF there are dramatic changes in the activity and concentration of the three NOS isoforms (Umar and van der Laarse, 2010). Many studies have shown that NOS1 is upregulated in cases of LV hypertrophy and HF (Damy et al., 2003, Damy et al., 2004, Loyer et al., 2007, Umar and van der Laarse, 2010). In addition, NOS1 is thought to translocate from the SR to the sarcolemma in HF, where NOS1 may target the sarcolemmal LTCC (Bendall et al., 2004). Under normal circumstances, NOS1 is thought to co-immunoprecipitate with xanthine oxidoreductase (XOR) in the SR, which produces reactive oxygen species and this physical association of NOS1 with XOR reduces the activity of XOR and thereby the production of reactive oxygen species (Khan et al., 2004, Saraiva et al., 2005). In addition, the translocation of NOS1 from the SR to the sarcolemma physically uncouples NOS1 and XOR, thereby increasing the risk of oxidant damage in the diseased myocardium (Bendall et al., 2004, Khan et al., 2004).

NOS2 is activated in association with the production of inflammatory cytokines and immune response, conditions typical of LV hypertrophy and HF (Kelly et al., 1996). It is therefore not too surprising that NOS2 is believed to be upregulated in LV hypertrophy and HF (Umar and van der Laarse, 2010). Activation of NOS2 has a negative inotropic effect through PKG phosphorylation of troponin I (reducing  $\text{Ca}^{2+}$  sensitivity of myofilaments) and phosphorylation of LTCC (reducing LTCC current) (Ziolo et al., 2008). In addition to the increased production of inflammatory cytokines associated with LV hypertrophy and HF, increased levels of inflammatory cytokines are also evident in cases of acute MI (Neumann et al., 1995). Indeed, NOS2 is believed to be upregulated in cases of acute MI (Umar and van der Laarse, 2010). Activation of NOS2 has been shown to promote contractile dysfunction and increase infarct size in models of MI (Wildhirt et al., 1999). As NOS2 does not significantly contribute to the

regulation of cardiac EC-coupling in healthy individuals it will not be discussed further in the present investigation.

In addition, there is a decrease in the activity and concentration of NOS3 in LV hypertrophy and HF (Damy et al., 2004, Umar and van der Laarse, 2010). A decrease in the abundance and activity of NOS3 is detrimental, as studies using NOS3 gene KO mouse models, have identified these mice to exhibit increased  $\beta$ -adrenergic responsiveness, increased  $I_{Ca}$ , increased LV hypertrophy, increased incidence of after-depolarisations and arrhythmogenesis (Kubota et al., 2000, Barouch et al., 2002, Wang et al., 2008b), suggesting the importance of NOS3 in limiting the adrenergic response, limiting  $Ca^{2+}$  overload, limiting LV remodelling and protecting against arrhythmogenesis.

Under normal circumstances, all three isoforms of NOS will produce NO, which can have cGMP-dependent and cGMP-independent effects in terms of effector proteins. This NO production acts locally due to the localisation and compartmentalisation of each NOS isoform and their downstream signalling components to the SR in the case of NOS1 and the sarcolemma/ caveolae in the case of NOS3.

However, in conditions of cardiovascular disease, NOS are thought to produce superoxide in addition to NO (Ziolo et al., 2008). The production of superoxide is detrimental as it will interact with NO to form peroxynitrite ( $ONOO^-$ ), a potent oxidant, responsible for the disruption and oxidation of lipid membranes (Radi et al., 1991). Peroxynitrite has been shown to modulate the function of the SR, namely, it is thought to irreversibly oxidate RyR2, which results in the increased open probability of the channel, increased spontaneous SR  $Ca^{2+}$  release and subsequent decreased SR  $Ca^{2+}$  content and contraction (Khan et al., 2004, Sun et al., 2008, Ziolo et al., 2008). Furthermore, peroxynitrite is thought to oxidise SERCA 2a thereby reducing its activity which reduces SR  $Ca^{2+}$  reuptake and promotes the pro-arrhythmic extrusion of  $Ca^{2+}$  through forward mode NCX (Khan et al., 2004, Sun et al., 2008, Ziolo et al., 2008). Under normal circumstances, NOS3 is believed to be associated with superoxide dismutase (Wang et al., 2008b), a potent scavenger of superoxide and this scavenging of

superoxide decreases the amount of superoxide that is free to interact with NO, producing ONOO<sup>-</sup>. As NOS3 is decreased in LV hypertrophy and HF this means less NOS3 is available to scavenge superoxide which may result in increased production of ONOO<sup>-</sup> and abnormal Ca<sup>2+</sup> homeostasis and contraction. Therefore, changes in NOS activity could contribute to abnormal EC-coupling, reduced contractile strength and arrhythmic activity in LV hypertrophy and HF.

#### **1.6.4 The development of several cardiomyopathies results in disruption to circadian clock and altered diurnal cycling.**

LV hypertrophy and HF are cardiomyopathies associated with the increased incidence of ventricular arrhythmias and SCD due to changes in key Ca<sup>2+</sup> handling proteins. In particular, the generation of ventricular arrhythmias is often associated with changes in SR function, namely through changes in expression of RyR2, SERCA 2a and PLB; changes in LTCC density; changes in NCX density and changes in the expression of K<sup>+</sup> channels. Of these, NCX surface expression and K<sup>+</sup> channel expression have been reported to exhibit diurnal variation (Yamashita et al., 2003, Shen et al., 2007). As many of the genes encoding these proteins may be under the influence of the circadian clock, this may contribute to the time-of-day dependent increase in ventricular arrhythmias observed in LV hypertrophy and HF.

Many cardiomyopathies including pressure-overload induced hypertrophy, are associated with severe disruptions to the circadian clock with both the diurnal variation in circadian clock gene and resulting output genes such as myocardial metabolic gene expression, either depressed in terms of the magnitude of cycling or that there is a change in the timing of the diurnal variation. For example, induction of myocardial ischaemia/ reperfusion (I/R) injury and streptozotocin-induced diabetes in the rat, have been shown to result in the attenuation of diurnal variation in circadian clock gene expression (Young et al., 2002, Kung et al., 2007). Pressure-overload induced

hypertrophy is also associated with severe disruptions to the normal pattern of diurnal variations in circadian clock gene expression (Young et al., 2001b) and cardiovascular metabolism (Young et al., 2001a). Young *et al* (2001a) induced pressure-overload induced hypertrophy in adult male Wistar rats through aortic banding, which resulted in the development of characteristic changes associated with LV hypertrophy, namely increased heart weight-to-body weight (HW/BW) ratios and induction of the expression of the foetal gene, myosin heavy chain  $\beta$  (*mhc* $\beta$ ). It was also shown that in pressure-overload induced hypertrophy, diurnal variation in the expression of carbohydrate, fatty acid and mitochondrial metabolic genes observed in control rats was blunted (Young et al., 2001a). However, very little is known about the impact of these changes in diurnal variation on the effector proteins of EC-coupling, namely LTCC, RyR2, SERCA 2a, PLB and NCX1.

## ***1.7 Aims and objectives***

In the mammalian myocardium, CO, HR, SV and BP, the cardiac AP, sympathetic activity and the expression of many cardiac genes including those responsible for cardiac metabolism exhibit patterns of diurnal cycling (Guo and Stein, 2003), however, to date it is unknown how variation in these parameters impacts on EC-coupling and the responsiveness of the ventricular myocardium to  $\beta$ -adrenergic stimulation. As diurnal variation has been documented in  $\text{Ca}^{2+}$  regulation in other organs including the brain, we hypothesised that diurnal variation is present in cardiac EC-coupling in the rat myocardium.

The aims and objectives of the present investigation were:

- 1) *To determine whether diurnal variation is present in EC-coupling and to determine any possible underlying cellular mechanisms which might account for*

*the documented diurnal variation in haemodynamic parameters such as CO & SV.*

To examine diurnal variation in EC-coupling, two opposing time-points from the *resting period* and the *active period* of the rats 24 hour cycle were chosen. As contraction reflects a complex interplay of electrical and  $\text{Ca}^{2+}$ -regulation mechanisms, we examined the  $\text{Ca}^{2+}$  transient, contraction strength and SR  $\text{Ca}^{2+}$  content in left ventricular myocytes isolated during the resting period (ZT3) and active period (ZT15) of the rat. In addition, we performed quantitative real-time RT-PCR to examine mRNA levels of key genes involved in EC-coupling.

2) *To determine whether diurnal cycling exists in the responsiveness of the ventricular myocardium to sympathetic stimulation and the cellular mechanisms responsible for this.*

We hypothesised that the diurnal variation in levels of sympathetic activity may in part impose time-of-day dependent variation in responsiveness of EC-coupling to sympathetic stimulation. We therefore examined the responsiveness of the  $\text{Ca}^{2+}$  transient to the sympathomimetic, non-specific  $\beta$ -adrenergic receptor agonist, isoproterenol (ISO), in left ventricular myocytes isolated during the resting period and active period of the rat.

3) *To determine the possible cellular mechanisms responsible for the time-of-day peak in ventricular arrhythmias.*

As there is a morning peak in the onset of SCD which is strongly associated with the generation of ventricular arrhythmias and an increase in sympathetic activity, we sought to determine whether the threshold for ISO-induced arrhythmias exhibit diurnal cycling.

4) *To determine whether NOS-signalling plays a role in diurnal variation in EC-coupling and  $\text{Ca}^{2+}$  regulation.*

Sympathetic stimulation activates  $\beta_3$ -adrenergic receptors resulting in a negative inotropic effect mediated through the downstream activation of NOS, which antagonises the  $\beta_1/\beta_2$  response. We set out to determine whether activation of the  $\beta_3$ -adrenergic

receptor and its downstream signalling pathways i.e. NOS, may play a role in diurnal variation in sympathetic responsiveness.

*5) To determine whether hypertension-induced hypertrophy influences diurnal cycling in EC-coupling and responsiveness to sympathetic stimulation.*

Many cardiomyopathies, such as pressure-overload induced hypertrophy, are associated with an increased incidence of ventricular arrhythmias. One possible cause for this may be altered circadian clock gene cycling. We hypothesised that diurnal variation in EC-coupling and its responsiveness to ISO would be depressed in a genetic model of hypertension-induced hypertrophy (SHR).

## **Chapter 2: Materials and methods**

### ***2.1 Experimental Animals and time-points***

#### **2.1.1 Animals**

Adult male Wistar rats (300-350g) used in the present investigation were at least 24 weeks old at the time of dispatch and were used to investigate EC-coupling, as they are not prone to any underlying cardiovascular pathology.

Young *et al* (2001) have shown that the diurnal variations in circadian clock genes and numerous metabolic genes are attenuated in an aortic banded rat model of pressure-overload induced hypertrophy (Young et al., 2001a, Young et al., 2001b). In order to investigate the effects of pressure-overload induced hypertrophy on EC-coupling, we used the genetic model of pressure-overload, the Spontaneously Hypertensive Rat (SHR). The SHR is a popular animal model of essential/ genetic hypertension, developed through outbreeding a hypertensive adult male Wistar rat with a female rat with mild hypertension, the resulting offspring were inbred until they had developed spontaneous hypertension (Okamoto and Aoki, 1963, Henry et al., 1990). The adult Wistar-Kyoto (WKY) rat was used as a normotensive age-matched control to the adult SHR. The WKY rats were obtained as a result of out-breeding from the strain of Wistar rat from which the SHR was originally out-bred (Okamoto and Aoki, 1963, Henry et al., 1990).

Adolescent SHR and WKY rats used were 6 weeks old at time of dispatch, as SHR rats do not develop spontaneous hypertension until approximately 10-15 weeks (Okamoto and Aoki, 1963). The SHR develop hypertrophy and reduced CO at 24 weeks (6 months) and HF at 18-24 months (Pfeffer and Pfeffer, 1983, Conrad et al., 1991, Boluyt and Bing, 2000), therefore, the adult SHR and WKY rats were used at 24 weeks to ensure hypertension and LV hypertrophy had developed in the SHR. The SHR/ WKY

rats were supplied from a colony housed and maintained in the biomedical services division at the University of Leicester, and were originally obtained from Charles River laboratories.

### **2.1.2 Time-points**

To study diurnal variation in EC-coupling, suitable time-points that correspond to the active and resting periods of the nocturnal rat, were selected and classified according to the convention of Zeitgebers and Zeitgeber Time (ZT). A Zeitgeber, translated to mean “time giver”, which in mammals is most commonly a light stimulus, is known to set/reset the mammalian circadian clock, allowing synchronisation of the clock with the Zeitgeber (Edery, 2000, Durgan et al., 2005). Therefore, ZT refers to the period of time from which light is first present (Edery, 2000, Durgan et al., 2005). In a 12 hour light cycle environment, ZT0 refers to the application of the light stimulus i.e. lights on, and ZT12 refers to removal of light stimulus i.e. lights off.

In order to obtain animals from time-points separated by 12 hours, all rats were randomly assigned to one of two rooms with either a normal or reverse 12 hour light/dark (L/D) cycle, for at least 4 weeks prior to experimentation. In the normal light cycle room, lights were turned on at 6am, which corresponds to ZT0, and switched off at 6pm, which corresponds to ZT12. In the reverse light cycle room, lights were turned off at 6am, which corresponds to ZT12 and the lights switched on at 6pm, which corresponds to ZT0/24. Animals were dispatched at 9.00 am, which corresponds to ZT3 in animals from the normal light cycle, and ZT15 from the reverse-light cycle room (shown in figure 2.1). Ventricular myocytes were isolated immediately and in this investigation “resting period (ZT3) myocytes” refers to ventricular myocytes isolated from rats at ZT3 and “active period (ZT15) myocytes” from rats at ZT15. This nomenclature also applies to left ventricular free-wall samples. In addition, adolescent and adult SHR / WKY rats were treated in a similar fashion with regard to ZT time-points.

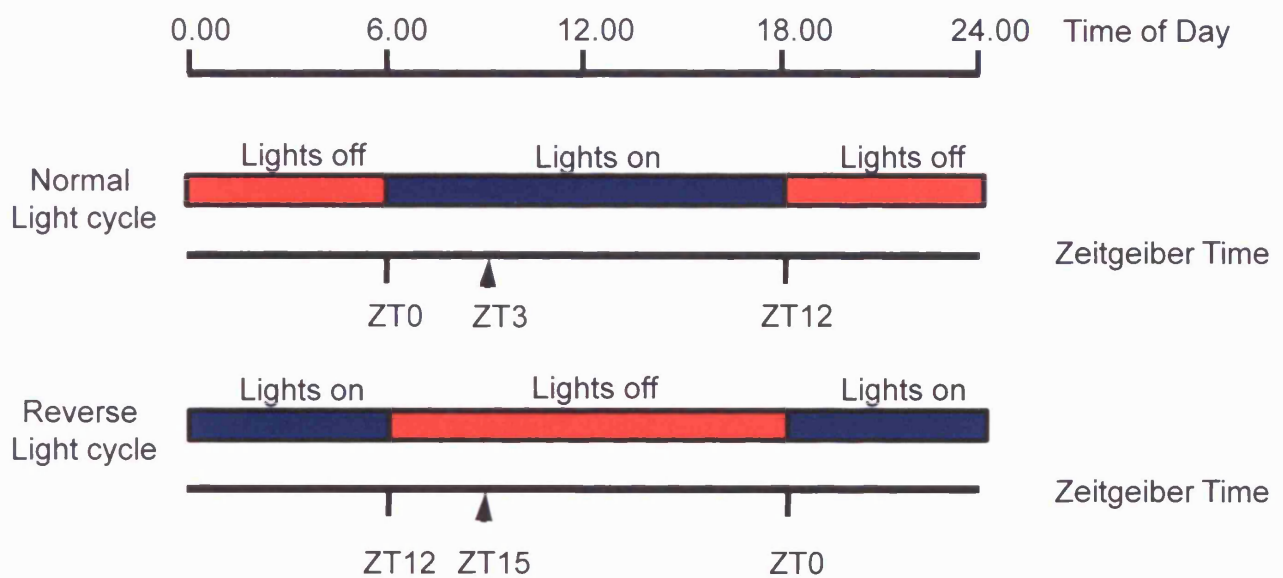


**Figure 2.1- Light/ dark cycle and Zeitgeber time (ZT)**

This figure shows the separate 12 hour light/ dark cycles in which the Wistar, SHR and WKY rats used in this investigation were kept. For normal light cycle rats, lights were switched on at 6 am (corresponding to ZT0) and lights were switched off at 6pm (corresponding to ZT12). For reverse light cycle rats, lights were switched off at 6am (corresponding to ZT12) and lights were switched on at 6pm (corresponding to ZT0). The figure also shows the ZT time points investigated; ZT3 (corresponding to 3 hours after lights switched on in normal light cycle) and ZT15 (corresponding to 3 hours after lights switched off in reverse light cycle).

## ***2.2 Isolation of single rat ventricular myocytes***

Single ventricular myocytes were isolated using the method previously described by Lawrence & Rodrigo (1999), which is a modification of the method originally described by Mitra & Morad (1985). Male Wistar, WKY and SHR were sacrificed humanely in accordance with Home office guidelines, as outlined in the Animals (Scientific procedures) Act, 1986. Rats were stunned by a blow to the head and sacrificed by cervical dislocation. Following this, a thorcotomy was performed and the heart rapidly excised and placed into cold  $\text{Ca}^{2+}$ -free Tyrode. The excised heart was rapidly cannulated at the aorta, which involved placing a flanged cannula into the aorta, secured distal to the openings of the coronary vessels. The heart was then retrogradely perfused with  $\text{Ca}^{2+}$ -free Tyrode for 6 minutes using a Langendorff apparatus (see figure 2.2). The heart was then subjected to enzymatic digestion by perfusion with  $\text{Ca}^{2+}$ -free Tyrode containing type I Collagenase (1.7 mg/ml) and type XIV Protease (1 mg/ml), for 5-8 minutes, during which time the enzyme was recirculated. After enzymatic digestion, the heart was perfused with normal Tyrode for 3 minutes to inactivate and wash off the enzymes, during which time the atria and the right ventricle were removed. The remaining left ventricle was removed from the cannula and placed into a conical flask containing normal Tyrode (10mls), scissor minced and placed into a 37°C Stuart SBS40 shaking water bath. Once the flask was turbid with cells, the remaining digested left ventricle was placed in a new flask with fresh normal Tyrode and this stage was repeated until the left ventricle was completely dissociated. The cell suspensions were sieved using a 200 $\mu\text{m}^2$  pore stainless steel sieve and placed into test tubes to settle, the supernatant removed and the cell pellet washed twice with normal Tyrode. The resulting cell fractions were placed into Petri dishes prior to use and were inoculated with 200 $\mu\text{l}$  of 10,000 units/ml Penicillin/ 10mg/ml Streptomycin (2000 units/ ml Penicillin/ 2mg/ml Streptomycin). A successful isolation of single ventricular myocytes typically produced 70-80% striated, rod-shaped myocytes. All cells isolated using this method were stored

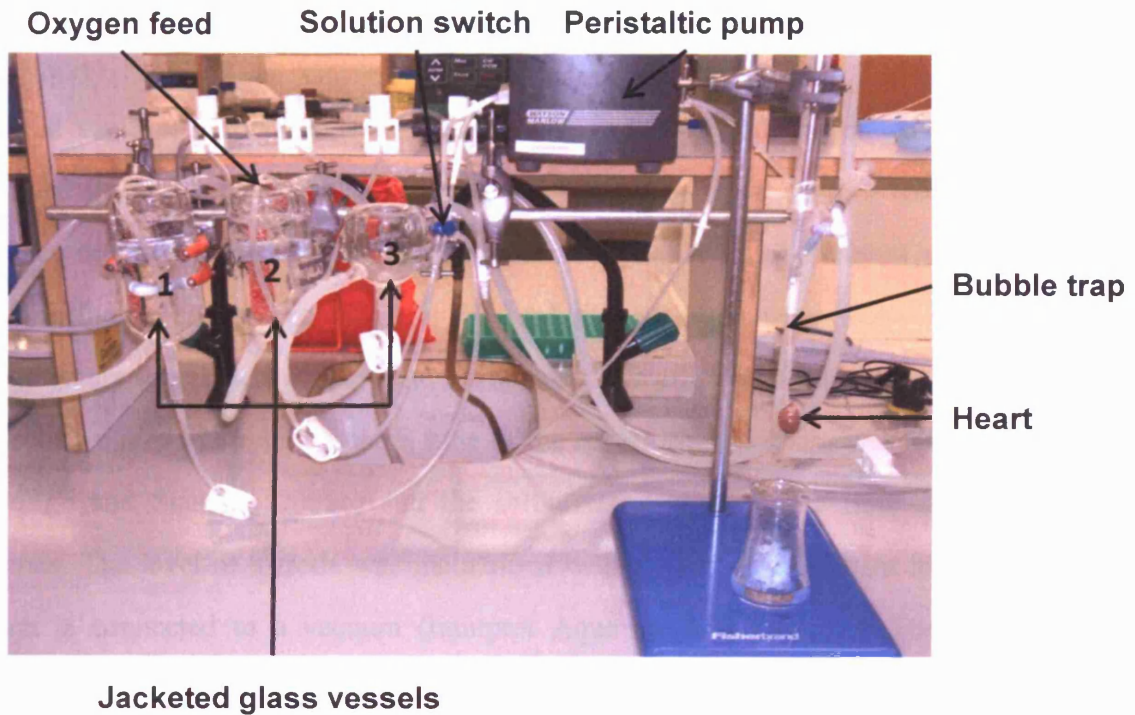


**Figure 2.2– Langendorff perfusion apparatus.**

This figure shows the Langendorff perfusion apparatus used during the isolation of single ventricular myocytes. The apparatus consists of the following components: three jacketed glass vessels containing [1]  $\text{Ca}^{2+}$ -free Tyrode [2] Normal Tyrode [3] Enzyme-containing Tyrode; a constant oxygen supply to each jacketed vessel; a solution switch to switch between Tyrode solutions; a peristaltic pump to ensure a constant perfusion rate and a bubble trap to remove air bubbles in the perfused Tyrode solutions.

at room temperature and were used on the day of isolation. All solutions were kept at 37°C and oxygenated throughout the duration of the isolation.

### ***2.3 Superfusion of ventricular myocytes***

Isolated ventricular myocytes were placed into normal Tyrode contained in a 500µl diamond shaped perspex superfusion chamber located on the stage of a Nikon diaphot inverted microscope (Nikon, Japan), shown in figure 2.3. The myocytes were left to settle in the superfusion chamber for 5-10 minutes prior to experimentation and then continuously superfused with normal Tyrode at a rate of 3-4mls/ minute by means of a peristaltic pump where the washout time of the superfusion chamber was < 40 seconds (Rodrigo and Standen, 2005b) and the solution exchanger had a time delay of ~5 seconds. The level of Tyrode was maintained with the aid of a constant level device, which is connected to a vacuum (Interpret Aqua air AP3 pump). The perfusion chamber was constantly maintained at the optimum temperature of  $35 \pm 2^{\circ}\text{c}$  by a Warner temperature controller during each experiment, incorporating a pre-heater. Two platinum stimulation electrodes were placed opposite each other in the superfusion chamber and were connected to a Harvard research stimulator, which allowed the continuous electrical field stimulation of myocytes. All myocytes were stimulated at 1Hz, unless otherwise stated, and cells not contracting synchronously at the start of superfusion were not used.

#### **2.3.1 Contraction studies**

The Nikon Diaphot inverted microscope was coupled to a charge coupled device (CCD) camera (Panasonic), which allowed the superfused myocytes to be viewed on a video monitor (Panasonic WV-5340). This system was used to determine cell-shortening using a video edge detection system or for studies investigating the development of arrhythmic activity.

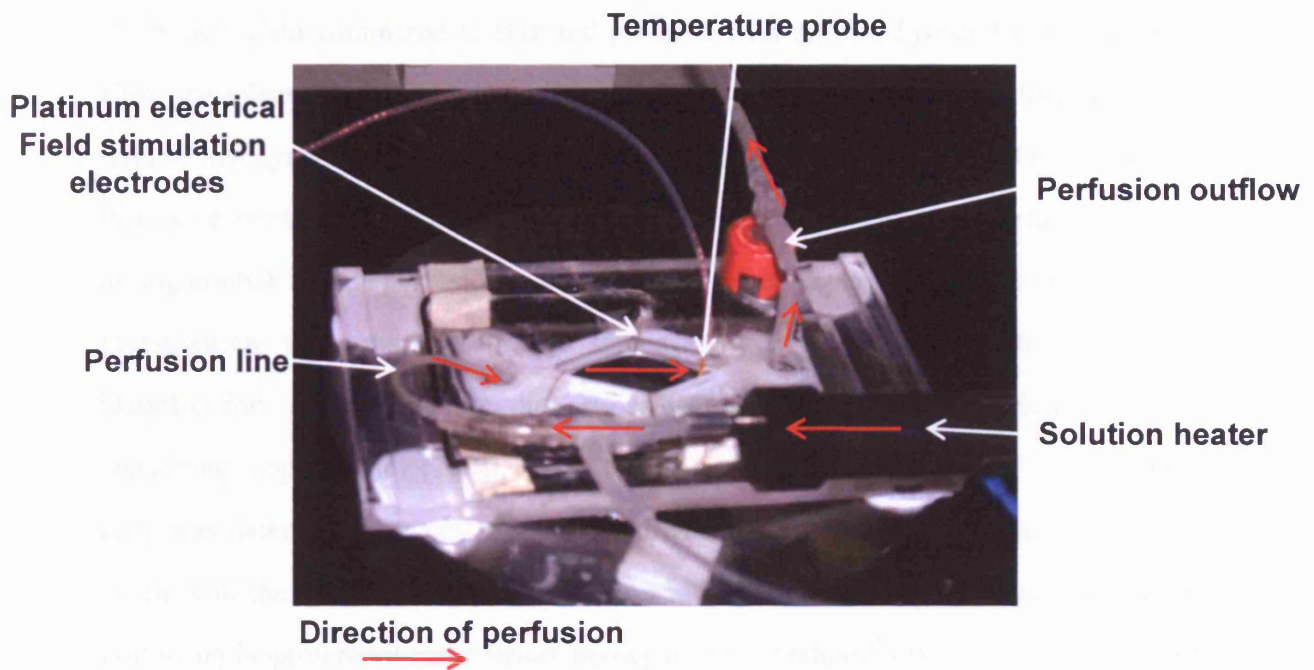


**Figure 2.3 – Myocyte superfusion chamber**

This figure shows the 500  $\mu$ l diamond-shaped cell superfusion chamber, used in all fluorescence experiments. The superfusing Tyrode solutions were maintained at  $35 \pm 2^\circ\text{C}$  by means of the solution preheater, connected to a temperature controller (Warner). The cells were superfused at a constant rate of  $\sim 3\text{-}4\text{mls/ min}$ , by a peristaltic pump and the level of Tyrode was maintained with the aid of a constant level suction device, connected to a vacuum. The platinum electrodes allowed electrical field stimulation of the myocytes.

To determine the development of arrhythmic activity, ventricular myocytes were electrically field stimulated at 1Hz and perfused with normal Tyrode for 5 minutes, to allow the selection of a field approximately 10-20 synchronously contracting cells. The field of myocytes was viewed as a video image using a x10 objective. Only myocytes that were contracting synchronously in response to 1Hz electrical field stimulation during normal Tyrode perfusion were selected for each experiment and these cells under investigation were marked on the screen of the video monitor, to allow easy identification. Myocytes were then superfused for 5 minutes with normal Tyrode containing isoproterenol (3, 10, 50 & 100nM) after which the number of arrhythmic cells was determined. A cell was assessed as arrhythmic if it was contracting out of synchrony with the electrical stimulator at the end of 5 minutes isoproterenol superfusion. Following isoproterenol superfusion, myocytes were perfused with normal Tyrode for 5 minutes, to allow the myocytes to recover

Cellular contraction strength was determined from changes in cell length, measured in single ventricular myocytes using video cell-edge detection (Crescent electronics, model no VED 103). Briefly, this involved placing two moveable cursors, produced by the edge detection equipment, onto opposite ends of a contracting cell viewed on the video monitor. The edge detection system generates a continuous output proportional to the distance length of the cell on the monitor. During these experiments, each cell was viewed using a x40 objective and cell length was sampled at a rate of 50Hz, which is a sampling frequency routinely documented in the literature and used in this laboratory. In the present investigation, the sampling frequency of 50Hz was sufficient to accurately examine the time course and peak of contraction as in continuous cell-length traces we saw no evidence of aliasing, which occurs when the sampling rate is too slow and also length traces were recorded continuously and for analysis 10 consecutive contractions were averaged.

### **2.3.2 Fluorescence studies**

A Nikon Diaphot inverted microscope was housed in a light proof chamber and measurements taken from a single myocyte using a x40 oil immersion fluorescence objective (fluor 40/1.30 oil). Cells were superfused using a Ismatec peristaltic pump during fluorescence experiments. Unlike contraction studies, the output of the microscope in fluorescence studies was directed to a photomultiplier (see section 2.4). Any cells that had a resting diastolic Fura-2 ratio of  $> 1$  (~250-300nM) during initial normal Tyrode superfusion were excluded from analysis.

To determine SR  $\text{Ca}^{2+}$  loading, ventricular myocytes loaded with Fura-2 were stimulated at a rate of 1Hz and perfused for 5 minutes with normal Tyrode, by means of a peristaltic pump, to establish a constant calcium transient. The electrical stimulator was switched off for 10 seconds and the cells were simultaneously and rapidly perfused with normal Tyrode containing 20mM Caffeine for 5 seconds until a caffeine-induced  $\text{Ca}^{2+}$  transient was visible. After which, the electrical stimulator was re-started and cells were perfused with normal Tyrode for 5 minutes, to allow the recovery of resting calcium transients. In the present investigation, caffeine was applied at  $35 \pm 2$  °C through a separate; 3-way tap based gravity-fed perfusion line which was connected to the solution pre-heater.

## ***2.4 Fluorescence microscopy***

The cell was excited with light from the monochromator (high speed Delta Ram X, PTI) directed to the cell with an excitation dichroic mirror, see figure 2.4. The light emitted from the cells was transmitted at the emission wavelength of the fluorescent dye in use using an emission dichroic mirror and emission filters, which both allow the transmission of light emitted at the emission wavelength of the fluorescent dye in use and prevent the transmission of other wavelengths. The emitted light is detected by the

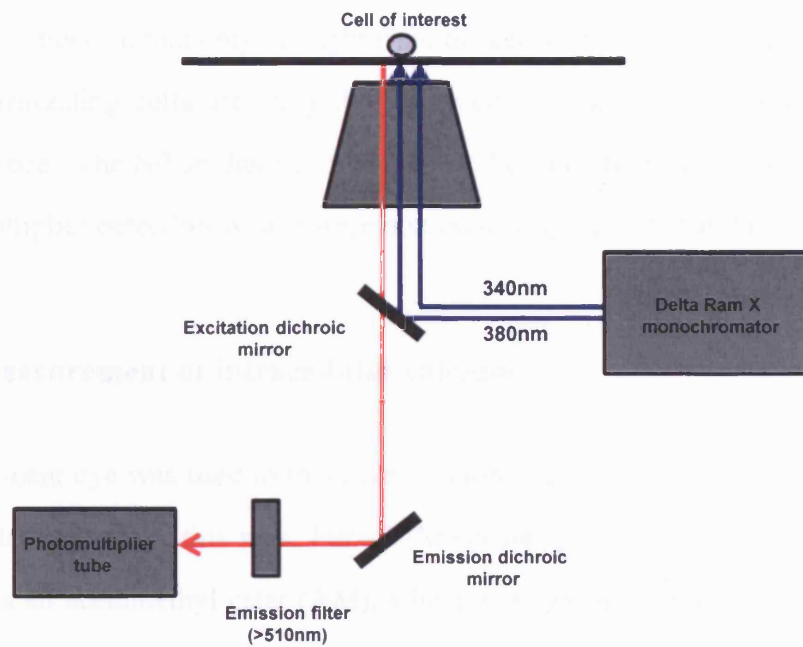


**Figure 2.4- Schematic of fluorescence excitation/ emission pathways .**  
 This schematic shows the light pathway for a dual excitation-single emission fluorescent dye. An example of a dual excitation-single emission dye is the calcium sensitive dye, Fura-2 AM. Loaded cells were excited alternately at both 340/380nm and the emission was collected at >510nm.

photomultiplier tube detection system (PTI Felix 32 product guide). The emitted light from the cell of interest was directed to the photomultiplier tube through the side port of the fluorescence microscope. The cell of interest was screened using horizontal and vertical shutters, so that only the light from the cell was collected, which prevented light from surrounding cells affecting the fluorescence data and also limited background fluorescence. The Nikon diaphot microscope, the Delta Ram X monochromator and the photomultiplier detection system were housed in a lightproof chamber.

#### **2.4.1 Measurement of intracellular calcium**

A fluorescent dye was used in this investigation to measure intracellular  $\text{Ca}^{2+}$ , in single ventricular myocytes, this was: Fura-2 (Molecular probes, Invitrogen). The dye was loaded as an acetomethyl ester (AM), where ester groups render the dye lipid soluble, allowing them to cross the cell membrane. Once the dye enters the cell, the acetoxymethyl ester is cleaved from the dye by intracellular esterases, producing the fluorescent salt of the dye. At this point the desired fluorophore is lipid-insoluble and unable to leave the cell. Fura-2 is a ratiometric dye, which means the excitation ratio of Fura-2 (340/380nm) is proportional to the concentration of intracellular  $\text{Ca}^{2+}$ . Ratiometric dyes are beneficial as they allow for differences in dye loading, leakage of dye from a loaded cell and movement of the loaded cell, for example during contraction (Takahashi et al., 1999).

Fura-2 was dissolved in Dimethyl sulfoxide (DMSO) containing 5% Pluronic acid by weight to produce a 2mM stock concentration, prior to dye loading. Isolated ventricular myocytes were loaded at room temperature with Fura-2 (5 $\mu\text{M}$ ) for 20 minutes. After loading, the cells were washed with normal Tyrode twice, to remove excess dye, and left for 30 minutes prior to experimentation. Fura-2 is a dual excitation, single emission dye (see figure 2.4) and loaded cells were excited alternately at both 340/380nm and the emission was collected at >510nm. The data were collected at a rate of 60Hz. To analyse  $\text{Ca}^{2+}$  transients, values for systolic [ $\text{Ca}^{2+}$ ], diastolic [ $\text{Ca}^{2+}$ ] and amplitude of  $\text{Ca}^{2+}$

transient were determined for each myocyte, as illustrated in figure 2.5 A. In order to reduce sampling error during analysis, systolic  $[Ca^{2+}]_i$ , diastolic  $[Ca^{2+}]_i$  and amplitude of  $Ca^{2+}$  transient from 10  $Ca^{2+}$  transients from each myocyte were averaged, see figure 2.5 B

#### **2.4.2 *In-vivo* Calibration of Fura-2 signal**

We used an *in vivo* calibration to calibrate data obtained using Fura-2 and this method of *in vivo* calibration has been successfully used previously (Williams and Fay, 1990, Henke et al., 1996). This *in vivo* Fura-2 calibration utilised the  $Ca^{2+}$  dissociation constant ( $K_d$ ) obtained from Groden *et al* (1991) which was reported to be 285nM at 37°C. The calibration involved the determination of  $R_{min}$ , which was achieved by loading cells with the calcium chelator, BAPTA AM (2mM) for 60 minutes prior to loading with Fura-2. The ratio obtained in these cells was taken as the  $R_{min}$ . To obtain a value for  $R_{max}$ , a microelectrode was manoeuvred close to the myocyte and the cell was damaged to allow the entry of calcium from the extracellular normal Tyrode, containing 2mM  $Ca^{2+}$ . The ratio of  $F_{380_{max}}/ F_{380_{min}}$  was also determined in order to calibrate the Fura-2 ratio and was the ratio of fluorescence of bound  $Ca^{2+}$  to unbound  $Ca^{2+}$  measured at 380nm.  $R_{min}$  and  $R_{max}$  were performed in 41 cells obtained from 4 different hearts at the beginning of the investigation and therefore were not calculated in every Fura-2 loaded cell. However, as the mean  $R_{min}$  and  $R_{max}$  values obtained were consistent between hearts and there was no significant difference between diastolic and systolic ratios at any particular time-point, this suggests that loading and  $Ca^{2+}$  binding characteristics were consistent.  $R_{min}$ ,  $R_{max}$ , the calcium  $K_d$  and  $F_{380_{max}}/ F_{380_{min}}$  ratio were used to calculate  $[Ca^{2+}]_i$  using the following equation:

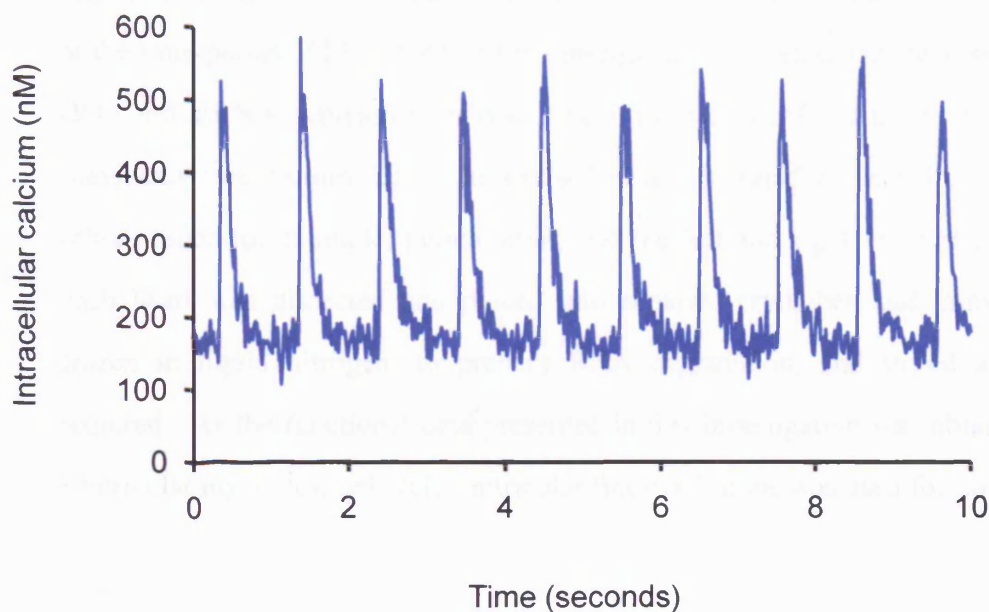
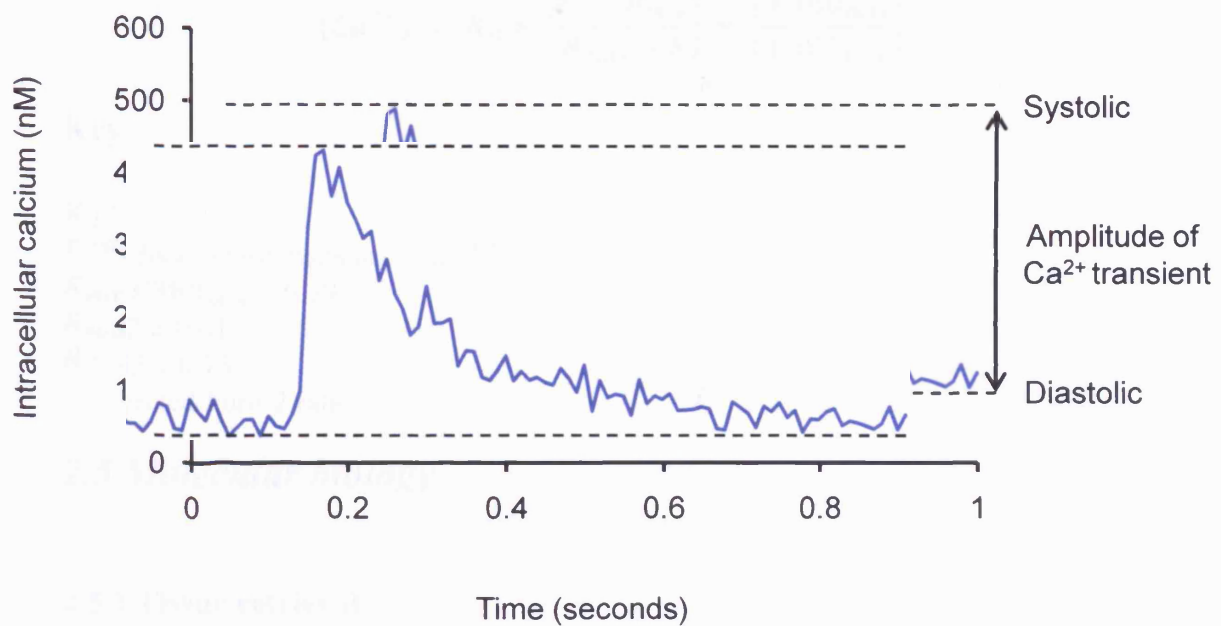


**Figure 2.5- Analysis of the basal  $\text{Ca}^{2+}$  transient**

- A. Example of a  $\text{Ca}^{2+}$  transient recorded from a single resting period (ZT3) myocyte superfused with normal Tyrode and stimulated at 1Hz.
- B. Example recording of 10  $\text{Ca}^{2+}$  transients recorded from a single resting period (ZT3) myocyte superfused with normal Tyrode and stimulated at 1Hz. 10 measurements of systolic  $[\text{Ca}^{2+}]$ , diastolic  $[\text{Ca}^{2+}]$  and amplitude of  $\text{Ca}^{2+}$  transient were obtained from each myocyte and averaged, prior to statistical analysis.

$$[Ca^{2+}] = K_d \times \left[ \frac{R - R_{min}}{R_{max} - R} \right] \times \left[ \frac{F380_{max}}{F380_{min}} \right]$$

## Key

$K_d$  =  $Ca^{2+}$  dissociation constant, 285nM

$F380_{max}/F380_{min} = 6.39$

$R_{min} = 0.42 \pm 0.01$

$R_{max} = 5.02 \pm 0.13$

$R$  = uncalibrated Fura-2 ratio

## 2.5 Molecular biology

### 2.5.1 Tissue retrieval

Hearts were excised from adult male rats (Wistar, adolescent/ adult male SHR & WKY) at the time-points, ZT3 and ZT15 for subsequent RNA extraction, reverse transcription (RT) and mRNA expression analysis. Each rat was sacrificed in the manner outlined previously (see section 2.2). The excised heart was rapidly cleaned of blood, fat and other tissues for example, pericardium, and the left and right ventricular free-wall of each heart was dissected and placed into separate cryotubes and immediately snap frozen in liquid nitrogen, to prevent RNA degradation, and stored at  $-80^{\circ}C$  until required. As the functional data presented in this investigation was obtained from left ventricular myocytes, only left ventricular free-wall tissue was used for mRNA analysis.

### 2.5.2 RNA extraction

The two main methods of RNA extraction used in the field of molecular biology are; the traditional phenol/ chloroform based method, for example the use of TriZOL and its synonymous alternatives or, the column-based guanidine-isothiocyanate methods, for example, the RNeasy plus mini kit offered by Qiagen (Bustin and Nolan, 2004, Chomczynski and Sacchi, 2006, Fleige and Pfaffl, 2006). On investigation, the RNeasy plus mini kit was preferable to the phenol/ chloroform method of extraction, as the latter

has been shown to contaminate RNA with high levels of genomic DNA (Siebert and Chenchik, 1993, Chomczynski and Sacchi, 2006) and the two compounds used, are highly toxic (Goda and Minton, 1995). In initial RNA extractions (data not included), the manufacturer's protocol was followed in its entirety, however, subsequently this has been modified at certain stages in order to maximise RNA yields and integrity. The major modifications to the existing Qiagen RNeasy protocol were; 1) the use of less starting material, 2) the extension of centrifugation times, 3) the use of less buffer at certain stages, 4) the incorporation of an on-column DNase step and 5) the final elution of a smaller volume of concentrated RNA. All RNA used for subsequent reverse transcription experiments was extracted using the modified Qiagen protocol.

### ***Sample preparation***

The entire workstation and pipettes were decontaminated and cleaned prior to use with RNase zap solution (Ambion) and aseptic technique was preferred throughout. Left ventricular free-wall tissue samples retrieved previously and stored at  $-80^{\circ}\text{C}$ , were placed on dry ice, alongside Petri dishes, blades, forceps and Eppendorff tubes, to prevent the tissue from thawing, which can lead to RNA degradation (Bustin and Nolan, 2004, Fleige and Pfaffl, 2006, Nolan et al., 2006). Each sample was placed on a Petri dish in the dry ice. In initial RNA extractions (data not included) approximately 30mg of tissue was cut, weighed and collected per sample, as indicated in the manufacturer's protocol. However, this was problematic as at this weight the tissue overloaded the RNeasy spin column, reducing the total RNA yield. Therefore, a tissue weight between 18 and 25mg per sample was preferred in all extractions and resulted in high RNA yields and integrity. Each tissue sample was then cut into at least 4-5 smaller pieces, to aid subsequent homogenisation, and placed into separate pre-cooled Eppendorffs.

### ***Lysis and homogenisation***

A mix of “Buffer RLT plus” (Qiagen) and  $\beta$ -mercaptoethanol was prepared on the day of each extraction and is referred to as “buffer RLT plus” for simplicity. Buffer RLT plus is a denaturing guanidine-isothiocyanate lysis buffer, added to tissue samples to aid homogenisation and to prevent RNase activity (Goda and Minton, 1995). To each sample-containing Eppendorff, Buffer RLT plus (600 $\mu$ l) was added and each sample individually homogenised with a rotor stator homogeniser with a 5mm tip (Powergen 125 IKA R104 Fisher scientific) until the tissue sample was fully dispersed i.e. the sample was homogenous, and then placed on ice until required (see stage 1, figure 2.6). The homogeniser was cleaned using IMS and Milli-Q water in between each sample to reduce contamination of samples and to prevent carry over of any tissue.

### ***Genomic DNA removal***

The samples were then centrifuged at 13,400 rpm for 5 minutes, supernatant was removed and added to a genomic-DNA (gDNA) eliminator column and centrifuged at 10,000 rpm for 2 minutes (see stage 2, figure 2.6). The gDNA eliminator column allows the collection of gDNA on the column membrane allowing the total RNA to pass through the membrane free of gDNA.

### ***Ethanol addition and RNA binding***

70% ethanol was then added at a volume of 500-550 $\mu$ l, instead of the stated 600 $\mu$ l, to each sample, pipette mixed and was added to a RNeasy spin column and centrifuged at 10,000 for 2 minutes until all the sample had passed through the column. The addition of ethanol at this stage allows RNA to bind to the column membrane allowing subsequent solutions passing through the column to be discarded (see stage 3, figure 2.6).

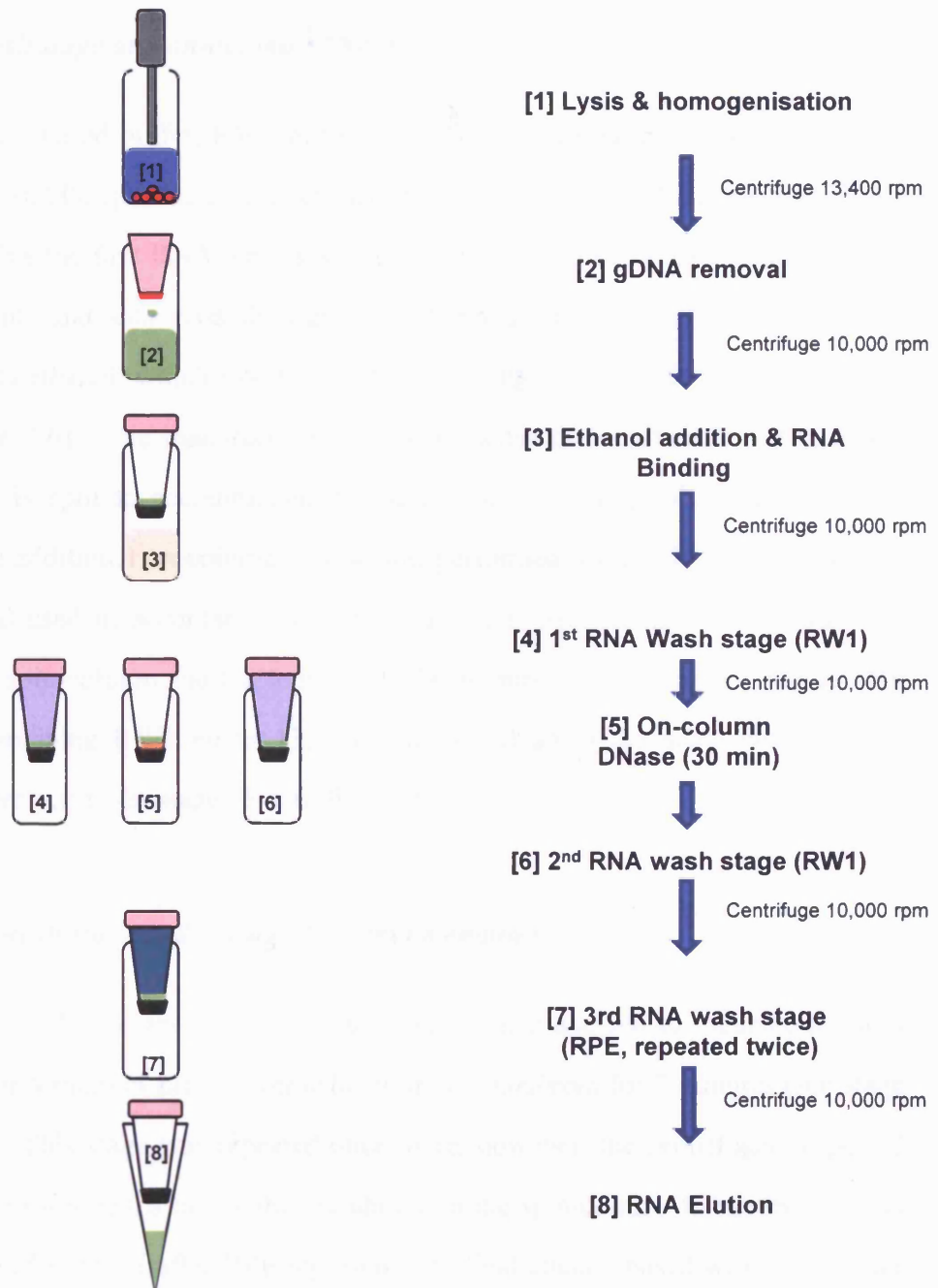


**Figure 2.6- Steps involved in RNA extraction using an RNeasy plus mini kit**

This figure shows the main stages involved in RNA extraction using an RNeasy plus mini kit. RNA extraction begins with the homogenisation of cardiac tissue in buffer RLT plus. The homogenate is placed into a genomic DNA eliminator column to remove contaminating DNA. 70% ethanol is added to the gDNA free homogenate to bind total RNA to the RNeasy spin column. The bound RNA is washed with RW1 buffer, then on-column DNase is applied to the column and left to incubate for 30 minutes. The remaining RW1 buffer is added to the spin column to further wash the RNA. The bound RNA is subjected to two further wash steps using RPE buffer. The total RNA is eluted from the column membrane using RNase-free water. A key is located on the right.

### ***First RNA wash stage and on-column DNase***

Another ethanol based buffer, RW1 buffer (350µl) was then added to the column and centrifuged at 10,000 rpm for 2 minutes (see stage 4, figure 2.6). The addition of RW1 buffer highlights the first RNA wash stage, in which application, allows contaminating protein, solvents and salts pass through the column to be discarded and dilutes any remaining 70% ethanol, which interfere with the activity of the on-column DNase (see stage 5, figure 2.6). The manufacturer's protocol states the addition of 700µl RW1; however, this is split to accommodate an additional on-column DNase treatment in between. The additional on-column DNase was performed using a Qiagen RNase-free DNase set and used in accordance with manufacturers instructions. The DNase was added to each spin-column and left to incubate for 30 minutes at room temperature after which, the remaining RW1 buffer (350µl) was added under the same conditions as previously mentioned (see stages 5 & 6, figure 2.6).

### ***Second RNA wash stage and drying of column membrane***

Buffer RPE (500µl) was then added to each spin-column and left to incubate at room temperature for 5 minutes prior to centrifugation at 10,000rpm for 2 minutes (see stage 7, figure 2.6). This stage was repeated once more, however, the centrifugation period was extended to 4 minutes to dry the membrane in the spin-column to prevent solvent contamination of RNA. Buffer RPE represents the final ethanol based wash stage prior to elution of the RNA from the spin-column membrane. To further dry the spin-column membrane, an additional "dry spin" was performed at 10,000 rpm for 5 minutes with a clean collection tube.

### ***RNA elution***

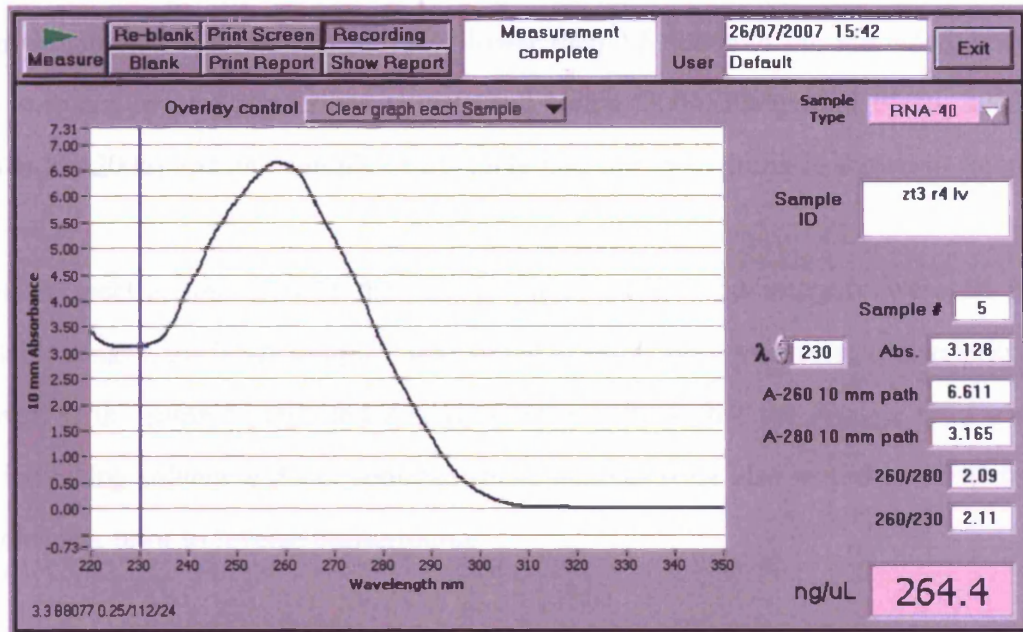
The collection tubes were replaced with individual RNase-free Eppendorff tubes and 25µl of RNase-free water was added to each spin column and centrifuged at 10,000 rpm

for 2 minutes in order to elute the RNA. The sample was then passed through the column and centrifuged again at 10,000 rpm for 2 minutes (see stage 8, figure 2.6). The eluted RNA samples were then placed on ice until spectrophotometric analysis of the RNA yield and quality (mentioned next) could be performed to prevent RNA degradation and were later stored at  $-80^{\circ}\text{C}$  until required.

### **2.5.3 Spectrophotometric assessment of RNA yield and quality**

RNA quality and integrity are critical to reverse transcription and its downstream applications, as in the case of real-time PCR, some contaminants can result in the inhibition of PCR or even the production of spurious data (Bustin and Nolan, 2004, Fleige and Pfaffl, 2006, Nolan et al., 2006). In order to assess the quality and integrity of the extracted RNA samples, each RNA sample was analysed spectrophotometrically to determine RNA yield ( $\text{ng}/\mu\text{l}$ ),  $A_{260/280}$  ratio (nm) and  $A_{260/230}$  ratio (nm) using an 8 sample Nanodrop ND-8000 spectrophotometer and the relevant ND-8000 V1 0.3 software. Spectrophotometry was performed immediately following RNA extraction. The RNA samples were kept on ice until the spectrophotometer was set up and blanked, in order to prevent RNA degradation and inaccurate Nanodrop data. All Nanodrop wells were cleaned prior to use and  $2\mu\text{l}$  of RNase free water (from the Qiagen RNeasy plus mini kit) was pipetted on to the centre of each well. A Nanodrop reading was taken of the RNase free water to blank the machine and this was then removed and  $2\mu\text{l}$  of each RNA sample was tested individually. After each sample had been analysed on the Nanodrop, the RNA yield,  $A_{260/280}$  ratio (nm) and  $A_{260/230}$  ratio were recorded. The  $A_{260/280}$  ratio is an indicator of protein contamination and the  $A_{260/230}$  ratio is an indicator of salt and solvent contamination within RNA samples, the importance and impact of both is the topic of extensive debate, however, it is common practice to take ratios of 2 in both to represent “pure” RNA samples (Bustin and Nolan, 2004, Fleige and Pfaffl, 2006, Nolan et al., 2006). Figure 2.7A shows Nanodrop readings from a high quality RNA sample, where RNA yield is high and the two ratios are  $\sim 2$ . For the purposes of

A



B

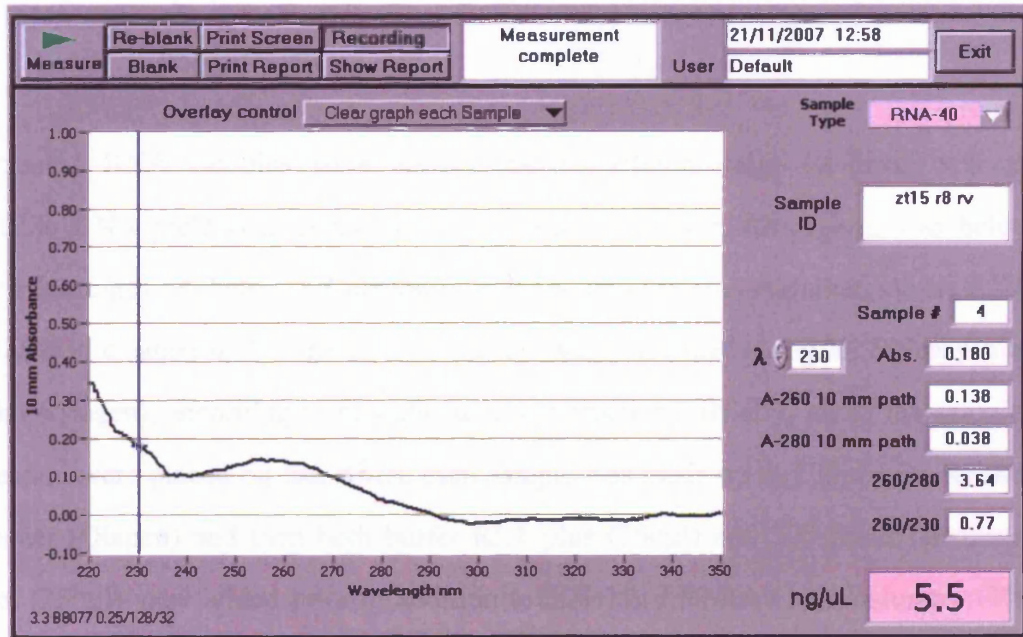


**Figure 2.7- Spectrophotometric analysis of RNA yield and quality**

- A. Nanodrop reading taken from a high quality RNA sample following RNA extraction. The RNA yield,  $A_{260/280}$  and  $A_{260/230}$  are all within acceptable ranges and RNA of this quality was used in the present investigation. All samples undergoing RNA cleanup were re-analysed spectrophotometrically and only used if they are of similar quality to the representative high quality RNA sample shown in A.
- B. Nanodrop reading taken from a poor quality RNA sample following RNA extraction. The RNA yield is poor (5.5ng/ $\mu$ l), as Qiagen quote that the average RNA yield from heart tissue should be  $\sim 4\mu$ g in total. The recommended  $A_{260/280}$  should be roughly 1.8-2 to indicate pure, protein-free RNA, however, the sample here is heavily contaminated and degraded. The  $A_{260/230}$  ratio should be above 1.8, as samples below this indicate solvent and salt contamination.

this investigation, samples with ratios of lower than 1.8 for both the aforementioned ratios were not reverse transcribed (Bustin and Nolan, 2004, Fleige and Pfaffl, 2006, Nolan et al., 2006) and an example of a sample meeting this criteria is shown in figure 2.7B.

Following spectrophotometry if the sample yield, quality and integrity were all in acceptable ranges, the RNA samples were stored at  $-80^{\circ}\text{C}$  prior to reverse transcription. However, if the sample yield and  $A_{260/280}$  were acceptable but the  $A_{260/230}$  ratio was poor, indicating solvent and salt contamination, samples were also stored at  $-80^{\circ}\text{C}$  for RNA cleanup, prior to reverse transcription.

#### **2.5.4 RNA cleanup**

If extracted RNA samples were shown spectrophotometrically to have both an acceptable RNA yield ( $\text{ng}/\mu\text{l}$ ) and an  $A_{260/280}$  ratio, however, the  $A_{260/230}$  was below acceptable ranges i.e. below 1.8 indicating salt and/or solvent contamination, the RNA sample was “cleaned up”. The RNA clean up was performed using an RNeasy plus mini kit (Qiagen), according to manufacturer’s instructions. Briefly, all of the samples for cleanup were placed on ice, where each sample was made up to  $100\mu\text{l}$  with RNase-free water (Qiagen) and then both buffer RLT plus ( $350\mu\text{l}$ ) and 200 proof (absolute) ethanol ( $250\mu\text{l}$ ) were added prior to addition to individual RNeasy spin-columns. The spin-columns were centrifuged to allow the RNA to re-bind to the spin-column membrane, after which, buffer RPE ( $500\mu\text{l}$ ), was added to the column to wash the RNA and this was repeated twice. The RNA was then eluted from the spin column using  $25\mu\text{l}$  RNase-free water and then the eluted RNA was passed through the column once more to collect any remaining RNA.

The cleaned up RNA samples were then analysed spectrophotometrically and if the  $A_{260/230}$  ratio had improved to acceptable ranges (i.e. above 1.8), the sample was stored at  $-80^{\circ}\text{C}$  for subsequent RT experiments. However, if these criteria were not met, the

sample was excluded from investigation as initial practice quantitative real-time RT-PCR indicated bad  $A_{260/230}$  ratios lead to the generation of spurious data due to the presence of salt and solvent contaminants which inhibit PCR (data not included). The RNA cleanup did not involve any DNA removal stage as this was previously performed during the original RNA extraction.

### **2.5.5 Denaturing agarose gel electrophoresis of RNA**

To complement the spectrophotometric analysis of RNA integrity and to see if the RNA was intact and not degraded following isolation, denaturing agarose gel electrophoresis was performed, see figure 2.8 (Goda and Minton, 1995). This involved making a 1% TBE agarose gel from 1x TBE solution (see experimental solutions for composition) and 1% molecular grade agarose. This mix was then heated, stirred and allowed to partially cool, so that ethidium bromide could be added safely, which enables the visualisation of the gel under UV light. The gel was then poured into a gel holder and a comb was placed into the pre-set gel to create wells in which to place RNA, bubbles were removed with a pipette tip and the gel placed in a fume hood to set for approximately 30 minutes.

Whilst the gel was setting, the RNA was prepared. This involved diluting 2-3 $\mu$ g of RNA with nuclease-free water (Ambion) until a 10 $\mu$ l volume of 0.5-1 $\mu$ g RNA had been produced. The diluted RNA samples were then heated to 70°C for 10 minutes on a techgene thermal cycler, in order to denature the RNA, and then placed on ice for 2 minutes. Prior to application to the gel, the denatured RNA was pulse spun and then 3-4 $\mu$ l of RNA gel loading dye was added to each sample. The RNA gel loading dye was composed of 50% formamide and 50% glycerol. The formamide within the RNA gel loading dye helps to protect against RNA degradation (Chomczynski, 1992).

The agarose gel was taken from the fume hood and placed into a gel tank containing 1x TBE solution and the gel was pre-run for 5 minutes to warm the gel, after which, the dye-containing RNA samples were loaded into individual wells and in the far left well

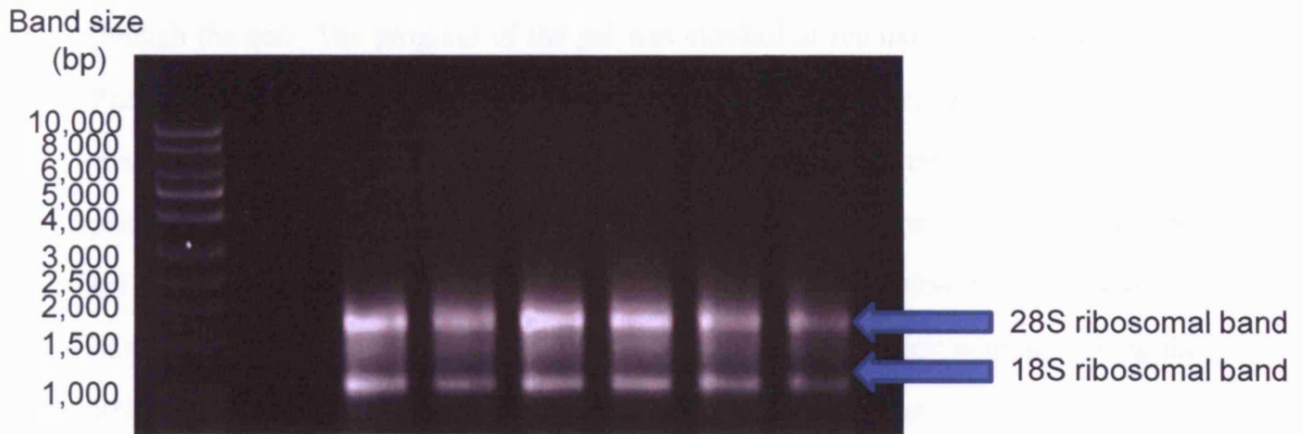


**Figure 2.8- Denaturing agarose gel electrophoresis of RNA samples**

This gel image shows an example of denaturing agarose gel electrophoresis performed using high quality RNA samples. Each RNA sample will produce two ribosomal bands, 28S and 18S, and ideally they should be in a 2:1 ratio, respectively. In samples where the 2:1 ratio is absent, this indicates a relative degree of RNA degradation has occurred. The smudge effect seen in each well above the ribosomal bands indicates the presence of DNA contamination, which is dealt with in section 2.5.7.

5µl of the 1Kb DNA ladder, Hyperladder I (Bioline) was added to determine the size of each band on the gel. The gel was then connected to the electrophoresis anodes and cathodes, set to 60V and left to run until the DNA ladder had successfully migrated through the gel. The progress of the gel was checked at regular intervals using a UV illuminator block (Alpha innotech corporation) and when the gel had been successfully run, it was transferred to a Syngene Gene genius bioimaging system for analysis and gel photography. If the clarity or intensity of the bands was poor upon UV examination, the gel was restained with ethidium bromide (Goda and Minton, 1995). It is also possible, however not common practice, to run RNA on normal agarose gels without heating the RNA and in my experience this process renders similar results (data not included).

### **2.5.6 Semi-quantitative PCR of 18S**

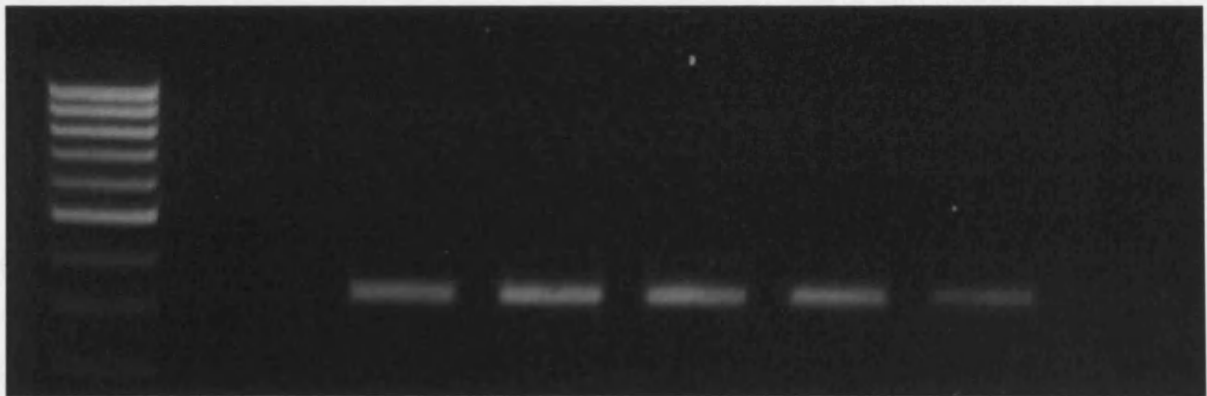
After RNA quality and integrity had been established, the level of gDNA contamination was assessed using semi-quantitative PCR of the single exon spanning gene, 18S. Semi-quantitative PCR differs from quantitative real-time RT-PCR in that it only measures the amount of product at the end of PCR rather than throughout the entirety of the reaction. All components were thawed on ice and pulse spun on a centrifuge prior to use and all of the PCR tubes were handled and opened minimally in order to reduce contamination. As additional precaution, all apparatus and pipettes were decontaminated with RNase zap solution (Ambion). An 18S PCR mix was produced in mass, to reduce pipetting error associated with pipetting smaller volumes, with the following components per reaction: 10x reaction buffer, Mg<sup>2+</sup>, 10mM deoxynucleoside triphosphates (dNTPS), 18S primers, Taq DNA polymerase and nuclease-free water (Abgene). Excess 18S PCR mix was produced for two additional PCR reactions to allow for solution carryover when pipetting and to account for the natural error (±10%) produced when pipetting (Bustin and Nolan, 2004, Nolan et al., 2006). The 18S PCR mix was added to 1µl of each RNA sample to create a final volume of 20µl and also as a negative control, 18S PCR mix was added to 1µl of water to create the same volume.

Once 18S PCR mix had been added to all samples and the negative control, each was pipette mixed and a small drop of mineral oil added to prevent evaporation of the sample during PCR. The oil-covered samples were pulse spun on a centrifuge and placed in a Techgene thermal cycler set with the following PCR conditions: 95°C for 5 minutes; 30 cycles of 95°C for 45 seconds, 60°C for 45 seconds and 72°C for 45 seconds, hold at 4°C, as indicated by the manufacturer. After PCR, the samples were carefully removed from the covering oil and added to a bromophenol blue containing loading dye and immediately loaded into the relevant wells of a 1% TBE agarose gel including ethidium bromide. A 100bp DNA ladder (Norgen Biotek Corporation) was placed in the far left well on the agarose gel to indicate the size of any formed bands. The gel was run for 30 minutes at 60V, during which time the gel was removed and examined under a UV illuminator to check the gel progress, and once the gel had migrated 2-3cm it was removed and examined using a Syngene Gene genius bioimaging system.

If large amounts of contaminating gDNA were present within a sample a significant band will be present when run on an agarose gel, as seen in figure 2.9 (top). The 18S product produces a band at ~340bp on the gel and is an indicator of DNA contamination. If a significant band was present upon analysis of the agarose gel, the relevant samples were subject to additional DNase treatment. As all of the RNA samples had a degree of DNA contamination, a small aliquot of each sample was DNase treated and only used when analysing the expression of the single exon spanning genes: nitric oxide synthase 3 (eNOS/NOS3) and  $\beta_1$ -adrenergic receptor (Adrb1), as the Taqman probes encoding these genes readily amplify contaminating DNA along with cDNA. As no DNase treatment is 100% efficient at removing DNA contamination, the DNase treated samples were not completely free of DNA, therefore, to tackle this problem non-enzyme controls were performed in subsequent reverse transcription and PCR reactions.

Band size  
(bp)

1000  
900  
800  
700  
600  
500  
400  
300  
200



1000  
900  
800  
700  
600  
500  
400  
300  
200



### Figure 2.9 – 18S semi-quantitative PCR of RNA samples

The gel images show an example of 18S semi-quantitative PCR performed on RNA samples that were contaminated with genomic DNA (Top) and an example of 18S semi-quantitative PCR performed on RNA samples following additional DNase treatment prior to reverse transcription (bottom). The presence of a gel band at 340 indicates the presence of DNA contamination, as seen in samples A-E. Water (H<sub>2</sub>O) is used as control as it should not contain DNA and therefore no band is present on the gel. If samples show the presence of gel bands like those seen in the top agarose gel, they were subjected to an additional DNase treatment only if they were required for use with Taqman gene expression probes (eNOS & Adrb1) that span a single exon and amplify contaminating genomic DNA. Ideally, the absence of a gel band after 18S quantitative PCR is desirable as it indicates no contaminating genomic DNA, however, no known DNase treatment can effectively remove all contamination and therefore, non-enzyme controls must be included at reverse transcription.

### **2.5.7 Additional DNase treatment of RNA for the analysis of single exon spanning genes**

Prior to reverse transcription, a small aliquot of each extracted RNA sample was taken individually for an additional DNase treatment so that the cDNA produced from these samples could be used for those genes under investigation that span a single exon and are therefore capable of amplifying gDNA as well as cDNA, which may skew any resultant quantitative real-time RT-PCR results (Bustin and Nolan, 2004, Nolan et al., 2006).

The additional DNase treatment was performed with amplification grade DNase I from Sigma and was used in accordance with the manufacturer's protocol. Briefly, this protocol involved diluting approximately 1µg of each high quality RNA sample in nuclease-free water (8µL), to which both reaction buffer (1µL) and DNase I (1µL) were added. The samples were mixed and left at room temperature for 15 minutes, to allow the DNase time to successfully remove any contaminating DNA. After which, a "stop solution" containing 50mM EDTA, which stops the DNase by chelating calcium and magnesium in the reaction buffer, was added to stop the reaction and then all the samples were heated to 70°C for 10 minutes on a Techgene thermal cycler. Heating of the RNA not only contributes to the inactivation of the DNase, but also, denatures the RNA secondary structure (Wu and Tinoco, 1998, Sambrook and Russell, 2001). Following the DNase treatment all samples were immediately reverse transcribed, in order to prevent additional freeze-thaw cycles on the RNA samples, as this may also jeopardize the subsequent quantitative real-time RT-PCR results.

### **2.5.8 Reverse transcription**

Complementary DNA, also known as cDNA, is produced from the reverse transcription of RNA using specific mRNA primers and is the required template for quantitative real-time RT-PCR (Bustin, 2000). It is possible to conduct a one-step PCR in which the

reverse transcription and the subsequent RT-PCR reaction are carried out in the same well, however, the cDNA cannot be kept for future use (Bustin, 2000). Two-step RT-PCR involves a separate reverse transcription and PCR stage so that cDNA can be stored for future use allowing the study of a broad range of genes of interest rather than just one and therefore, two-step RT-PCR was preferred (Bustin, 2000). A high capacity RNA-to-cDNA kit (Applied Biosystems) was used to produce cDNA. This particular kit was selected as it contained the following RT primers within the included 2x RT buffer mix: random hexamers and Oligo d(T)<sub>16</sub>, and these were present in a 10:1 ratio, respectively. The Oligo d(T)<sub>16</sub> allows the reverse transcription of all short mRNAs containing a poly A tail, however, if the poly A tail is in anyway degraded reverse transcription may not occur as efficiently, therefore, the addition of random hexamers allows the amplification of longer mRNAs all along the transcript rather than just at the poly A tail and therefore can be used on samples with degradation (Resuehr and Spiess, 2003, Nolan et al., 2006).

Approximately 1µg of each high quality RNA sample was reverse transcribed into cDNA, in accordance with the manufacturer's protocol. Briefly, this protocol involved thawing both the RNA samples and the RT kit components on ice and once thawed, an RT + mix containing 2x RT buffer mix and 20x RT enzyme mix, was prepared for the production of experimental cDNA. To test for DNA contamination within the RNA samples, an additional RT mix was prepared containing nuclease-free water in place of the 20 x RT enzyme to act as a non-enzyme control and is referred to as RT - mix. In addition, non-template controls were prepared using nuclease-free water instead of the normal template of RNA in order to test for DNA contamination within the RT kit or water used. Both Non-template and non-enzyme controls were performed to test for gDNA contamination, which was of particular importance when looking at genes which are capable of amplifying gDNA (Bustin and Nolan, 2004, Nolan et al., 2006).

Once all reactions were prepared in individual PCR tubes, they were pulse spun in a centrifuge and placed in a PTC-200 Peltier thermal cycler and reverse transcribed under the following conditions: 37°C for 60 minutes; 95°C for 5 minutes and finally held at

4°C, as indicated by manufacturers protocol. The resultant cDNA was pulse spun and stored at -20°C until required for future quantitative real-time RT-PCR reactions.

Within this investigation, reverse transcriptions were all performed on the same day using the same RT mix, and if possible were placed on the thermal cycler together and this was done to keep the conditions constant.

### **2.5.9 Quantitative real-time reverse transcription PCR**

Quantitative real-time RT-PCR, unlike semi-quantitative methods, offers the ability to monitor gene expression changes in real time rather than conventional end point analysis of PCR products. There are two popular and extensively used methods in current mRNA analysis, these being Taqman fluorescent probe based technology or the fluorescence based SYBR green method, however, for the purposes of this investigation the Taqman fluorescent probe based technology was preferred as the SYBR green method is subject to extensive optimisation.

#### ***Choice of Taqman endogenous control gene (housekeeping gene)***

To control for inter-sample variation, pipetting errors and to normalise cDNA levels during quantitative real-time RT-PCR, a Taqman endogenous control gene was required (Thellin et al., 1999). An endogenous control gene or “*housekeeping gene*”, is one which does not change expression and remains constant within the tested target tissue and allows comparison of mRNA Levels between two or more different experimental conditions (Thellin et al., 1999).

As this investigation looks at diurnal variation in genes involved in cardiac EC-coupling,  $\beta$ -adrenergic stimulation and the impact of hypertension-induced remodelling, it is important to use an endogenous control gene that does not exhibit patterns of either circadian or diurnal variation, as this would lead to the generation of

spurious data. On investigation it was found that many common endogenous control genes vary in this manner, for example Glyceraldehyde-3-phosphate dehydrogenase (GAPDH) expression was seen to vary with time of day (Shinohara et al., 1998). It was also important to use a control gene that does not amplify genomic DNA, therefore, for the basis of Taqman gene expression experiments, control genes which amplify DNA spanning a single exon were excluded, for example 18S. For the purposes of this study,  $\beta$ -actin (ACTB) was preferred for use as the control gene as it has not been shown by Youngs experimental group to vary in expression with time of day (Young et al., 2001a, Young et al., 2001b, Young et al., 2002), and this was confirmed by the presence of a constant expression level within all time-points (ZT3 & ZT15) and rat strains (Wistar, WKY & SHR) studied in the present investigation (see section 3.2.4). In addition, it does not amplify gDNA. Ideally, various control genes should be studied to find and select an appropriately expressed gene (Vandesompele et al., 2002); however, due to the observed constant expression of  $\beta$ -actin, this was deemed not necessary.

### ***Taqman gene expression assays (Taqman Probes)***

All Taqman probes used in this investigation, as shown in figure 2.10, were purchased from Applied Biosystems as inventoried Taqman gene expression assays, of which the primer and probe concentrations per reaction were 900nM and 250nM, respectively. In addition, all Taqman assays selected for use had amplicon lengths of less than 100, in order to improve the efficiency of the resultant PCR (Cha and Thilly, 1993, Bustin, 2000).

### ***Standard curves***

To ensure the efficient replication of each examined gene during quantitative real-time RT-PCR and for subsequent accuracy in mRNA analysis, the efficiency of each Taqman

| Gene type                     | Gene name (alias)                                                      | Gene symbol | Applied biosystems assay I.D. |
|-------------------------------|------------------------------------------------------------------------|-------------|-------------------------------|
| Circadian clock genes         | Period homolog 2 (PER2)                                                | Per2        | Rn00581577_m1                 |
|                               | Circadian locomotor output cycles kaput (CLOCK)                        | Clock       | Rn00573120_m1                 |
| Mitochondrial metabolic genes | Uncoupling protein 2                                                   | Ucp2        | Rn00571166_m1                 |
|                               | Uncoupling protein 3                                                   | Ucp3        | Rn00565874_m1                 |
| Sarcoplasmic reticulum genes  | Ryanodine receptor 2 (RyR)                                             | RyR2        | Rn01470303_m1                 |
|                               | Phospholamban (PLB)                                                    | Pln         | Rn01434045_m1                 |
|                               | Sarcoplasmic/endoplasmic reticulum calcium ATPase (SERCA 2a)           | Atp2a2      | Rn00568762_m1                 |
| Sarcolemmal genes             | Sodium/ calcium exchanger (NCX1)                                       | Slc8a1      | Rn00570527_m1                 |
|                               | Sodium/ Hydrogen exchanger (NHE1)                                      | Slc9a1      | Rn00561924_m1                 |
|                               | Voltage dependent L-type Ca <sup>2+</sup> channel, $\alpha$ 1c subunit | Cacna1c     | Rn00709287_m1                 |
|                               | $\beta_1$ -adrenergic receptor (Adrb1)                                 | Adrb1       | Rn00824536_s1*                |
|                               | $\beta_3$ -adrenergic receptor (Adrb3)                                 | Adrb3       | Rn00565393_m1                 |
| NOS- signalling genes         | Neuronal nitric oxide synthase 1 (nNOS)                                | Nos1        | Rn00583793_m1                 |
|                               | Endothelial nitric oxide synthase 3 (eNOS)                             | Nos3        | Rn02132634_s1*                |
|                               | Neuronal nitric oxide synthase 1 adaptor protein (CAPON)               | Nos1ap      | Rn00594475_m1                 |

**Figure 2.10- Taqman gene expression probe based assays used in this investigation**

Table shows the Taqman gene expression probe based assays used to assess the mRNA levels of various circadian clock, mitochondrial metabolic, EC-coupling and NOS-signalling genes. Within the assay I.D. of each Taqman probe, the “Rn” refers to the assay being compatible with the species, *Rattus norvegicus* and the “\_m1” or “\_s1” located at the end of each assay I.D. refers to the way in which the assay binds to the template cDNA. The “\_m1” probes react with cDNA at a junction between two exons and therefore, no contaminating genomic DNA (gDNA) is amplified; however, “\_s1” probes span a single exon and as a result are capable of amplifying any contaminating gDNA present within the cDNA samples and are marked with an asterisk (\*). Most of the Taqman probes selected where those ending in “\_m1”, however, if this were not possible and “\_s1” probes were required, cDNA samples were treated with an additional DNase step prior to reverse transcription (see section 2.5.7).

probe used in this investigation was determined. For efficiency to be calculated, a standard curve of known concentrations of cDNA is produced by serial dilution. Originally a ten-fold dilution of cDNA (100ng, 10ng, 1ng, 0.1ng, 0.01ng and 0.001ng) was used to produce standard curves, however, this proved difficult for many samples as the less concentrated dilutions were often not in the dynamic range of the Taqman probe and therefore failed to amplify (data not included). Due to this, a two-fold dilution was used which contained the following concentrations of cDNA: 100ng, 50ng, 25ng, 12.5ng, 6.25ng and 3.125ng, in which the cDNA was diluted by 50% each time with nuclease-free water (Ambion) and as a result, dynamic range was met in all Taqman probes (with the exception of the  $\beta_3$ -adrenergic receptor (Adrb3) probe, due to its low abundance).

Quantitative real-time RT-PCR was then performed using the two-fold serial dilutions of cDNA with each desired Taqman probe in triplicate for the cDNA concentrations above 10ng and in quadruplicate in the cDNA dilutions with concentrations below 10ng, as at these low concentrations; more variation will occur in CT values, as single copy number is reached, so the production of extra reactions allows for a larger number of comparisons to be made (Bustin and Nolan, 2004, Nolan et al., 2006). All standard curve cDNA samples were run at a volume of 20 $\mu$ l on a 96-well optical PCR plate sealed with optical film, using an Applied Biosystems ABI-PRISM 7900HT sequence detector real-time PCR machine. The data was collected using Applied Biosystems SDS 2.1 software and the slope of a plot of Log cDNA concentration versus the CT value (see figure 2.11), used to determine efficiency in the following equation:

$$\text{Efficiency} = 10^{(-1/\text{slope})} - 1 \times 100$$

According to Applied Biosystems, all of their Taqman gene expression assays have efficiencies of 100%  $\pm$  10% and do not require a standard curve to be determined. However, this was not always the case with some of the assays used in this investigation as efficiencies between 80 and 110% were common. Standard curves were produced

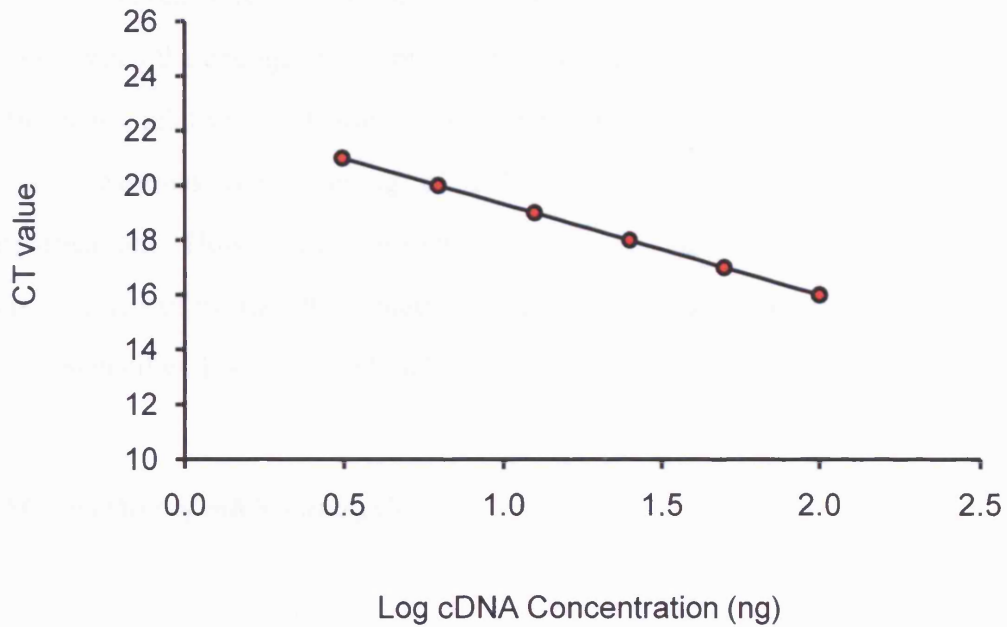


**Figure 2.11- Example 2-fold standard curve plot of 100% PCR efficiency**

This figure shows a theoretical plot of CT value and Log cDNA concentration when the efficiency of the PCR reaction is 100%. In cases where efficiency is 100%, the slope of the plot is 3.32 and a good indicator of 100% efficiency in a 2-fold standard curve dilution is that the CT values increase by 1 with each descending cDNA concentration.

for each Taqman probe in the following samples: adult Wistar (data given in appendix 1 & 3), adolescent and adult SHR samples (data given in appendix 4).

Standard curves were used to determine the method for analysing mRNA expression levels. When the endogenous control gene and the gene of interest have the same PCR efficiencies, relative quantification can be performed via the comparative  $\Delta\Delta C_T$  method as this assumes the doubling of PCR products with each cycle (exponential amplification). However, if these efficiencies are not equal then the mRNA expression was assessed using the Pfaffl method of correction. Both the  $\Delta\Delta C_T$  method and the Pfaffl method will be explained, in brief, below.

#### ***$\Delta\Delta C_T$ method of mRNA analysis***

As stated previously, the comparative  $\Delta\Delta C_T$  method of analysing mRNA expression is employed when the PCR efficiencies of the gene of interest and endogenous control gene are equal (Livak and Schmittgen, 2001, Schmittgen and Livak, 2008). The formula used for the comparative  $\Delta\Delta C_T$  method is outlined below and includes the parameters used:

$$\Delta C_T = \text{mean } C_T^{(\text{Gene of interest})} - \text{mean } C_T^{(\text{Endogenous control gene, } \beta\text{-actin})}$$

$$\Delta\Delta C_T = \Delta C_T^{(\text{Unknown, ZT15})} - \Delta C_T^{(\text{Calibrator, ZT3})}$$

$$\text{Fold change} = 2^{-\Delta\Delta C_T}$$

### ***Pfaffl method of mRNA analysis***

When the efficiencies of the gene of interest and endogenous control gene ( $\beta$ -actin) are not equal then it is inappropriate to use the comparative  $\Delta\Delta C_T$  method of mRNA analysis, as it assumes an exponential PCR amplification ( $\pm 5\%$ ). Therefore, the Pfaffl correction was used, as it takes into account the difference in efficiencies during analysis (Pfaffl, 2001). The Pfaffl correction equation is outlined below:

$$\text{Ratio (Fold change)} = \frac{(E \text{ gene of interest})^{\Delta CP \text{ gene of interest (control-sample)}}}{(E \text{ control gene})^{\Delta CP \text{ control gene (control-sample)}}$$

**E gene of interest** = efficiency of gene of interest

**E control gene** = efficiency of control gene. Control gene used was  $\beta$ -actin

**$\Delta CP$  gene of interest** = mean CT of gene of interest (control sample) – mean CT of gene of interest (sample). Control sample refers to ZT3 samples and sample refers to ZT15 samples.

**$\Delta CP$  control gene** = mean CT of control gene (control sample) – mean CT of control gene (sample). Control sample refers to ZT3 samples and sample refers to ZT15 samples.

### ***Quantitative real-time RT-PCR of genes of interest***

Following the production of individual standard curves, quantitative real-time RT-PCR was performed on the control gene and each gene of interest. Each individual gene of interest was performed on a separate plate; however, the control gene was examined on every plate. Briefly, cDNA samples and the Taqman probes for  $\beta$ -actin and the gene of interest were placed on ice to thaw. Whilst thawing, the entire workstation and pipettes were decontaminated and cleaned prior to use. Taqman universal PCR mastermix was vortexed and placed on ice. To reduce pipetting error, each  $1\mu\text{g}$  cDNA sample was diluted with nuclease-free water to give a final concentration of  $50\text{ng}$ , creating a “cDNA mastermix” for each sample, sufficient to produce three PCR plates. In addition, a

“PCR mix” was produced using Taqman universal PCR mastermix and Taqman probe, of which an individual mix was created for both the control gene and the gene of interest with an excess of 4 additional reactions in each, to allow for pipette carryover. To an optical 96-well PCR plate, 50ng of cDNA for each sample was added in triplicate for both the control gene and gene of interest. The PCR mix containing the control gene probe was added to the first sample triplicates, followed by the addition of the PCR mix containing the gene of interest probe, which was added to the second set of triplicates for each sample. The total volume of 20 $\mu$ l per well on the PCR plate was composed of: 9 $\mu$ l cDNA, 10 $\mu$ l of Taqman universal mastermix and 1 $\mu$ l Taqman probe (control gene or gene of interest). The PCR plate was sealed with optical film, a PCR cover was then placed on top of the film and the plate including cover were briefly centrifuged prior to running the plate on the PCR machine. The PCR amplification was performed using an Applied Biosystems ABI-PRISM 7900HT real time PCR system, in accordance with the manufacturer’s protocol, this was briefly: 95°C for 10 minutes followed by 40 cycles of 95°C for 15 seconds and 60°C for 1 minute. At the end of each PCR run, CT values for each sample were collected using SDS 2.1 software. CT values correspond to the number of individual PCR cycles it takes a specific fluorescent probe, in this case, a Taqman probe, to reach the threshold for detection (Bustin and Nolan, 2004, Nolan et al., 2006, Schmittgen and Livak, 2008). Collected CT values were subsequently exported to Microsoft Excel for additional analysis. 50ng of cDNA template was used for all genes investigated in order to keep the amount of cDNA constant (with the exception of the  $\beta_3$ -adrenergic receptor due to its low abundance in left ventricular tissue). For the analysis of all gene expression experiments, in terms of diurnal variation, the resting period (ZT3) time-point was used as the calibrator, to which all active period (ZT15) samples were compared. In the developmental analysis of gene expression between adolescent and adult SHR, the adolescent SHR was used a calibrator (see discussion 6).

## ***2.6 Experimental solutions***

Unless otherwise stated, all chemicals, solutions and drugs were purchased directly from Sigma.

### **2.6.1 Myocyte isolation and superfusion**

The Tyrode solutions used to isolate and superfuse the isolated myocytes in this investigation are based upon the solutions used by members of this laboratory (Rodrigo et al., 2002, Rodrigo et al., 2004, Rodrigo and Standen, 2005b, Rodrigo and Samani, 2008, Collins and Rodrigo, 2010). Normal Tyrode solution contained the following (in mM): NaCl 135, KCl 6, MgCl<sub>2</sub> 1, CaCl<sub>2</sub> 2, NaH<sub>2</sub>PO<sub>4</sub> 0.33, Na-pyruvate 5, Glucose 10, HEPES 10. The pH of the solution was titrated to 7.4 by the addition of 1M NaOH or 1M HCl (Merck).

The enzyme-containing Tyrode used during the myocyte isolation process contained type I collagenase (1mg/ml)/ Type XIV protease (0.67mg/ml) and Bovine serum albumin (BSA, 1.67mg/ml) in Ca<sup>2+</sup>-free Tyrode. Ca<sup>2+</sup>-free Tyrode solution used in the myocyte isolation process was the same as normal Tyrode; however, 2mM CaCl<sub>2</sub> was not added. All solutions were made using Milli-Q de-ionised water (Millipore).

### **2.6.2 Experimental drugs**

(-)-Isoproterenol hydrochloride (ISO) was made up as a stock solution of 10mM in 200 proof (absolute) ethanol and this stock solution was kept refrigerated in a foil covered bottle and used within 4 weeks. A separate stock solution of 1μM ISO was prepared on the day of experiment from the 10mM stock from which various experimental dilutions were produced (discussed in chapter 4). N-ω-nitro-L-arginine (L-NNA) was made up as a 500μM stock solution which was prepared on the day of experiment, by the addition of solid L-NNA to normal Tyrode. For experiments involving the

measurement of SR  $\text{Ca}^{2+}$  content, a stock solution of 20mM caffeine was produced by the addition of caffeine to normal Tyrode.

### **2.6.3 Fluorescent dyes**

Fura-2 AM was purchased from Molecular Probes (Invitrogen); kept wrapped in foil, to prevent photobleaching of the dye, and stored in a freezer ( $-20^{\circ}\text{C}$ ). In addition, Fura-2 (2mM) was dissolved in DMSO containing 5% by weight Pluronic acid.

### **2.6.4 Molecular biology**

$\beta$ -mercaptoethanol was added to buffer RLT, from the Qiagen RNeasy plus mini kit, on the morning of each RNA isolation, as indicated by manufacturers protocol. 70% ethanol used during RNA extraction was produced by the addition of 200 proof (absolute) ethanol to Milli-Q de-ionised water. The RNase-free DNase set (Qiagen) and the additional DNase protocol which both utilized an amplification grade DNase I were prepared and used as indicated in the manufacturer's instructions. For quantitative real-time RT-PCR, RNA and cDNA samples were diluted using nuclease-free water purchased from Ambion. A stock solution of 0.5M ethylenediamine tetraacetic acid (EDTA) was produced by the addition of EDTA to Milli-Q de-ionised water and the pH was titrated to pH 8, as EDTA is soluble at this pH. Tris-borate-EDTA (TBE) buffer used to make and run RNA gels was produced by the addition of the following to Milli-Q water: 890nM Tris base, 890nM Boric acid and 20mM pH8 0.5M EDTA. A 10mg/ml ethidium bromide stock solution was prepared by the addition Milli-Q de-ionised water, of which 0.5  $\mu\text{g}/\text{ml}$  was required for the visualization of each gel.

## ***2.7 Data acquisition and statistics***

Fluorescence data were collected using a PTI bryte box acquisition system and analysed in PTI Felix 32 software. Cell length data were collected using Clampfit 9.2 software. Quantitative real-time RT-PCR data were collected using Applied Biosystems SDS 2.1 software in combination with an Applied Biosystems ABI-PRISM 7900HT sequence detector real-time PCR machine. RNA spectrophotometry results were collected using nanodrop software ND-8000 V1 0.3 and all data files were saved as picture files (j.peg). All gel pictures were visualised using a Syngene Gene genius bioimaging system and its relevant software, Genesnap. Data sets from all experiments were exported to and tabulated in Microsoft Excel, prior to graphical and statistical analysis in Graphpad prism 4.

Prior to statistical analysis, data sets were analysed for the presence of normal (Gaussian) distribution using a D'Agostino & Pearson omnibus normality test and if data sets were normally distributed, parametric statistical tests were applied. Statistical significance of parametric data was calculated using either a student's *t*-test, when comparing two single variables, or a two way ANOVA followed by a Bonferroni *post-hoc* test, when comparing multiple variables, where  $p < 0.05$  was considered statistically significant. All statistical tests are indicated in the text and were performed using Graphpad Prism 4.

All experiments were performed at  $35 \pm 2^\circ\text{C}$  at pH 7.4 and cells were stimulated at 1Hz, unless otherwise stated. For fluorescence experiments, where one myocyte was equal to one experiment,  $n$  = number of experiments/hearts; in experiments where measurements were taken from a field of multiple myocytes, for example arrhythmia experiments,  $n$  = number of cells; number of experiments; hearts and in PCR experiments,  $n$  = number of sample hearts. For all of the data sets presented in this investigation, at least 3 experimental animals from each time-point were used and are indicated in the text (with the exception of  $\text{Ca}^{2+}$  measurements obtained at a stimulation frequency of 2Hz, see

chapter 4). Where possible the data are presented as mean  $\pm$  standard error of the mean (S.E.M.), unless otherwise stated in the text.

## **Chapter 3: Diurnal variation in excitation-contraction coupling in rat ventricular myocytes**

### ***3.1 Introduction***

The onset of ventricular arrhythmias associated with SCD, has been shown to peak in the hours after waking in man, typically between the hours of 6am and 10am, and is believed to reflect a decrease in the arrhythmic threshold of the ventricular myocardium (Arntz et al., 1993, Goldstein et al., 1996). The morning increase in myocardial sensitivity is thought to be a result of diurnal changes in the following underlying factors: cardiovascular haemodynamics, the cardiac AP, sympathetic stimulation and cardiac metabolism (Guo and Stein, 2003). However, the increased morning incidence of ventricular arrhythmias may also reflect  $\text{Ca}^{2+}$  mismanagement and therefore may suggest that diurnal variation exists in  $\text{Ca}^{2+}$  regulation.

In recent years, the presence of molecular elements of the circadian clock have been shown to exist in the cardiomyocyte (Davidson et al., 2005, Durgan et al., 2005). This peripheral cardiomyocyte clock has been shown to regulate cardiac metabolic gene expression and this regulation of the metabolic gene expression is suggested to account for the time-of-day dependent response of the myocardium to I/R injury (Durgan et al., 2005, Durgan et al., 2010).

Indeed, the documented percentage of rodent cardiac genes believed to exhibit diurnal patterns of expression is thought to be approximately 10-15% (Storch et al., 2002, Martino et al., 2004). Of these, Young *et al* (2001a) have shown that a strong diurnal pattern exists in the expression of many cardiac carbohydrate, fatty acid and mitochondrial metabolic genes, which peak in expression between ZT15-18, when the nocturnal rat is active and this shows a similar dependence on time-of-day to cardiac power,  $\text{O}_2$  consumption and carbohydrate oxidation. The authors linked the diurnal changes in cardiac metabolic genes to the intrinsic expression of circadian clock genes

(Young et al., 2001a). The diurnal variations in BP, HR, and SV may result from a similar diurnal variation in EC-coupling; however, this is yet to be shown. This is important as diurnal variations seen in BP, HR and SV (Veerman et al., 1995), K<sup>+</sup> channels (Kv4.2 and Kv1.5) (Yamashita et al., 2003), QT interval (Bexton et al., 1986, Yi et al., 1998), cardiac conduction and refractoriness (Cinca et al., 1986, Kong et al., 1995), contractile performance (Young et al., 2001a), alpha myosin heavy chain (MHC) expression (Wang et al., 1999) and sympathetic stimulation (Hayano et al., 1990, Dodt et al., 1997) may have an impact on Ca<sup>2+</sup> homeostasis, EC-coupling and therefore the arrhythmic threshold of the myocardium.

Cardiac EC-coupling is the physiological process that links the AP, Ca<sup>2+</sup> homeostasis and contraction. During the cardiac ventricular AP, a wave of depolarisation spreads across the surface of the ventricular myocyte and into the T-tubules, opening LTCC and allowing Ca<sup>2+</sup> to enter the myocyte. Reverse-mode NCX is also believed to contribute to Ca<sup>2+</sup> entry (Bers, 2002). The entry of Ca<sup>2+</sup> triggers CICR from the SR through the opening of RyR2, resulting in the release of Ca<sup>2+</sup> from the SR lumen, the increase in cytoplasmic [Ca<sup>2+</sup>]<sub>i</sub> and subsequent binding of Ca<sup>2+</sup> to the contractile proteins to initiate contraction. Relaxation occurs as this inward Ca<sup>2+</sup> current inactivates promoting cardiac AP repolarisation and the dissociation of Ca<sup>2+</sup> bound to the contractile myofilaments. In the rat, Ca<sup>2+</sup> is removed from the cytoplasm, mainly by the action of SERCA, in which Ca<sup>2+</sup> re-enters the SR and to a lesser extent NCX, in which Ca<sup>2+</sup> leaves the myocyte (see section 1.3 of introduction). Therefore, diurnal variations in Ca<sup>2+</sup>-regulation could result from numerous cell processes.

Diurnal variation has been reported in intracellular Ca<sup>2+</sup> levels, LTCC current and TTCC receptor expression in the brain (Milhaud et al., 1972, Pennartz et al., 2002, Nordskog et al., 2006) and intracellular Ca<sup>2+</sup> levels in small intestine (Wrobel and Nagel, 1979) and blood serum (Wills, 1970). However, it is not known whether a diurnal variation exists in the processes involved in EC-coupling and Ca<sup>2+</sup>-homeostasis within the heart. We have therefore set out to determine whether any diurnal variation exists in normal EC-coupling in rat ventricular myocytes with respect to the Ca<sup>2+</sup>

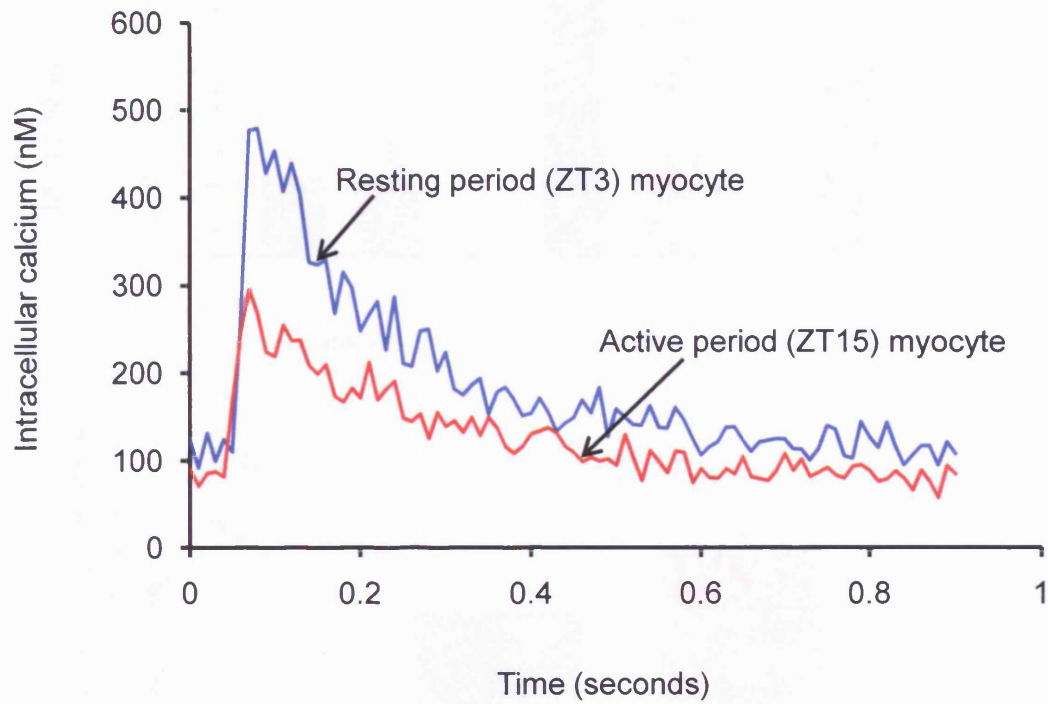
transient, cell contraction strength and SR  $\text{Ca}^{2+}$  content. We also looked at the expression of several key components of EC-coupling to see whether any difference reflects changes in gene expression.

## **3.2 Results**

### **3.2.1 Diurnal variation in the basal $\text{Ca}^{2+}$ transient**

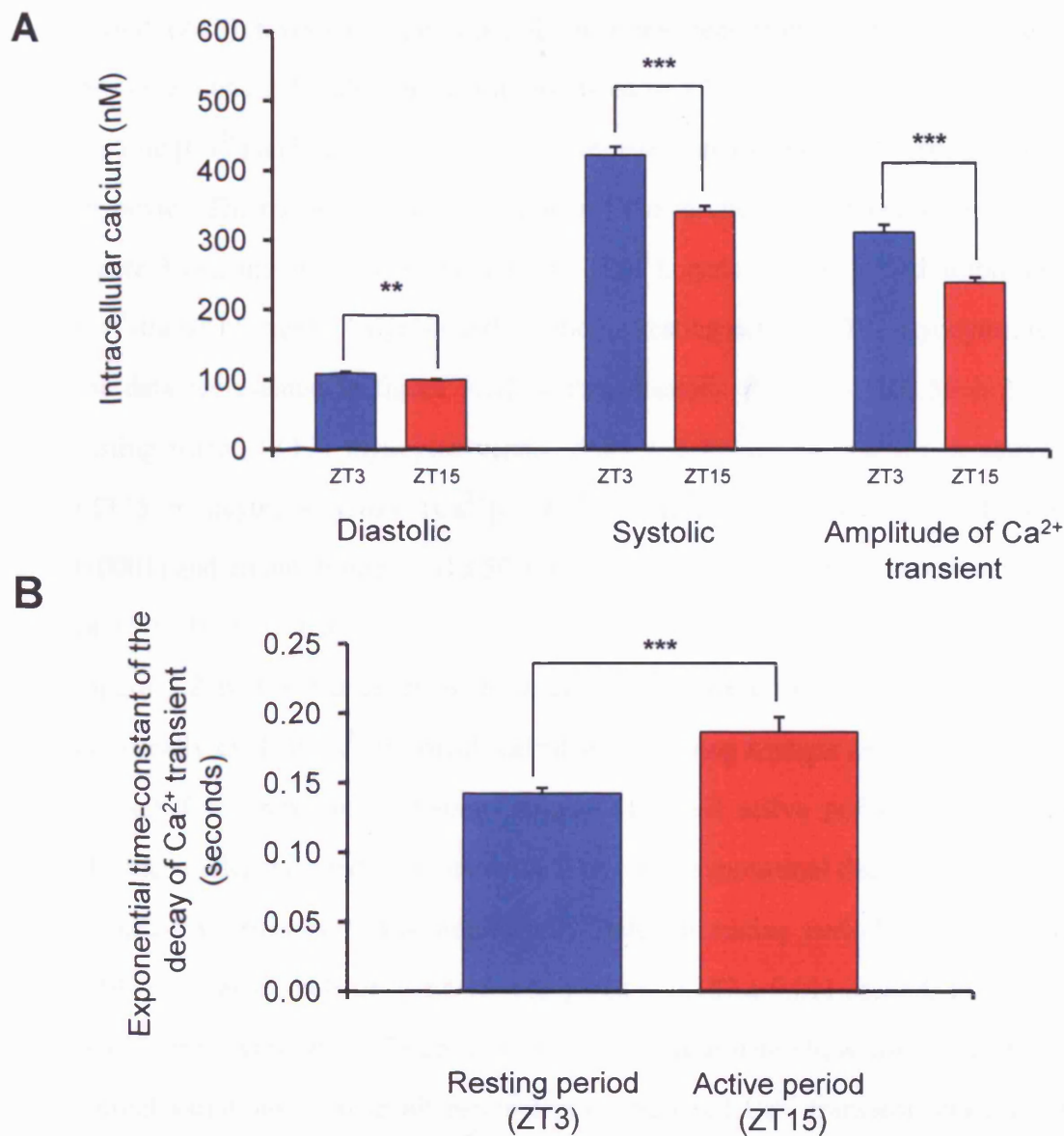
Intracellular  $\text{Ca}^{2+}$  is integral for normal cardiac EC-coupling, through a process that links electrical excitation to  $\text{Ca}^{2+}$  and contraction. We hypothesised that  $\text{Ca}^{2+}$  homeostasis during contraction, may exhibit diurnal variation, as cardiac contractile performance,  $\text{O}_2$  consumption and SV are increased in the early hours of the morning in man (Veerman et al., 1995, Young et al., 2001a). These parameters are likely to impact on  $\text{Ca}^{2+}$  homeostasis, as  $\text{Ca}^{2+}$  and contraction are linked. To investigate whether diurnal variation exists in the basal  $\text{Ca}^{2+}$  transient, measurements of  $[\text{Ca}^{2+}]_i$  were made using the fluorescent dye, Fura-2, in resting period (ZT3) and active period (ZT15) myocytes. Fura-2 loaded cells were superfused with normal Tyrode and stimulated by electrical field stimulation at 1Hz and the resulting  $\text{Ca}^{2+}$ -transients were recorded and the following measurements made: diastolic  $[\text{Ca}^{2+}]$ , systolic  $[\text{Ca}^{2+}]$ , amplitude of  $\text{Ca}^{2+}$  transient and the exponential decay of the electrically-evoked  $\text{Ca}^{2+}$  transient, calculated by fitting a single exponential to the slope of  $\text{Ca}^{2+}$  transient. Myocytes in which the diastolic Fura-2 ratio was  $>1$  (diastolic  $\text{Ca}^{2+}$   $\sim 250\text{-}300\text{nM}$ ) when superfused with normal Tyrode were not selected for experimentation.

Figure 2.5 A shows an experimental trace of a typical basal  $\text{Ca}^{2+}$ -transient recorded from a single resting period (ZT3) myocyte superfused with normal Tyrode and stimulated at 1Hz, in which diastolic  $[\text{Ca}^{2+}]$ , systolic  $[\text{Ca}^{2+}]$  and amplitude of  $\text{Ca}^{2+}$  transient are indicated. Figure 3.1 is a record of a single  $\text{Ca}^{2+}$ -transient from a resting



**Figure 3.1- The  $\text{Ca}^{2+}$  transient of resting period (ZT3) and active period (ZT15) myocytes recorded in normal Tyrode.**

Example of a representative  $\text{Ca}^{2+}$  transient recorded from a resting period (ZT3) myocyte (blue) and an active period (ZT15) myocyte (red) superfused with normal Tyrode and stimulated at 1Hz.



**Figure 3.2- The parameters of the Ca<sup>2+</sup> transient of resting period (ZT3) and active period (ZT15) myocytes recorded in normal Tyrode.**

A. Bar chart showing the diastolic [Ca<sup>2+</sup>] (left), systolic [Ca<sup>2+</sup>] (middle) and amplitude of the Ca<sup>2+</sup> transient (right) recorded from resting period (ZT3; blue) and active period (ZT15) myocytes (red), stimulated at 1Hz and superfused with normal Tyrode. Values are the mean  $\pm$  S.E.M; number of experiments/ hearts = resting period (ZT3) myocyte,  $n = 166/ 15$  and active period (ZT15) myocyte,  $n = 176/ 16$ ; \*\*  $p < 0.05$ , \*\*\*  $p < 0.0001$ , unpaired students  $t$  test.

B. Bar chart showing the exponential time-constant of the decay of the electrically-evoked Ca<sup>2+</sup> transient from resting period (ZT3) myocytes (blue) and active period (ZT15) myocytes (red). The exponential decay of the Ca<sup>2+</sup> transient was calculated by fitting a single exponential to the slope of Ca<sup>2+</sup> transient. Values are the mean  $\pm$  S.E.M; number of experiments/ hearts = resting period (ZT3) myocyte,  $n = 166/ 15$  and active period (ZT15) myocyte,  $n = 176/ 16$ ; \*\*\*  $p < 0.0001$ , unpaired students  $t$  test.

period (ZT3) myocyte superimposed on a transient from an active period (ZT15) myocyte, obtained under the conditions stated in 3.1A, and shows that diastolic  $[Ca^{2+}]_i$ , systolic  $[Ca^{2+}]_i$  and the amplitude of  $Ca^{2+}$ -transient are higher in the resting period (ZT3) myocyte. The mean data obtained from such experiments, is shown in the bar chart in figure 3.2A, and shows that the diastolic  $[Ca^{2+}]_i$ , systolic  $[Ca^{2+}]_i$ , and amplitude of the  $Ca^{2+}$ -transient, were all significantly higher in resting period (ZT3) myocytes, reflecting the data represented in figure 3.1B, with a diastolic  $[Ca^{2+}]_i$  of  $108.56 \pm 2.23$  nM in resting period (ZT3) myocytes versus  $99.89 \pm 1.79$  nM ( $p < 0.05$ ) in active period (ZT15) myocytes; a systolic  $[Ca^{2+}]_i$  of  $422.05 \pm 12.23$  nM versus  $340.79 \pm 8.69$  nM ( $p < 0.0001$ ) and an amplitude of  $313.50 \pm 11.06$  nM versus ( $n = 166/ 15$ )  $240.92 \pm 7.50$  nM ( $n = 176/ 16; p < 0.0001$ ).

Figure 3.2 B is a bar chart of the mean data showing the exponential decay of the electrically-evoked  $Ca^{2+}$  transient, calculated by fitting a single exponential to the slope of each  $Ca^{2+}$  transient in resting period (ZT3) and active period (ZT15) myocytes, obtained under the conditions stated in 3.1A. The exponential decay of the electrically-evoked  $Ca^{2+}$  transients was significantly faster in resting period (ZT3) myocytes, at  $0.142 \pm 0.004$  seconds ( $n = 166/15$ ) compared to  $0.187 \pm 0.011$  seconds in active period (ZT15) myocytes ( $n = 176/16; p < 0.0001$ ). These data show for the first time that diurnal variations exist in all parameters of the basal  $Ca^{2+}$  transient (diastolic  $[Ca^{2+}]_i$ , systolic  $[Ca^{2+}]_i$  and amplitude  $Ca^{2+}$  of the transient), which may reflect underlying changes in components of EC-coupling.

### **3.2.2 Diurnal variation in basal contraction**

We have shown that the basal diastolic  $[Ca^{2+}]_i$ , systolic  $[Ca^{2+}]_i$  and amplitude  $Ca^{2+}$  of the transient are significantly higher in resting period (ZT3) than active period (ZT15) myocytes. Due to the strong physiological relationship existing between intracellular  $Ca^{2+}$  and the mechanical process of contraction in EC-coupling (Bers, 2002), and given

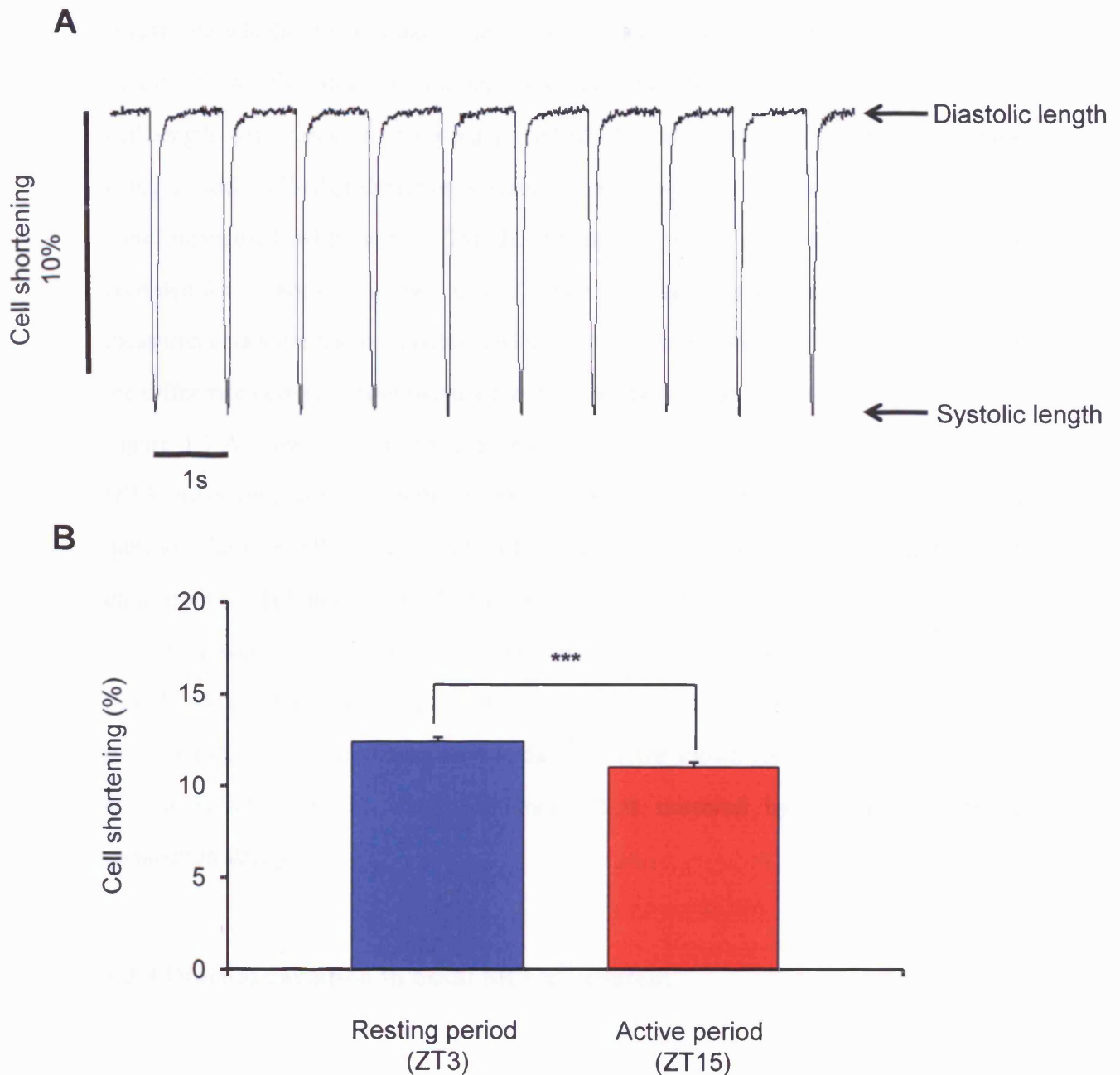


**Figure 3.3 – Percentage cell shortening of resting period (ZT3) and active period (ZT15) myocytes recorded in normal Tyrode**

A. Example recording of contraction (cell shortening) from a resting period (ZT3) myocyte, perfused with normal Tyrode and stimulated at a rate of 1Hz. Data were collected as diastolic and systolic lengths from which percentage cell shortening was obtained.

B. Bar chart showing contraction strength, assessed as percentage cell shortening, recorded from resting period (ZT3) myocytes (blue) and active period (ZT15) myocytes (red). Values are the mean  $\pm$  S.E.M; number of experiments/ hearts = resting period (ZT3) myocyte  $n = 209/ 4$  and active period (ZT15) myocyte  $n = 216/ 4$ , \*\*\*  $p < 0.0001$ , unpaired students  $t$  test.

the documented diurnal variation in SV (Veerman et al., 1995), we decided to investigate whether the diurnal variation in  $\text{Ca}^{2+}$  is mirrored in contraction strength. To investigate whether diurnal variation exists in contraction strength, measurements of cell length were made from resting period (ZT3) and active period (ZT15) myocytes using a video cell-edge detection system. To measure basal contraction strength, cells were superfused with normal Tyrode and stimulated at 1Hz and cell length was recorded for 30 seconds in each cell to obtain a stable constant trace, from which two measurements were taken, diastolic and systolic cell length (shown in figure 3.3 A) and the difference between these two used to calculate percentage cell shortening.

Figure 3.3 A shows an experimental trace of cell length from a typical resting period (ZT3) myocyte superfused with normal Tyrode and stimulated at 1Hz and the cell in question shows a cell shortening of ~12%. Figure 3.3B is a bar chart showing the mean data, from experiments described in figure 3.3A, and shows that basal percent cell shortening was significantly higher in resting period (ZT3) myocytes at  $12.41 \pm 0.22 \%$  ( $n = 209/4$ ) compared to  $11.02 \pm 0.26 \%$  in active period (ZT15) myocytes ( $n = 216/4$ ;  $p < 0.0001$ ). Therefore, based on this data, we have shown for the first time that the diurnal variation in the basal  $\text{Ca}^{2+}$ -transient is mirrored by similar changes in contraction strength.

### **3.2.3 Diurnal variation in basal SR $\text{Ca}^{2+}$ content**

An important component of the EC-coupling pathway, which could be responsible for the enhanced  $\text{Ca}^{2+}$ -transient in resting period (ZT3) myocytes, is SR  $\text{Ca}^{2+}$  content. Many physiological stimuli that increase contraction strength and the  $\text{Ca}^{2+}$ -transient do so by increasing the  $\text{Ca}^{2+}$ -content of the SR (Bassani et al., 1995, Bers, 2002). The data shows a faster rate of decay of the electrically-evoked  $\text{Ca}^{2+}$ -transient in resting period (ZT3) myocytes, which probably reflects an increase in SERCA activity as SERCA is the predominant mechanism by which  $\text{Ca}^{2+}$  is sequestered during relaxation in the rat

myocyte and this might be expected to lead to an increase in SR  $\text{Ca}^{2+}$ -content (Bassani et al., 1994, Bers, 2001, Bers, 2002). As the  $\text{Ca}^{2+}$ -transient dynamics and contraction are dependent upon the amount of  $\text{Ca}^{2+}$  released from the SR during activation; we next looked at whether the SR  $\text{Ca}^{2+}$  content displays diurnal variation by determining SR  $\text{Ca}^{2+}$  loading in resting period (ZT3) and active period (ZT15) myocytes. To investigate whether diurnal variation exists in SR  $\text{Ca}^{2+}$  content, we rapidly applied 20mM caffeine to release SR  $\text{Ca}^{2+}$ . Fura-2 loaded cells were stimulated at 1Hz and superfused with normal Tyrode for 5 minutes, until a constant  $\text{Ca}^{2+}$ -transient was recorded. The electrical stimulator was switched off for 10 seconds and the cells were rapidly perfused with normal Tyrode containing 20mM caffeine for 5 seconds, which resulted in the release of  $\text{Ca}^{2+}$  from the SR, visible as a large  $\text{Ca}^{2+}$ -transient. After the caffeine-induced  $\text{Ca}^{2+}$  transient had declined, the stimulation was re-started and cells were perfused with normal Tyrode to allow recovery of basal  $\text{Ca}^{2+}$ -transients. Any experiment where the magnitude of the  $\text{Ca}^{2+}$ -transient was significantly altered following the rapid application of caffeine (i.e. less than 80% of the basal  $\text{Ca}^{2+}$  transient) was discarded. From each caffeine-induced  $\text{Ca}^{2+}$  transient, two measurements were taken, these were: the peak caffeine-induced  $\text{Ca}^{2+}$  transient, which reflects SR  $\text{Ca}^{2+}$  content, and the exponential rate of decay of the transient, calculated by fitting a single exponential to the slope of each caffeine  $\text{Ca}^{2+}$  transient, which reflects the activity of the NCX1 and PMCA (Bassani et al., 1994).

Figure 3.4 A shows experimental traces of typical caffeine  $\text{Ca}^{2+}$  transients recorded from a resting period (ZT3) myocyte (top; blue) and an active period (ZT15) myocyte (bottom; red) superfused with normal Tyrode and shows that the peak of the caffeine  $\text{Ca}^{2+}$  transient is greater in the resting period (ZT3) myocyte in comparison to the active period (ZT15) myocyte. These differences are highlighted in figure 3.4B, where the caffeine  $\text{Ca}^{2+}$  transients shown in figure 3.4A are overlapped. The mean data of the basal SR  $\text{Ca}^{2+}$  content, assessed as the peak  $\text{Ca}^{2+}$  in response to 20mM caffeine, is shown in the bar chart in figure 3.5A, and shows that basal SR  $\text{Ca}^{2+}$  content was significantly higher in resting period (ZT3) myocytes at  $672.8 \pm 20.5$  nM ( $n = 71/3$ ) than active

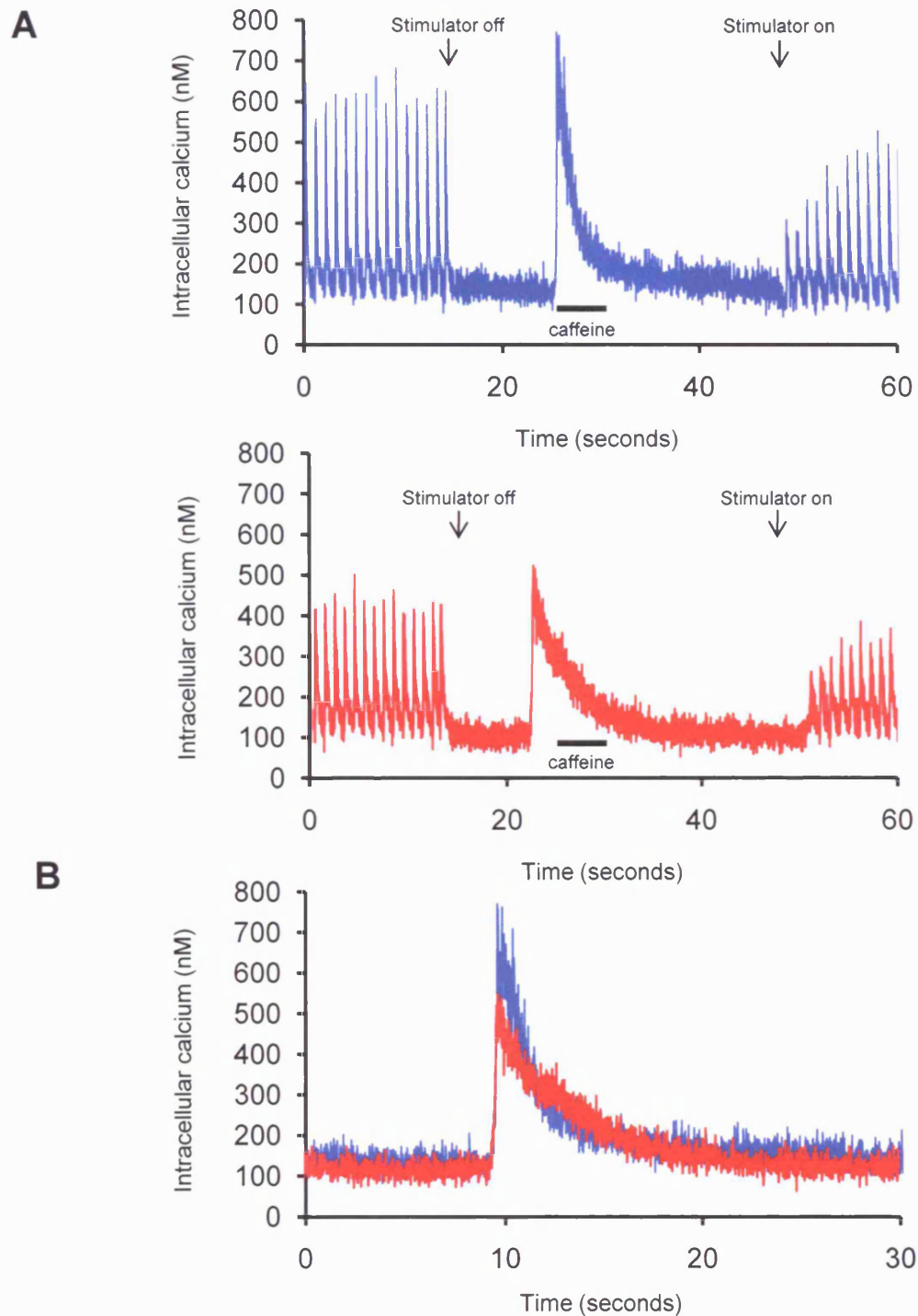


**Figure 3.4- Caffeine-induced  $\text{Ca}^{2+}$  transients in ZT3 and ZT15 ventricular myocytes recorded in normal Tyrode.**

A. Example record of intracellular calcium from a single ZT3 myocyte (top; blue) and a ZT15 myocyte (bottom; red). The cell stimulator was switched off for ~10 seconds before superfusing the myocytes with normal Tyrode containing 20mM caffeine for 5 seconds.

B. Expanded trace of the caffeine-induced  $\text{Ca}^{2+}$  transients obtained in A.

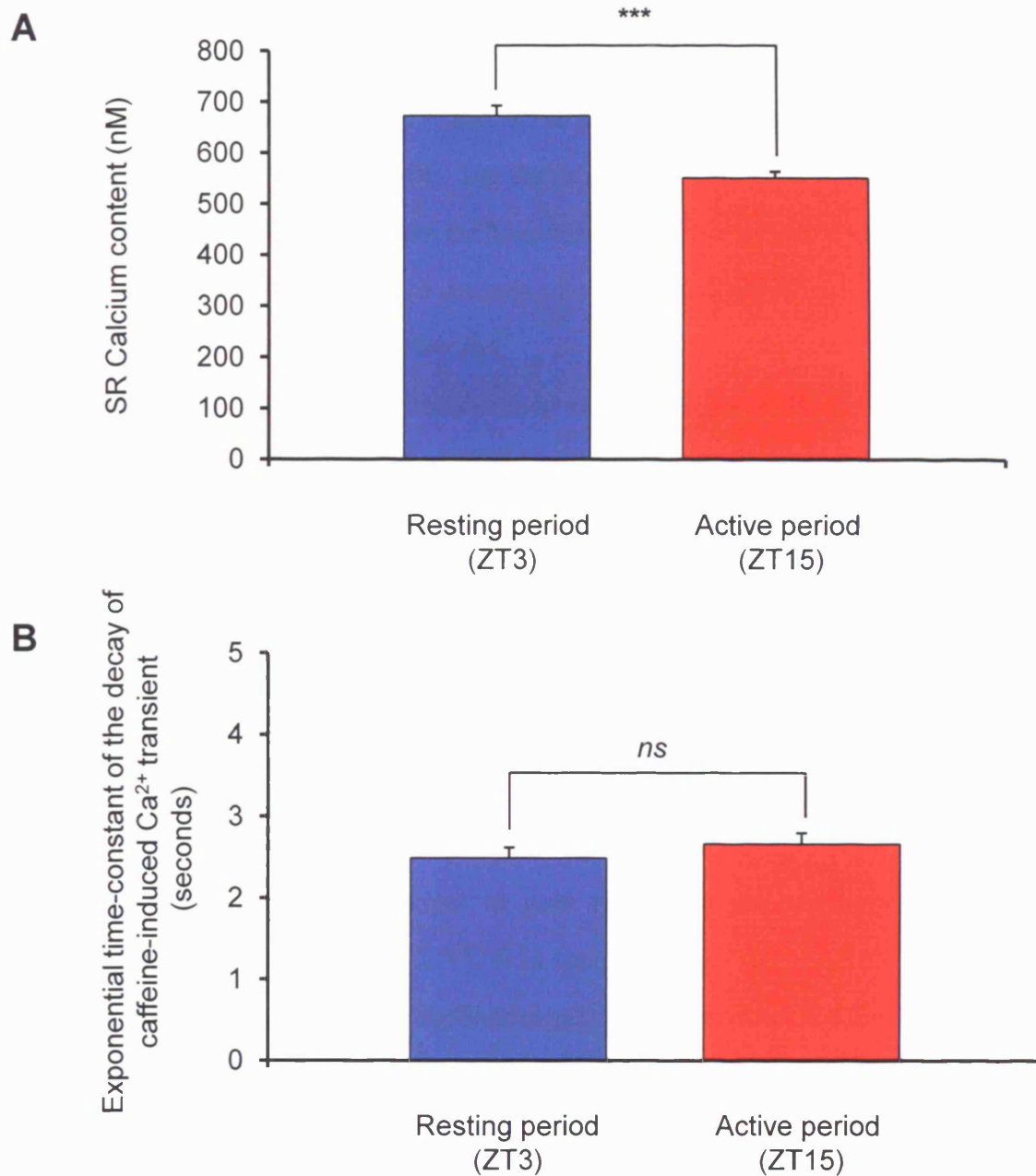


**Figure 3.5- The sarcoplasmic reticulum  $\text{Ca}^{2+}$  content in resting period (ZT3) and active period (ZT15) myocytes recorded in normal Tyrode**

- A. Bar chart showing the sarcoplasmic reticulum  $\text{Ca}^{2+}$  content recorded from resting period (ZT3) myocytes (blue) and active period (ZT15) myocytes (red). Values are the mean  $\pm$  S.E.M.; numbers of experiments/ hearts = resting period (ZT3) myocyte,  $n = 71/3$  and active period (ZT15) myocyte,  $n = 97/4$ , \*\*\*  $p < 0.0001$ , unpaired students  $t$  test.
- B. Bar chart showing the exponential time-constant of the decay of the caffeine-induced  $\text{Ca}^{2+}$  transient recorded from resting period (ZT3) myocytes (blue) and active period (ZT15) myocytes (red). Values are the mean  $\pm$  S.E.M.; numbers of experiments/ hearts = resting period (ZT3) myocyte,  $n = 71/3$  and active period (ZT15) myocyte,  $n = 97/4$ ; unpaired students  $t$  test.

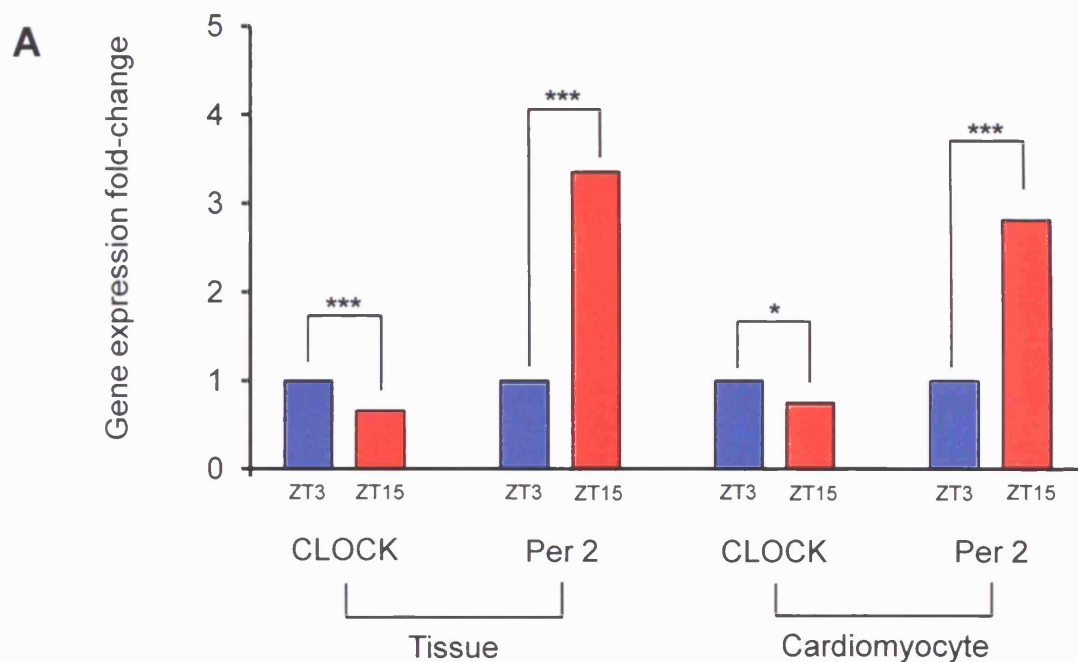
period (ZT15) myocytes at  $551.0 \pm 12.8$  nM ( $n = 97/4$ ;  $p < 0.0001$ ). Figure 3.5B is a bar chart of the mean data showing the exponential decay of the caffeine-induced  $\text{Ca}^{2+}$  transient in resting period (ZT3) and active period (ZT15) myocytes, obtained under the conditions stated in figure 3.4A. The data show that there is no significant difference in rate of exponential decay of the caffeine-induced  $\text{Ca}^{2+}$  transient between resting period (ZT3) myocytes at  $2.58 \pm 0.16$  seconds ( $n = 71/3$ ) and active period (ZT15) myocytes at  $3.16 \pm 0.32$  seconds, ( $n = 97/4$ ; *ns*).

These data show that a significant diurnal variation exists in SR  $\text{Ca}^{2+}$  content in resting period (ZT3) and active period (ZT15) myocytes, which may play a causal role, or contribute to the observed variations in basal  $\text{Ca}^{2+}$  transient and contraction strength between resting period (ZT3) and active period (ZT15) myocytes.

### 3.2.4 Diurnal variation in circadian clock and metabolic genes

In order to examine whether the underlying diurnal variation in basal EC-coupling we have identified, reflects changes in gene expression and transcription of the key elements of EC-coupling e.g. LTCC ( $\alpha 1c$  subunit), NCX1, NHE1, SERCA 2a, PLB and RyR2, we next looked at whether diurnal variation exists in mRNA levels.

In order to study diurnal variation in gene expression, the possibility of diurnal variation in the chosen *housekeeping gene* needed to be eliminated, as it is known that many commonly used *housekeeping genes*, for example, GAPDH, show diurnal variation (Shinohara et al., 1998). Therefore, to check that expression of the *housekeeping gene*,  $\beta$ -actin used in the present investigation, was not subject to diurnal variation, quantitative real-time Taqman RT-PCR was performed on the left ventricular free-wall tissue isolated from Wistar rat hearts at time-points during the resting period (ZT3) and active period (ZT15) (see section 2.5.9 of methods). The CT expression of  $\beta$ -actin did not significantly differ between left ventricular free-wall tissue isolated during the resting period (ZT3) at  $18.66 \pm 0.02$  ( $n = 5$ ) and active period (ZT15) at  $18.64 \pm 0.07$  ( $n$



**B**

| Gene of interest |               | $\Delta$ CT (normalised to $\beta$ -actin) |                      | <i>p</i> -value (from $\Delta$ CT) | Fold change ZT15 (Pfaffl) |
|------------------|---------------|--------------------------------------------|----------------------|------------------------------------|---------------------------|
|                  |               | Resting period (ZT3)                       | Active period (ZT15) |                                    |                           |
| Per 2            | Tissue        | 7.90 $\pm$ 0.22                            | 6.14 $\pm$ 0.12      | <i>p</i> = 0.0003<br>***           | 3.35<br>#                 |
| CLOCK            |               | 5.23 $\pm$ 0.05                            | 5.90 $\pm$ 0.10      | <i>p</i> = 0.0004<br>***           | 0.66<br>#                 |
| Per 2            | Cardiomyocyte | 6.42 $\pm$ 0.08                            | 4.79 $\pm$ 0.06      | <i>p</i> < 0.0001<br>***           | 2.81<br>#                 |
| CLOCK            |               | 3.96 $\pm$ 0.11                            | 4.44 $\pm$ 0.19      | <i>p</i> = 0.05<br>*               | 0.75<br>#                 |

**Figure 3.6- Gene expression levels of the circadian clock genes, CLOCK and Per2, in Wistar rat hearts isolated during the resting period (ZT3) and active period (ZT15).**

A. Bar chart showing quantitative real-time RT-PCR of CLOCK and Per2 mRNA expression as fold-changes in left ventricular free-wall (left) and ventricular myocytes (right) isolated during the resting period (ZT3; blue) and active period (ZT15; red) of the Wistar rat. Both CLOCK and Per2 mRNA was normalised to  $\beta$ -actin mRNA. Fold-change of CLOCK and Per2 mRNA were calculated using the Pfaffl method (#, see appendix 1 figure 1) relative to the control (ZT3; blue bars). The results are mean  $\pm$  S.E.M.; Number of samples = resting period (ZT3) *n* = 5 and active period (ZT15) *n* = 5. \* *p* < 0.05, \*\*\* *p* < 0.001, unpaired students *t* test performed on  $\Delta$ CT values.

B. Table showing the data used to produce the bar chart in figure 3.6A.

= 6;  $p = 0.77$ , *ns*, data not shown as figure). This data shows that  $\beta$ -actin gene expression does not exhibit diurnal cycling, and was therefore an appropriate *housekeeping gene* to which diurnal cycling of other genes investigated could be normalised.

Young *et al* (2001a), amongst others, have studied diurnal variation in the circadian clock genes, *Per2* and *CLOCK*, and the mitochondrial metabolic genes, *UCP2* and *UCP3*, normalised to  $\beta$ -actin expression (Naito *et al.*, 2003, Yamamoto *et al.*, 2004). They have shown that *Per2* expression peaks between ZT15-18 during the active period of the rat and that *CLOCK* shows an opposite pattern and peaks in expression between ZT0-3 during the resting period of the rat.

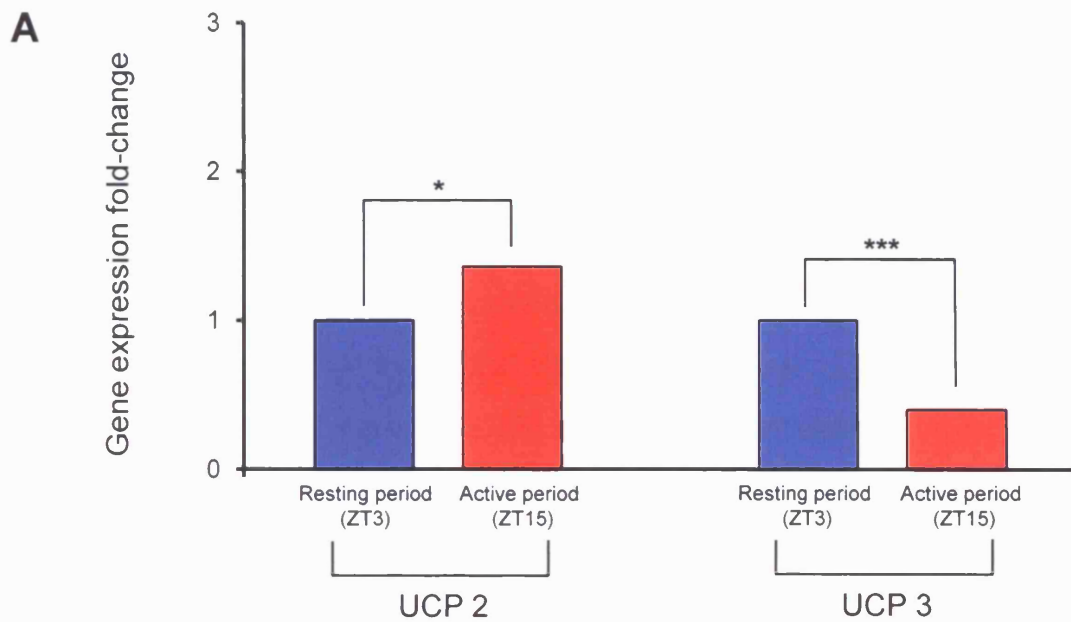
To validate our technique for determining gene expression, we performed quantitative real-time Taqman RT-PCR on the circadian clock genes, *Per2* and *CLOCK*, to check for consistency with published data and to determine whether the isolation of single ventricular myocytes had any effect on the intrinsic circadian clock in myocardial cells. Gene expression was normalised to the control gene  $\beta$ -actin and fold-changes were calculated using the Pfaffl method (see appendix 1 for details). Statistics were performed on the  $\Delta$ CT values. The resting period (ZT3) sample was used as a reference sample or “calibrator” to which the active period (ZT15) samples were compared, and therefore has an average fold change of 1 in each PCR dataset.

Figure 3.6 A is a bar chart showing gene expression fold-change measurements for *Per2* and *CLOCK*, in snap frozen left ventricular free-wall tissue (left) and isolated left ventricular myocytes (right). *CLOCK* expression was significantly higher in both tissue and myocytes isolated during the resting period (ZT3) in comparison to active period (ZT15), which corresponded to a fold-change of 0.66 in active period (ZT15) tissue ( $p = 0.0004$ ) and 0.75 in active period (ZT15) myocytes ( $p = 0.05$ ). *Per2* expression was significantly higher in both tissue and myocytes isolated during the active period (ZT15) in comparison to the resting period (ZT3), which corresponded to a fold-change of 3.35 in active period (ZT15) tissue ( $p = 0.0003$ ) and 2.81 in active period (ZT15) myocytes ( $p < 0.0001$ ). There was no statistical difference between the PCR data

obtained from tissue and isolated myocytes within the active period (ZT15) time-point for Per2 expression ( $p = 0.25$ ) and CLOCK expression ( $p = 0.46$ , not shown on figure). All Per2 and CLOCK gene expression were consistent with data published (Young et al., 2001a, Naito et al., 2003, Yamamoto et al., 2004).

Young *et al* (2001a) have also shown that UCP2 peaks in expression, like Per2, between ZT15-18, when the rat is active, however, there is conflicting data for UCP3 expression, as in rat whole heart, UCP3 has a peak expression during the active period (ZT15) and a trough expression at ZT9 (Young et al., 2001a) and the same group later showed that UCP3 has a peak expression during the resting period (ZT3) and a trough expression at ZT9 in whole rat heart (Durgan et al., 2005). To further validate our technique for determining gene expression, we performed additional quantitative real-time Taqman RT-PCR on the mitochondrial metabolic genes, UCP2, to check for consistency with published data and UCP3, to establish its diurnal profile. Figure 3.7 A is a bar chart showing gene expression fold-change measurements for UCP2 and UCP3 in left ventricular free-wall tissue isolated during the resting period (ZT3) and the active period (ZT15) of the Wistar rat, normalised to the expression of  $\beta$ -actin. UCP2 expression was significantly higher during the active period (ZT15) in comparison to the resting period (ZT3) in the Wistar rat, which corresponded to a fold change of 1.36 in active period (ZT15) tissue ( $p = 0.01$ ). UCP3 expression was significantly higher during the resting period (ZT3) in comparison to the active period (ZT15) in the Wistar and corresponded to a fold change of 0.40 in active period (ZT15) tissue ( $p = 0.0006$ ) and corroborated the data of Durgan *et al* (2005).

Therefore, due to the reliability of  $\beta$ -actin as a *housekeeping gene*, the confirmation of diurnal expression in both circadian clock and metabolic genes and lack of effect that our myocyte isolation process had on the expression of circadian clock genes, we looked at the expression of key components of EC-coupling in the same samples.



**B**

| Gene of interest |        | $\Delta$ CT (normalised to $\beta$ -actin) |                      | <i>p</i> -value (from $\Delta$ CT) | Fold change ZT15 ( $\Delta\Delta$ CT) |
|------------------|--------|--------------------------------------------|----------------------|------------------------------------|---------------------------------------|
|                  |        | Resting period (ZT3)                       | Active period (ZT15) |                                    |                                       |
| UCP 2            | Tissue | 0.48 $\pm$ 0.14                            | 0.04 $\pm$ 0.03      | <i>p</i> = 0.01<br>*               | 1.36<br>\$                            |
| UCP 3            |        | 5.56 $\pm$ 0.16                            | 7.07 $\pm$ 0.21      | <i>p</i> = 0.0006<br>***           | 0.40<br>\$                            |

**Figure 3.7- Gene expression levels of the mitochondrial metabolic genes, UCP2 and UCP3, in Wistar rat hearts isolated during the resting period (ZT3) and active period (ZT15).**

A. Bar chart showing quantitative real-time RT-PCR of UCP2 and UCP3 mRNA expression as fold-changes in left ventricular free-wall isolated during the resting period (ZT3; blue) and active period (ZT15; red) of the Wistar rat. Both UCP2 and UCP3 mRNA was normalised to  $\beta$ -actin mRNA. Fold-change of UCP2 and UCP3 mRNA were calculated using  $\Delta\Delta$ CT (UCP2 and UCP3, \$, see appendix 1 figure 1) relative to the control (ZT3; blue bars). The results are mean  $\pm$  S.E.M.; Number of samples = resting period (ZT3), *n* = 5 and active period (ZT15), *n* = 5. \* *p* < 0.05, \*\*\* *p* < 0.001, unpaired students *t* test performed on  $\Delta$ CT values.

B. Table showing the data used to produce the bar chart in figure 3.7A.

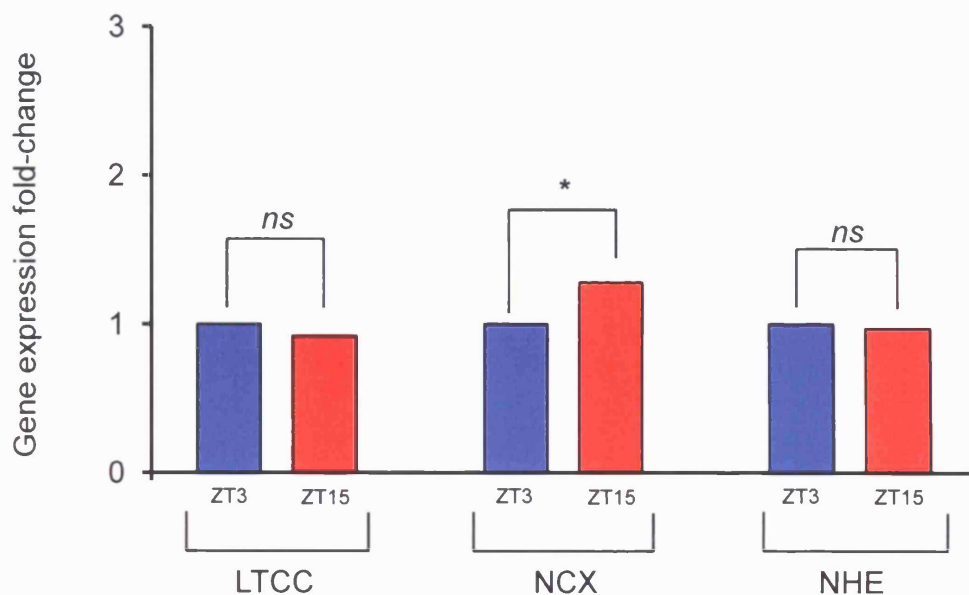
### 3.2.5 Diurnal variation in EC-coupling genes

As our data show that the basal  $\text{Ca}^{2+}$  transient, contraction and SR  $\text{Ca}^{2+}$  content are all higher in resting period (ZT3) myocytes rather than active period (ZT15) myocytes, we hypothesised that  $\text{Ca}^{2+}$  homeostasis may be different due to underlying changes in the expression and transcription of genes involved in EC-coupling.

To determine whether the diurnal changes in the basal  $\text{Ca}^{2+}$  transient, contraction strength and SR  $\text{Ca}^{2+}$  content we have shown, result from changes to gene expression of key components of EC-coupling, we looked at the real-time expression of the following genes involved in EC-coupling: LTCC ( $\alpha 1c$  subunit), NCX1, NHE1, PLB, SERCA 2a and RyR2. In order to look at these genes, quantitative real-time Taqman RT-PCR was performed on the left ventricular free-wall tissue isolated from Wistar rat hearts at time-points during the resting period (ZT3) and active period (ZT15) (see section 2.5.9 of methods).

Figure 3.8 shows the gene expression fold-change measurements for the EC-coupling proteins located in the myocyte sarcolemmal membrane, which are: LTCC ( $\alpha 1c$  subunit), NCX1 & NHE1 in left ventricular free-wall tissue isolated from rats during the resting period (ZT3) and active period (ZT15), normalised to  $\beta$ -actin expression. NCX1 expression was significantly higher during the active period (ZT15) in comparison to the resting period (ZT3), which corresponded to a fold-change of 1.28 in active period (ZT15) tissue ( $p = 0.01$ ). The expression of the LTCC ( $p = 0.28$ , *ns*) and NHE1 ( $p = 0.53$ , *ns*) were not significantly different between the resting period (ZT3) and the active period (ZT15).

Figure 3.9 shows the gene expression fold-change measurements for the EC-coupling proteins located on the SR membrane, which are: PLB, SERCA 2a and RyR2 in left ventricular free-wall tissue isolated during the resting period (ZT3) and the active period (ZT15), normalised to  $\beta$ -actin expression. The expression of PLB ( $p = 0.07$ , *ns*), SERCA 2a ( $p = 0.07$ , *ns*) and RyR2 ( $p = 0.60$ , *ns*) were not significantly different between the resting period (ZT3) and the active period (ZT15).

**A****B**

| Gene of interest |        | $\Delta$ CT (normalised to $\beta$ -actin) |                      | <i>p</i> -value (from $\Delta$ CT) | Fold change ZT15 ( $\Delta\Delta$ CT/Pfaffl) |
|------------------|--------|--------------------------------------------|----------------------|------------------------------------|----------------------------------------------|
|                  |        | Resting period (ZT3)                       | Active period (ZT15) |                                    |                                              |
| LTCC             | Tissue | 5.03 $\pm$ 0.05                            | 5.17 $\pm$ 0.12      | <i>p</i> = 0.2821<br><i>ns</i>     | 0.92<br>\$                                   |
| NCX1             |        | 3.45 $\pm$ 0.07                            | 3.10 $\pm$ 0.06      | <i>p</i> = 0.0126<br>*             | 1.28<br>#                                    |
| NHE1             |        | 6.34 $\pm$ 0.05                            | 6.39 $\pm$ 0.04      | <i>p</i> = 0.5347<br><i>ns</i>     | 0.97<br>#                                    |

**Figure 3.8- Gene expression levels of the sarcolemmal EC-coupling genes, LTCC, NCX1 and NHE1 in Wistar rat hearts isolated during the resting period (ZT3) and active period (ZT15).**

A. Bar chart showing quantitative real-time RT-PCR of LTCC, NCX1 & NHE1 mRNA expression as fold-changes in left ventricular free-wall isolated during the resting period (ZT3; blue) and active period (ZT15; red) of the Wistar rat. LTCC, NCX & NHE mRNA was normalised to  $\beta$ -actin mRNA. Fold-changes were calculated using either the  $\Delta\Delta$ CT (\$, LTCC) or Pfaffl method (#, NCX1 & NHE1; see appendix 1 figure 1) relative to the control (ZT3; blue bars). The results are mean  $\pm$  S.E.M.; Number of samples = resting period (ZT3), *n* = 5 and active period (ZT15), *n* = 5. \* *p* < 0.05, unpaired students *t* test performed on  $\Delta$ CT values.

B. Table showing the data used to produce the bar chart in figure 3.8A.

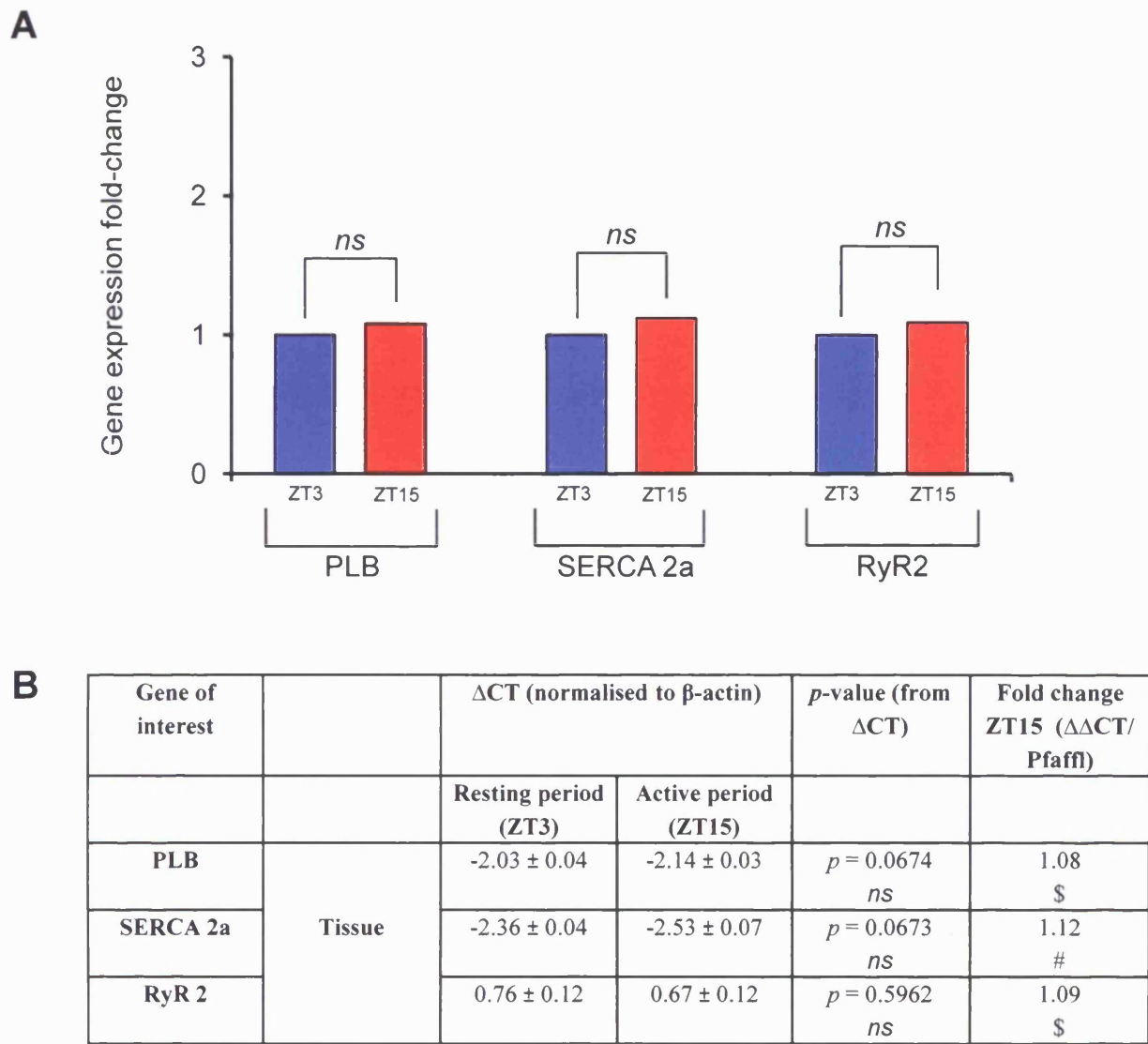


**Figure 3.9- Gene expression levels of the sarcoplasmic reticulum EC-coupling genes, PLB, SERCA 2a & RyR2 in Wistar rat hearts isolated during the resting period (ZT3) and active period (ZT15).**

A. Bar chart showing quantitative real-time RT-PCR of PLB, SERCA 2a & RyR2 mRNA expression as fold changes in left ventricular free-wall isolated during the resting period (ZT3; blue) and active period (ZT15; red) of the Wistar rat. PLB, SERCA 2a & RyR2 mRNA was normalised to  $\beta$ -actin mRNA. Fold changes were calculated using either the  $\Delta\Delta$ CT method (\$; PLB and RyR2) or the Pfaffl method (#, SERCA 2a, see appendix 1 figure 1) relative to the control (ZT3; blue bars). The results are mean  $\pm$  S.E.M.; Number of samples = resting period (ZT3), *n* = 5 and active period (ZT15), *n* = 5; unpaired students *t* test performed on  $\Delta$ CT values.

B. Table showing the data used to produce the bar chart in figure 3.9A.

We have shown that NCX1 mRNA expression is significantly higher in left ventricular free-wall isolated during the active period (ZT15) in comparison to resting period (ZT3), which if translated to protein levels in the SR, may contribute to the decreased  $\text{Ca}^{2+}$  transient in active period (ZT15) myocytes (see discussion).

### ***3.3 Discussion***

In the present chapter, we have shown for the first time that basal EC-coupling in rat ventricular myocytes is subject to diurnal variation. To investigate this time-of-day dependent variation in EC-coupling, we recorded the  $\text{Ca}^{2+}$  transient, resulting contraction strength and SR  $\text{Ca}^{2+}$  content from ventricular myocytes isolated at two opposing time points during the resting period (ZT3) and active period (ZT15) of adult Wistar rats, under basal conditions (superfusion with normal Tyrode). The data show that diastolic  $[\text{Ca}^{2+}]$ , systolic  $[\text{Ca}^{2+}]$ , amplitude of  $[\text{Ca}^{2+}]$  transient and  $\text{Ca}^{2+}$  transient relaxation (the rate of exponential decline of the electrically-evoked  $\text{Ca}^{2+}$  transient) were all significantly higher in resting period (ZT3) myocytes than active period (ZT15) myocytes. The differences in the  $\text{Ca}^{2+}$  transient recorded under basal conditions were mirrored by contraction strength and SR  $\text{Ca}^{2+}$  content, as resting period (ZT3) myocytes had a significantly larger percent cell shortening and SR  $\text{Ca}^{2+}$  content in comparison to active period (ZT15) myocytes. On the basis of this data, we also determined whether the differences in basal EC-coupling were the result of changes in the expression of EC-coupling genes. The gene expression data show that NCX1 mRNA levels are greater in hearts isolated from active period (ZT15) rats. These findings are novel as diurnal variation in  $\text{Ca}^{2+}$  homeostasis and EC-coupling have yet to be reported in cardiac tissue.

### **3.3.1 Is the isolated ventricular myocyte an appropriate model to study diurnal cycling in ventricular function?**

To study the parameters of diurnal variation in the ventricular myocardium, we used the isolated single ventricular myocytes, which facilitates analysis of cellular mechanisms involved in EC-coupling, as our experimental model. However, it was essential we validated our model and quantitative real-time RT-PCR technique. The isolation of single ventricular myocytes is a traumatic and stressful event for the myocardium and the process of isolation may affect many intracellular processes, which may themselves exhibit diurnal variation. The extraction of the heart and isolation of ventricular myocytes are associated with changes in temperature,  $[Ca^{2+}]_i$ , brief periods of ischaemia and serum starvation/shock, all of which have been shown to affect circadian/diurnal variation in cardiac gene expression and function (Mitra and Morad, 1985, Durgan et al., 2005). Serum starvation followed by serum shock of cardiomyocytes has been shown to reset the circadian clock and promote circadian clock gene cycling (Balsalobre et al., 1998, Durgan et al., 2005). Indeed, Durgan *et al* (2005) have shown that long-term exposure (~2 hours) of cultured cardiomyocytes to 50% foetal calf serum (FCS) results in significant circadian clock gene cycling. In the same study, Durgan and colleagues also reported that short-term exposure to the standard cell culture concentration of FCS (2.5% FCS) was also sufficient to permit circadian clock gene cycling following serum starvation but not of the same magnitude as the application of 50% FCS (Durgan et al., 2005). During the ventricular myocyte isolation process used in the present study, cells were exposed for 5 minutes to < 1% bovine serum albumin (BSA) during enzymatic digestion (see section 2.6.1 of methods for detail). Therefore, in order to rule out the effects of the whole isolation process including any effects of BSA on circadian clock gene expression, we looked at the expression of the circadian clock genes, Per2 and CLOCK, in both isolated single ventricular myocytes and immediately snap-frozen LV free-wall. In our study, neither the isolation process nor the involvement of BSA had any effect on the circadian profile of the clock genes, Per2

and CLOCK, as expression was similar between isolated ventricular myocytes and LV free-wall, which was consistent with previously published data (Young et al., 2001a, Naito et al., 2003, Yamamoto et al., 2004). The similarity in the gene expression profiles of Per2 and CLOCK in isolated cardiomyocytes and LV free-wall also indicate that isolating cardiomyocytes does not disrupt the circadian clock. This gene expression data is not surprising as in comparison to Durgan and colleagues, the concentration of BSA that was used in the present study was minimal in comparison to the FCS they used, as in the present study < 1% BSA was used compared with 2.5% and 50% FCS (Durgan et al., 2005). The duration of exposure also differed between the two studies, in that myocytes were exposed to BSA for 5 minutes in the present study whereas Durgan and colleagues exposed cultured myocytes to FCS for ~2 hours (Durgan et al., 2005). In addition, differences between the compositions of both FCS and BSA may contribute to the differing effects on circadian clock gene expression, as FCS is known to contain various growth factors, albumins, minerals, vitamins, immunoglobulins, lipids, which may themselves promote circadian clock gene cycling where as BSA does not contain these components and is typically a very pure and specific albumin (Durgan et al., 2005). Culturing of myocytes may also enhance circadian clock gene cycling as the culture media itself contains several components such as cortisol and retinoic acid which have been previously reported to reset the circadian clock (Balsalobre et al., 2000, McNamara et al., 2001, Durgan et al., 2005).

It is well established that a peripheral circadian clock exists in the cardiomyocyte, which has been shown to be involved in the control of cardiac metabolic gene transcription and expression (Durgan et al., 2005); however, it is unknown whether the cardiomyocyte circadian clock is still active following ventricular myocyte isolation. We therefore wanted to check whether the circadian clock was still active in our isolated myocytes and whether this would influence the comparison of the basal  $Ca^{2+}$  transient, contraction strength and SR  $Ca^{2+}$  content between resting period (ZT3) and active period (ZT15) myocytes. It is possible that if the endogenous circadian clock in the myocyte was still active following isolation, that this may result in the continued

cycling of the basal  $\text{Ca}^{2+}$  transient, contraction strength and SR  $\text{Ca}^{2+}$  content, over the course of the experimental day (~8 hours). So that a resting period (ZT3) myocyte would effectively become and behave like an active period (ZT15) myocyte during the experimental day following isolation, and vice-versa for the active period (ZT15) myocyte. Therefore, in order to rule out the presence of an active cardiomyocyte circadian clock post isolation, we analysed the basal  $\text{Ca}^{2+}$  transient, contraction and SR  $\text{Ca}^{2+}$  content at the beginning of the experimental day and the end of the experimental day, corresponding to 0-4 hours and 4-8 hours after isolation, respectively. We found no significant difference in the basal  $\text{Ca}^{2+}$  transient, contraction strength and SR  $\text{Ca}^{2+}$  content between 0-4 hours and 4-8 hours, indicating that the intrinsic cardiomyocyte circadian clock is inactive in our isolated myocytes. This is likely to be the case as our isolated myocytes were stored at room temperature in normal Tyrode solution, conditions of which are unlikely to promote changes in gene transcription and protein production and also it may be the case that perhaps FCS may be required for continued circadian clock gene cycling in isolated myocytes in a similar manner as cultured cells. Studies of circadian variation typically use a wide range of time-points throughout the resting and active periods of nocturnal rodents, to obtain a 24 hour representation of cycling. In the present chapter, basal  $\text{Ca}^{2+}$  transient, contraction strength and SR  $\text{Ca}^{2+}$  content data were obtained using only single ventricular myocytes and LV free-wall from adult Wistar rat hearts isolated during the resting period (ZT3) and the active period (ZT15). To verify that the time-points selected were representative of the resting period (ZT3) and the active period (ZT15) and to verify that the circadian clock cycles as expected and is not affected by the myocyte isolation process, we looked at the gene expression of Per2 and CLOCK at ZT9 and ZT21 in addition to ZT3 and ZT15 (see appendix 1 figures 2 & 3). We found that the 24 hour expression profiles of the circadian clock genes, Per2 and CLOCK, were consistent with previously published data (Young et al., 2001a, Naito et al., 2003, Yamamoto et al., 2004) and that our selected time-points (ZT3 and ZT15) represented periods in which clear rhythmic differences in circadian clock gene expression were evident. In addition, we did not

choose time-points on the borderline of the transition from the resting period to the active period, for example, ZT0, or the transition from the active period to the resting period, for example, ZT12, as this will represent a sudden change in activity level and sympathetic drive, which may mean cellular processes such as diurnal changes in gene transcription and protein expression may have not yet occurred. Moreover, the time at which each animal enters the resting period and active period will vary between each animal and also the rest-activity pattern may not be consistent on a daily basis. We therefore selected time-points in the present investigation that represent ~3 hours after the beginning of either the resting period or the active period of the rat in which the animals behaviour had time to change and they had definitely entered either the resting or active period.

The expression of a number of frequently used *housekeeping genes* has been shown to be highly variable (Dheda et al., 2004) and also vary with the time of day (Kawai and Kin, 1975, Bredow et al., 1997). In particular, the expression of GAPDH has been shown to change throughout the day (Shinohara et al., 1998). In the present study, it was essential to select a *housekeeping gene* that is not regulated by the circadian clock, as this may introduce errors in the interpretation of the mRNA analysis. We therefore, compared the expression of the *housekeeping gene*,  $\beta$ -actin, between LV free-wall isolated from adult Wistar rats during the resting (ZT3) and active (ZT15) period. The data showed that  $\beta$ -actin expression did not vary between LV free-wall tissue isolated from resting (ZT3) and active (ZT15) period rats and as a result we used  $\beta$ -actin to normalise all genes of interest to. Ideally, a number of *housekeeping genes* should have been selected for analysis (Vandesompele et al., 2002); however, due to the stable expression of  $\beta$ -actin and time constraints we deemed it not necessary.

To further validate our quantitative real-time RT-PCR technique, we also looked at the expression of the mitochondrial metabolic proteins, UCP2 and UCP3. Our UCP2 gene expression data confirm previously published reports by Young *et al* (2001a), as in both studies, UCP2 expression was greater in rat hearts isolated during the active period (ZT15) than the resting period (ZT3). Our gene expression data for UCP3 is in

agreement with some of the previously published data as Durgan *et al* (2005) have shown that UCP3 expression is increased during the resting period (ZT3) of the rat. However, in a separate study from the same experimental group, Young and colleagues looked specifically at UCP3 expression; they found that UCP3 expression was in fact increased during the active period (ZT15) of the rat (Young *et al.*, 2001a). The conflict in the literature regarding the expression of UCP3 may result from methodological differences, as in the study by Young *et al* (2001a) they used freshly isolated ventricular myocytes whereas Durgan *et al* (2005) were using serum-cultured ventricular myocytes, which suggests that culturing ventricular myocytes in serum may affect gene expression through resetting of the circadian clock (see earlier) or that the culturing of myocytes themselves infers certain properties on the cells that affect cell function and signalling that may impact on gene expression, for example, in culture ventricular myocytes often differentiate.

In addition, Martino *et al* (2004) used a high density microarray in mice to examine diurnal variation in gene expression and they found no such differences in the expression of both UCP2 and UCP3, suggesting that UCP2 and UCP3 may not differ with time-of-day, which does not support either the data of the present investigation nor that of Young's experimental group (Young *et al.*, 2001a). However, these differences in UCP2 and UCP3 expression may result from genetic variation between mice and rats, as diurnal variation in these genes in the rat is well documented (Young *et al.*, 2001a) and rats and mice do not share 100% similar genetic homology.

### **3.3.2 Diurnal variation in cardiac EC-coupling**

The diurnal variation we see in basal EC-coupling in the heart is novel, however; it is not surprising as diurnal variation in  $\text{Ca}^{2+}$  homeostasis has been documented in other organs. In the brain,  $[\text{Ca}^{2+}]_i$  levels, LTCC current and TTCC receptor expression all exhibit patterns of diurnal cycling (Milhaud *et al.*, 1972, Pennartz *et al.*, 2002, Nordskog

et al., 2006). In addition, diurnal variation has been shown in  $[Ca^{2+}]_i$  levels in both the small intestine (Wrobel and Nagel, 1979) and blood serum (Wills, 1970). Our data is supportive of the documented diurnal cycling of  $Ca^{2+}$  homeostasis in other organs, as in previous studies  $[Ca^{2+}]_i$  levels in the SCN of the brain and blood serum in the rat were increased during the day-time, corresponding to the resting period of the rat (Nielsen et al., 1991, Colwell, 2000). In the present chapter we showed that the parameters of the basal  $Ca^{2+}$  transient (diastolic, systolic and amplitude of  $Ca^{2+}$  transient), contraction strength and SR  $Ca^{2+}$  content were all higher in resting period (ZT3) myocytes than active period (ZT15) myocytes. This is paradoxical as the resting period of the rat is associated with a passive, resting state, one in which the  $Ca^{2+}$  transient, contraction strength, CO, and metabolic demands are all decreased. In addition, one would expect that upon transition from the resting period to active period that these parameters would increase thereby heightening the responsiveness of the rat which could be evolutionarily important in terms of avoiding predation and foraging, however, this increased responsiveness is reversed in our data. The increase in the basal  $Ca^{2+}$  transient in resting period (ZT3) myocytes could reflect changes in the activity or expression of the key  $Ca^{2+}$  handling proteins, LTCC, RyR2, SERCA/PLB and NCX1 and the possible contributions of these EC-coupling proteins to the increase in the  $Ca^{2+}$  transient of resting period (ZT3) myocytes will now be discussed individually.

### ***L-type $Ca^{2+}$ current***

An increase in LTCC current may underpin the paradoxical increase in the basal  $Ca^{2+}$  transient we see in resting period (ZT3) myocytes. However, contrary to this, data from our laboratory show that basal LTCC current density is significantly larger in active period (ZT15) myocytes where we observe a reduced  $Ca^{2+}$  transient (Collins and Rodrigo, 2010). This is inconsistent with the conventional sequence of EC-coupling, as an increase in the LTCC current would be expected to generate a larger trigger for

SR  $\text{Ca}^{2+}$  release thereby increasing the amplitude of the  $\text{Ca}^{2+}$  transient and subsequent contraction strength (Bassani et al., 1995, Takamatsu et al., 2003). The reduced basal LTCC current in the face of an increased  $\text{Ca}^{2+}$  transient in resting period (ZT3) myocytes could however be explained by  $\text{Ca}^{2+}$ -dependent inactivation of the LTCC. The LTCC is predominately inactivated by  $\text{Ca}^{2+}$  (Kass and Sanguinetti, 1984, Bers, 2001, Altamirano and Bers, 2007) which reduces  $\text{Ca}^{2+}$  entry and most of this inactivation results from SR  $\text{Ca}^{2+}$  release. Therefore, it is possible that the SR liberates a greater amount of  $\text{Ca}^{2+}$  in resting period (ZT3) myocytes, independently of changes in the LTCC density, possibly due to an increased SR  $\text{Ca}^{2+}$  content or opening of the RyR, which will contribute to a greater degree of inactivation and decreased  $\text{Ca}^{2+}$  entry, which may explain the reduced basal LTCC current observed in these myocytes. Indeed, many studies have shown that depleting SR  $\text{Ca}^{2+}$  with thapsigargin/ caffeine or buffering SR  $\text{Ca}^{2+}$  for example with the  $\text{Ca}^{2+}$  chelator BAPTA, results in less  $\text{Ca}^{2+}$  dependent inactivation of LTCC therefore increasing LTCC current and slowing inactivation (Adachi-Akahane et al., 1996, Delgado et al., 1999, Takamatsu et al., 2003, Pott et al., 2007). However,  $\text{Ca}^{2+}$ -dependent inactivation of LTCC is unlikely to occur in the present investigation as electrophysiological measurements of LTCC current density were performed in the presence of a high concentration of BAPTA (10mM), effectively blocking  $\text{Ca}^{2+}$  induced inactivation of LTCC. The increased basal  $\text{Ca}^{2+}$  transient observed in resting period (ZT3) myocytes could be explained by the changes in the number of functional LTCC channels. However, our data shows that there is no significant difference in LTCC expression between the rat hearts isolated during the resting period (ZT3) and active period (ZT15), which corroborates previously published data (Martino et al., 2004) and would suggest that the time-of-day dependent increase in the basal  $\text{Ca}^{2+}$  transient and reduction in LTCC current do not reflect changes in expression of functional LTCC. The reduction in LTCC current in resting period (ZT3) myocytes may reflect changes in the expression of active LTCC protein, as changes mRNA do not always reflect changes in active protein levels. Due to time constraints we were unable to examine LTCC protein expression in the resting period (ZT3) and

active period (ZT15) of the rat therefore, further work is required to determine whether the decreased LTCC current in resting period (ZT3) myocytes reflects a decreased expression of active protein or increased receptor trafficking at this time. It is possible that the reduction in LTCC current in resting period (ZT3) myocytes is the result of changes in sarcolemmal membrane trafficking of the LTCC. Shen *et al* (2007) have shown that NCX insertion into the cell membrane is time-of-day dependent, as NCX surface expression was increased during the active period and was decreased during the resting period of the mouse. In addition, the authors correlated these changes in the surface expression of NCX with changes in the concentration of PIP<sub>2</sub>, which is responsible for the internalisation and intracellular trafficking of NCX. Therefore, it is entirely possible that LTCC internalisation and trafficking may also be subject to similar changes, however, this requires further work to elucidate. In addition, the decreased LTCC current in resting period (ZT3) myocytes may reflect post-translational modification of the LTCC protein, as many cell signalling molecules have been shown to modify receptor activity for example S-nitrosylation of the LTCC by NO has been shown to reduce LTCC current (Sun *et al.*, 2007, Burger *et al.*, 2009). However, it is unlikely that the LTCC makes a major contribution to the increased basal Ca<sup>2+</sup> transient we observe in resting period (ZT3) myocytes, as the Ca<sup>2+</sup> entry through the LTCC (and NCX) only reflects ~10% of the total Ca<sup>2+</sup> that contributes to the Ca<sup>2+</sup> transient amplitude and resultant contraction strength in the rat. The remaining ~90% of Ca<sup>2+</sup> that contributes to the Ca<sup>2+</sup> transient in the rat originates from the SR (Bassani *et al.*, 1994, Bers, 2001) and therefore it is possible that the increased Ca<sup>2+</sup> transient in resting period (ZT3) myocytes reflects changes in the expression and activity of the SR proteins, RyR2, SERCA 2a and PLB and/or an increase in SR Ca<sup>2+</sup> content.

Our experiments involved determining the basal Ca<sup>2+</sup> transient and contraction strength in field-stimulated myocytes using current-clamp and as a result we were not able to control for changes in APD, therefore, the basal Ca<sup>2+</sup> transient may be depressed in active period (ZT15) myocytes through a reduction in APD. Indeed, APD has been reported to be reduced in a model of cardiac-specific over-expression of Kv1.5, which

gives rises to  $I_{Kur}$  (Brunner et al., 2003, Tanabe et al., 2006). Yamashita *et al* (2003) have documented diurnal variation in the expression of two  $K^+$  currents, one responsible for the early plateau stage and the long refractory period of the cardiac AP,  $Kv1.5$  ( $I_{Kur}$ ) peaks in expression during the active period, which would shorten the APD during the active period which may contribute to the depressed basal  $Ca^{2+}$  transient and contraction strength. Yamashita and colleagues also found that  $Kv4.2$  mRNA ( $I_{to}$ ) peaks in expression during the resting period of the nocturnal rat, and due to the role of  $I_{to}$  in the notch phase of AP, this would promote partial AP repolarisation and also provide a larger the driving force for  $Ca^{2+}$  entry during the plateau phase of the AP, which may contribute to a greater  $Ca^{2+}$  trigger for the SR and also a longer APD in resting period (ZT3) rats. This increase in APD will reduce the amount of time in which the heart remains in diastole during increased HR and therefore ventricular contraction will become less efficient and this may also increase the incidence of arrhythmic activity in these animals. Also, LTCC current data obtained from this laboratory were obtained under voltage clamp so it is possible that the paradoxical data we observe in the  $Ca^{2+}$  current data in resting period (ZT3) myocytes may reflect differences in APD between measurements of  $Ca^{2+}$  transient and LTCC current.

### ***Ryanodine receptor***

The increase in the basal  $Ca^{2+}$  transient observed in resting period (ZT3) myocytes may be explained by changes in the sensitivity of RyR2 to  $Ca^{2+}$ . The  $Ca^{2+}$  sensitivity of the RyR2 may be increased in resting period (ZT3) myocytes, which may mean that the RyR2 may be more fine-tuned to respond to a smaller trigger  $Ca^{2+}$  from the LTCC, which could promote greater SR  $Ca^{2+}$  release, thereby increasing the basal  $Ca^{2+}$  transient and contraction strength in these myocytes. These changes in the  $Ca^{2+}$  sensitivity of RyR2 may reflect changes in RyR2 activity. However, we did not study the sensitivity of RyR2 to  $Ca^{2+}$  or RyR2 activity in the present investigation; therefore,

we cannot confirm or rule out whether changes in of RyR2 activity contribute to the observed diurnal variation in the basal  $\text{Ca}^{2+}$  transient. The increase in the basal  $\text{Ca}^{2+}$  transient in resting period (ZT3) myocytes could also reflect changes in the number of active RyR2 channels. However, our gene expression data for RyR2 do not support the time-of-day dependent variation in the basal  $\text{Ca}^{2+}$  transient as these data show that RyR2 expression is not significantly different between resting period (ZT3) and active period (ZT15) myocytes, which supports previously published data (Martino et al., 2004). Our data do not rule out changes in the expression of RyR2 protein, however, due to time constraints we were unable to determine this. It is however possible that the time-of-day dependent variation in the basal  $\text{Ca}^{2+}$  transient may reflect modulation of RyR2 activity which may occur through post-translational changes in SR function for example the intracellular signalling molecule, NO has been shown to modulate RyR2 function (Stoyanovsky et al., 1997, Zahradnikova et al., 1997, Xu et al., 1998) or it is possible that this variation could be due to changes in the expression of associated RyR2 accessory proteins as changes in expression of these will modulate RyR function through the alteration of RyR2 open probability and sensitivity to  $\text{Ca}^{2+}$  and therefore may contribute to the reduced  $\text{Ca}^{2+}$  kinetics in active period (ZT15) myocytes. Triadin and junctin are examples of two known proteins associated with RyR, which anchor other proteins to the RyR-signalling complex, for example, calsequestrin (Beard et al., 2009, Chopra et al., 2009). They also modulate SR  $\text{Ca}^{2+}$  release in addition to buffering SR  $\text{Ca}^{2+}$  and both have been reported to modulate EC-coupling and RyR-function (Bers, 2002, Beard et al., 2009, Chopra et al., 2009). For example, cardiac-specific over-expression of triadin is reported to produce a decreased  $\text{Ca}^{2+}$  transient, contraction strength and SR  $\text{Ca}^{2+}$  content through an increase in RyR2 open probability (Terentyev et al., 2005, Chopra et al., 2009). We did not however examine either the activity of RyR-associated proteins or their expression in the present investigation therefore this requires further work to determine whether they contribute to the observed diurnal variation in the basal  $\text{Ca}^{2+}$  transient.

### ***Sarcoplasmic reticulum Ca<sup>2+</sup> content***

The larger basal Ca<sup>2+</sup> transient in resting period (ZT3) myocytes may be the result of a larger SR Ca<sup>2+</sup> content, as an increase in SR Ca<sup>2+</sup> content will increase the amplitude of the Ca<sup>2+</sup> transient (Bassani et al., 1995, Bers, 2002). An increase in SR Ca<sup>2+</sup> content in resting period (ZT3) myocytes may result from a direct increase in SERCA 2a activity (Bers, 2001, Bers, 2002). Increased SERCA 2a activity has two consequences in terms of Ca<sup>2+</sup> regulation, it will enhance SR Ca<sup>2+</sup> uptake during diastole increasing the rate of decline in the Ca<sup>2+</sup>-transient and therefore relaxation and also SR Ca<sup>2+</sup> content (Bers, 2001, Bers, 2002). In the rat SERCA 2a is responsible for the removal of ~90 % of cytosolic Ca<sup>2+</sup> and therefore the rate of relaxation is predominately driven by SERCA 2a (Bassani et al., 1994, Bers, 2001) and may mean that any increase in activity or expression of SERCA 2a is likely to contribute to the time-of-day dependent variation in the basal Ca<sup>2+</sup> transient. Our data supports the notion of an increase in SERCA2a activity, as the exponential decay of the electrically-evoked Ca<sup>2+</sup> transient was faster in resting period (ZT3) myocytes than active period (ZT15) myocytes, and this is also associated with an increased in SR Ca<sup>2+</sup> content.

The increase in SERCA 2a activity in resting period (ZT3) myocytes may occur as a result of an increase in SERCA 2a expression or possibly a decrease in PLB expression. However, our gene expression data do not support changes in the mRNA levels of either SERCA 2a or PLB in resting period (ZT3) and active period (ZT15) myocytes, which is supportive of published data from Martino *et al* (2004). The increase in SERCA 2a activity in resting period (ZT3) myocytes may reflect an increase in active SERCA 2a protein; however, due to time constraints we were unable to determine active protein levels. In addition, the increase in SERCA 2a activity in resting period (ZT3) myocytes may also be due to an increase in PLB phosphorylation. The activity of SERCA 2a is regulated by the phosphorylation status of PLB (Inui et al., 1986), which in its unphosphorylated state inhibits the activity of SERCA 2a and upon phosphorylation, for

example, during  $\beta$ -adrenergic stimulation, this inhibition is relieved and SERCA 2a activity is enhanced (Bers, 2001, Bers, 2002). In support of this, Rothermel and colleagues have reported that there is a time-of-day dependent variation in calcineurin activity in the mouse heart (Dey et al., 2008). As calcineurin is thought to phosphorylate PLB, this time-of-day dependent variation in calcineurin may impact on diurnal cycling in PLB phosphorylation and therefore SERCA activity. Therefore, changes in the phosphorylation status of PLB may contribute to the enhanced SERCA 2a activity allowing faster relaxation and uptake of SR  $\text{Ca}^{2+}$ , which in the case of the resting period (ZT3) myocyte would also contribute to observed increase in SR  $\text{Ca}^{2+}$  content. In addition, the increase in SR  $\text{Ca}^{2+}$  content and SERCA 2a activity in resting period (ZT3) myocytes, may reflect post-translational modification of SERCA 2a and/or PLB, similar to LTCC, as for example SERCA/PLB have been shown to be targeted by NOS dependent signalling in the heart (Xu et al., 1999, Sears et al., 2003, Wang et al., 2008a, Zhang et al., 2008) and therefore requires further work to elucidate the specific post-translational changes that may occur.

### ***Sodium/calcium exchanger***

The increase in the basal  $\text{Ca}^{2+}$  transient in resting period (ZT3) myocytes may also be explained by changes in NCX expression/ activity. Indeed, our gene expression data did show changes in NCX1 expression between the active period (ZT15) and resting period (ZT3), as NCX1 expression was significantly greater during the active period (ZT15) however, this increase was very modest (1.28 fold). Our NCX1 gene expression data contrast with previously published data as Martino *et al* (2004) have reported that NCX expression is not time-of-day dependent. In addition, Shen *et al* (2007) have shown that the surface expression of NCX was increased during the active period (dark phase) of the mouse due to decreased receptor internalisation and trafficking by  $\text{PIP}_2$  and that NCX was decreased during the resting period (ZT3) due to increased  $\text{PIP}_2$

activity. Our gene expression data does not support an increase in NCX activity during the active period (ZT15), as an increase in the activity of the reverse-mode NCX, for example, during phase 0 (upstroke) of the AP, will increase  $\text{Ca}^{2+}$  entry and therefore may contribute to an increase in the amplitude of  $\text{Ca}^{2+}$  transient (Sher et al., 2008) however, our basal  $\text{Ca}^{2+}$  transient data do not reflect this as the basal  $\text{Ca}^{2+}$  transient is depressed in active period (ZT15) myocytes. Conversely, it is possible that the increase in the basal  $\text{Ca}^{2+}$  transient in resting period (ZT3) myocytes may reflect a reduction in NCX activity which may enhance the basal  $\text{Ca}^{2+}$  transient through reduced  $\text{Ca}^{2+}$  extrusion from the myocyte during diastole, which due to reduced competition with SERCA 2a for  $\text{Ca}^{2+}$ , will contribute to an increase in SR  $\text{Ca}^{2+}$  uptake and content (Weber et al., 2002, Sher et al., 2008). However, our data suggests that the activity of NCX1 does not exhibit time-of-day dependent variation, as the decay of the caffeine-induced  $\text{Ca}^{2+}$  transient, which reflects the activity of NCX1 in addition to PMCA (Bassani et al., 1994), was not significantly different between resting (ZT3) and active (ZT15) period myocytes. This may mean that even though NCX1 gene expression is slightly greater during the active period (ZT15), NCX activity may be unchanged as active NCX1 protein levels may not differ between resting (ZT3) and active (ZT15) period myocytes. Further work is required to examine the role of the NCX1 in the time-of-day dependent variation in basal EC-coupling and to support the present data simultaneous measurements of caffeine fluorescence with electrophysiological measurements of the transient inward current ( $I_{\text{ti}}$ , NCX) should be made to provide a more reliable measure of SR  $\text{Ca}^{2+}$  content and kinetics of the NCX. However, the contribution of NCX to the time-of-day dependent variation we observe in the basal  $\text{Ca}^{2+}$  transient is likely to be small, as the gene expression data is modest and in the rat myocardium  $\text{Ca}^{2+}$  efflux through NCX has been reported to contribute ~10% of cytosolic  $\text{Ca}^{2+}$  removal whereas SR  $\text{Ca}^{2+}$  uptake through SERCA 2a has been reported to contribute ~90% (Bassani et al., 1994, Bers, 2001). As our data show that the increase in basal  $\text{Ca}^{2+}$  transient in resting period (ZT3) myocytes reflects an increase in

SR  $\text{Ca}^{2+}$  content and SERCA 2a activity, the variation in the basal  $\text{Ca}^{2+}$  transient is more likely to reflect changes in SR function.

### **3.3.3 Diurnal variation in contraction**

Contraction is a graded on the concentration of intracellular  $\text{Ca}^{2+}$ ; therefore, any given increase in  $\text{Ca}^{2+}$  will result in a proportional increase in contraction strength (Bers, 2001, Bers, 2002). Our data show that the  $\text{Ca}^{2+}$  transient and resultant contraction strength are both increased in resting period (ZT3) myocytes. In addition to this variation in the systolic  $[\text{Ca}^{2+}]_i$ , this increase in contraction strength in resting period (ZT3) myocytes could be due to increased sensitivity of the contractile myofilaments to  $\text{Ca}^{2+}$ . It is possible that these changes in the sensitivity of the myofilaments could be due to alterations to the pCa-tension curve that may contribute to increase in contraction strength in resting period (ZT3) myocytes. Although the increase in contraction strength in resting period (ZT3) myocytes is most likely to reflect the observed increase in SR function and SR  $\text{Ca}^{2+}$  content in these myocytes due to the overwhelming presence and activity of the SR in the rat, our data, however, does not rule out changes in the sensitivity of contractile myofilaments as it is possible that the large difference in the  $\text{Ca}^{2+}$  transient may not be fully reflected as changes in contraction (see section 3.3.4 for additional detail).

### **3.3.4 What are the physiological implications of the reduced $\text{Ca}^{2+}$ transient during the active period?**

A decrease in the basal  $\text{Ca}^{2+}$  transient and resultant contraction strength in active period (ZT15) myocytes would seem paradoxical, as the active period of an animal is associated with an increase in  $\text{O}_2$  consumption, cardiac power, sympathetic activity and the expression of cardiac metabolic genes, all of which have been documented previously (Hashimoto et al., 1999, Young et al., 2001a) and these act to heighten the

responsiveness of the animal allowing the animal to forage successfully whilst avoiding predation. In addition, HR has been reported to be increased during the active period in response to the increase in sympathetic activity (Richards et al., 1986, Scheer et al., 2004) therefore, CO, a product of HR and SV, could still be higher during the active period (ZT15) in the face of the observed decrease in the basal  $\text{Ca}^{2+}$  transient and contraction strength in active period (ZT15) myocytes. It is possible that the reduction in basal systolic  $[\text{Ca}^{2+}]_i$  we observe in active period (ZT15) myocytes may be a mechanism through which EC-coupling efficiency is enhanced, through a left shift in the pCa-tension relationship, so that the active period (ZT15) myocyte functions at lower systolic  $[\text{Ca}^{2+}]_i$  levels. Although our data shows that contraction strength and the  $\text{Ca}^{2+}$  transient both increase in active period (ZT15) myocytes, the percentage increase in the  $\text{Ca}^{2+}$  transient is much greater than that of contraction strength. However, additional work is required to determine whether changes in the pCa-tension relationship exhibits diurnal variations.

The decreased  $\text{Ca}^{2+}$  transient and contraction strength during the active period (ZT15) could also be a possible means of conserving ATP as EC-coupling is a high energy demanding process involving many ATP hydrolysing ion pumps (ATPases). For example, the activity of the ATPase, SERCA 2a is reduced in active period (ZT15) myocytes which in addition to reducing SR  $\text{Ca}^{2+}$  uptake and content may also reduce the demand for ATP.

The reduced  $\text{Ca}^{2+}$  transient and contraction strength in the active period (ZT15) myocytes may also reflect a protective mechanism in which the myocardium is protected from  $\text{Ca}^{2+}$  overload and aberrant arrhythmic activity during periods of increased sympathetic activity.

There is a pronounced morning peak and a smaller afternoon peak both in the concentration of the circulating catecholamines, epinephrine and norepinephrine, and the increase in sympathetic activity in man (Prinz et al., 1979, Linsell et al., 1985, Dodt et al., 1997), which is reversed by 12 hours in the rat (Hashimoto et al., 1999). Therefore, in the next chapter we will examine whether  $\beta$ -adrenergic stimulation of

resting period (ZT3) and active period (ZT15) myocytes with the non-selective  $\beta$ -adrenoceptor agonist, ISO, effects the observed diurnal variation in basal EC-coupling.

## **Chapter 4: Diurnal variation in the response of ventricular myocytes to $\beta$ -adrenergic stimulation with isoproterenol**

### ***4.1 Introduction***

The occurrence of ventricular arrhythmias associated with SCD is greatest in the early hours of the morning, peaking between 6am and 10am in man (Arntz et al., 1993, Goldstein et al., 1996). This morning increase in ventricular arrhythmias and associated SCD in man is linked to a parallel increase in sympathetic activity, resulting in an increase in the levels of the circulating and neurally released catecholamines, epinephrine and norepinephrine, both of which have positive inotropic, chronotropic and lusitropic effects in the mammalian myocardium (Guo and Stein, 2003). However, in the rat myocardium, this increase in sympathetic activity occurs during the active period of the nocturnal rat, typically in the evening. This is physiologically important as an increase in sympathetic activity will enhance EC-coupling and contractile performance through an increase in the systolic  $\text{Ca}^{2+}$  transient, its rate of relaxation and contraction strength (Bers, 2002). In addition, the morning surge in sympathetic activity in man is physiologically important as blood flow must be increased in order to match the demands of the active individual which is reflected by sympathetic mediated increases in HR, SV, BP and CO in man (Narkiewicz et al., 2002, Sherwood et al., 2002, Scheer et al., 2004).

Epinephrine and norepinephrine bind to the sarcolemmal  $\beta$ -adrenergic receptors on ventricular cells. The mammalian ventricular myocardium expresses several isoforms of  $\beta$ -adrenergic receptors and these consist of the  $\beta_1$ ,  $\beta_2$  and  $\beta_3$  isoforms. Of these, the  $\beta_1$  isoform is the most abundant  $\beta$ -adrenergic receptor, comprising of ~75% of all the cardiac  $\beta$ -adrenergic receptors, the remainder of which (~25%) is composed of the  $\beta_2$

and  $\beta_3$  isoforms (Bristow et al., 1986, Bers, 2002, Wallukat, 2002). The positive inotropic, chronotropic and lusitropic effects of sympathetic stimulation are mediated by the activation of the  $\beta_1$  and  $\beta_2$  adrenergic receptors; however, the  $\beta_1$ -adrenergic receptor is more responsive to sympathetic stimulation than the  $\beta_2$  isoform (Brodde, 1993, Rodefeld et al., 1996) (see section 1.4 of introduction for detail). Sympathetic activation of the  $\beta_1$ -adrenergic receptor results in the activation of AC through the stimulatory G-protein,  $G_s$ , which increases cAMP concentration and activates PKA. PKA is known to phosphorylate 4 key EC-coupling components, they are: LTCC, RyR2, PLB and troponin I.

***L-type  $Ca^{2+}$  channel:*** PKA-mediated phosphorylation of the LTCC increases  $I_{Ca}$ , and due to close proximity of the LTCC to the RyR, any increase in  $I_{Ca}$  will impact on SR  $Ca^{2+}$  release as a localised increase in  $Ca^{2+}$  concentration in the vicinity of the RyR2 will be detected which will increase RyR open probability thereby contributing to a greater SR  $Ca^{2+}$  release and therefore a positive inotropic effect (Tsien et al., 1986, Walsh et al., 1989).

***Ryanodine receptor:*** Phosphorylation of RyR2 increases the open probability of the RyR by increasing the sensitivity of RyR to a given  $I_{Ca}$  stimulus which results in increased SR  $Ca^{2+}$  release during electrical activation and in response to  $I_{Ca}$ , also contributing to a positive inotropic effect (Marx et al., 2000, Bers, 2002).

***Sarcoplasmic reticulum proteins:*** In its unphosphorylated form, PLB inhibits the activity of the SR  $Ca^{2+}$  pump, SERCA 2a (Inui et al., 1986). Phosphorylation of PLB by PKA reduces the level of inhibition exerted on SERCA 2a, which allows SR  $Ca^{2+}$  uptake to occur at a faster rate, which contributes to an increased rate of relaxation (positive lusitropic effect). In addition, this increase in SR  $Ca^{2+}$  uptake will increase SR  $Ca^{2+}$  content which contributes to a positive inotropic effect ((Li et al., 2000, Bers, 2002); see section 1.4.2 of introduction for detail). The phosphorylation of PLB produces the most of the positive inotropic and lusitropic effects of sympathetic stimulation in the rat (Li et al., 2000, Bers, 2002).

**Contractile proteins:** Phosphorylation of troponin I contributes to the lusitropic effect of sympathetic stimulation as it leads to an increased relaxation rate as  $\text{Ca}^{2+}$  dissociates faster from the contractile proteins due to a decrease in the sensitivity of the myofilaments to  $\text{Ca}^{2+}$  upon phosphorylation (Ray and England, 1976, Okazaki et al., 1990, Li et al., 2000, Bers, 2002) (see section 1.4.2 of introduction for detail).

Sympathetic activation of the  $\beta_2$ -adrenergic receptor is similar to  $\beta_1$ -adrenergic receptor activation; however, the positive inotropic effect mediated through  $\beta_2$ -adrenergic receptor activation is weaker than  $\beta_1$ -adrenergic receptor activation as there is an increased abundance of  $\beta_1$ -adrenergic receptors in the ventricular myocardium (Brodde, 1993, Rodefeld et al., 1996). In addition,  $\beta_2$ -adrenergic receptor downstream signalling is restricted to the sarcolemmal membrane and caveolae in which PKA only targets LTCC rather than the SR proteins (RyR & PLB) and myofilaments (troponin I) to mediate a positive inotropic effect. (Xiao et al., 1994, Calaghan et al., 2008) (see section 1.4 of introduction for detail).

In the previous chapter, we demonstrated the presence of diurnal variation in the basal  $\text{Ca}^{2+}$  transient; contraction strength and SR  $\text{Ca}^{2+}$  content of ventricular myocytes, as all of these parameters were depressed in the active period (ZT15) myocyte in comparison to resting period (ZT3) myocyte. As an increase in sympathetic activity is coupled to an increase in SV and CO and as sympathetic stimulation increases contraction by modulating cardiac EC-coupling through an increase in the  $\text{Ca}^{2+}$  transient and SR  $\text{Ca}^{2+}$  content through the activation of  $\beta_1$  and  $\beta_2$ -adrenergic receptors, we postulated that the responsiveness of the  $\text{Ca}^{2+}$  transient to  $\beta$ -adrenergic stimulation would also exhibit diurnal variation. We therefore set out to determine whether diurnal variation exists in the response of EC-coupling to  $\beta$ -adrenergic stimulation. Sympathetic stimulation can be mimicked *in vitro* using  $\beta$ -adrenergic receptor agonists, like the non-specific  $\beta$ -adrenergic receptor agonist, isoproterenol (ISO), which has been shown to increase the systolic  $\text{Ca}^{2+}$  transient, amplitude of  $\text{Ca}^{2+}$  transient, contraction strength and SR  $\text{Ca}^{2+}$  content in rat ventricular myocytes (Bers, 2001, Bers, 2002). We looked at the  $\text{Ca}^{2+}$  transient, contraction strength and SR  $\text{Ca}^{2+}$  content in response to stimulation of the  $\beta$ -

adrenoreceptor system using ISO in rat ventricular myocytes. In addition, strong  $\beta$ -adrenergic stimulation can result in spontaneous activity and triggered arrhythmias due to  $\text{Ca}^{2+}$ -overload and the development of after-depolarisations, we then looked at whether diurnal variation exists in the threshold for the generation of arrhythmias in response to ISO.

## **4.2 Results**

### **4.2.1 Diurnal variation in the response of the $\text{Ca}^{2+}$ transient to $\beta$ -adrenergic stimulation with isoproterenol**

We postulated that the increase in sympathetic activity may be coupled to an increase in the responsiveness of the  $\text{Ca}^{2+}$  transient and hypothesised that the  $\text{Ca}^{2+}$  transient will be increased in active period (ZT15) myocytes in response to  $\beta$ -adrenergic stimulation in comparison to the resting period (ZT3) myocyte. To investigate whether the responsiveness of the  $\text{Ca}^{2+}$  transient to  $\beta$ -adrenergic stimulation exhibits diurnal variation, we measured  $[\text{Ca}^{2+}]_i$  in resting period (ZT3) and active period (ZT15) myocytes using Fura-2 in response to the non-specific  $\beta$ -adrenergic receptor agonist, ISO. Fura-2 loaded myocytes were electrically-field stimulated at 1Hz, unless otherwise stated, and were superfused with normal Tyrode for 5 minutes, to establish stable resting  $\text{Ca}^{2+}$  transients. Any trace in which the resting diastolic Fura-2 ratio was  $> 1$  ( $\sim 250\text{-}300\text{nM}$ ) was discarded. Myocytes were then superfused for 5 minutes in succession with normal Tyrode containing the following concentrations of ISO (nM): 0.1, 0.5, 1, 3, 10, 50 & 100 (see figure 4.1A).  $\text{Ca}^{2+}$  transients were recorded for 20 seconds at the end of each ISO exposure, when the ISO response was maximal and had reached steady state, to reduce the effect of photobleaching and measurements of diastolic  $[\text{Ca}^{2+}]$ , systolic  $[\text{Ca}^{2+}]$  and amplitude of  $\text{Ca}^{2+}$  transient were made. Following ISO superfusion, myocytes were superfused with normal Tyrode for 5 minutes, to allow

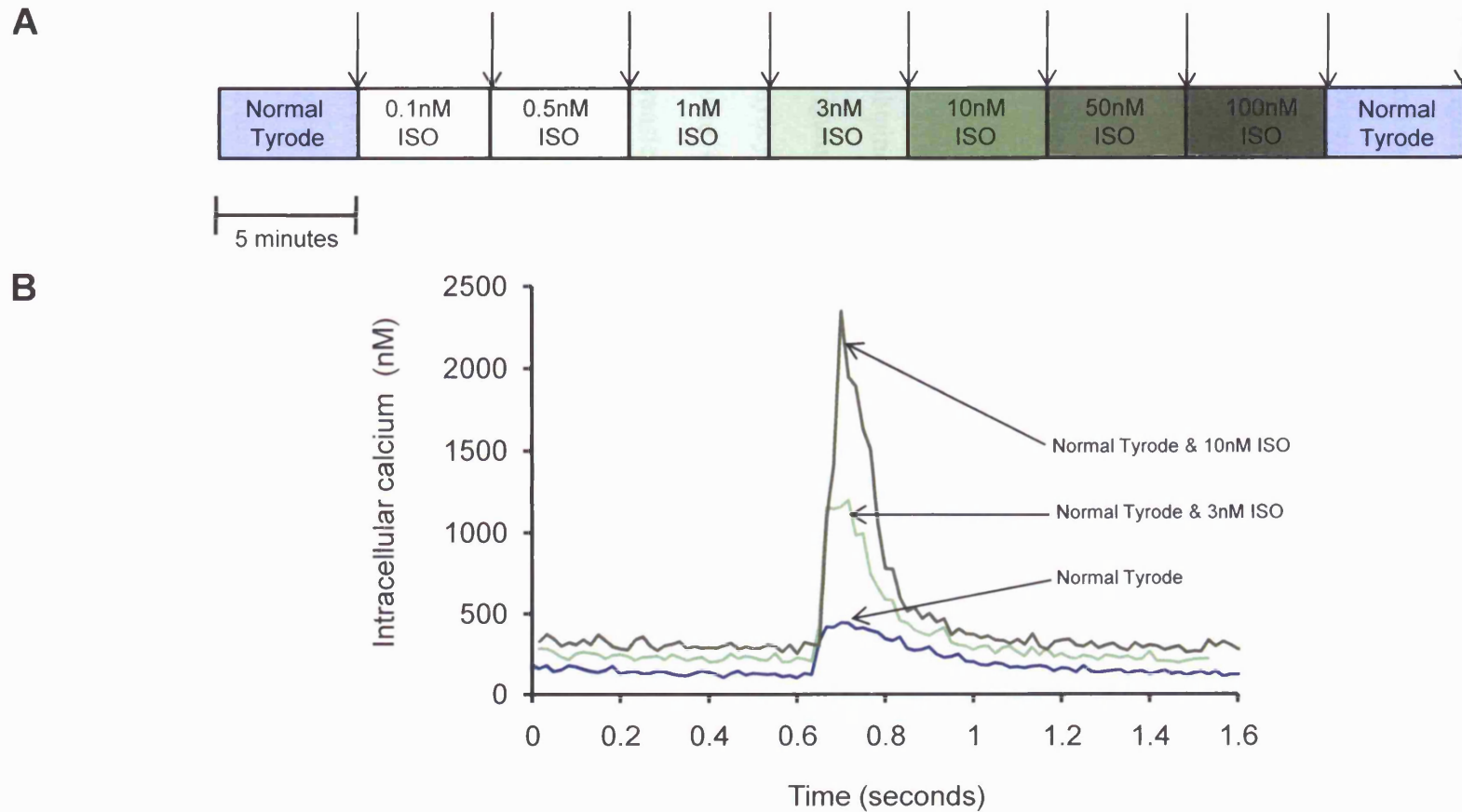


**Figure 4.1- Protocol to determine the concentration-dependent effect of isoproterenol (ISO) on the  $\text{Ca}^{2+}$  transient in resting period (ZT3) and active period (ZT15) myocytes.**

Myocytes were stimulated at either 0.5Hz, 1Hz or 2Hz and superfused with normal Tyrode for 5 minutes. Myocytes were then superfused for 5 minutes with normal Tyrode containing ISO in the following concentrations (nM): 0.1, 0.5, 1, 3, 10, 50 & 100. Myocytes were superfused with normal Tyrode for 5 minutes to wash off ISO and allow the recovery of calcium transients. The calcium transients were recorded for 20 seconds at the end of 5 minutes exposure to ISO (indicated by arrows) to limit photobleaching.

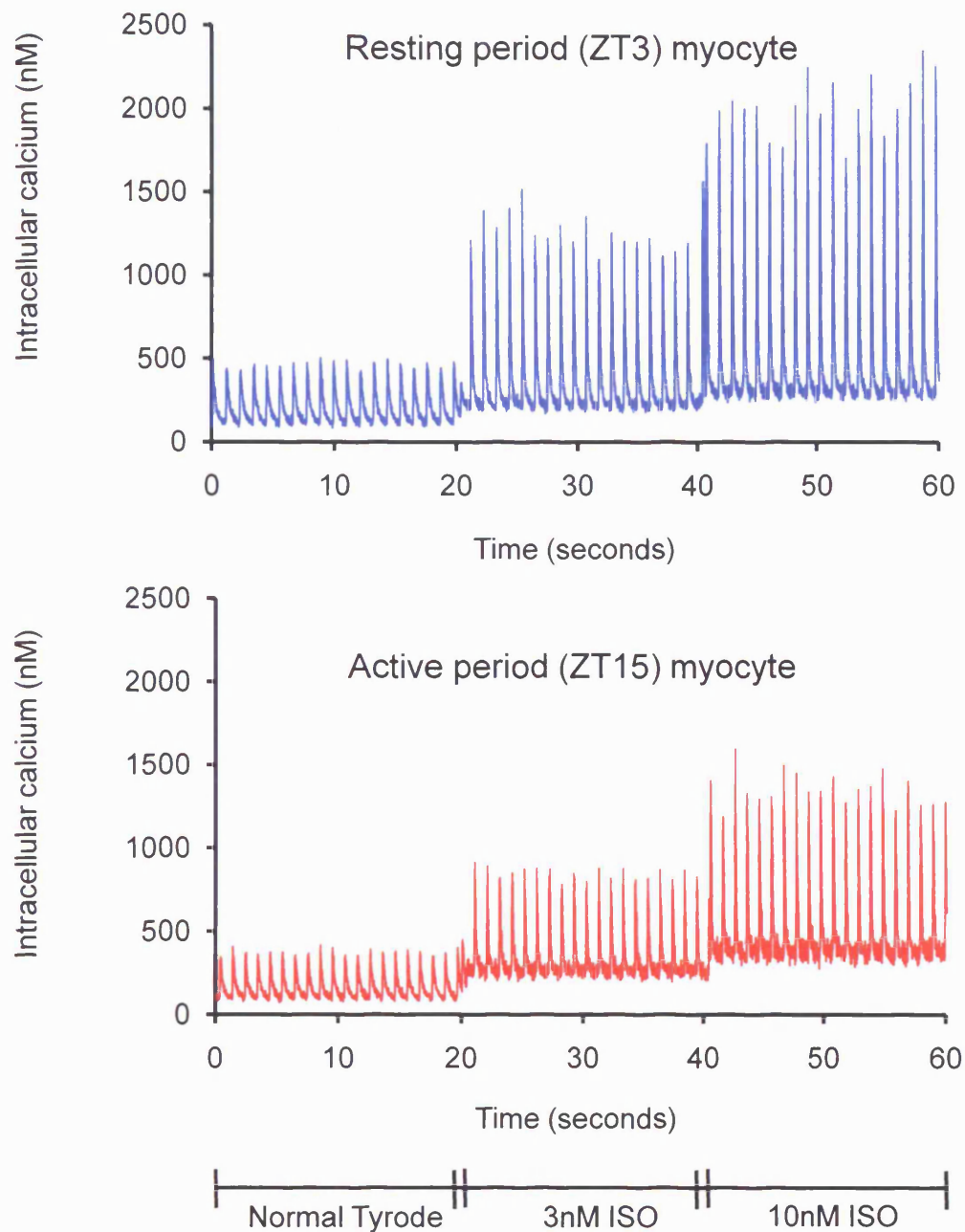
recovery of resting  $\text{Ca}^{2+}$  transients. Any data where the  $\text{Ca}^{2+}$  transient amplitude failed to recover to within ~80% of control following ISO were discarded.

Figure 4.1B is a recording of intracellular  $\text{Ca}^{2+}$  from a single resting period (ZT3) myocyte using this protocol, and shows the  $\text{Ca}^{2+}$ -transient recorded in normal Tyrode (blue); normal Tyrode containing 3nM ISO (light green) and normal Tyrode containing 10nM ISO (dark green) during 1Hz electrical field stimulation. The record shows a concentration-dependent increase in diastolic  $[\text{Ca}^{2+}]_i$ , systolic  $[\text{Ca}^{2+}]_i$  and the amplitude of  $\text{Ca}^{2+}$  transient to increasing ISO concentrations.

Experiments described in figure 4.1A, were also repeated using only a few concentrations of ISO, to exclude the effects of  $\beta$ -adrenergic receptor desensitisation in the response of resting period (ZT3) and active period (ZT15) myocytes to ISO and we found there was no difference between data obtained in this manner compared to that obtained using the protocol described in figure 4.1A (data not shown).

Figure 4.2 is a recording of intracellular  $\text{Ca}^{2+}$  from a single resting period (ZT3) myocyte (top; blue) and a single active period (ZT15) myocyte (bottom; red). Myocytes were superfused with normal Tyrode for 5 minutes, at the end of which the  $\text{Ca}^{2+}$ -transients reached a steady-state and were recorded. The myocytes were subsequently superfused with normal Tyrode containing 3 & 10nM ISO for 5 minutes and the  $\text{Ca}^{2+}$ -transient recorded at the end. The record shows that ISO stimulation increases diastolic  $[\text{Ca}^{2+}]_i$ , systolic  $[\text{Ca}^{2+}]_i$  and amplitude of  $\text{Ca}^{2+}$  transient in both resting period (ZT3) and active period (ZT15) myocytes, however, contrary to expectations, the resting period (ZT3) myocyte is more responsive to 3 & 10nM ISO in comparison the active period (ZT15) myocyte, as the systolic  $[\text{Ca}^{2+}]_i$  and amplitude of  $\text{Ca}^{2+}$  transient are both greater in the resting period (ZT3) myocyte.

Figures 4.3 are the dose-response curves of diastolic  $[\text{Ca}^{2+}]_i$  (A), systolic  $[\text{Ca}^{2+}]_i$  (B) and the amplitude of the  $\text{Ca}^{2+}$ -transient (C) recorded from resting period (ZT3; blue symbols) and active period (ZT15) myocytes (red symbols), obtained from experiments described previously (see figure 4.1A). Figure 4.3A shows that diastolic  $[\text{Ca}^{2+}]_i$  increases in a sigmoidal dose-dependent manner in response to increasing ISO



**Figure 4.2- The  $\text{Ca}^{2+}$  transient of resting period (ZT3) and active period (ZT15) myocytes recorded during  $\beta$ -adrenergic stimulation with isoproterenol (ISO).**

Example of  $\text{Ca}^{2+}$  transients recorded from a single resting period (ZT3) myocyte (top; blue) and a single active period (ZT15) myocyte (bottom; red) during 1Hz electrical field stimulation and superfused with normal Tyrode for 5 minutes, 3nM ISO-containing Tyrode for 5 minutes and 10nM ISO-containing Tyrode for 5 minutes.  $\text{Ca}^{2+}$  transients were recorded for 20 seconds at end of the perfusion of each solution to reduce effects of photobleaching.

concentrations, and that there was no significant difference in the sensitivity to ISO between resting period (ZT3) myocytes with an  $EC_{50}$  of  $4.69 \pm 0.86$  nM ( $n = 28-56/ 10$ ) compared to  $3.76 \pm 0.49$  nM in active period (ZT15) myocytes ( $n = 25-51/ 11$ ; *ns*). The data also show that the response of diastolic  $[Ca^{2+}]$  to the maximal concentration of ISO (100 nM) was not significantly different between resting period (ZT3) myocytes at  $321 \pm 23$  nM ( $n = 28/ 10$ ) compared to active period (ZT15) myocytes at  $326 \pm 34$  nM ( $n = 25/ 11$ ; *ns*).

Figure 4.3 B shows that systolic  $[Ca^{2+}]$  increases in a sigmoidal dose-dependent manner in response to increasing ISO concentrations, and there was no significant difference in the sensitivity to ISO between resting period (ZT3) myocytes, with an  $EC_{50}$  of  $3.65 \pm 0.87$  nM ( $n = 28-56/ 10$ ) compared to  $3.05 \pm 0.34$  nM in active period (ZT15) myocytes ( $n = 25-51/ 11$ ; *ns*). However, the data show that the systolic  $[Ca^{2+}]$  dose-response relationship diverges at concentrations  $> 3$ nM ISO, with resting period (ZT3) myocytes having significantly higher systolic  $[Ca^{2+}]$  in comparison to active period (ZT15) myocytes in the presence of any given ISO concentration. The data also show that the response of systolic  $[Ca^{2+}]$  to the maximal concentration of ISO (100nM) was significantly different between resting period (ZT3) myocytes at  $2330 \pm 402$  nM ( $n = 28/ 10$ ) compared to active period (ZT15) myocytes at  $1385 \pm 109$  nM ( $n = 25/ 11$ ,  $p < 0.05$ ).

Figure 4.3 C shows that the amplitude of  $Ca^{2+}$  transient increases in a sigmoidal dose-dependent manner in response to increasing ISO concentrations, and there was no significant difference in the sensitivity to ISO between resting period (ZT3) myocytes with an  $EC_{50}$  of  $3.89 \pm 0.92$  nM ( $n = 28-56/ 10$ ) compared to  $3.58 \pm 0.78$  nM in active period (ZT15) myocytes ( $n = 25-51/ 11$ ; *ns*). Like that of systolic  $[Ca^{2+}]$  shown in figure 4.3 B, the data in figure 4.3 C shows that amplitude of  $Ca^{2+}$  transient dose-response relationship also diverges at concentrations  $> 3$ nM ISO, with resting period (ZT3) myocytes having significantly higher amplitude of  $Ca^{2+}$  transient in comparison to active period (ZT15) myocytes. The data also show that the response of the amplitude of  $Ca^{2+}$  transient to the maximal concentration of ISO (100nM) was

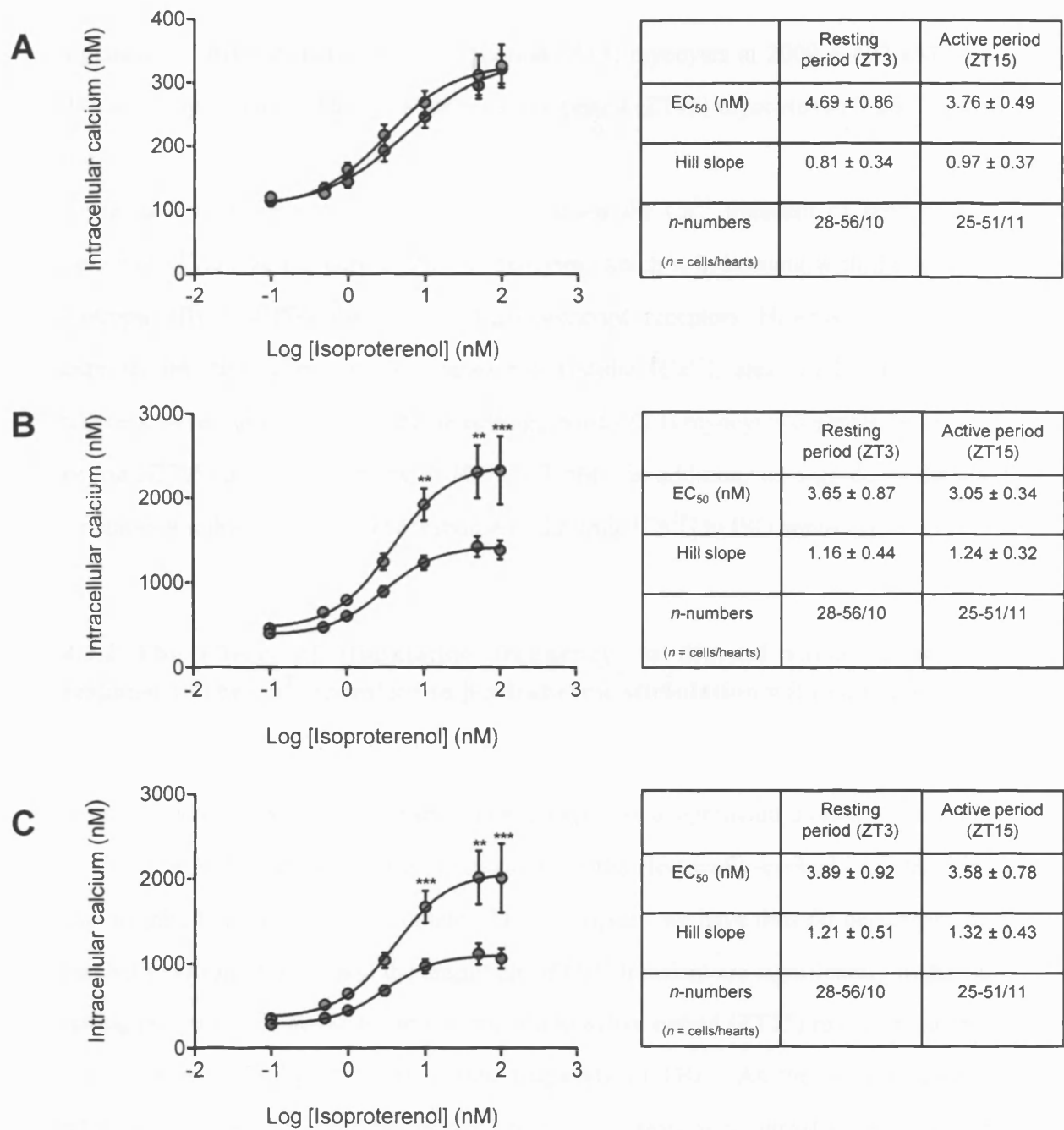


**Figure 4.3- Dose-response curves of diastolic [Ca<sup>2+</sup>], systolic [Ca<sup>2+</sup>] and amplitude of Ca<sup>2+</sup> transient to  $\beta$ -adrenergic stimulation with isoproterenol (ISO) in resting period (ZT3) and active period (ZT15) myocytes.**

Dose-response curve of the effects of ISO on diastolic [Ca<sup>2+</sup>] (A), systolic [Ca<sup>2+</sup>] (B) and amplitude of Ca<sup>2+</sup> transient (C) in resting period (ZT3) myocytes (blue circles) and active period (ZT15) myocytes (red circles). Myocytes were superfused at 35°C and electrically field stimulated at 1Hz. Values are mean ± S.E.M; numbers of cells / hearts = resting period (ZT3) myocyte, *n* = 28-56/ 10 and active period (ZT15) myocyte, *n* = 25-51/ 11. \*\* *p* < 0.01; \*\*\* *p* < 0.001, two way ANOVA followed by Bonferroni *post hoc* test.

significantly different between resting period (ZT3) myocytes at  $2009 \pm 407$  nM ( $n = 28/10$ ) compared to  $1058 \pm 114$  nM in active period (ZT15) myocytes ( $n = 25/11$ ;  $p < 0.05$ ).

These data show that ISO significantly increases the  $\text{Ca}^{2+}$  transient of both resting period (ZT3) and active period (ZT15) myocytes, which is in keeping with the positive inotropic effect of ISO stimulation of  $\beta_1$ -adrenergic receptors. However, contrary to expectations, the dose-response curves for systolic  $[\text{Ca}^{2+}]_i$  and amplitude of  $\text{Ca}^{2+}$  transient were significantly greater in resting period (ZT3) myocytes compared to active period (ZT15) at concentrations of ISO  $> 3$  nM. In addition, no significant diurnal variation was documented in the response of diastolic  $[\text{Ca}^{2+}]_i$  to ISO application.

#### **4.2.2 The effects of stimulation frequency on diurnal variation in the response of the $\text{Ca}^{2+}$ transient to $\beta$ -adrenergic stimulation with isoproterenol**

In the previous chapter, we have shown the presence of a significant diurnal variation in SR-function reflected by the rate of relaxation of the electrically-evoked  $\text{Ca}^{2+}$  transient and magnitude of the SR  $\text{Ca}^{2+}$  content. In this chapter, we have thus far demonstrated, that both systolic  $[\text{Ca}^{2+}]_i$  and the amplitude of  $\text{Ca}^{2+}$  transient are significantly higher in resting period (ZT3) myocytes in comparison to active period (ZT15) myocytes at ISO concentrations  $> 3$ nM, at a stimulation frequency of 1Hz. As the force-frequency relationship (FFR) impinges on SR  $\text{Ca}^{2+}$  content and there is a diurnal variation in SR function, we therefore postulated that the diurnal variation in the dose-response relationship of systolic  $[\text{Ca}^{2+}]_i$  to ISO would be influenced by stimulation-frequency.

To investigate whether the diurnal variation in the dose-response curves of systolic  $[\text{Ca}^{2+}]_i$  and the amplitude of  $\text{Ca}^{2+}$  transient to ISO are altered by frequency, we determined the dose-dependent effects of ISO on  $[\text{Ca}^{2+}]_i$ , as outlined in figure 4.1A, in resting period (ZT3) and active period (ZT15) myocytes, stimulated at 0.5Hz and 2Hz. However, it is important to note that when pacing at a rate of 2Hz, some myocytes

quickly developed asynchronous or arrhythmic activity along with a high resting diastolic  $[Ca^{2+}]$  concentration and therefore, these myocytes were excluded from analysis.

Figure 4.4 are the dose-response curves of diastolic  $[Ca^{2+}]_i$  (top), systolic  $[Ca^{2+}]_i$  (middle) and the amplitude of the  $Ca^{2+}$ -transient (bottom) recorded from resting period (ZT3; blue symbols) and active period (ZT15) myocytes (red symbols), at 0.5Hz (A) and 2Hz (B). Figure 4.4 A shows that diastolic  $[Ca^{2+}]$ , systolic  $[Ca^{2+}]_i$  and amplitude of  $Ca^{2+}$  transient all increase in a sigmoidal dose-dependent manner in response to increasing ISO concentrations at 0.5Hz electrical field stimulation. There was no significant difference in the sensitivities of diastolic  $[Ca^{2+}]$ , systolic  $[Ca^{2+}]$  and the amplitude of  $Ca^{2+}$  transient to ISO ( $EC_{50}$ ) between resting period (ZT3) myocytes ( $n = 12-26/6$ ) and active period (ZT15) myocytes ( $n = 16-22/6$ ) during 0.5Hz electrical field stimulation (see appendix 2 figure 1 for  $EC_{50}$  data). The data also shows that systolic  $[Ca^{2+}]$  and the amplitude of  $Ca^{2+}$  transient dose-response relationships both diverge at concentrations  $> 3nM$  ISO during 0.5Hz electrical field stimulation, with resting period (ZT3) myocytes having significantly higher systolic  $[Ca^{2+}]$  and amplitude of  $Ca^{2+}$  transient in comparison to active period (ZT15) myocytes, similar to data obtained at 1Hz (see figure 4.3). The responses of systolic  $[Ca^{2+}]$  and the amplitude of  $Ca^{2+}$  transient to maximal ISO stimulation (100nM) were also significantly higher in resting period (ZT3) myocytes than active period (ZT15) myocytes during 0.5Hz electrical field stimulation (see appendix 2 figure 2 for maximal ISO stimulation data). In addition, the diastolic  $[Ca^{2+}]$  dose-response relationship does not diverge and its response to maximal ISO stimulation (100nM) was not significantly different between resting period (ZT3) and active period (ZT15) myocytes during 0.5Hz electrical field stimulation.

Figure 4.4 B shows that diastolic  $[Ca^{2+}]$ , systolic  $[Ca^{2+}]_i$  and amplitude of  $Ca^{2+}$  transient all increase in a sigmoidal dose-dependent manner in response to increasing ISO concentrations during at 2Hz electrical field stimulation. There was no significant difference in the sensitivities of diastolic  $[Ca^{2+}]$ , systolic  $[Ca^{2+}]$  and the amplitude of

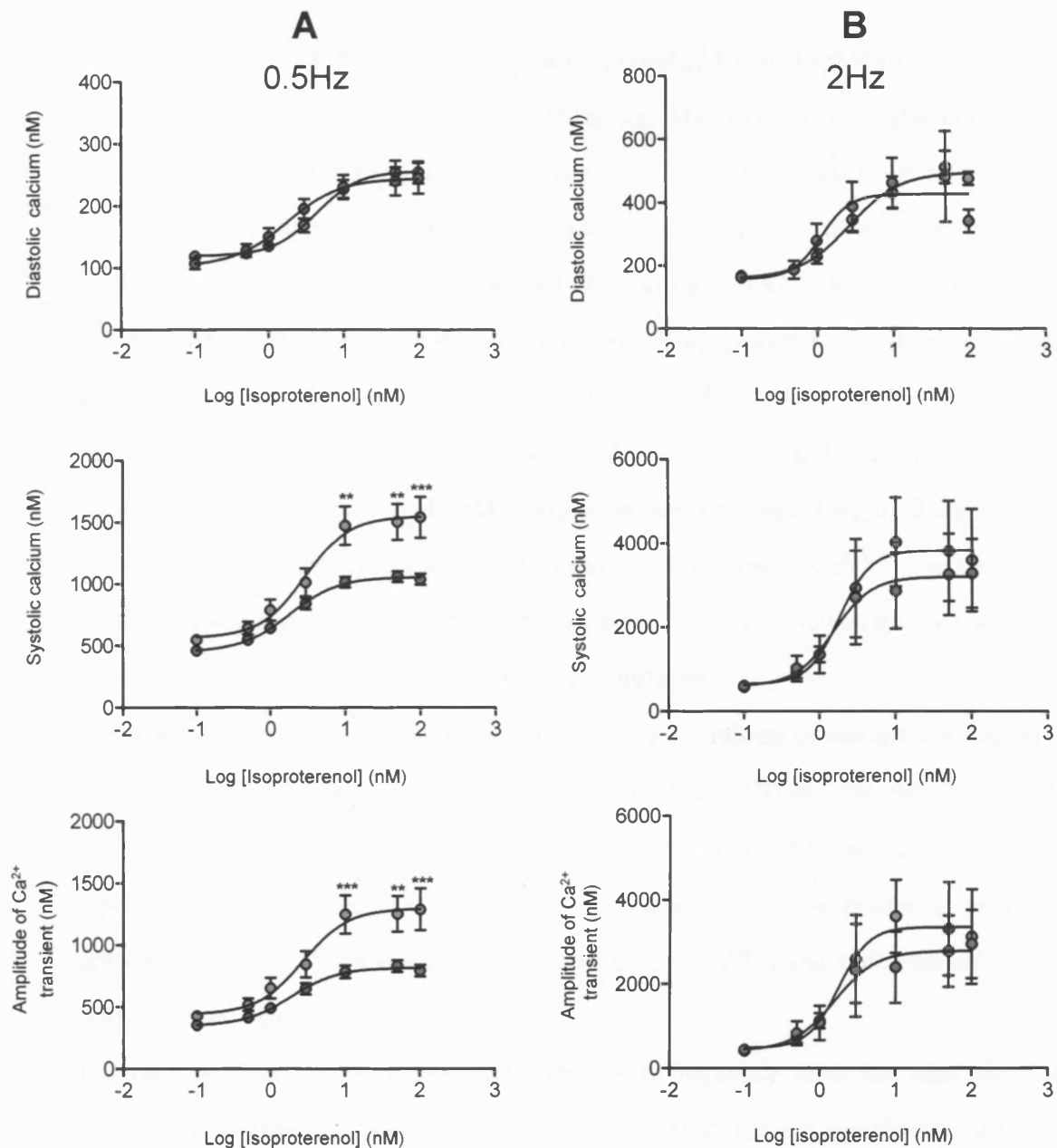


**Figure 4.4- Effect of stimulation frequency on dose-response curves of diastolic [Ca<sup>2+</sup>], systolic [Ca<sup>2+</sup>] and amplitude of Ca<sup>2+</sup> transient to  $\beta$ -adrenergic stimulation with isoproterenol (ISO) in resting period (ZT3) and active period (ZT15) myocytes.**

Dose-response curves of diastolic [Ca<sup>2+</sup>] (top), systolic [Ca<sup>2+</sup>] (middle) and amplitude of Ca<sup>2+</sup> transient (bottom) to ISO showing the effects of 0.5Hz (A) and 2Hz (B) electrical field stimulation in resting period (ZT3) myocytes (blue circles) and active period (ZT15) myocytes (red circles). Values are mean  $\pm$  S.E.M.; numbers of experiments/ hearts = resting period (ZT3) myocyte (0.5Hz  $n = 12-26/6$ ; 2Hz  $n = 4-15/3$ ) and active period (ZT15) myocyte (0.5Hz  $n = 16-22/6$ ; 2Hz  $n = 5-9/2$ ). \*\*  $p < 0.01$ , \*\*\*  $p < 0.001$ , two way ANOVA followed by a Bonferroni *post hoc* test. Note- graphs in A and B have different scales.

Ca<sup>2+</sup> transient to ISO (EC<sub>50</sub>) between resting period (ZT3) myocytes ( $n = 4-15/3$ ) and active period (ZT15) myocytes ( $n = 5-9/2$ ) during 2Hz electrical field stimulation (see appendix 2 figure 1 for EC<sub>50</sub> data). The data also shows that diastolic [Ca<sup>2+</sup>]<sub>i</sub>, systolic [Ca<sup>2+</sup>]<sub>i</sub> and the amplitude of Ca<sup>2+</sup> transient dose-response relationships do not significantly diverge at any ISO concentrations during 2Hz electrical field stimulation, due large error bars as a result of low  $n$  numbers. The responses of systolic [Ca<sup>2+</sup>]<sub>i</sub> and the amplitude of Ca<sup>2+</sup> transient to maximal ISO stimulation (100nM) were not significantly different between resting period (ZT3) myocytes and active period (ZT15) myocytes during 2Hz electrical field stimulation (see appendix 2 figure 2 for maximal ISO stimulation data). In addition, the response of diastolic [Ca<sup>2+</sup>]<sub>i</sub> to maximal ISO stimulation was significantly higher in resting period (ZT3) myocytes than active period (ZT15) myocytes during 2Hz electrical field stimulation.

Figure 4.5 are bar charts of the mean data showing the effects of stimulation frequency (0.5, 1 and 2 Hz) on diastolic [Ca<sup>2+</sup>]<sub>i</sub> (A); systolic [Ca<sup>2+</sup>]<sub>i</sub> (B) and the amplitude of the Ca<sup>2+</sup>-transient (C) in resting period (ZT3) and active period (ZT15) myocytes following superfusion of 10nM ISO, which is the concentration of ISO that produces the largest differences in the Ca<sup>2+</sup> transient between resting period (ZT3) and active period (ZT15) myocytes (see figure 4.2 and 4.3).

The data in figure 4.5A shows that stimulation frequency does not alter the ISO response with respect to diastolic Ca<sup>2+</sup>, as diastolic [Ca<sup>2+</sup>]<sub>i</sub> is not significantly different between resting period (ZT3) and active period (ZT15) myocytes at 0.5Hz, 1Hz & 2Hz electrical stimulation. (See appendix 2 figure 3 for data). This is expected as no significant diurnal variation was observed in diastolic Ca<sup>2+</sup> in response to ISO.

Figure 4.5B shows that diurnal variation in the responsiveness of systolic [Ca<sup>2+</sup>]<sub>i</sub> to 10nM ISO persists at stimulation frequencies <1Hz, as systolic [Ca<sup>2+</sup>]<sub>i</sub> is significantly higher in resting period (ZT3) myocytes at 0.5Hz ( $p < 0.01$ ) and 1Hz electrical field stimulation ( $p < 0.01$ ) in comparison to active period (ZT15) myocytes. However, the response of systolic [Ca<sup>2+</sup>]<sub>i</sub> to ISO stimulation is not significantly different between

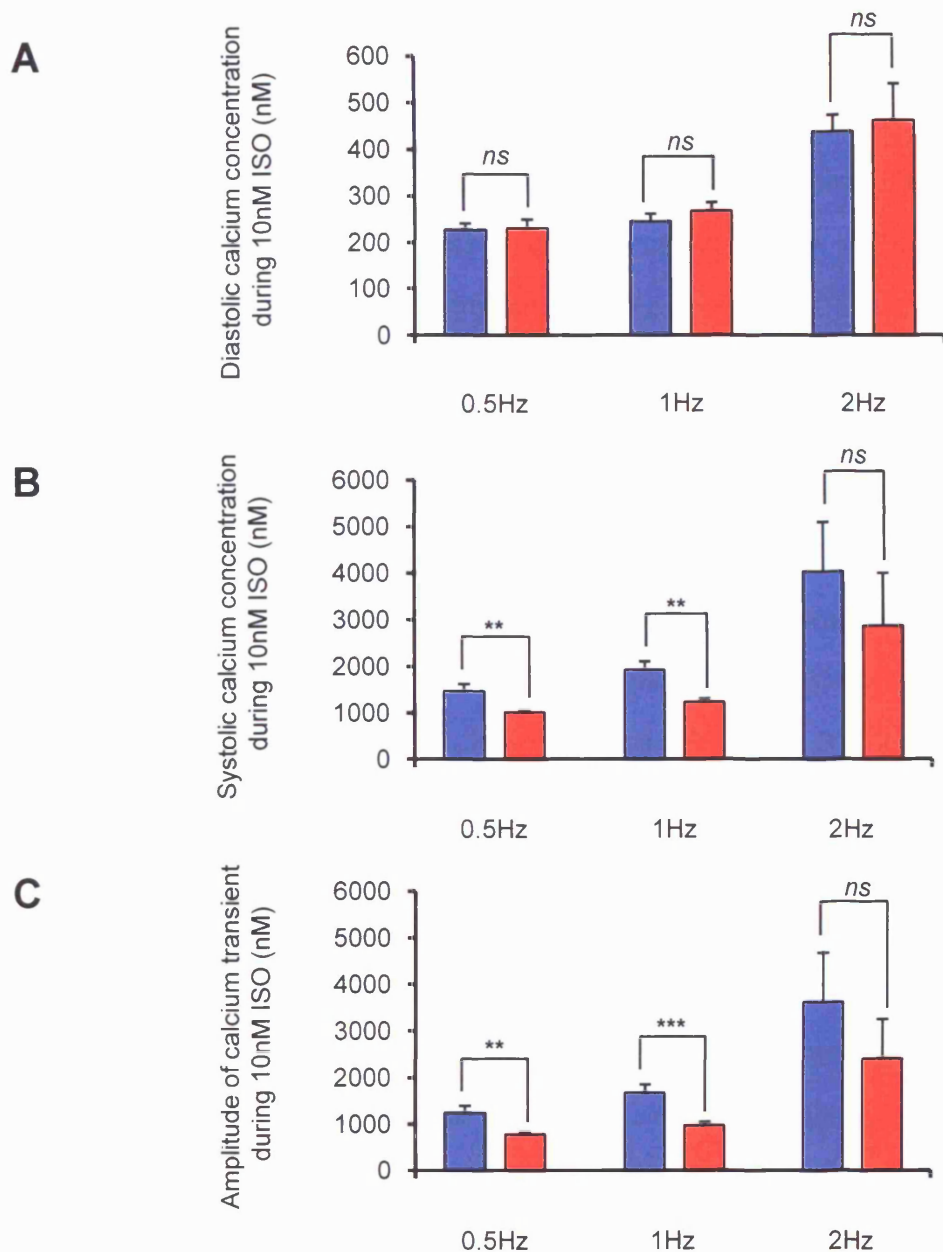


**Figure 4.5- The effect of stimulation frequency on diastolic [Ca<sup>2+</sup>], systolic [Ca<sup>2+</sup>] and amplitude of Ca<sup>2+</sup> transient to  $\beta$ -adrenergic stimulation with 10nM isoproterenol (ISO) in resting period (ZT3) and active period (ZT15) myocytes.**

Bar charts showing levels of diastolic [Ca<sup>2+</sup>] (A), systolic [Ca<sup>2+</sup>] (B) and amplitude of Ca<sup>2+</sup> transient (C) during superfusion of 10nM ISO and electrical field stimulation at 0.5 Hz, 1Hz and 2Hz in resting period (ZT3) myocytes (blue) and active period (ZT15) myocytes (red), obtained from experiments described in figure 4.1. Values are mean  $\pm$  S.E.M.; number of experiments/ hearts = resting period (ZT3) myocyte (0.5Hz:  $n = 16/6$  ; 1Hz :  $n = 47/10$ ; 2Hz:  $n = 4/3$ ) and active period (ZT15) myocyte (0.5Hz:  $n = 20/6$  ; 1Hz:  $n = 49/11$ ; 2Hz:  $n = 7/2$ ). \*\*  $p < 0.01$ , \*\*\*  $p < 0.001$ , unpaired students  $t$  test.

resting period (ZT3) and active period (ZT15) myocytes during 2Hz stimulation (See appendix 2 figure 3 for data).

Figure 4.5 C shows that diurnal variation in the responsiveness of the amplitude of  $\text{Ca}^{2+}$  transient to 10nM ISO persists at stimulation frequencies <1Hz, as the amplitude of  $\text{Ca}^{2+}$  transient is significantly higher in resting period (ZT3) myocytes at both 0.5Hz ( $p < 0.01$ ) and 1Hz electrical field stimulation ( $p < 0.001$ ) in comparison to active period (ZT15) myocytes. However, the amplitude of  $\text{Ca}^{2+}$  transient is not significantly different between resting period (ZT3) and active period (ZT15) myocytes during 2Hz stimulation (See appendix 2 figure 3 for data). These data show that diurnal variation in the dose-response relationships of systolic  $[\text{Ca}^{2+}]$  and amplitude of  $\text{Ca}^{2+}$  transient to ISO in resting period (ZT3) and active period (ZT15) myocytes were similar at stimulation frequencies <1Hz, indicating that stimulation frequency does not alter the diurnal influence on the ISO response. It is difficult to rely on the statistical significance of the dose-response data collected at 2Hz, as the low  $n$  numbers observed in the dose-response relationships of the  $\text{Ca}^{2+}$  transient (diastolic, systolic and amplitude) to ISO were the result of a larger number of myocytes being excluded from analysis due to the development of asynchronous arrhythmic activity and a high resting diastolic  $[\text{Ca}^{2+}]$ , which could have resulted in the loss of significance in the response of the  $\text{Ca}^{2+}$  transient to ISO at 2Hz between resting period (ZT3) and active period (ZT15) myocytes.

#### **4.2.3 Diurnal variation in the response of contraction strength to $\beta$ -adrenergic stimulation with isoproterenol**

In the previous chapter, we showed that the resting  $\text{Ca}^{2+}$  transient and contraction strength are both significantly higher in resting period (ZT3) myocytes than active period (ZT15) myocytes and in the present chapter we have extended these findings to show that at high concentrations of ISO (> 3nM), the increase in systolic  $[\text{Ca}^{2+}]$  is

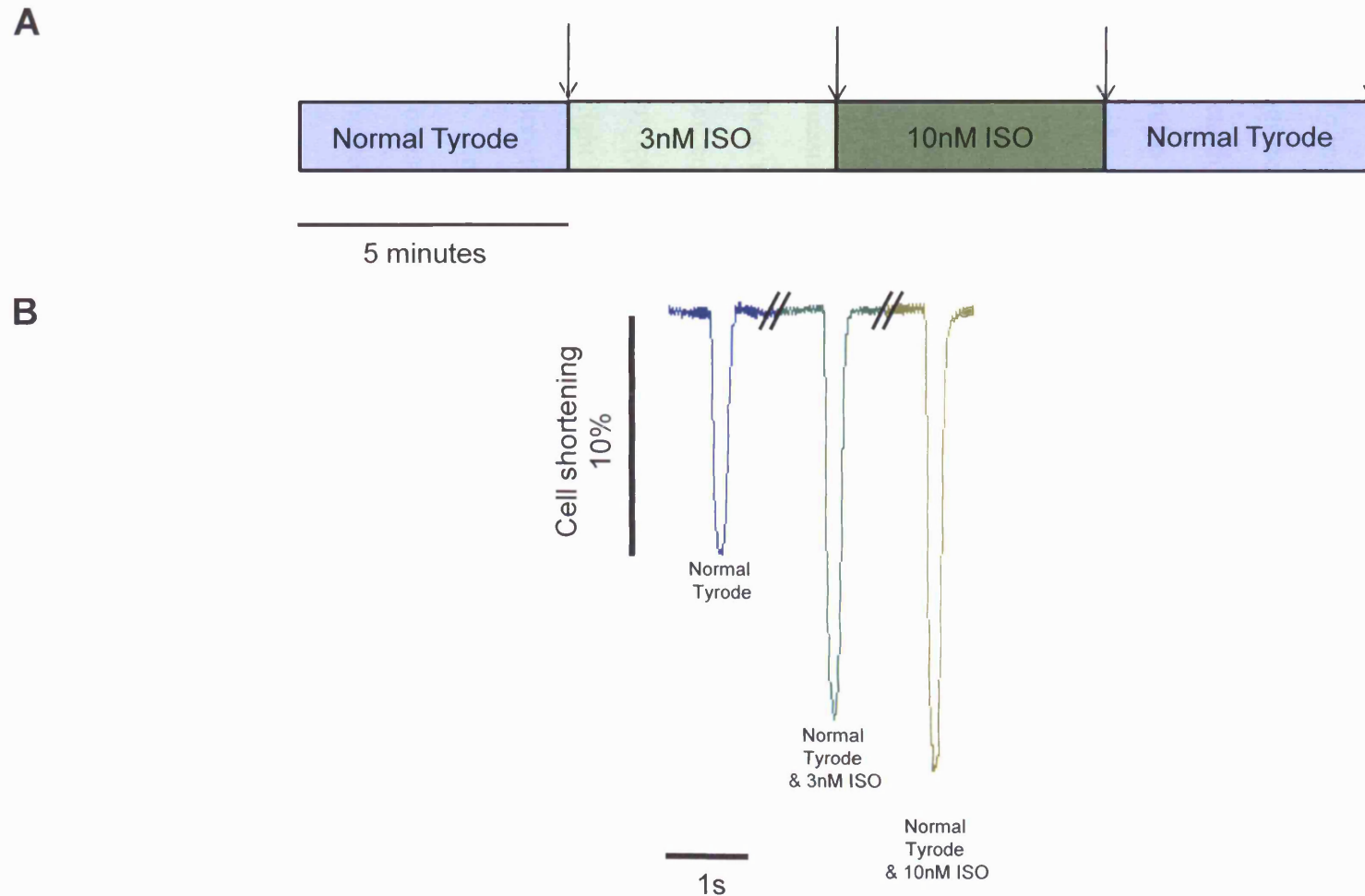


**Figure 4.6- Protocol to determine the concentration-dependent effect of isoproterenol (ISO) on percentage cell shortening in resting period (ZT3) and active period (ZT15) myocytes.**

Video cell-edge detection was used to assess percentage cell shortening in ventricular myocytes. Myocytes were stimulated at a rate of 1Hz and superfused with normal Tyrode for 5 minutes. Myocytes were then superfused with normal Tyrode containing 3nM ISO and normal Tyrode containing 10nM ISO in succession for 5 minutes each. Myocytes were superfused with normal Tyrode to wash off ISO and to allow recovery of cell shortening to basal levels. Data were collected at the end of 5 minutes of ISO exposure (as indicated by the arrows) as diastolic and systolic lengths from which percentage cell shortening was obtained.

significantly greater in resting period (ZT3) myocytes than active period (ZT15) myocytes. Therefore, due to diurnal variation in the responsiveness of the  $\text{Ca}^{2+}$ -transient to ISO, we postulated that this would be reflected by a similar diurnal variation in response of contraction strength to ISO.

To investigate whether the diurnal variation seen in response of the  $\text{Ca}^{2+}$  transient to  $\beta$ -adrenergic stimulation with ISO translates to contraction strength, measurements of cell length were made from resting period (ZT3) and active period (ZT15) myocytes using a video cell-edge detection system. Myocytes were electrically field stimulated at 1Hz and superfused for 5 minutes in succession with normal Tyrode, normal Tyrode containing 3nM ISO and normal Tyrode containing 10nM ISO (see figure 4.6A). ISO was washed off with Normal Tyrode for 5 minutes to allow recovery of contraction. Cell length was followed continuously for the duration of the protocol and cell length was recorded for 30 seconds when it had reached steady state (~ 5minutes), from which measurements of diastolic and systolic length were taken and the difference between these two used to calculate percentage cell shortening. Figure 4.6 B is a recording of cell contraction, assessed as percent cell shortening, from a single resting period (ZT3) myocyte, superfused with normal Tyrode (blue); normal Tyrode containing 3nM ISO (light green) and normal Tyrode containing 10nM ISO (dark green) during 1Hz electrical field stimulation, using the protocol shown in figure 4.6A. The record shows a concentration-dependent increase in contraction strength to increasing ISO concentrations.

Figure 4.7 is a bar chart of the mean data, from such experiments, showing percent cell shortening in normal Tyrode (left) and in response to  $\beta$ -adrenergic stimulation with 3nM ISO (middle) and 10nM ISO (right) in resting period (ZT3) and active period (ZT15) myocytes. Percent cell shortening in normal Tyrode was higher in resting period (ZT3) myocytes at  $12.93 \pm 0.43 \%$  ( $n = 30/3$ ) compared to  $11.14 \pm 0.44 \%$  in active period (ZT15) myocytes ( $n = 41/4$ , *ns*). Percent cell shortening following stimulation with 3nM ISO was significantly higher in resting period (ZT3) myocytes at  $14.68 \pm 0.51$  ( $n = 30/3$ ) compared to  $11.85 \pm 0.49$  in active period (ZT15) myocytes ( $n =$

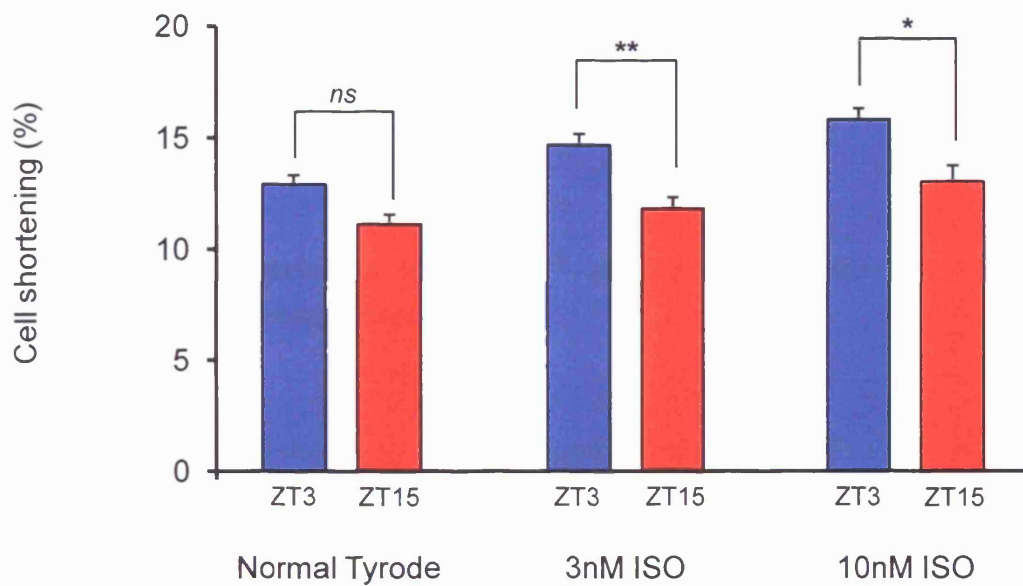


**Figure 4.7- The effect of  $\beta$ -adrenergic stimulation with isoproterenol (ISO) on percentage cell shortening in resting period (ZT3) and active period (ZT15) myocytes.**

Bar chart showing contraction strength, assessed as percentage cell shortening, recorded from resting period (ZT3) myocytes (blue) and active period (ZT15) myocytes (red) stimulated at a rate of 1Hz. Each myocyte was superfused with normal Tyrode, 3nM ISO-containing Tyrode and 10nM ISO-containing Tyrode sequentially for 5 minutes each, as described in figure 4.6. Values are the mean  $\pm$  S.E.M.; number of experiments/hearts = resting period (ZT3) myocyte,  $n = 30/3$  and active period (ZT15) myocyte,  $n = 21-41/4$ , \*  $p < 0.05$ , \*\*  $p < 0.001$ , two way ANOVA followed by a Bonferroni *post hoc* test.

41/4;  $p < 0.001$ ), and after 10nM ISO was significantly higher in resting period (ZT3) myocytes at  $15.82 \pm 0.40$  ( $n = 30/3$ ) compared to  $13.03 \pm 0.72$  in active period (ZT15) myocytes ( $n = 21/2$ ;  $p < 0.05$ ). These data show that ISO increases contraction strength in both resting period (ZT3) and active period (ZT15) myocytes i.e. ISO has a positive inotropic effect; however, this increase is more profound in the resting period (ZT3) myocyte which also reflects the increased  $\text{Ca}^{2+}$  transients seen in resting period (ZT3) myocytes during ISO stimulation.

#### **4.2.4 Diurnal variation in SR $\text{Ca}^{2+}$ content in response to $\beta$ -adrenergic stimulation with isoproterenol.**

The non-specific  $\beta$ -adrenergic receptor agonist ISO is believed to mediate most of its inotropic effects via the phosphorylation of PLB in the rat (Li et al., 2000), which increases the activity of SERCA 2a, resulting in greater sequestration of  $\text{Ca}^{2+}$  into the SR, which increases SR  $\text{Ca}^{2+}$  content and therefore the amount of  $\text{Ca}^{2+}$  available for release (Bers, 2001, Bers, 2002). Due to our finding that, systolic  $[\text{Ca}^{2+}]_i$  is greater in resting period (ZT3) myocytes compared to the active period (ZT15) myocytes in response to stimulation with ISO, we postulated that this may reflect an increase in SR  $\text{Ca}^{2+}$  content in resting period (ZT3) myocytes. To investigate whether the increase in the  $\text{Ca}^{2+}$  transient in response to stimulation with ISO seen in resting period (ZT3) myocytes compared to active period (ZT15) myocytes reflects an increase in SR  $\text{Ca}^{2+}$  content, we looked at whether the ISO-induced increase in SR  $\text{Ca}^{2+}$  content exhibits a similar diurnal variation, by determining SR  $\text{Ca}^{2+}$  loading during  $\beta$ -adrenergic stimulation with ISO. To determine the effects of ISO stimulation on SR  $\text{Ca}^{2+}$  loading, myocytes were electrically-field stimulated at 1Hz and superfused with normal Tyrode. When the  $\text{Ca}^{2+}$ -transients had reached a steady-state (usually after 5 minutes), the stimulator was switched off and the cell rapidly superfused with normal Tyrode containing 20mM caffeine (5 second pulse), which resulted in a caffeine-induced  $\text{Ca}^{2+}$

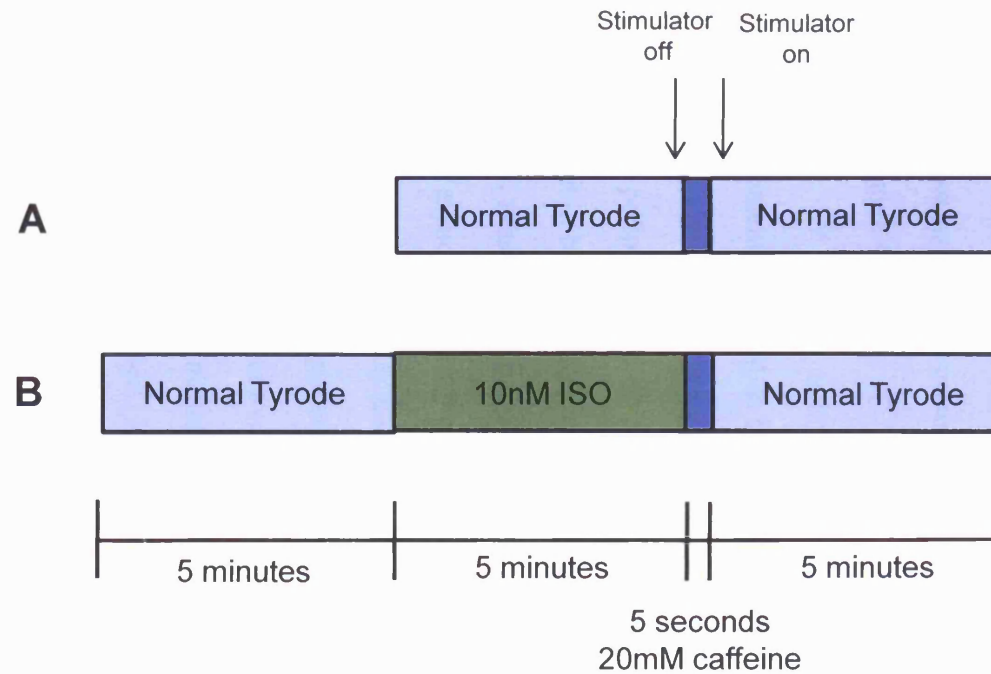


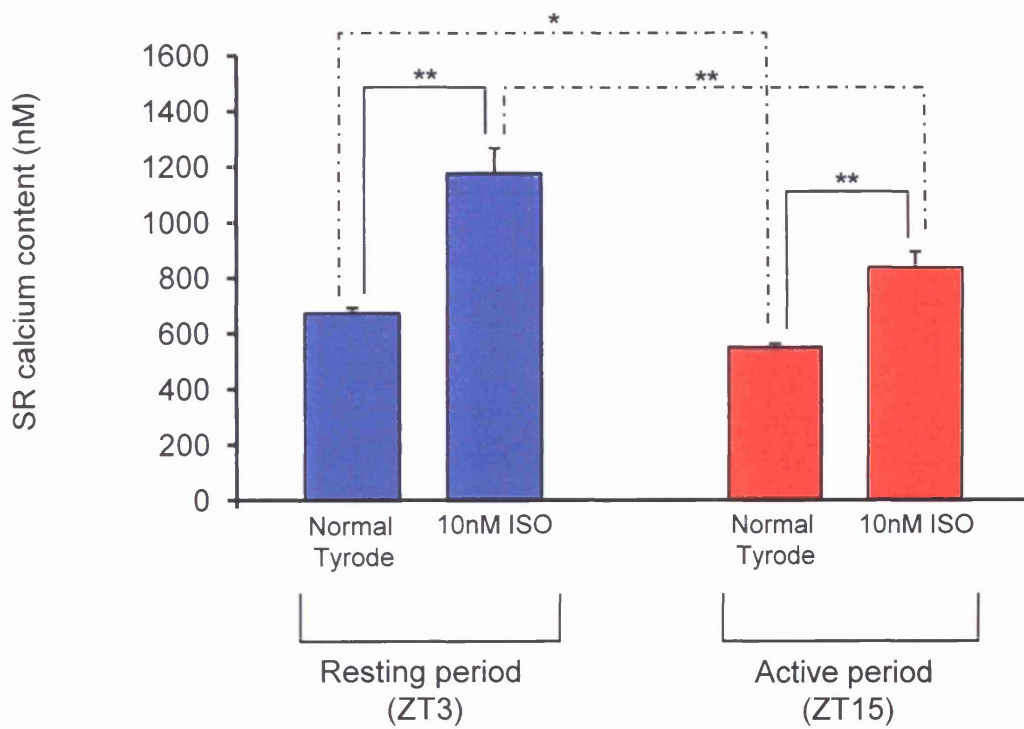
**Figure 4.8- Protocol used to obtain caffeine-induced calcium transients in resting period (ZT3) and active period (ZT15) myocytes during control conditions and  $\beta$ -adrenergic stimulation with isoproterenol (ISO).**

- A. Myocytes were superfused with normal Tyrode for 5 minutes during 1Hz electrical field stimulation. After which, the cell stimulator was switched off for ~10 seconds before superfusing the myocytes with normal Tyrode containing 20mM caffeine for 5 seconds. Normal Tyrode was then perfused to allow recovery of calcium transients.
- B. Myocytes were treated as in A; however, prior to caffeine superfusion normal Tyrode containing 10nM ISO was superfused for 5 minutes.

transient. Following this, the stimulator was switched on and myocytes superfused with normal Tyrode, to allow recovery of  $\text{Ca}^{2+}$  transients. Any experiment where the magnitude of the electrically-evoked  $\text{Ca}^{2+}$  transient was significantly altered following the rapid application of caffeine was discarded (i.e. if  $\text{Ca}^{2+}$  transients had not returned to within 80% of the control  $\text{Ca}^{2+}$  transients following caffeine application). The modulating effects of ISO were determined by superfusing the myocytes for 5 minutes with normal Tyrode containing 10nM ISO immediately prior to application of caffeine (see figure 4.8).

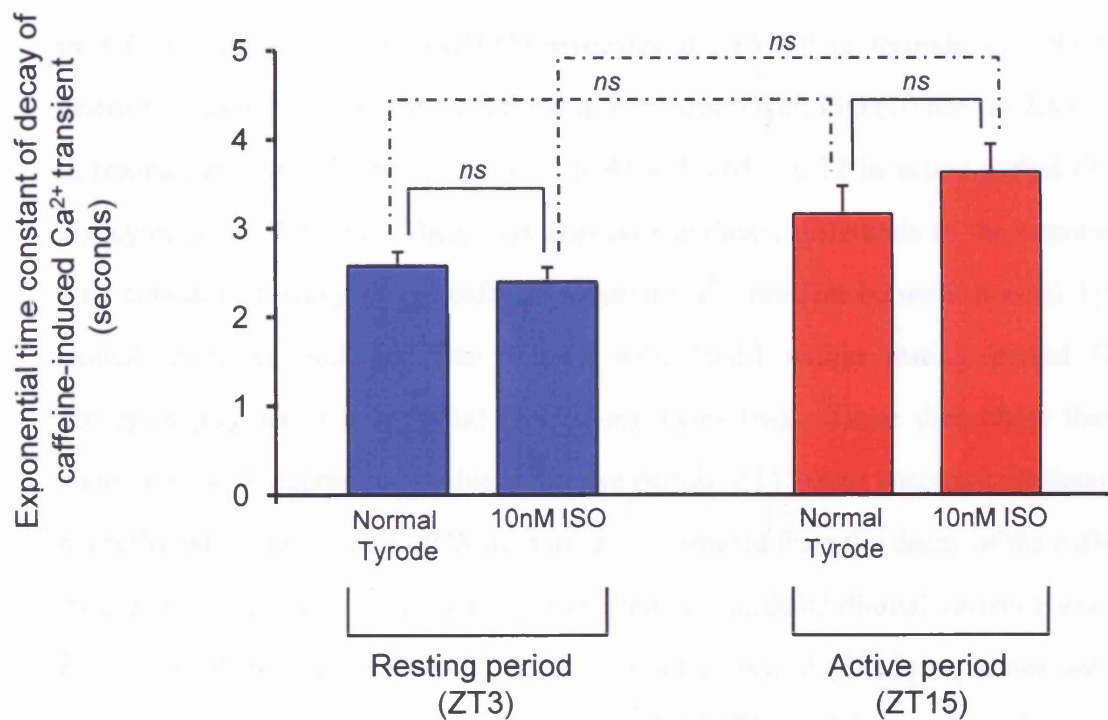
Figure 4.9 is a bar chart of the mean data from such experiments, and shows SR  $\text{Ca}^{2+}$  content, assessed as the peak  $\text{Ca}^{2+}$  in response to 20mM caffeine, in normal Tyrode and following  $\beta$ -adrenergic stimulation with 10nM ISO in resting period (ZT3) and active period (ZT15) myocytes. The data show that ISO-stimulation increases SR  $\text{Ca}^{2+}$  content in both resting period (ZT3) ( $p < 0.001$ ) and active period (ZT15) myocytes ( $p < 0.001$ ), which corresponded to an increase in SR  $\text{Ca}^{2+}$  content of 75% in resting period (ZT3) myocytes and 52% in active period (ZT15) myocytes following the superfusion of 10nM ISO. Under basal conditions i.e. the superfusion of normal Tyrode, the SR  $\text{Ca}^{2+}$  content was significantly higher in resting period (ZT3) myocytes at  $672.8 \pm 20.5$  nM ( $n = 71/3$ ) than active period (ZT15) myocytes at  $551.0 \pm 12.8$  nM ( $n = 97/4$ ;  $p < 0.01$ ). Following stimulation with 10nM ISO, the SR  $\text{Ca}^{2+}$  content was significantly higher in resting period (ZT3) myocytes at  $1177.4 \pm 90.5$  ( $n = 24/4$ ) compared to active period (ZT15) myocytes at  $837.7 \pm 59.0$  ( $n = 19/3$ ;  $p < 0.001$ ). In addition, to determine whether the increase in NCX1 mRNA in hearts isolated during the active period (ZT15), shown in the previous chapter, reflects an increase in NCX1 activity in response to ISO stimulation, we looked at the rate of relaxation (or decay) of the caffeine-induced  $\text{Ca}^{2+}$  transient, as this reflects the activity of NCX1 (Bassani et al., 1994).

Figure 4.10 is a bar chart of the mean data showing the exponential time constant of decay of the caffeine-induced  $\text{Ca}^{2+}$  transient in normal Tyrode and following  $\beta$ -adrenergic stimulation with 10nM ISO in resting period (ZT3) and active period (ZT15)



**Figure 4.9- The effect of  $\beta$ -adrenergic stimulation with isoproterenol (ISO) on the sarcoplasmic reticulum  $\text{Ca}^{2+}$  content in resting period (ZT3) and active period (ZT15) myocytes.**

Bar chart showing the sarcoplasmic reticulum  $\text{Ca}^{2+}$  content recorded from resting period (ZT3) myocytes (blue) and active period (ZT15) myocytes (red), obtained from experiments described in figure 4.8. Values are the mean  $\pm$  S.E.M.; numbers of experiments/ hearts = resting period (ZT3) myocyte (normal Tyrode  $n = 71/3$ ; 10nM ISO  $n = 24/4$ ) and active period (ZT15) myocyte (normal Tyrode  $n = 97/4$ ; 10nM ISO  $n = 19/3$ ), \*  $p < 0.01$ , \*\*  $p < 0.001$ , two way ANOVA followed by a Bonferroni *post hoc* test.



**Figure 4.10- The effect of  $\beta$ -adrenergic stimulation with isoproterenol (ISO) on the exponential time constant of decay of the caffeine-induced  $\text{Ca}^{2+}$  transient in resting period (ZT3) and active period (ZT15) myocytes.**

Bar chart showing the exponential time constant of decay of the caffeine-induced  $\text{Ca}^{2+}$  transient recorded from resting period (ZT3) myocytes (blue) and active period (ZT15) myocytes (red) in normal Tyrode superfusion and 10nM ISO-containing Tyrode, obtained from experiments described in figure 4.8. The exponential time constant of decay of the caffeine  $\text{Ca}^{2+}$  transient was calculated by fitting a single exponential to the slope of each caffeine  $\text{Ca}^{2+}$  transient. Values are the mean  $\pm$  S.E.M.; numbers of experiments/ hearts = resting period (ZT3) myocyte (normal Tyrode  $n = 71/3$ ; 10nM ISO  $n = 24/4$ ) and active period (ZT15) myocyte (normal Tyrode  $n = 97/4$ ; 10nM ISO  $n = 19/3$ ); two way ANOVA followed by a Bonferroni *post hoc* test. Note- statistics performed in combination with data presented in figure 5.4.

myocytes, from experiments described in figure 4.9. The exponential time constant of decay of the caffeine-induced  $\text{Ca}^{2+}$  transient was calculated by fitting a single exponential to the slope of each caffeine-induced  $\text{Ca}^{2+}$  transient. The data show that there is no significant difference in exponential time constant of decay of the caffeine-induced  $\text{Ca}^{2+}$  transient between resting period (ZT3) myocytes at  $2.58 \pm 0.16$  seconds ( $n = 71/3$ ) and active period (ZT15) myocytes at  $3.16 \pm 0.32$  seconds, ( $n = 97/4$ ; *ns*) determined in normal Tyrode, or following stimulation with ISO (10 nM) at  $2.40 \pm 0.16$  in resting period (ZT3) myocytes ( $n = 24/4$ ) and  $3.63 \pm 0.32$  in active period (ZT15) myocytes ( $n = 19/3$ , *ns*). There was also no significant difference in the exponential time constant of decay of the caffeine-induced  $\text{Ca}^{2+}$  transient between normal Tyrode treated myocytes and myocytes treated with 10nM within resting period (ZT3) myocytes (*ns*) and active period (ZT15) myocytes (*ns*). These data show that the increase in NCX expression during the active period (ZT15) (see chapter 3 for data) was not reflected by an increase NCX activity, as determined from the decay of the caffeine-induced  $\text{Ca}^{2+}$  transient. The data also show that a significant diurnal variation exists in SR  $\text{Ca}^{2+}$  content in resting period (ZT3) and active period (ZT15) myocytes and this variation is enhanced by the application of 10nM ISO, which may contribute to the observed variations in the  $\text{Ca}^{2+}$  transient and contraction in response to  $\beta$ -adrenergic stimulation with ISO in resting period (ZT3) and active period (ZT15) myocytes.

#### **4.2.5 Diurnal variation in the development of arrhythmic activity in ventricular myocytes in response to $\beta$ -adrenergic stimulation with isoproterenol**

Excessive  $\beta$ -adrenergic stimulation results in the generation of spontaneous arrhythmic activity *in vitro* in isolated ventricular myocytes and *in vivo* in intact heart from adult male Wistar rats (Penna and Bassani, 2010), Swine (Wei et al., 2002), Guinea pigs (Song et al., 2001) and humans (Meredith et al., 1991, Anderson, 2003). Indeed, in our hands, adult male Wistar rat ventricular myocytes stimulated at 1Hz and superfused

with normal Tyrode containing ISO developed asynchronous/ arrhythmic activity in response to ISO concentrations  $> 3\text{nM}$ , using the protocol illustrated in figure 4.1. The generation of arrhythmic activity in response to ISO is due to either early after-depolarisations (EADs), caused by LTCC reactivation, or delayed after-depolarisations (DADs), which are due to spontaneous SR  $\text{Ca}^{2+}$  release (see section 1.5 of introduction for detail). As resting period (ZT3) myocytes respond to ISO with a greater increase in SR  $\text{Ca}^{2+}$  content, we postulated that more resting period (ZT3) myocytes would develop arrhythmic activity in response to ISO superfusion. To determine whether the threshold for arrhythmic activity, to excessive  $\beta$ -adrenergic stimulation with ISO, exhibits diurnal variation, we measured the percentage of resting period (ZT3) and active period (ZT15) myocytes developing arrhythmic activity in response to  $\beta$ -adrenergic stimulation with increasing concentrations of ISO. Myocytes were superfused with normal Tyrode for 5 minutes, then superfused for 5 minutes in succession with normal Tyrode containing ISO in the following concentrations (nM): 3, 10, 50 and 100, during which time fields of  $\sim 10\text{-}20$  myocytes were assessed for arrhythmic activity. Following this, myocytes were superfused with normal Tyrode for 5 minutes to allow recovery from ISO superfusion. Myocytes were deemed arrhythmic if they were contracting asynchronously in response to 1Hz electrical field stimulation at the end of 5 minutes ISO superfusion (see section 2.3.1 for detail).

Figure 4.11 is a bar chart of the mean data showing the percentage of myocytes that develop arrhythmic activity in response to  $\beta$ -adrenergic stimulation with ISO (3, 10, 50 & 100nM). The data show that a significant percentage of both resting period (ZT3) and active period (ZT15) myocytes develop asynchronous/arrhythmic activity in response to ISO and that there is a concentration-dependent increase in the percentage of myocytes developing arrhythmic activity. The data also show that significantly more resting period (ZT3) myocytes developed arrhythmic activity than active period (ZT15) myocytes at concentrations of ISO between 3 and 10 nM, with  $43.3 \pm 4.8\%$  of resting period (ZT3) myocytes ( $n = 238; 18; 5$ , where  $n = \text{cells; experiments; hearts}$ , see section 2.9 for detail) versus  $13.6 \pm 1.8\%$  of active period (ZT15) myocytes ( $n = 257; 19; 5; p$

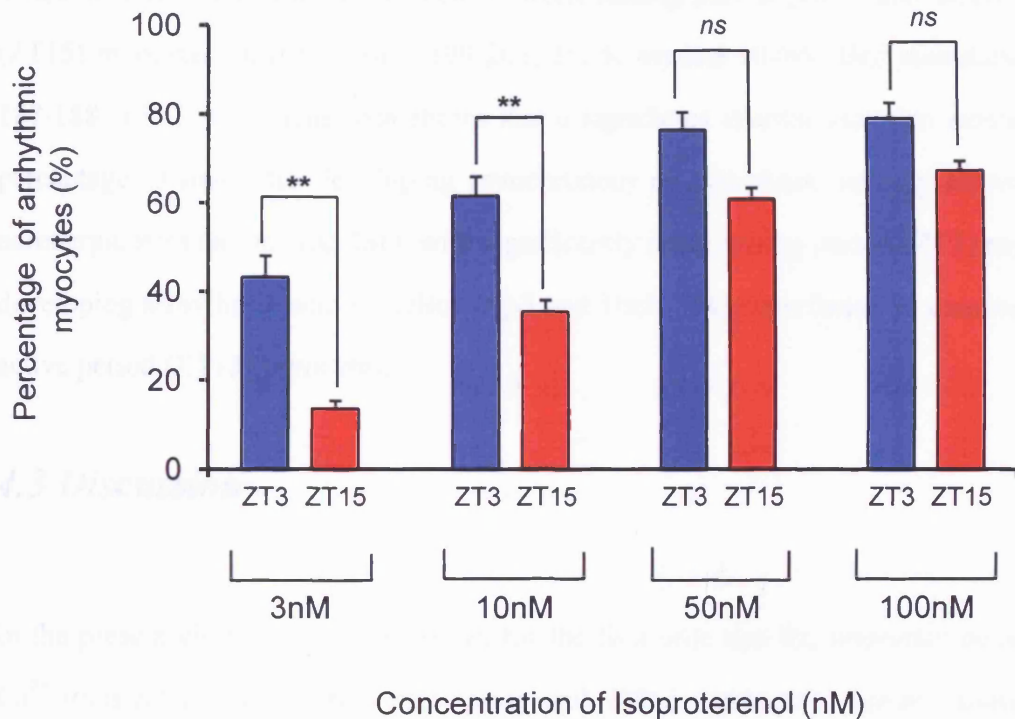


**Figure 4.11- Diurnal variation in the percentage of ventricular myocytes developing arrhythmic activity in response to  $\beta$ -adrenergic stimulation with isoproterenol (ISO).**

Bar chart showing the percentage of resting period (ZT3) myocytes (blue) and active period (ZT15) myocytes (red) from fields of ~10-20 cells, that develop asynchronous, arrhythmic activity after superfusion with normal Tyrode containing 3, 10, 50 or 100nM ISO for 5 minutes during 1Hz electrical field stimulation. Values are mean  $\pm$  S.E.M.; number of cells; experiments; hearts = resting period (ZT3) myocyte (3nM  $n = 238$ ; 18; 5, 10nM  $n = 244$ ; 18; 5, 50nM  $n = 199$ ; 15; 5 & 100nM  $n = 187$ ; 15; 5) and active period (ZT15) myocyte (3nM  $n = 257$ ; 19; 5, 10nM  $n = 237$ ; 18; 5, 50nM  $n = 205$ ; 15; 5 & 100nM  $n = 188$ ; 15; 5); \*\*  $p < 0.001$ , two way ANOVA followed by a Bonferroni *post hoc* test.

< 0.001) developing arrhythmic activity in 3nM ISO and with  $61.6 \pm 4.4$  % of resting period (ZT3) myocytes ( $n = 244$ ; 18; 5) versus  $35.5 \pm 2.6$  % of active period (ZT15) myocytes ( $n = 237$ ; 18; 5;  $p < 0.001$ ) developing arrhythmic activity in 10nM ISO. There was no significant difference between resting period (ZT3) and active period (ZT15) myocytes during 50 ( $n = 199-205$ ; 15; 5, *ns*) and 100nM ISO stimulation ( $n = 187-188$ ; 15; 5, *ns*). This data shows that a significant diurnal variation exists in the percentage of myocytes developing asynchronous or arrhythmic activity following  $\beta$ -adrenergic stimulation with ISO, with significantly more resting period (ZT3) myocytes developing arrhythmic activity following 3 and 10nM ISO superfusion in comparison to active period (ZT15) myocytes.

### ***4.3 Discussion***

In the present chapter, we have shown for the first time that the responsiveness of the  $\text{Ca}^{2+}$  transient to  $\beta$ -adrenergic stimulation with ISO is subject to diurnal variation. To investigate this, we recorded the  $\text{Ca}^{2+}$  transient from myocytes isolated from adult Wistar rats during the resting period (ZT3) and the active period (ZT15) in response to increasing concentrations of ISO. The data show paradoxically that the responsiveness of systolic  $[\text{Ca}^{2+}]$  and amplitude of  $[\text{Ca}^{2+}]$  transient to ISO were both significantly greater in myocytes isolated during the resting period (ZT3). The differences in the responsiveness of systolic  $[\text{Ca}^{2+}]$  and amplitude of  $\text{Ca}^{2+}$  transient to ISO stimulation reflected increases in SR  $\text{Ca}^{2+}$  content and contraction strength as resting period (ZT3) myocytes had a significantly larger percent cell shortening and SR  $\text{Ca}^{2+}$  content in comparison to active period (ZT15) myocytes in response to ISO. Moreover, this time-of-day dependent influence on the responsiveness of systolic  $[\text{Ca}^{2+}]$  and amplitude of  $\text{Ca}^{2+}$  transient to ISO stimulation was not altered by changes in stimulation frequency <1Hz. The increased responsiveness of resting period (ZT3) myocytes to ISO

stimulation was also reflected by a higher percentage of field-stimulated resting period (ZT3) myocytes developing arrhythmic activity in response to ISO.

#### **4.3.1 Diurnal variation in the responsiveness of the $\text{Ca}^{2+}$ transient to isoproterenol**

In the rat myocardium, stimulation of  $\beta$ -adrenergic receptors with ISO results in positive inotropic and lusitropic effects through the PKA dependent phosphorylation of LTCC, RyR2, PLB and troponin I (see section 1.4.3 of the introduction for detail). Therefore, the time-of-day dependent variation in the responsiveness of systolic  $[\text{Ca}^{2+}]$  and amplitude of  $\text{Ca}^{2+}$  transient in response to ISO, which was greater in resting period (ZT3) myocytes, could result from changes in these proteins. More specifically, this could be the result of a greater increase in LTCC current density, resulting in enhanced activation of RyR2 or due to increased SR  $\text{Ca}^{2+}$  release as a result of an increase in SR  $\text{Ca}^{2+}$  loading. PKA dependent phosphorylation of LTCC increases the open probability and open duration of LTCC thereby increasing  $I_{\text{Ca}}$ , which increases the signal for CICR (Tsien et al., 1986, Walsh et al., 1989). Indeed, data from this laboratory show that the increase in LTCC in response to ISO is greater in resting period (ZT3) myocytes than active period (ZT15) myocytes. This is unlikely to reflect an increase in channel density, as our previous chapter (chapter 3) suggests that the time-of-day variation in basal LTCC current density does not reflect an increase in LTCC mRNA levels (Collins and Rodrigo, 2010), and the acute effects of ISO are unlikely to increase LTCC through the increase in the expression of active channels. The diurnal variation in the magnitude of the increase in LTCC current density is unlikely to make a major contribution to the time-of-day dependent variation in the increase in the systolic  $[\text{Ca}^{2+}]$  and amplitude of  $\text{Ca}^{2+}$  transient between resting period (ZT3) and active period (ZT15) myocytes, as it only contributes around 10% to the  $\text{Ca}^{2+}$ -transient (Bassani et al., 1994, Bers, 2001) therefore due to this a drastic difference in LTCC would be required to explain our data.

As the SR has a large contribution in terms of EC-coupling in the rat myocardium, due to ~90% of released  $\text{Ca}^{2+}$  originating from the SR (Bassani et al., 1994, Bers, 2001), the diurnal variation we observe could be the result of changes in SR function, as the large contribution of the SR would mean that only a modest variation in the sensitivity of the SR to ISO could explain our data. ISO stimulation targets SR function through PKA-dependent phosphorylation of RyR2 which increases the open probability and open duration of the SR  $\text{Ca}^{2+}$  release channels, thereby contributing to greater SR  $\text{Ca}^{2+}$  release (Marx et al., 2000, Bers, 2002). In addition, PKA-dependent phosphorylation of PLB relieves SERCA 2a inhibition thereby increasing SERCA 2a activity which increases both SR  $\text{Ca}^{2+}$  uptake and SR  $\text{Ca}^{2+}$  content (Li et al., 2000, Bers, 2002). Therefore, it is not surprising that the time-of-day dependent increase in systolic  $[\text{Ca}^{2+}]$  and amplitude of  $\text{Ca}^{2+}$  transient in response to ISO in resting period (ZT3) myocytes reflects an increase in SR  $\text{Ca}^{2+}$  content (see figures 4.3 and 4.9). This increased SR  $\text{Ca}^{2+}$  content in resting period (ZT3) myocytes means that a greater amount of  $\text{Ca}^{2+}$  can be released which increases the amplitude of the  $\text{Ca}^{2+}$  transient and increases contraction strength. The increase in SR  $\text{Ca}^{2+}$  content in resting period (ZT3) myocytes is likely to be the result of increased SERCA 2a activity. In chapter 3, we determined SERCA 2a activity in resting period (ZT3) and active period (ZT15) myocytes from the decay of the electrically-evoked  $\text{Ca}^{2+}$  transient. We would expect that if the increase in SR  $\text{Ca}^{2+}$  content we observe in resting period (ZT3) myocytes in response to ISO is the result of increased SERCA 2a activity that there would be a faster rate of decay of the electrically-evoked  $\text{Ca}^{2+}$  transient in these myocytes. However, due to time constraints, we were unable to determine the rate of decay of the electrically-evoked  $\text{Ca}^{2+}$  transient in response to ISO stimulation and therefore were unable to determine whether SERCA 2a activity reflects the time-of-day dependent variation shown in the responsiveness of the  $\text{Ca}^{2+}$  transient and SR  $\text{Ca}^{2+}$  content in resting period (ZT3) myocytes.

In addition to changes in SERCA activity, the time-of-day dependent variation in the response of systolic  $[\text{Ca}^{2+}]$  and amplitude of  $\text{Ca}^{2+}$  transient to ISO in resting period

(ZT3) myocytes could also be due to changes in SR  $\text{Ca}^{2+}$  release which may reflect changes in RyR2 activity and/or SR  $\text{Ca}^{2+}$  content. This could reflect either changes in RyR2 density, changes in PLB protein levels or phosphorylation of PLB & RyR2 during the resting period (ZT3). In the previous chapter, we showed that the expression levels of RyR2, SERCA 2a and PLB mRNA during the resting period (ZT3) and active period (ZT15) and found that there was no time-of-day dependent difference in the expression of these SR located proteins, therefore, any difference in the functional activity of these proteins must be due to post-translational modification. However, due to time constraints we did not look at protein expression levels or protein phosphorylation levels during the resting period (ZT3) or the active period (ZT15) and therefore this requires further work to determine.

If the modest increase in NCX expression during the active period (ZT15) shown in the previous chapter translates to active protein in the cell membrane, any resulting increase in NCX activity would result in greater efflux of  $\text{Ca}^{2+}$  on the exchanger during diastole and therefore less  $\text{Ca}^{2+}$  returning to the SR. Therefore, if NCX1 activity is modulated by ISO this would lead to a competition between NCX-mediated  $\text{Ca}^{2+}$  extrusion and SERCA driven SR  $\text{Ca}^{2+}$  uptake which would ultimately decrease SR  $\text{Ca}^{2+}$  content as more  $\text{Ca}^{2+}$  is extruded from the myocyte. However, Bers and colleagues, amongst others, have shown that  $\beta$ -adrenergic stimulation with ISO does not modulate NCX1 and common to most studies to date, this is likely to have been performed during the animals resting period rather than active period (Ginsburg and Bers, 2005, Lin et al., 2006). Our data also confirms that ISO does not have significant effect on the decay of the caffeine-induced  $\text{Ca}^{2+}$  transient, a measure of NCX1 activity, in resting period (ZT3) and active period (ZT15) myocytes. This is not consistent with the modest increase in NCX1 mRNA during the active period (ZT15) we have shown previously in chapter 3 and may suggest that the increase in NCX1 mRNA that we see is not correlated to active protein or that post-translational modification occurs. The increase in NCX1 expression that we observe in hearts isolated during the active period (ZT15) of the rat in the previous chapter has also been shown previously by Shen *et al* (2007). Shen and

colleagues found that in the nocturnal mouse  $\text{PIP}_2$  which is responsible for the internalisation and membrane trafficking of NCX1 is greatest during the resting period and the surface expression of NCX1 was in fact greatest during the active period, which supports our data (Shen et al., 2007).

The cardiac force-frequency relationship of larger mammals like rabbits and humans is typically positive which refers to increased contraction strength in response to an increase in stimulation frequency and this is often also named the Treppe or staircase effect (Frampton et al., 1991, Bers, 2001). At higher stimulation frequencies, there is greater SR loading and therefore more SR  $\text{Ca}^{2+}$  is available for release and this increase in SR  $\text{Ca}^{2+}$  content and subsequent release contributes to an increase in  $\text{Ca}^{2+}$  transient amplitude and greater contraction (Frampton et al., 1991, Bers, 2001). Therefore, the force-frequency relationship is related to changes in SR function, namely it impinges in SR loading and in recent years, Meyer *et al* (1999) have shown that the cardiac force-frequency relationship is determined by the PLB/SERCA 2a ratio (Meyer et al., 1999).

Interestingly, both positive and negative force-frequency relationships have been reported in the rat myocardium (Schouten and ter Keurs, 1986, Frampton et al, 1991)

In the previous chapter (chapter 3) we suggested that the SR has a dominant role in the time-of-day dependent changes we observe in EC-coupling and as loading of the SR has been shown to be frequency-dependent, we wanted to see whether changes in stimulation frequency would impact on diurnal variation in the responsiveness of the  $\text{Ca}^{2+}$  transient to ISO in the rat. Therefore, to establish whether the time-of-day dependent variation in systolic  $[\text{Ca}^{2+}]$  and amplitude of  $\text{Ca}^{2+}$  transient is frequency-dependent we looked at the force frequency relationship.

In contrast to the negative force-frequency relationship reported in the rat, we only observed a positive force-frequency relationship in the rat in response to increasing stimulation frequency (0.5-1-2Hz). In addition, our data show that stimulation frequency does not affect the diurnal influence on the responsiveness of the  $\text{Ca}^{2+}$  transient to ISO, as the responses of systolic  $[\text{Ca}^{2+}]$  and the amplitude of the  $\text{Ca}^{2+}$  transient to ISO between resting period (ZT3) and active period (ZT15) myocytes were

similar at stimulation frequencies of 0.5Hz and 1Hz. This trend was less obvious between resting period (ZT3) and active period (ZT15) myocytes stimulated at 2Hz. As, a large number of myocytes developed arrhythmic activity and increased diastolic  $[Ca^{2+}]$  in response to 2Hz and as a result were excluded from analysis, which reduced the  $n$  numbers below statistical relevance ( $< 3$  animals) and produced large error bars in the data.

#### **4.3.2 Diurnal variation in the generation of arrhythmic activity**

The morning peak in the incidence of both SCD and related arrhythmias in man have been correlated with the morning surge in the activity of the sympathetic nervous system and increase in circulating catecholamines (Guo and Stein, 2003). In the nocturnal rat, this surge in the activity of the sympathetic nervous system has been shown to occur during its active period i.e. during the evening (Hashimoto et al., 1999). Prolonged or excessive  $\beta$ -adrenergic stimulation is associated with an increased incidence of triggered arrhythmias in many species (Meredith et al., 1991, Barbieri et al., 1994, Veldkamp et al., 2001). Indeed, increased exposure to the non-specific  $\beta$ -adrenergic receptor agonist, ISO, has been shown to be associated with an increased incidence of triggered arrhythmias in the form of early (EAD) and delayed after-depolarisations (DAD).

Our data show that diurnal variation exists in the propensity for ISO-induced arrhythmic activity, with the result that there is a time-of-day dependent increase in the frequency of arrhythmic activity, as resting period (ZT3) myocytes developed more arrhythmic activity than active period (ZT15) myocytes in response to similar ISO stimulation. This increase in arrhythmic activity in resting period (ZT3) myocytes could be due to either an increase in the incidence of EADS or DADs. The increase in arrhythmic activity we see in resting period (ZT3) myocytes in response to ISO could be the result of an increase in the incidence of EADs, as data from this laboratory have shown that

LTCC current is significantly greater in resting period (ZT3) myocytes compared with active period (ZT15) myocytes during ISO stimulation (Collins and Rodrigo, 2010). The increase in arrhythmic activity in resting period (ZT3) myocytes could also reflect an increased incidence of EADs as the increase in arrhythmic activity was reflected by an increase in systolic  $[Ca^{2+}]$  and SR  $Ca^{2+}$  content in response to ISO. It seems likely that the arrhythmic activity we see is the result of an increased incidence of DADs rather than EADs, as DADs are favoured by high  $Ca^{2+}$  which is a consequence of  $\beta$ -adrenergic stimulation whereas EADs are favoured by long APs and slow HRs (Priori and Corr, 1990, Fozzard, 1992, De Ferrari et al., 1995). The increased SR  $Ca^{2+}$  content in resting period (ZT3) myocytes in response to ISO could promote spontaneous SR  $Ca^{2+}$  release and the subsequent generation of the transient inward current ( $I_{ti}$ ), both of which are also associated with the generation of DADs. Indeed, data obtained in this laboratory has since revealed that the increase in arrhythmic activity that we show in resting period (ZT3) myocytes is the result of an increase in the propensity of DADs (Collins and Rodrigo, 2010).

The time-of-day dependent increase in the frequency of sympathetic-induced arrhythmic activity, namely DADs, in resting period (ZT3) myocytes is therefore likely to reflect either changes in SR function; namely changes in SERCA 2a activity which impact on SR  $Ca^{2+}$  loading/ content and RyR2 instability, changes in NCX density and/or changes in the expression of  $K^+$  channels, which also exhibit diurnal variation and the impact of each will now be discussed individually.

### ***Sarcoplasmic reticulum function***

The development of ventricular arrhythmias is often associated with increased SR  $Ca^{2+}$  loading (see introduction, section 1.5). Indeed, our data demonstrates that the increased propensity for arrhythmic activity, namely DADs, in resting period (ZT3) myocytes is

associated with a heightened response to ISO culminating in an increase in SR  $\text{Ca}^{2+}$  content in these myocytes. DADs occur as a result of increased SR  $\text{Ca}^{2+}$  loading and result in the spontaneous release of SR  $\text{Ca}^{2+}$  which triggers the generation of  $I_{\text{li}}$  and DADs (January et al., 1991, De Ferrari et al., 1995). However, a given increase in SR  $\text{Ca}^{2+}$  content does not necessarily result in the generation of ventricular arrhythmias, this increase in SR  $\text{Ca}^{2+}$  content is more likely to lead to an increased risk of arrhythmogenesis if it occurs in association with RyR2 instability. RyR2 instability may occur if the RyR2 become sensitised to  $\text{Ca}^{2+}$  or responds to a very low level of diastolic  $\text{Ca}^{2+}$  which may make the receptor unstable and more likely to open. This could be exacerbated by the increase in SR  $\text{Ca}^{2+}$  content, as an increase in SR luminal  $\text{Ca}^{2+}$  increases the open probability of RyR2, leading to spontaneous SR  $\text{Ca}^{2+}$  release (Lukyanenko et al., 1996). Therefore, the increase in arrhythmic activity during ISO-stimulation we observe in resting period (ZT3) myocytes could be the result of RyR instability in addition to SR  $\text{Ca}^{2+}$  loading. RyR2 instability may result from modulation of RyR2 during  $\beta$ -adrenergic stimulation which could arise either through phosphorylation by PKA (see for introduction for details), or could arise following the activation of  $\beta_3$ -adrenergic receptor and downstream NOS-signalling cascade which has been reported to target RyR2 function through both PKG mediated phosphorylation (Takasago et al., 1991) and NO- mediated S-nitrosylation of RyR2 (Xu et al., 1998, Gonzalez et al., 2007). Modulation of RyR2 by NOS may impact on the frequency of arrhythmic activity in both resting period (ZT3) and active period (ZT15) myocytes as NOS isoforms are characteristically anti-arrhythmic and therefore may explain the reduction of arrhythmic activity in active period (ZT15) myocytes we observe in response to ISO. The instability in RyR2 could also result from phosphorylation of proteins associated with the RyR2 signalling complex which may impact on SR function and therefore the frequency of arrhythmic activity in resting period (ZT3) myocytes. The RyR2 has been reported to be physically associated with calmodulin, FKBP12.6, sorcin, triadin, junctin and calsequestrin and phosphorylation of RyR2 also affects the function of these proteins (Bers, 2002). The increased incidence of

arrhythmic activity we observe in resting period (ZT3) myocytes could reflect the changes in these RyR-associated proteins. In support of this, phosphorylation of RyR2 by PKA during  $\beta$ -adrenergic stimulation results in dissociation of FKBP12.6 from the RyR2 signalling complex which thought to be pro-arrhythmic, as this increases the open probability of RyR2 and as a consequence, increases SR  $\text{Ca}^{2+}$  release (Wehrens et al., 2003, Gellen et al., 2008). This increase in SR  $\text{Ca}^{2+}$  release could also promote the generation of the ventricular arrhythmias and DADs through the production of the NCX1 mediated transient inward current.

### ***Sodium/calcium exchange expression***

One possible mechanism for the time-of-day dependent increase in arrhythmic activity, namely the increase in the incidence of DADs, in response to ISO stimulation in resting period (ZT3) myocytes may be due to changes in the activity and expression of NCX1 in addition to changes in SR function, as the size of NCX1 contributes to the magnitude of DADs and NCX1 has been shown to be the predominate contributor to the transient inward current ( $I_{ti}$ ) which is associated with the generation of DADs (January et al., 1991, Fozzard, 1992, De Ferrari et al., 1995, Bers, 2001).

As the increase in arrhythmic activity in resting period (ZT3) myocytes we show has been associated with the generation of DADs (Collins and Rodrigo, 2010) one would expect that NCX1 current be increased in response to ISO in order to contribute to transient inward current ( $I_{ti}$ ) and subsequent DADS. However, current literature does not support the modulation of NCX1 during  $\beta$ -adrenergic stimulation with ISO (see section 4.3.1 for detail). Shen *et al* (2007) have also shown that there is a time-of-day dependent variation in NCX1 levels and membrane trafficking in that the surface expression of NCX1 peaks during the active period of the mouse (see section 4.3.1 for detail). Our gene expression data supports Shen *et al* (2007) as we showed that NCX1 mRNA was also increased in active period (ZT15) rather than resting period, and this

could lead to an increase in magnitude of any DAD. However, our functional data does not support this as a mechanism for the increased arrhythmic activity, as this increase in mRNA was not reflected by an increase in NCX1 activity (see chapter 3). In addition, studies involving cardiac specific NCX1 over-expression have shown that increased NCX1 is correlated with a reduced responsiveness to  $\beta$ -adrenergic stimulation (Ranu et al., 2002, Sato et al., 2004). These findings would suggest that NCX1 is increased when the animal is active and is contrary to our finding of increased arrhythmic activity, namely DADs, in resting period (ZT3) myocytes and therefore this may suggest that changes in SR function may contribute more to the generation of ventricular arrhythmias in resting period (ZT3) myocytes than changes in NCX1 expression.

### ***K<sup>+</sup> channel expression***

The time-of-day dependent increase in the generation of ventricular arrhythmias in resting period (ZT3) myocytes may also be contributed to by changes in the expression of K<sup>+</sup> channels, as changes in the contribution of K<sup>+</sup> channels underlying the AP is often associated with the generation of long QT syndrome and ventricular arrhythmias (Tristani-Firouzi et al., 2001). In support of this, diurnal variations have been reported in the expression of two K<sup>+</sup> channels underlying the cardiac AP. Yamashita *et al* (2003) have shown that expression of Kv4.2 (I<sub>to</sub>) mRNA peaks during the resting period (ZT6) of the rat and this channel is of particular importance for the notch phase of the cardiac AP and impacts on APD. This may indicate that the APD may be changed in our resting period (ZT3) myocytes as increased I<sub>to</sub> would permit faster partial repolarisation of the AP and will increase the driving force for Ca<sup>2+</sup> entry during the plateau phase of the AP, contributing to an larger Ca<sup>2+</sup> current. This increase in I<sub>to</sub> could prolong APD by an increase in LTCC; alternatively, the resulting increase in SR Ca<sup>2+</sup> release could lead to rapid inactivation of the LTCC resulting in a shortened APD. A prolonged APD will also reduce the length of diastole during increased HRs and therefore may increase

the incidence of arrhythmic activity (see discussion 3 section 3.3.2). As, prolonged and shortened APDs are associated with the generation of ventricular arrhythmias, the variation in the arrhythmic activity we see in resting period (ZT3) and active period (ZT15) myocytes may therefore reflect changes in APD.

#### **4.3.3 The time-of-day dependent decrease in the responsiveness of the $\text{Ca}^{2+}$ transient to isoproterenol in active period myocytes is paradoxical**

In the present chapter, we show that the responsiveness of the  $\text{Ca}^{2+}$  transient to  $\beta$ -adrenergic stimulation with the non-specific  $\beta$ -adrenergic receptor agonist, ISO, exhibits time-of-day dependent variation, as the increase in systolic  $[\text{Ca}^{2+}]$  and the amplitude of  $\text{Ca}^{2+}$  transient in response to ISO were significantly lower in active period (ZT15) versus resting period (ZT3) myocytes, and this was reflected by reduced contraction strength and SR  $\text{Ca}^{2+}$  content in active period (ZT15) myocytes. This data is contrary to expectations as one would expect that an animal would have a heightened response to sympathetic stimulation during its active period, providing the animal with an evolutionary advantage in terms of avoiding predation and successful foraging. Our data showing that the responsiveness of myocytes to ISO stimulation is greatest during the resting period (ZT3) of the rat conflicts with previously published data by Rau and Meyer (1975), who show *in vivo* ISO-mediated protein synthesis peaks during the active period (ZT15) of the rat. In addition, Bray *et al* (2008) have shown that epinephrine-mediated changes in CO are most significant during the active period (ZT18) of the mouse in comparison to its resting period. It is important to note however, that the data reported by Bray *et al* (2008) were obtained using a very high concentration of epinephrine (1 $\mu\text{M}$ ) in “free-running” animals, where heart rates was not controlled and typically rose from 300-500 beats per min. Such rapid HRs, may well compromise ventricular filling rendering the mouse heart less efficient, reducing SV. In addition, during increased stimulation frequency,  $\text{K}^+$  driven variations in APD (see previous

section) may affect refractory period during high HRs and may also affect diastolic filling time and therefore, preload.

In contrast, our experiments were performed in isolated myocytes using ISO concentrations  $<1\mu\text{M}$  and at constant HRs in electrically stimulated isolated myocytes. Differences between our data and that of Bray *et al* (2008) could simply arise from species-dependent differences between the rat and mouse heart and also between the differential sensitivity of cardiac  $\beta$ -adrenergic receptors to ISO and epinephrine (Hoffmann *et al.*, 2004).

Most studies using the  $\beta$ -adrenergic receptor agonist, ISO, including Bray *et al* (2008) (see earlier) have used high concentrations ( $\sim 1\mu\text{M}$ ), however, we found that this concentration adversely increased diastolic  $[\text{Ca}^{2+}]$  and promoted arrhythmic activity in our cells. In our study, ISO concentrations between 0.1-100nM were adopted, which represents physiological conditions, as studies have shown that plasma norepinephrine is  $\sim 3.5\text{nM}$  during resting conditions and increases to  $\sim 12\text{nM}$  during exercise in the dog (Coker *et al.*, 1997) and these levels of norepinephrine were also similar in the rat and in man (Buhler *et al.*, 1978).

The decreased responsiveness of active period (ZT15) myocytes to ISO stimulation may be the result of  $\beta$ -adrenergic receptor desensitisation/ downregulation in active period (ZT15) myocytes, driven by the surge in sympathetic activity which occurs in moving from the resting to the active period. In an attempt to determine whether this was likely, we examined the responsiveness of active period (ZT15) myocytes to ISO stimulation 0-4 hours after isolation (beginning of experimental day) and 4-8 hours after isolation (end of experimental day), with the premise that any change in receptor sensitivity, driven by the surge in sympathetic activity, would recover in the isolated cells. One would expect that if there is a time-of-day dependent desensitisation or downregulation of the cardiac  $\beta$ -adrenergic receptor that the myocytes would recover the ability to respond to ISO over a period of 8-12 hours. However, our cells did not recover this ability as our data shows that the responsiveness of active period (ZT15) myocytes to ISO stimulation was not significantly different between the start and end of the

experimental day (data not shown). Receptor desensitisation and downregulation are also unlikely to persist following myocyte isolation as our myocytes were kept at room temperature in normal Tyrode solution, which are conditions which are not favoured for protein synthesis and turnover. Our data, however, is not definitive and cannot exclude the possibility of  $\beta$ -adrenergic receptor desensitisation or downregulation in active period (ZT15) myocytes and therefore requires further experimentation and elucidation.

#### **4.3.4 Possible mechanisms for diurnal variation in $\beta$ -adrenergic responsiveness**

ISO is a non-specific  $\beta$ -adrenergic receptor agonist and is therefore capable of stimulating all three  $\beta$ -adrenergic receptors ( $\beta_1$ ,  $\beta_2$ ,  $\beta_3$ ). The activation of  $\beta_3$ -adrenergic receptors is associated with a negative inotropic effect mediated through NOS and NO. In particular, NOS1 and NOS3 have been shown to be anti-adrenergic and protective against the generation of arrhythmic activity (Kubota et al., 2000, Barouch et al., 2002, Burger et al., 2009) and also models of cardiac specific NOS1 over-expression are associated with depressed  $\text{Ca}^{2+}$  transient amplitude, contraction strength and SR  $\text{Ca}^{2+}$  content (Burkard et al., 2007). The decreased responsiveness of active period (ZT15) myocytes to ISO and the decreased incidence of arrhythmic activity may therefore reflect the activation of the  $\beta_3$ -adrenergic receptor and its downstream NOS signalling pathway, possibly through an increase in NOS1. In the next chapter we will determine whether the paradoxical depression of the  $\text{Ca}^{2+}$  transient, contraction strength, SR  $\text{Ca}^{2+}$  content and arrhythmogenesis we have observed in active period (ZT15) myocytes in response to ISO are the result of NOS signalling.

# **Chapter 5: The role of nitric oxide synthase in the diurnal variation in responsiveness of ventricular myocytes to $\beta$ -adrenergic stimulation with isoproterenol**

## ***5.1 Introduction***

The non-specific nature of the  $\beta$ -adrenergic receptor agonist, ISO, means that it is capable of stimulating not only  $\beta_1$ -adrenergic receptors, but also  $\beta_2$  and  $\beta_3$ -adrenergic receptors.  $\beta$ -adrenergic stimulation with ISO induces a positive inotropic response through the activation of  $\beta_1$  and  $\beta_2$ -adrenergic receptors, which activate AC producing a global increase in cAMP concentration ( $\beta_1$ -adrenergic receptor) (Bers, 2002) or a localised increase in cAMP concentration in caveolae ( $\beta_2$ -adrenergic receptor) both of which activate PKA (Jurevicius and Fischmeister, 1996, Balijepalli et al., 2006, Calaghan et al., 2008). PKA phosphorylates the LTCC, RyR2, PLB and troponin I in  $\beta_1$ -adrenergic receptor signalling. However, in the case of  $\beta_2$ -adrenergic receptor signalling; PKA signalling is restricted to the sarcolemmal membrane where it targets LTCC and therefore does not target the SR proteins, RyR2 and PLB or the contractile myofilament, troponin I as they are not in close proximity to PKA (Xiao et al., 1994, Calaghan et al., 2008) (see section 1.4 of introduction for detail).

Activation of the cardiac  $\beta_3$ -adrenergic receptor has a negative inotropic effect in the mammalian myocardium (Gauthier et al., 2000), as the receptor is coupled to the inhibitory G-protein,  $G_i$ , which inhibits the activation of AC, thereby reducing cAMP concentration and PKA activation (Taussig et al., 1993). The negative inotropic effects of  $\beta_3$ -adrenergic receptor activation are also believed to be mediated via the activation of NOS and the subsequent production of NO. NO activates GC resulting in an increase in cGMP, which is responsible for the activation of PKG. PKG is thought to phosphorylate the contractile myofilaments, to reduce  $Ca^{2+}$  sensitivity, and the LTCC, to

reduce inward  $\text{Ca}^{2+}$  current which both contribute to a depression in contraction strength (Layland et al., 2002, Yang et al., 2007, Wang et al., 2008b) (see introduction section 1.4). PKG also targets SR function through the modulation of SERCA 2a/PLB (Raeymaekers et al., 1988) and RyR2 (Takasago et al., 1991, Lim et al., 2008) (see introduction section 1.4 for detail). NO can also act independently of cGMP and PKG, through the direct S-nitrosylation of LTCC (Sun et al., 2006, Sun et al., 2007), RyR2 (Xu et al., 1998, Wang et al., 2010), SERCA 2a (Sun et al., 2007) and PLB (Garofalo et al., 2009).

In chapter 4, we have shown that the non-specific  $\beta$ -adrenergic agonist, ISO, produces a significantly smaller increase in contraction strength, reflecting a reduced effect on the  $\text{Ca}^{2+}$  transient and SR  $\text{Ca}^{2+}$  content, which also resulted in a lower percentage of arrhythmic activity in active period (ZT15) myocytes in comparison to resting period (ZT3) myocytes. We postulated that this may result from the activation of the  $\beta_3$ -adrenergic receptor, NOS, NO and PKG, resulting in a negative inotropic action that antagonises the positive inotropism of  $\beta_1$  and  $\beta_2$ -adrenergic receptor activation (Gauthier et al., 1998). There are two mechanisms which could promote the antagonist effect of the  $\beta_3$ -adrenergic receptor on the  $\beta_1$  and  $\beta_2$ -adrenergic receptors. Firstly, there may be an increased concentration of NOS, which would enhance NO concentration and subsequent downstream signalling. Secondly, there may be changes in receptor population with respect to the positive inotropic  $\beta_1/\beta_2$ -adrenergic receptors and the negative inotropic  $\beta_3$ -adrenergic receptor, so that the ratio of  $\beta_1/\beta_2:\beta_3$  is changed.

We have therefore set out to determine whether NOS is responsible for the depressed response of the  $\text{Ca}^{2+}$  transient and SR  $\text{Ca}^{2+}$  content in active period (ZT15) myocytes to ISO using the non-specific NOS inhibitor, L-NNA. To see whether any difference in the response of the  $\text{Ca}^{2+}$  transient to  $\beta$ -adrenergic stimulation reflects changes in the ratio of  $\beta_1$  to  $\beta_3$ -adrenergic receptors, we looked at the expression of the genes encoding the  $\beta_1$ -adrenergic receptor (*Adrb1*) and the  $\beta_3$ -adrenergic receptor (*Adrb3*). In addition, as the downstream signalling pathway of the  $\beta_3$ -adrenergic receptor involves NOS, we looked at the expression of the genes encoding neuronal nitric oxide synthase (*NOS1*)

and endothelial nitric oxide synthase (NOS3) and the NOS1-associated protein (NOS1AP) CAPON in adult Wistar rat hearts isolated during the resting period (ZT3) and active period (ZT15).

## ***5.2 Results***

### **5.2.1 The effect of NOS inhibition on the diurnal variation in the response of the Ca<sup>2+</sup> transient to $\beta$ -adrenergic stimulation with isoproterenol.**

We postulated that if the decreased responsiveness of active period (ZT15) myocytes with respect to the Ca<sup>2+</sup> transient, contraction strength and SR Ca<sup>2+</sup> content in response to  $\beta$ -adrenergic stimulation with ISO (see chapter 4) was the result of the activation of the  $\beta_3$ -adrenergic receptor and NOS, then simultaneous inhibition of NOS during ISO stimulation should reverse this effect.

To investigate the involvement of NOS in the depressed responsiveness of the Ca<sup>2+</sup> transient to  $\beta$ -adrenergic stimulation with ISO in active period (ZT15) myocytes (described in chapter 4), we determined the effects of NOS inhibition, using L-NNA, on the response of Ca<sup>2+</sup> transients from resting period (ZT3) myocytes compared to active period (ZT15) myocytes to ISO stimulation. Fura-2 loaded cells were electrically-field stimulated at a rate of 1Hz and were superfused with normal Tyrode for 5 minutes, to establish stable resting Ca<sup>2+</sup> transients. Myocytes were then superfused with normal Tyrode containing 10nM ISO for 5 minutes, followed by the superfusion of normal Tyrode containing 10nM ISO and the NOS inhibitor L-NNA for 5 minutes. Any record in which the resting diastolic Fura-2 ratio during normal Tyrode superfusion was > 1 was discarded (~250-300nM). Ca<sup>2+</sup> transients were recorded for 20 seconds at the end of ISO exposure and ISO + L-NNA, to reduce photobleaching and measurements of diastolic [Ca<sup>2+</sup>], systolic [Ca<sup>2+</sup>] and amplitude of Ca<sup>2+</sup> transient were made.

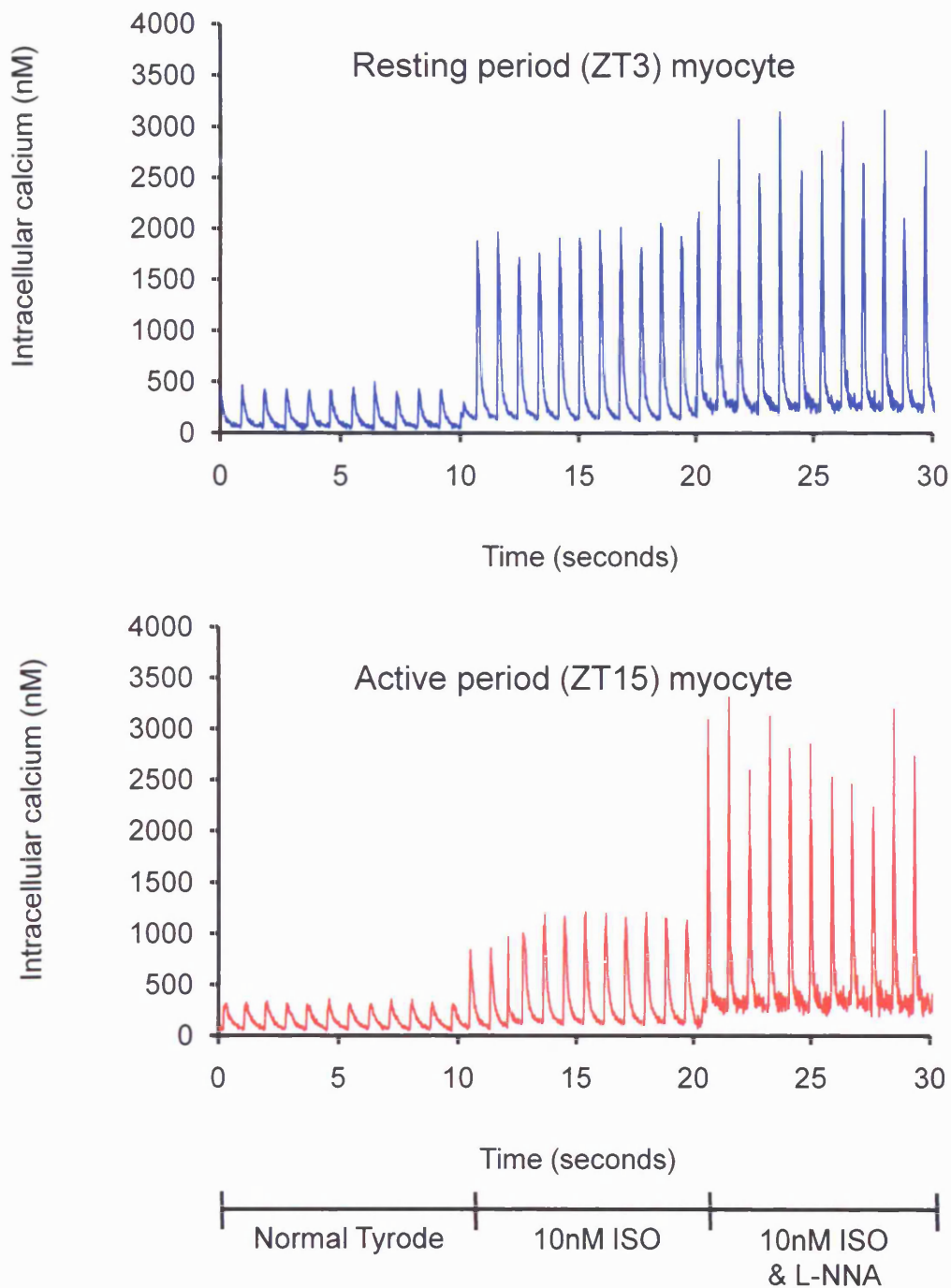


**Figure 5.1- The  $\text{Ca}^{2+}$  transient recorded from resting period (ZT3) and active period (ZT15) myocytes during  $\beta$ -adrenergic stimulation with isoproterenol (ISO) and during NOS inhibition with L-NNA.**

Example of a  $\text{Ca}^{2+}$  transients recorded from a single resting period (ZT3) myocyte (top; blue) and a single active period (ZT15) myocyte (bottom; red) superfused with normal Tyrode for 5 minutes, 10nM ISO-containing Tyrode for 5 minutes and Tyrode containing 10nM ISO & 500 $\mu\text{M}$  L-NNA for 5 minutes during 1Hz electrical field stimulation.  $\text{Ca}^{2+}$  transients were recorded for 20 seconds at end of the 5 minute perfusion of each experimental solution to reduce effects of photobleaching.

Figure 5.1 is a recording of intracellular  $\text{Ca}^{2+}$  from a single resting period (ZT3) myocyte (top; blue) and a single active period (ZT15) myocyte (bottom, red), stimulated at 1Hz and superfused with normal Tyrode for 5 minutes at the end of which  $\text{Ca}^{2+}$  transients reached a steady-state and were recorded to determine resting diastolic, systolic and  $\text{Ca}^{2+}$ -transient amplitudes. The myocytes were subsequently superfused with normal Tyrode containing 10nM ISO then normal Tyrode containing 10nM ISO and 500 $\mu\text{M}$  L-NNA for 5 minutes each and the  $\text{Ca}^{2+}$  transient recorded at the end of the 5 minute period, during which the response had reached a new steady-state. The records show that the resting period (ZT3) myocyte is more responsive to stimulation with 10nM ISO in comparison to the active period (ZT15) myocyte, as the increase in both systolic  $[\text{Ca}^{2+}]$  and the amplitude of  $\text{Ca}^{2+}$  transient are greater in the resting period (ZT3) myocyte compared to the active period (ZT15) myocyte. This is in keeping with the data presented in the previous chapter (chapter 4; section 4.2.1). The record also shows that upon superfusion with the NOS inhibitor L-NNA in the continued presence of ISO, that there is a further increase in the  $\text{Ca}^{2+}$ -transient that is greater in the active period (ZT15) myocytes than the resting period (ZT3) myocytes, so that the final  $\text{Ca}^{2+}$ -transient (ISO + NOS-inhibition) is not dissimilar between resting period (ZT3) and active period (ZT15) myocytes.

Figure 5.2 shows the bar charts of the mean data of diastolic  $[\text{Ca}^{2+}]$ , systolic  $[\text{Ca}^{2+}]$  and amplitude of the  $\text{Ca}^{2+}$  transient, from such experiments. The data in figure 5.2A show that diastolic  $[\text{Ca}^{2+}]$  was not significantly different between resting period (ZT3) and active period (ZT15) myocytes during 10nM ISO-stimulation, at  $253.9 \pm 15.1$  nM in resting period (ZT3) myocytes ( $n = 47/9$ ) versus  $268.4 \pm 18.5$  nM in active period (ZT15) myocytes ( $n = 49/9$ ; *ns*) and during superfusion of 10nM ISO & L-NNA, at  $236.2 \pm 13.8$  nM in resting period (ZT3) myocytes ( $n = 26/4$ ) versus  $260.5 \pm 36.4$  nM in active period (ZT15) myocytes ( $n = 19/3$ ; *ns*). There was also no significant difference in diastolic  $[\text{Ca}^{2+}]$  between myocytes treated with 10nM ISO and myocytes treated with 10nM ISO & L-NNA in the resting period (ZT3) (*ns*) and in the active period (ZT15; *ns*). However, the data in figure 5.2B show that systolic  $[\text{Ca}^{2+}]$  is significantly higher in

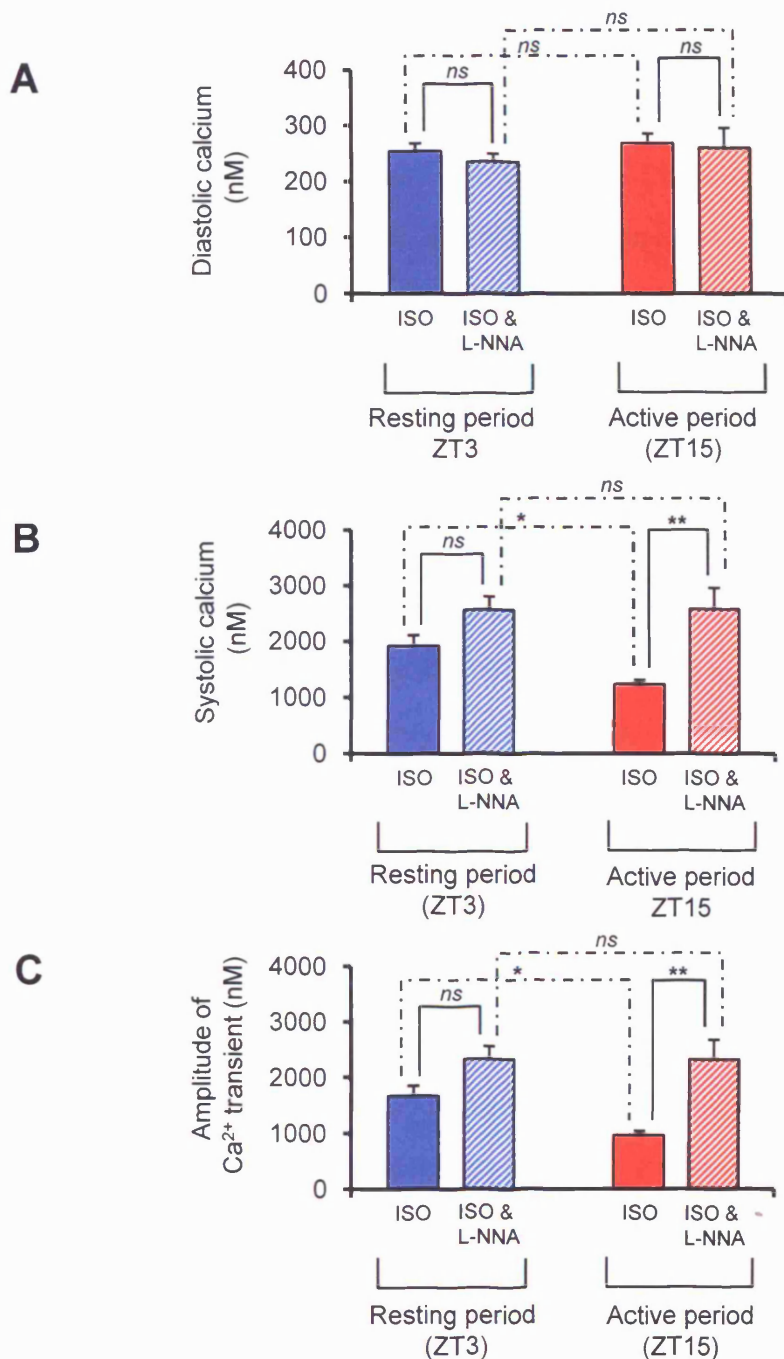


**Figure 5.2- The parameters of the Ca<sup>2+</sup> transient of resting period (ZT3) and active period (ZT15) myocytes during  $\beta$ -adrenergic stimulation with isoproterenol (ISO) and during NOS inhibition with L-NNA.**

Bar chart of the mean data from experiments described in figure 5.1, showing the diastolic calcium (A), systolic calcium (B) and amplitude of Ca<sup>2+</sup> transient (C) recorded from resting period (ZT3; blue) and active period (ZT15) myocytes (red), stimulated at 1Hz and superfused with either normal Tyrode containing 10nM ISO (open bars) or normal Tyrode containing 10nM ISO and 500 $\mu$ M L-NNA for 5 minutes (hatched bars). Values are the mean  $\pm$  S.E.M.; number of experiments/ hearts = Resting period (ZT3) myocyte (ISO  $n = 47/8$ ; ISO & L-NNA  $n = 26/4$ ) and active period (ZT15) myocyte (ISO  $n = 49/10$ ; ISO & L-NNA  $n = 19/3$ ); \*  $p < 0.05$ , \*\*  $p < 0.001$ , two way ANOVA followed by a Bonferroni *post hoc* test.

resting period (ZT3) myocytes compared to active period (ZT15) myocytes during 10nM ISO superfusion, with a systolic  $[Ca^{2+}]$  of  $1921.1 \pm 191.9$  nM in resting period (ZT3) myocytes ( $n = 47/9$ ) versus  $1234.0 \pm 81.8$  nM in active period (ZT15) myocytes ( $n = 49/9$ ,  $p < 0.05$ ). Furthermore, this difference appeared to disappear when NOS was inhibited simultaneously during ISO-stimulation, with no difference in systolic  $[Ca^{2+}]$  between resting period (ZT3) and active period (ZT15) myocytes during superfusion of 10nM ISO & L-NNA, at  $2574.7 \pm 230.9$  nM in resting period (ZT3) myocytes ( $n = 26/4$ ) versus  $2583.4 \pm 385.0$  nM in active period (ZT15) myocytes ( $n = 19/3$ ; *ns*). This may reflect a greater NOS activity in active period (ZT15) myocytes, as the data show that L-NNA significantly increases systolic  $[Ca^{2+}]$  in the presence of 10nM ISO in active period (ZT15) myocytes ( $p < 0.001$ ); however, there was no significant effect of L-NNA in resting period (ZT3) myocytes (*ns*). The data in figure 5.2C show that the amplitude of  $Ca^{2+}$  transient reflects the difference in systolic  $[Ca^{2+}]$  (see figure 5.2B), as the amplitude of  $Ca^{2+}$  transient is significantly higher in resting period (ZT3) myocytes compared to active period (ZT15) myocytes during 10nM ISO superfusion, with an amplitude of  $Ca^{2+}$  transient of  $1667.2 \pm 187.7$  nM in resting period (ZT3) myocytes ( $n = 47/9$ ) versus  $965.6 \pm 82.2$  nM in active period (ZT15) myocytes ( $n = 49/9$ ;  $p < 0.05$ ). In addition, reflecting systolic  $[Ca^{2+}]$ , there was no difference in amplitude of  $Ca^{2+}$  transient between resting period (ZT3) and active period (ZT15) myocytes during superfusion of 10nM ISO & L-NNA, with an amplitude of  $Ca^{2+}$  transient of  $2338.5 \pm 225.2$  nM in resting period (ZT3) myocytes ( $n = 26/4$ ) versus  $2322.9 \pm 359.1$  nM in active period (ZT15) myocytes ( $n = 19/3$ ; *ns*). The data also show that L-NNA significantly increases the amplitude of  $Ca^{2+}$  transient in the presence of 10nM ISO in active period (ZT15) myocytes ( $p < 0.001$ ); however, there was no significant effect of L-NNA in resting period (ZT3) myocytes (*ns*).

These data show that the increase in systolic  $[Ca^{2+}]$  and amplitude of  $Ca^{2+}$  transient in response to ISO stimulation is enhanced by inhibition with the NOS inhibitor, L-NNA in both resting period (ZT3) and active period (ZT15) myocytes and this increase in systolic  $[Ca^{2+}]$  and amplitude of  $Ca^{2+}$  transient was greater in the active period (ZT15)

myocytes. The result is that NOS inhibition significantly enhances the effects of ISO in active period (ZT15) myocytes and abolishes diurnal variation seen in the response of systolic  $[Ca^{2+}]$  and amplitude of  $Ca^{2+}$  transient to  $\beta$ -adrenergic stimulation with ISO, suggesting that NOS is responsible for the diurnal differences in the  $Ca^{2+}$  transient.

### **5.2.2 The effect of NOS inhibition on the diurnal variation in SR $Ca^{2+}$ content in response to $\beta$ -adrenergic stimulation with isoproterenol**

In the previous chapter, we showed that the increase in the  $Ca^{2+}$  transient and SR  $Ca^{2+}$  content following  $\beta$ -adrenergic stimulation with ISO, were all greater in resting period (ZT3) myocytes in comparison to active period (ZT15) myocytes. In the present chapter, we have shown that inhibition of NOS with L-NNA during  $\beta$ -adrenergic stimulation with ISO increases systolic  $[Ca^{2+}]_i$  to a greater extent in active period (ZT15) than resting period (ZT3) myocytes, such that the systolic  $[Ca^{2+}]_i$  was no longer different between time-points. We postulated that this increase in systolic  $[Ca^{2+}]_i$  during NOS inhibition in active period (ZT15) myocytes may reflect an increase in SR  $Ca^{2+}$  content.

To determine the effects of NOS on SR  $Ca^{2+}$  loading during ISO stimulation, we used the NOS inhibitor, L-NNA. Myocytes were electrically-field stimulated at 1Hz and superfused with normal Tyrode for 5 minutes, to obtain stable resting  $Ca^{2+}$  transients. SR  $Ca^{2+}$  loading was determined by a rapid caffeine pulse following pre-treatment with ISO (10nM) in the presence and absence of the NOS inhibitor, L-NNA (500 $\mu$ M). To investigate the involvement of NOS in diurnal variation in SR  $Ca^{2+}$  content in response to  $\beta$ -adrenergic stimulation with ISO, we measured peak of the  $Ca^{2+}$  transient in response to 20mM caffeine, an indicator of SR  $Ca^{2+}$  content, and the exponential time constant of decay of the caffeine-induced  $Ca^{2+}$  transient, an indicator of NCX and plasma membrane  $Ca^{2+}$  ATPase (PMCA) activity (Bassani et al., 1994), in resting period (ZT3) and active period (ZT15) myocytes during NOS inhibition with L-NNA, using the method described in chapter 4 section 4.2.4.

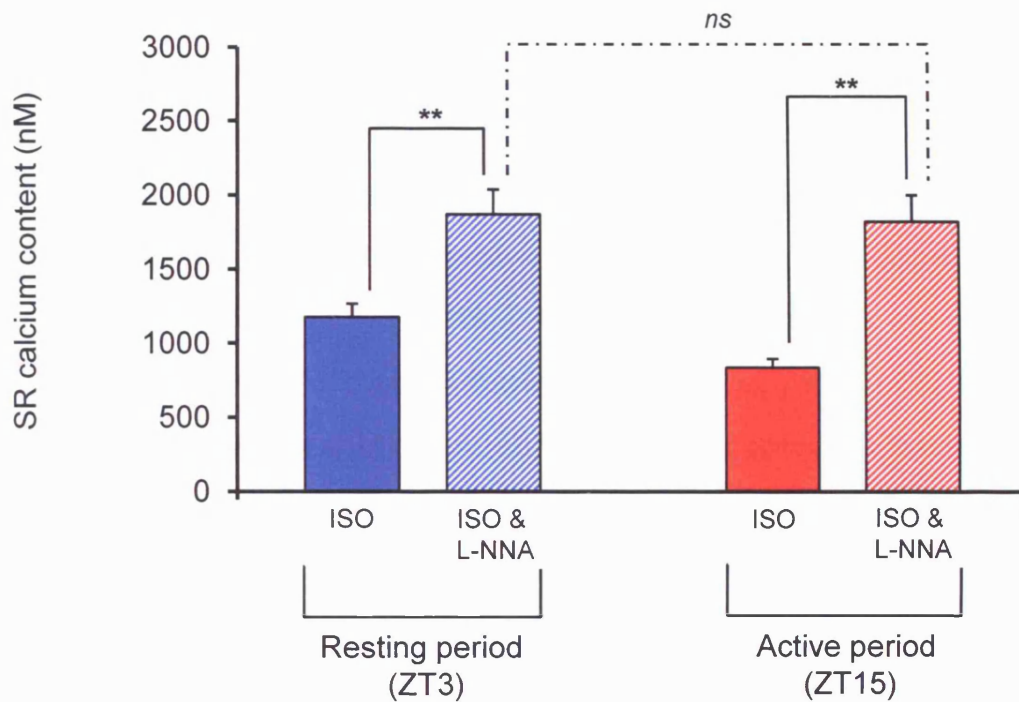


**Figure 5.3- The effect of  $\beta$ -adrenergic stimulation with isoproterenol (ISO) and of NOS inhibition with L-NNA on the sarcoplasmic reticulum  $\text{Ca}^{2+}$  content in resting period (ZT3) and active period (ZT15) myocytes.**

Bar chart showing the sarcoplasmic reticulum  $\text{Ca}^{2+}$  content, determined by the application of 20mM caffeine, recorded from resting period (ZT3; blue) and active period (ZT15) myocytes (red) following superfusion of normal Tyrode containing 10nM ISO (open bars) or 10nM ISO & 500 $\mu$ M L-NNA (hatched bars) for 5 minutes prior to application of 20mM caffeine. Values are mean  $\pm$  S.E.M.; number of experiments/ hearts = resting period (ZT3) myocyte (ISO  $n = 24/4$ ; ISO & L-NNA  $n = 27/4$ ) and active period (ZT15) myocyte (ISO  $n = 19/3$ ; ISO & L-NNA  $n = 17/3$ ); \*\*  $p < 0.001$ , two way ANOVA followed by a Bonferroni *post hoc* test.

Figure 5.3 is a bar chart of the mean data, from such experiments, showing SR  $\text{Ca}^{2+}$  content, assessed as the peak  $\text{Ca}^{2+}$  in response to 20mM caffeine, following  $\beta$ -adrenergic stimulation with 10nM ISO (open bars) and following inhibition of NOS with L-NNA during  $\beta$ -adrenergic stimulation with 10nM ISO (hatched bars) in resting period (ZT3) and active period (ZT15) myocytes. The data show that NOS inhibition with L-NNA during 10nM ISO superfusion induced a significant increase in SR  $\text{Ca}^{2+}$  content from levels seen with ISO alone in both resting period (ZT3) myocytes ( $p < 0.001$ ) and active period (ZT15) myocytes ( $p < 0.001$ ). SR  $\text{Ca}^{2+}$  content following simultaneous inhibition of NOS with L-NNA during  $\beta$ -adrenergic stimulation with 10nM ISO was not significantly different between resting period (ZT3) and active period (ZT15) myocytes, at  $1871.4 \pm 167.5$  nM in resting period (ZT3) myocytes ( $n = 24/4$ ) versus  $1822.7 \pm 178.9$  nM in active period (ZT15) myocytes ( $n = 17/4$ ; *ns*).

Figure 5.4 is a bar chart of the mean data of the exponential time constant of decay of the caffeine-induced  $\text{Ca}^{2+}$  transient following  $\beta$ -adrenergic stimulation with 10nM ISO (open bars) and following inhibition of NOS with L-NNA during  $\beta$ -adrenergic stimulation with 10nM ISO (hatched bars) in resting period (ZT3) and active period (ZT15) myocytes. The exponential time constant of decay of the caffeine-induced  $\text{Ca}^{2+}$  transient was calculated by fitting a single exponential to the slope of each caffeine-induced  $\text{Ca}^{2+}$  transient. In contrast to basal values (see chapter 3 figure 3.5B), there was a trend in which  $\beta$ -adrenergic stimulation with 10nM ISO prolonged the exponential time constant of decay of the caffeine-induced  $\text{Ca}^{2+}$  transient in active period (ZT15) myocytes, at  $2.40 \pm 0.16$  seconds in resting period (ZT3) myocytes ( $n = 24/4$ ) versus  $3.63 \pm 0.32$  seconds in active period (ZT15) myocytes ( $n = 19/3$ ; *ns*), however, this was not statistically significant. Moreover, following inhibition of NOS with L-NNA during  $\beta$ -adrenergic stimulation with 10nM ISO, this diurnal trend was abolished, with a exponential time constant of decay of the caffeine-induced  $\text{Ca}^{2+}$  transient of  $2.34 \pm 0.28$  seconds in resting period (ZT3) myocytes ( $n = 27/4$ ) versus  $2.33 \pm 0.34$  seconds in active period (ZT15) myocytes ( $n = 17/3$ ; *ns*).

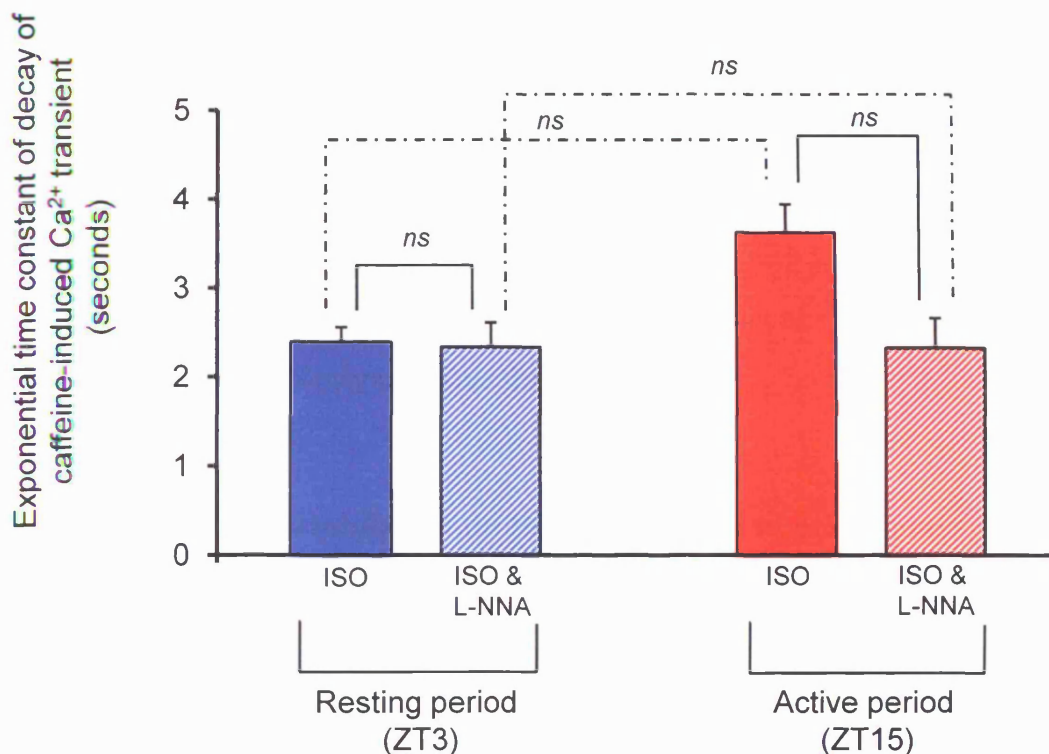


**Figure 5.4-** The effect of  $\beta$ -adrenergic stimulation with isoproterenol (ISO) and inhibition of NOS with L-NNA on the exponential time constant of decay of the caffeine-induced  $\text{Ca}^{2+}$  transient in resting period (ZT3) and active period (ZT15) myocytes.

Bar chart showing the exponential time constant of decay of the caffeine-induced  $\text{Ca}^{2+}$  transient recorded from resting period (ZT3; blue) and active period (ZT15) myocytes (red) following superfusion of normal Tyrode containing 10nM ISO (open bars) or 10nM ISO & 500 $\mu\text{M}$  L-NNA (hatched bars) for 5 minutes prior to application of 20mM caffeine. The exponential time constant of decay of the caffeine-induced  $\text{Ca}^{2+}$  transient was calculated by fitting a single exponential to the slope of each caffeine-induced  $\text{Ca}^{2+}$  transient. Values are the mean  $\pm$  S.E.M.; numbers of experiments/ hearts = resting period (ZT3) myocyte (ISO  $n = 24/4$ ; ISO & L-NNA  $n = 27/4$ ) and active period (ZT15) myocyte (ISO  $n = 19/3$ ; ISO & L-NNA  $n = 17/3$ ), two way ANOVA followed by a Bonferroni *post hoc* test. Note- statistics performed in combination with data presented in figure 4.10.

These data show that diurnal variation in SR  $\text{Ca}^{2+}$  content during ISO stimulation is absent following simultaneous NOS inhibition with L-NNA which suggests a significant role for NOS in the diurnal differences in basal SR  $\text{Ca}^{2+}$  content (see chapter 3; section 3.2.3) and SR  $\text{Ca}^{2+}$  content in response to ISO (see chapter 4; section 4.2.4). In addition, these data show that the diurnal trend in the exponential time constant of decay of the caffeine-induced  $\text{Ca}^{2+}$  transient which is present during 10nM ISO stimulation is absent following simultaneous NOS inhibition with L-NNA. As NCX is the principal current underlying the decay of the caffeine-induced  $\text{Ca}^{2+}$  transient, these data may suggest that NOS may modulate the activity of NCX.

### **5.2.3 The effect of NOS inhibition on the development of arrhythmic activity in ventricular myocytes in response to $\beta$ -adrenergic stimulation with isoproterenol**

In chapter 4, we showed that active period (ZT15) myocytes exhibit a reduced  $\text{Ca}^{2+}$  transient, contraction strength and SR  $\text{Ca}^{2+}$  content in response to ISO in comparison to resting period (ZT3) myocytes. We postulated this may be the result of the activation of the  $\beta_3$ -adrenergic receptor, as activation of the  $\beta_3$ -adrenergic receptor results in the activation of PKG through increases in NOS, NO, GC and cGMP, which produces a negative inotropic effect, that works against the positive inotropism of  $\beta_1$  and  $\beta_2$ -adrenergic receptor activation (see introduction section 1.4 for detail).

In the present chapter, we have shown that the inhibition of NOS activity with L-NNA attenuates the diurnal variation in the  $\text{Ca}^{2+}$  transient (diastolic, systolic and amplitude) and in SR  $\text{Ca}^{2+}$  content during  $\beta$ -adrenergic stimulation with ISO in resting period (ZT3) and active period (ZT15) myocytes. As a significantly smaller percentage of active period (ZT15) myocytes compared to resting period (ZT3) myocytes were shown to develop arrhythmic activity in response to 3 and 10nM ISO in chapter 4 and as activation of NOS has been suggested to be anti-arrhythmic (Burger et al., 2009), therefore, we postulated that this may be due to the protective action of the  $\beta_3$ -

adrenergic receptor and NOS and therefore, inhibition of NOS would abolish these diurnal differences. To determine whether NOS activity is responsible for diurnal variation in the development of arrhythmic activity, we measured the percentage of resting period (ZT3) and active period (ZT15) myocytes, stimulated at a rate of 1Hz, developing arrhythmic activity in response to  $\beta$ -adrenergic stimulation with ISO (3, 10nM) during NOS inhibition with the NOS inhibitor, L-NNA (500 $\mu$ M), using the method described in section 4.2.5 of chapter 4.

Figure 5.5 is a bar chart of the mean data, from such experiments, showing the percentage of myocytes that develop arrhythmic activity in response to  $\beta$ -adrenergic stimulation with ISO (3 & 10nM) and following inhibition of NOS with L-NNA. As seen in chapter 4, there is a significant diurnal variation in the percentage of myocytes developing arrhythmic activity in response to 3 and 10nM ISO, as at both concentrations, resting period (ZT3) myocytes develop a greater percentage of arrhythmic activity in comparison to active period (ZT15) myocytes (see section 4.2.5).

The data shows that inhibition of NOS with L-NNA has no effect on the percentage of resting period (ZT3) myocytes developing arrhythmic activity at either 3 or 10nM ISO, with  $43.3 \pm 4.8$  % of resting period (ZT3) myocytes developing arrhythmic activity in 3nM ISO ( $n = 18/5$ ) versus  $43.9 \pm 2.0$  % in 3nM ISO & L-NNA ( $n = 16/3$ ; *ns*) and  $61.6 \pm 4.4$  % of resting period (ZT3) myocytes developing arrhythmic activity in 10nM ISO ( $n = 18/5$ ) versus  $60.8 \pm 3.1$  % in 10nM ISO & L-NNA ( $n = 17/3$ ; *ns*). However, inhibition of NOS with L-NNA significantly increased the percentage of active period (ZT15) myocytes developing arrhythmic activity during 3nM ISO from  $13.6 \pm 1.8$  % ( $n = 19/5$ ) in 3nM ISO to  $31.2 \pm 1.5$  % in 3nM ISO & L-NNA ( $n = 22/4$ ;  $p < 0.001$ ) and during 10nM stimulation from  $35.5 \pm 2.6$  % ( $n = 18/5$ ) in 10nM ISO to  $53.0 \pm 2.1$  % ( $n = 21/4$ ;  $p < 0.001$ ) in 10nM ISO & L-NNA. The data also shows that inhibition of NOS reduces the difference between resting period (ZT3) and active period (ZT15) myocytes, as there was no significant difference in arrhythmic activity between resting period (ZT3) myocytes superfused with 3nM ISO and active period (ZT15) myocytes superfused with 3nM ISO & L-NNA (*ns*) and between resting period (ZT3) myocytes

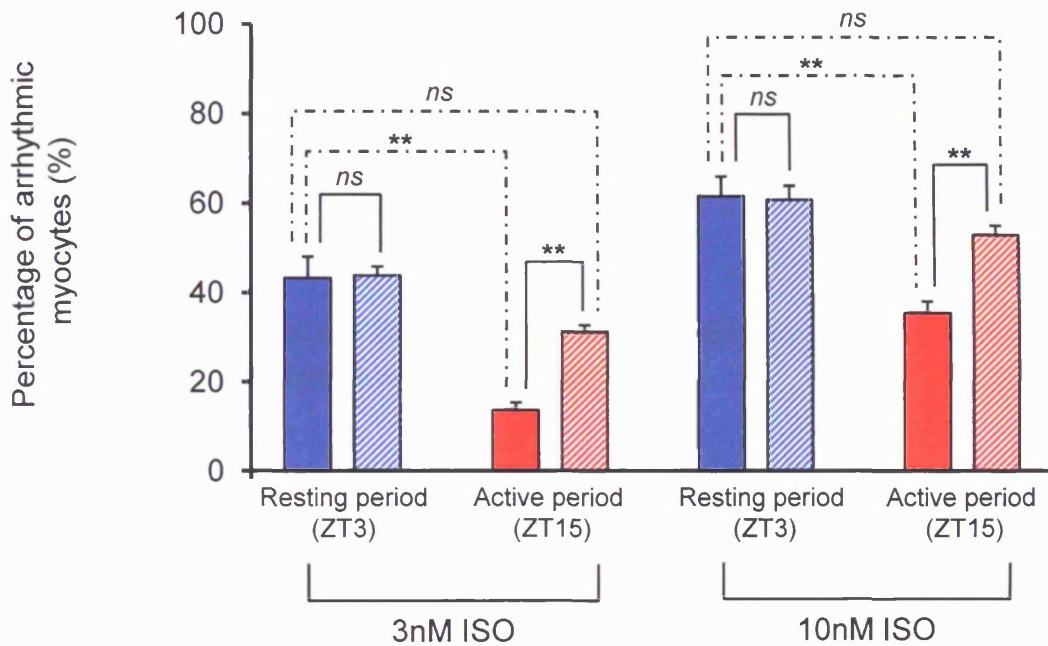


**Figure 5.5- The effect of NOS inhibition with L-NNA on the percentage of ventricular myocytes developing arrhythmic activity in response to  $\beta$ -adrenergic stimulation with isoproterenol (ISO).**

Bar chart showing the percentage of resting period (ZT3) myocytes (blue) and active period (ZT15) myocytes (red) calculated from a field of ~10-20 cells during 1Hz electrical field stimulation, that develop asynchronous, arrhythmic activity after 5 minutes superfusion with normal Tyrode containing either 3 or 10nM ISO (open bars) or after 5 minutes superfusion of normal Tyrode containing either 3 or 10nM ISO and 500µM L-NNA (hatched bars). Values are mean  $\pm$  S.E.M.; number of experiments/ hearts = resting period (ZT3) myocyte,  $n = 16-18/ 3-5$  and active period (ZT15) myocyte,  $n = 18-22/ 4-5$ ; \*\*  $p < 0.001$ , two way ANOVA followed by a Bonferroni *post hoc* test.

superfused with 10nM ISO and active period (ZT15) myocytes superfused with 10nM ISO & L-NNA (*ns*), suggesting that NOS may have an anti-arrhythmic role in active period (ZT15) myocytes and protects against catecholamine-induced arrhythmias.

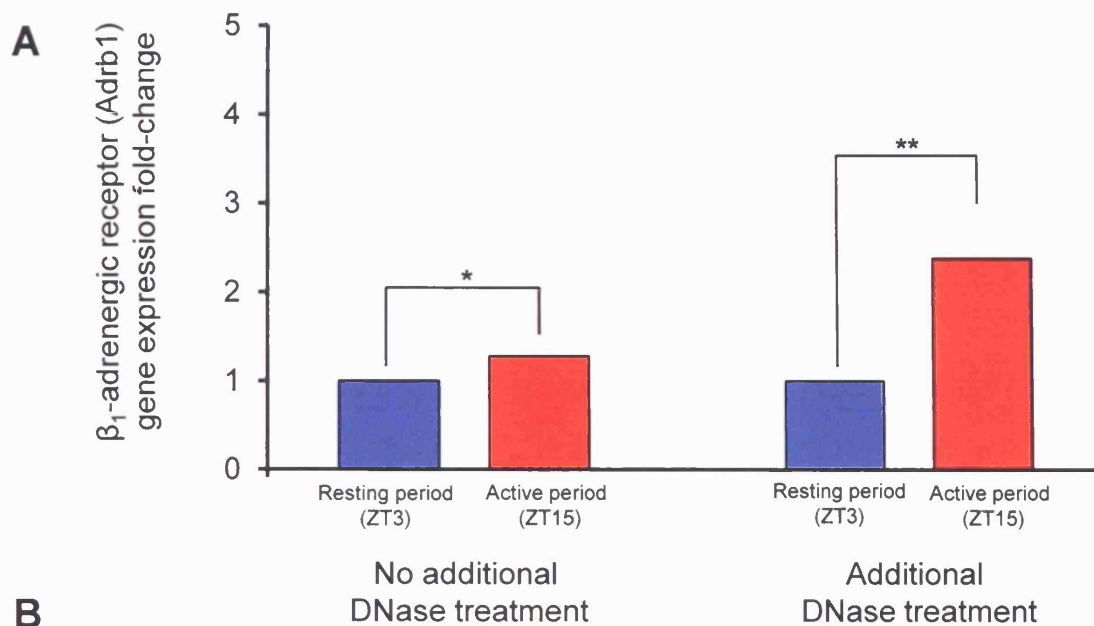
These data show that NOS inhibition with L-NNA increases the percentage of active period (ZT15) myocytes developing arrhythmic activity to similar levels seen in the resting period (ZT3) myocytes during ISO stimulation, suggesting a protective role for NOS in the prevention of arrhythmias.

#### **5.2.4 Diurnal variation in the $\beta_1$ -adrenergic receptor and the $\beta_3$ -adrenergic receptor mRNA expression in the adult Wistar**

As our data show a significant diurnal variation in the response of  $Ca^{2+}$  transient, contraction strength and SR  $Ca^{2+}$  content to  $\beta$ -adrenergic stimulation with the non-specific  $\beta$ -adrenergic receptor agonist, ISO, we hypothesised that this diurnal variation may reflect underlying changes in the expression and transcription of the  $\beta_1$ -adrenergic receptor (*Adrb1*) and  $\beta_3$ -adrenergic receptor (*Adrb3*).

To determine this we performed quantitative real-time Taqman RT-PCR on left ventricular free-wall tissue isolated from Wistar rat hearts at time points during the resting period (ZT3) and the active period (ZT15; see section 2.5.9 of methods). The Taqman probe used to amplify  $\beta_1$ -adrenergic receptor mRNA spans a single exon and therefore, amplifies contaminating DNA. To overcome DNA contamination, RNA samples were either treated at extraction with a gDNA eliminator column and on-column DNase (no additional DNase) or treated with gDNA eliminator column, on-column DNase and an additional Sigma DNase prior to RT (additional DNase; see methods 2.5.7).

Figure 5.6 shows the gene expression fold-change measurements for the  $\beta_1$ -adrenergic receptor (*Adrb1*) in samples without (left) and with an additional DNase treatment (right) prior to RT in left ventricular free-wall tissue isolated during the resting period



**B**

| Gene of interest                       | Treatment           | $\Delta$ CT (normalised to $\beta$ -actin) |                      | <i>p</i> -value (from $\Delta$ CT) | Fold change ZT15 ( $\Delta\Delta$ CT) |
|----------------------------------------|---------------------|--------------------------------------------|----------------------|------------------------------------|---------------------------------------|
|                                        |                     | Resting period (ZT3)                       | Active period (ZT15) |                                    |                                       |
| $\beta_1$ -adrenergic receptor (Adrb1) | No additional DNase | 4.96 $\pm$ 0.07                            | 4.61 $\pm$ 0.07      | <i>p</i> = 0.0141<br>*             | 1.28<br>\$                            |
|                                        | Additional DNase    | 6.36 $\pm$ 0.15                            | 5.20 $\pm$ 0.29      | <i>p</i> = 0.0046<br>**            | 2.38<br>\$                            |

**Figure 5.6- Gene expression levels of the  $\beta_1$ -adrenergic receptor (Adrb1) in Wistar rat hearts isolated during the resting period (ZT3) and active period (ZT15).**

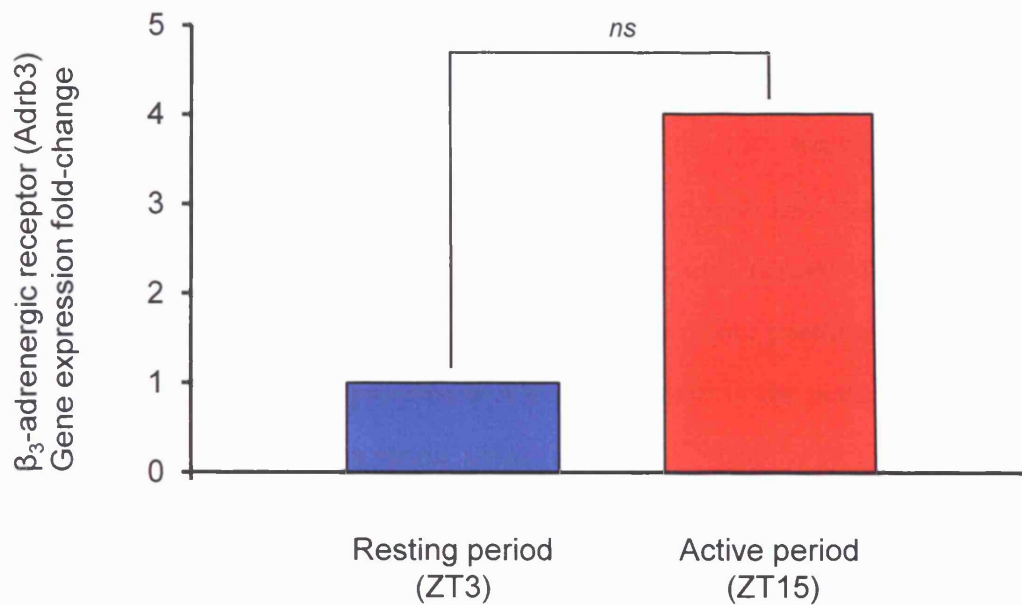
A. Bar chart showing the quantitative real-time RT-PCR of  $\beta_1$ -adrenergic receptor (Adrb1) mRNA expression as fold-changes in left ventricular free-wall isolated from resting period (ZT3; blue) and active period (ZT15; red) of the Wistar rat. As the Taqman probe for Adrb1 amplifies gDNA, the RNA was either subjected to two separate gDNA removal steps during RNA extraction (left bars) or the RNA was subject to two separate gDNA removal steps during RNA extraction and an additional DNase treatment prior to conversion to cDNA (right bars). Adrb1 expression was normalised to  $\beta$ -actin mRNA. Fold-changes in Adrb1 mRNA were calculated using the  $\Delta\Delta$ CT method (\$, see appendix 3 figure 1) relative to the control (ZT3; blue bars). The results are mean  $\pm$  S.E.M.. Number of samples = resting period (ZT3), *n* = 5 and active period (ZT15), *n* = 5. \* *p* < 0.05, \*\* *p* < 0.001, unpaired students *t* test performed on  $\Delta$ CT values.

B. Table showing the data used to produce the bar chart in figure 5.6A.

(ZT3; blue) and the active period (ZT15; red), normalised to  $\beta$ -actin expression. *Adrb1* expression was significantly higher during the active period (ZT15) in comparison to the resting period (ZT3) in cDNA samples without the application of an additional DNase stage, which corresponded to a fold-change of 1.28 in active period (ZT15) tissue ( $p = 0.0141$ ). This difference in expression appeared to be more marked following additional DNase treatment as *Adrb1* expression was significantly higher during the active period (ZT15) in comparison to the resting period (ZT3), which corresponded to a fold-change of 2.38 in active period (ZT15) tissue ( $p = 0.0046$ ). In addition, there was a borderline significant difference in *Adrb1* expression in between cDNA without additional DNase treatment and cDNA with additional DNase treatment in left ventricular free-wall tissue isolated during the active period (ZT15) ( $p < 0.06$ , *ns*, not shown on figure).

Figure 5.7 shows the gene expression fold-change measurements for the  $\beta_3$ -adrenergic receptor (*Adrb3*) in snap frozen left ventricular free-wall isolated during the resting period (ZT3) and active period (ZT15) of the adult Wistar rat. *Adrb3* expression was higher during the active period (ZT15) in comparison to the resting period (ZT3), which corresponded to a fold-change of 4.01 in active period (ZT15) tissue ( $p = 0.17$ , *ns*), however, based on statistics performed on  $\Delta$ CT values this increase in expression was not significantly different.

These data show that *Adrb1* expression is significantly higher in left ventricular free-wall isolated during the active period (ZT15) in comparison to the resting period (ZT3), which is enhanced through the application of an additional DNase stage prior to RT and this may indicate the presence of contaminating DNA in the samples that are not treated with an additional DNase that could be masking differences in the expression of *Adrb1*. These data also show that *Adrb3* mRNA expression is higher in left ventricular free-wall isolated during the active period (ZT15) in comparison to the resting period (ZT3); however, the data is not significantly different.

**A****B**

| Gene of interest                       | Sample | $\Delta$ CT (normalised to $\beta$ -actin) |                      | <i>p</i> -value (from $\Delta$ CT) | Fold change ZT15 ( $\Delta\Delta$ CT) |
|----------------------------------------|--------|--------------------------------------------|----------------------|------------------------------------|---------------------------------------|
|                                        |        | Resting period (ZT3)                       | Active period (ZT15) |                                    |                                       |
| $\beta_3$ -adrenergic receptor (Adrb3) | Tissue | 21.67 $\pm$ 0.40                           | 20.12 $\pm$ 0.76     | <i>p</i> = 0.1672<br><i>ns</i>     | 4.01<br>\$                            |

**Figure 5.7- Gene expression levels of the  $\beta_3$ -adrenergic receptor (Adrb3) in Wistar rat hearts isolated during the resting period (ZT3) and active period (ZT15).**

A. Bar chart showing the quantitative real-time RT-PCR of Adrb3 mRNA expression as fold-changes in left ventricular free-wall isolated during the resting period (ZT3; blue) and active period (ZT15; red) of the Wistar rat. Adrb3 mRNA expression was normalised to  $\beta$ -actin mRNA. Fold-change of Adrb3 mRNA was calculated using the  $\Delta\Delta$ CT method (\$) relative to the control (ZT3; blue bars). The results are mean  $\pm$  S.E.M.; number of samples = resting period (ZT3), *n* = 3 and active period (ZT15), *n* = 4; unpaired students *t* test performed on  $\Delta$ CT values

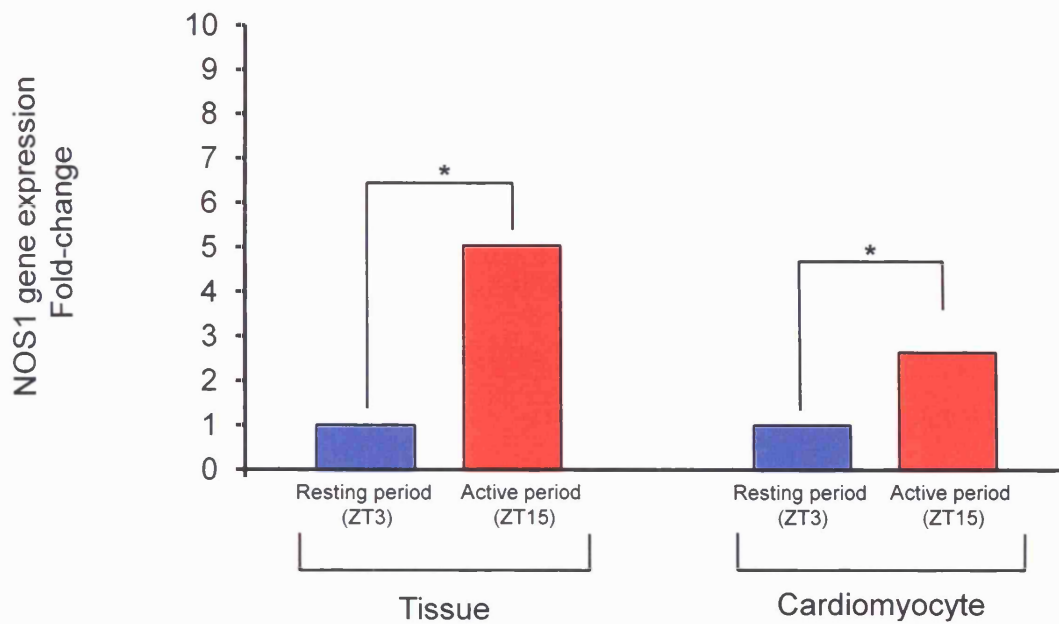
B. Table showing the data used to produce the bar chart in figure 5.7A

### **5.2.5 Diurnal variation in neuronal nitric oxide synthase, nitric oxide synthase 1 adaptor protein and endothelial nitric oxide synthase mRNA expression in adult Wistar.**

The NOS inhibitor L-NNA augments the response of the  $\text{Ca}^{2+}$  transient and SR  $\text{Ca}^{2+}$  content in active period (ZT15) myocytes to stimulation with ISO thereby attenuating the difference between resting period (ZT3) and active period (ZT15) myocytes suggesting the involvement of NOS-signalling. We therefore postulated that neuronal and endothelial NOS gene expression would be increased in the active period (ZT15) myocyte. In addition, as the nitric oxide synthase 1 adaptor protein, CAPON, is physically associated with NOS1 acting as an anchoring protein for NOS1 (Beigi et al., 2009), we also looked at the expression of CAPON during the resting period (ZT3) and active period (ZT15) of the nocturnal rat. To determine the expression levels of the genes encoding neuronal nitric oxide synthase (NOS1), endothelial nitric oxide synthase (NOS3) and CAPON, quantitative real-time Taqman RT-PCR was performed on the left ventricular free-wall isolated from Wistar rat hearts at time-points during the resting period (ZT3) and the active period (ZT15) (see section 2.5.9 of methods).

In chapter 3, we showed that expression of the circadian clock genes, *Per2* and *CLOCK*, was not significantly different between isolated ventricular myocytes and left ventricular free-wall tissue, suggesting that our method of isolating single ventricular myocytes does not adversely affect gene expression. To further re-enforce these data in chapter 3, we determined whether the process of isolating single ventricular myocytes had any effect on the expression of NOS1, through quantitative real-time Taqman RT-PCR of isolated left ventricular myocytes and left ventricular free-wall tissue from Wistar rat hearts isolated during the resting period (ZT3) and the active period (ZT15). Gene expression was normalised to the control gene,  $\beta$ -actin and fold changes were calculated using either the  $\Delta\Delta\text{CT}$  or Pfaffl method (see figure legends and appendix 3 for details). Statistics were performed on the  $\Delta\text{CT}$  values. The resting period (ZT3) sample was used as a reference sample or calibrator to which all active period (ZT15)

**A**



**B**

| Gene of interest | Sample        | $\Delta$ CT (normalised to $\beta$ -actin) |                      | <i>p</i> -value (from $\Delta$ CT) | Fold change ZT15 (Pfaffl) |
|------------------|---------------|--------------------------------------------|----------------------|------------------------------------|---------------------------|
|                  |               | Resting period (ZT3)                       | Active period (ZT15) |                                    |                           |
| NOS1             | Tissue        | 14.14 $\pm$ 0.77                           | 11.52 $\pm$ 0.64     | <i>p</i> = 0.03<br>*               | 5.04<br>#                 |
|                  | Cardiomyocyte | 12.26 $\pm$ 0.52                           | 10.85 $\pm$ 0.31     | <i>p</i> = 0.05<br>*               | 2.65<br>#                 |

**Figure 5.8- Gene expression levels of neuronal nitric oxide synthase (NOS1) in Wistar rat hearts isolated during the resting period (ZT3) and active period (ZT15).**

A. Bar chart showing the quantitative real-time RT-PCR of NOS1 mRNA expression as fold-changes in left ventricular free wall (left) and ventricular myocytes (right) isolated during the resting period (ZT3; blue) and active period (ZT15; red) of the Wistar rat. NOS1 mRNA expression was normalised to  $\beta$ -actin mRNA. Fold-change of NOS1 mRNA was calculated using the Pfaffl method (#, see appendix 3 figure 1) relative to the control (ZT3; blue bars). The results are mean  $\pm$  S.E.M.; number of samples = resting period (ZT3), *n* = 5 and active period (ZT15), *n* = 5. \* *p* < 0.05, unpaired students *t* test performed on  $\Delta$ CT values

B. Table showing the data used to produce the bar chart in figure 5.8 A

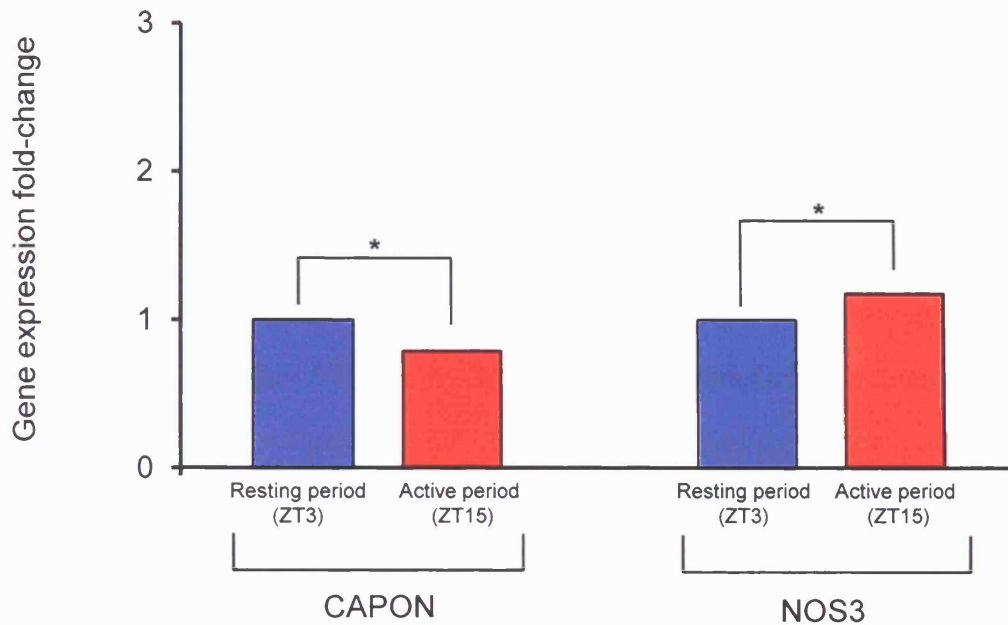
samples were compared and therefore has an average fold change of 1 in each PCR dataset.

Figure 5.8 is a bar chart showing the gene expression fold-change measurements for the gene encoding neuronal nitric oxide synthase (NOS1), in snap frozen left ventricular tissue (left) and isolated left ventricular myocytes (right), normalised to  $\beta$ -actin. NOS1 expression was significantly higher in both tissue and isolated myocytes during the active period (ZT15) in comparison to the resting period (ZT3), which corresponded to a fold change of 5.04 ( $p < 0.05$ ) in active period (ZT15) tissue and 2.65 ( $p < 0.05$ ) in active period (ZT15) isolated myocytes. There was no statistical difference between the PCR data obtained from tissue and isolated myocytes in the active period (ZT15) time-point ( $p = 0.55$ ; *ns*).

Figure 5.9 is a bar chart showing the gene expression fold-change measurements for the genes encoding nitric oxide synthase 1 adaptor protein, CAPON (left), and endothelial nitric oxide synthase, NOS3 (right), in snap frozen left ventricular free-wall from adult Wistar. CAPON expression was significantly higher during the resting period (ZT3) in comparison to the active period (ZT15), which corresponded to a fold change of 0.79 in active period (ZT15) tissue ( $p < 0.05$ ). NOS3 expression was significantly higher during the active period (ZT15) in comparison to the resting period (ZT3), which corresponded to a fold change of 1.18 in active period (ZT15) tissue ( $p < 0.05$ ).

The data show firstly that NOS1 gene expression is significantly higher in left ventricular free-wall tissue and myocytes isolated during the active period (ZT15) in comparison to the resting period (ZT3) and that NOS3 gene expression is also increased in Wistar left ventricular free-wall tissue from hearts isolated during the active period (ZT15) in comparison to the resting period (ZT3). However, the fold changes were greater for NOS1 than NOS3, suggesting an involvement of NOS1 in the depressed  $\text{Ca}^{2+}$  transient, contraction strength and SR  $\text{Ca}^{2+}$  content in active period (ZT15) myocytes. Paradoxically, the data also show that expression of the gene encoding the NOS1 associated protein, CAPON, is significantly higher left ventricular free-wall

**A**



**B**

| Gene of interest | Sample | $\Delta$ CT (normalised to $\beta$ -actin) |                      | <i>p</i> -value (from $\Delta$ CT) | Fold change ZT15 ( $\Delta\Delta$ CT/ Pfaffl) |
|------------------|--------|--------------------------------------------|----------------------|------------------------------------|-----------------------------------------------|
|                  |        | Resting period (ZT3)                       | Active period (ZT15) |                                    |                                               |
| CAPON            | Tissue | 6.94 $\pm$ 0.13                            | 7.32 $\pm$ 0.05      | <i>p</i> = 0.0288<br>*             | 0.79<br>\$                                    |
| NOS3             |        | 6.21 $\pm$ 0.06                            | 5.94 $\pm$ 0.10      | <i>p</i> = 0.0418<br>*             | 1.18<br>#                                     |

**Figure 5.9- Gene expression levels of neuronal nitric oxide synthase adaptor protein 1 (CAPON) and endothelial nitric oxide synthase (NOS3) in Wistar rat hearts isolated during the resting period (ZT3) and active period (ZT15).**

A. Bar chart showing the quantitative real-time RT-PCR of CAPON & NOS3 mRNA expression as fold-changes in left ventricular free-wall isolated during the resting period (ZT3; blue) and active period (ZT15; red) of the Wistar rat. Both CAPON & NOS3 mRNA expression were normalised to  $\beta$ -actin mRNA. Fold-changes in CAPON & NOS3 mRNA were calculated using either the  $\Delta\Delta$ CT (CAPON, \$) or Pfaffl method (NOS3, #, see appendix 3 figure 1) relative to the control (ZT3; blue bars). The results are mean  $\pm$  S.E.M.; number of samples = resting period (ZT3), *n* = 5 and active period (ZT15), *n* = 5. \* *p* < 0.05, unpaired students *t* test performed on  $\Delta$ CT values

B. Table showing the data used to produce the bar chart in figure 5.9 A

tissue isolated during the resting period (ZT3) in comparison to the active period (ZT15).

### ***5.3 Discussion***

In the present chapter, we have suggested for the first time that NOS-signalling exhibits diurnal variations in cardiac myocytes and is responsible for the variation in responsiveness of cardiac contractility to sympathetic stimulation, reported in the previous chapter. To investigate the role of NOS in the time-of-day dependent variation in EC-coupling, we recorded the effects of the non-specific NOS inhibitor, L-NNA on the response of the  $\text{Ca}^{2+}$  transient, SR  $\text{Ca}^{2+}$  content and resultant contraction strength from resting period (ZT3) and active period (ZT15) myocytes during  $\beta$ -adrenergic stimulation with ISO. The data shows that inhibition of NOS activity with L-NNA increases the responsiveness of active period (ZT15) myocytes to ISO thereby abolishing diurnal variation in systolic  $[\text{Ca}^{2+}]$  and amplitude of  $[\text{Ca}^{2+}]$  transient in these myocytes. This effect of inhibiting NOS-signalling was also observed in contraction strength and SR  $\text{Ca}^{2+}$  content in resting period (ZT3) and active period (ZT15) myocytes. Stimulation with high concentrations of the non-specific  $\beta$ -adrenergic receptor agonist, ISO, was shown in the previous chapter to induce arrhythmic activity, which is less pronounced in active period (ZT15) myocytes. The data shows that this apparent protection against arrhythmic activity in active period (ZT15) myocytes is lost in the presence of the NOS inhibitor L-NNA, suggesting NOS is responsible for reducing the incidence of sympathetic-induced arrhythmic activity in active period (ZT15) myocytes. On the basis of this data, we also determined whether the differences in EC-coupling were the result of changes in the expression of  $\beta$ -adrenergic and NOS-signalling genes. The gene expression data show that expression of the  $\beta_1$ -adrenergic receptor and  $\beta_3$ -adrenergic receptors were greater in hearts isolated during the active period (ZT15). In addition, we found that expression of NOS1 rather than NOS3

exhibited diurnal variations which were consistent with NOS1 being involved in the reduced responsiveness and reduced sympathetic-induced arrhythmic activity observed in active period (ZT15) myocytes. These findings are novel as the role of NOS in the diurnal variation in  $Ca^{2+}$  homeostasis and EC-coupling we observe have yet to be reported.

### **5.3.1 Is the relative contribution of $\beta_1$ and $\beta_3$ -adrenergic receptors responsible for the diurnal variation in the responsiveness to ISO?**

ISO and the endogenous catecholamines, epinephrine and norepinephrine, have been reported to activate  $\beta_2$  and  $\beta_3$ -adrenergic receptors in addition to  $\beta_1$ -adrenergic receptors (Bers, 2002, Wallukat, 2002). Activation of cardiac  $\beta_1$ -adrenergic receptors (and  $\beta_2$ -adrenergic receptors through local LTCC phosphorylation) results in positive inotropic and lusitropic effects mediated through PKA-dependent phosphorylation of LTCC, RyR2, PLB and troponin I, which contributes to an increase in  $Ca^{2+}$  transient amplitude, SR  $Ca^{2+}$  content and contraction strength (Bers, 2001, Bers, 2002). Conversely, activation of the cardiac  $\beta_3$ -adrenergic receptor produces a negative inotropic effect through the activation of NOS, which is responsible for the production of NO (Gauthier et al., 1998). This NO is thought to target the function of the LTCC, RyR2, SERCA 2a/PLB and troponin I through cGMP-dependent (PKG phosphorylation) and cGMP-independent (S-nitrosylation) signalling, thereby reducing  $Ca^{2+}$  transient amplitude, SR  $Ca^{2+}$  content and contraction strength, however, the exact targets and NOS isoform responsible for these changes are controversial (Ziolo, 2008, Ziolo et al., 2008).

As the overall inotropic response of the myocardium to ISO will reflect the balance between  $\beta_1/\beta_2$  and  $\beta_3$ -adrenergic receptor activation, the reduced responsiveness of active period (ZT15) myocytes to ISO stimulation we observe could reflect changes in the balance between  $\beta_1/\beta_2$  (positive inotropic) and  $\beta_3$ -adrenergic receptor (negative inotropic) activation. This could be the result of either a change in the ratio of  $\beta_1/\beta_2$ -

adrenergic receptors to  $\beta_3$ -adrenergic receptors or a change in the signalling pathways, which are different between receptor types (see introduction section 1.4). Therefore, if the diurnal variation we observe results from a shift in the balance of  $\beta_1/\beta_2$ :  $\beta_3$ -adrenergic receptors this may impact on the responsiveness of the myocardium to sympathetic stimulation in terms of both inotropy and also the development of ventricular arrhythmias.

The reduced responsiveness of active period (ZT15) myocytes to ISO may be due to a reduction in  $\beta_1$ -adrenergic receptor density, as reduction in the expression of the  $\beta_1$ -adrenergic receptor may mean that active period (ZT15) myocytes are less able to respond to sympathetic stimulation thereby preventing the positive inotropic effect associated with  $\beta_1$ -adrenergic receptor activation. However, our gene expression data for the  $\beta_1$ -adrenergic receptor (*Adrb1*) does not support this idea but rather showed an increase in the expression of the  $\beta_1$ -adrenergic receptor during the active period (ZT15) compared to resting period (ZT3).

The reduced responsiveness of active period (ZT15) myocytes to ISO may reflect increased desensitisation/down-regulation of the  $\beta_1$ -adrenergic receptor through phosphorylation by  $\beta$ -ARK1, driven by the increase in sympathetic activity at this time. The phosphorylation of cardiac  $\beta$ -adrenergic receptors by  $\beta$ -ARK1 typically occurs in cases of chronic sympathetic stimulation such as those associated with the development of LV-hypertrophy, although it is not known whether this also occurs to a lesser extent during shorter periods i.e in minutes of increased sympathetic activity (Castellano and Bohm, 1997, Post et al., 1999, Rockman et al., 2002, Wallukat, 2002). Therefore, it is possible that an increase in sympathetic activity associated with the active period of the rat may promote increased desensitisation and/or down-regulation of cardiac  $\beta$ -adrenergic receptors in active period (ZT15) myocytes. Desensitisation/down-regulation seems unlikely to have occurred in the present investigation as the responsiveness of  $\text{Ca}^{2+}$  transient to ISO stimulation did not differ in myocytes over the course of the experimental day or the application of different concentrations of ISO and active period (ZT15) myocytes did not recover the ability to respond to ISO over a

period of 8-12 hours (see chapter 4 discussion section 4.3.3 for detail). However, as our data does not definitively exclude the possibility of desensitisation/down-regulation we therefore cannot rule this out. In addition, the decreased responsiveness of active period (ZT15) myocytes could possibly reflect time-of-day dependent changes in the expression of active  $\beta_1$ -adrenergic receptor protein, which we did not determine, or time-of-day dependent changes in  $\beta_1$ -adrenergic receptor internalisation and trafficking in a similar manner to the time-of-day dependent changes in surface expression of NCX mediated by PIP<sub>2</sub> (Shen et al., 2007). The decreased responsiveness of active period (ZT15) myocytes to ISO could also be due to differences in  $\beta_1$ -adrenergic receptor affinity/efficacy in addition to changes in  $\beta_1/\beta_2$ -adrenergic receptor density, as it has been documented that the affinity of the cardiac  $\beta_1$ -adrenergic receptor differs between ISO and the endogenous catecholamines, norepinephrine and epinephrine (Hoffmann et al., 2004). Therefore, differences in  $\beta_1$ -adrenergic receptor affinity between epinephrine, norepinephrine and ISO may explain the differences between the data obtained in the present investigation and that of Young and colleagues. However, as we did not perform any  $\beta_1$ -adrenergic receptor binding studies with ISO, as part of the present investigation, we do not know whether this possible mechanism is indeed occurring, therefore, further work is required to examine this.

The decreased responsiveness of active period (ZT15) myocytes we observe in response to ISO may also be due to an increase in the expression of the negative inotropic  $\beta_3$ -adrenergic receptor, which would antagonise the positive inotropic effect of  $\beta_{1/2}$ -adrenergic receptor activation. If there was a time-of-day dependent increase in active  $\beta_3$ -adrenergic receptor protein in active period (ZT15) myocytes then the decreased responsiveness may be due to increased activation and signalling through the negative inotropic  $\beta_3$ -adrenergic receptor and downstream NOS signalling. In addition, increased activation of the negative inotropic  $\beta_3$ -adrenergic receptor in active period (ZT15) myocytes could be masking the positive inotropic effects of  $\beta_1/\beta_2$ -adrenergic receptors, in that the diurnal variation we observe in the responsiveness of active period (ZT15) myocytes to ISO may be the result of a shift in the balance of the ratio of

$\beta_1/\beta_2:\beta_3$ -adrenergic receptors. However, our gene expression data for  $\beta_3$ -adrenergic receptor (*Adrb3*) do not completely support the reduced responsiveness of active period (ZT15) myocytes, as although there is an increase in the magnitude of expression for the  $\beta_3$ -adrenergic receptor during active period (ZT15) compared to the resting period (ZT3), this difference was not significant and in our opinion these data may be unreliable due to issues with quantitative real-time RT-PCR of this gene (see section 5.3.5 limitations). In addition, this data cannot be explained by receptor desensitisation/down-regulation as the  $\beta_3$ -adrenergic receptor does not possess the phosphorylation sites required for  $\beta$ -ARK1 phosphorylation (Skeberdis, 2004). However, time-of-day dependent changes in the expression of the  $\beta_3$ -adrenergic receptor may occur in active protein in active period (ZT15) myocytes; however, in the present study we were unable to quantify protein, therefore, this requires additional work to determine.

### **5.3.2 The role of NOS-signalling in the time-of-day dependent variation in the responsiveness of the $\text{Ca}^{2+}$ transient to $\beta$ -adrenergic stimulation**

NOS has been implicated in the control of cardiac contraction and the modulation of  $\text{Ca}^{2+}$  homeostasis under basal conditions and during sympathetic stimulation (Hare, 2003, Casadei, 2006), where it targets LTCC, RyR2, SERCA 2a/PLB and troponin I through downstream activation of cGMP-dependent and independent pathways, which reduce the  $\text{Ca}^{2+}$  transient amplitude and contraction strength (Hare, 2003, Ziolo et al., 2008). Therefore, the decreased responsiveness of active period (ZT15) myocytes to ISO may be due to an increase in NOS activity. In support of this, our data show that the non-specific NOS inhibitor, L-NNA, significantly augmented the depressed response of systolic  $[\text{Ca}^{2+}]$  and the amplitude of  $\text{Ca}^{2+}$  transient in active period (ZT15) myocytes, to ISO stimulation, suggesting that NOS is involved in the diurnal variation in the responsiveness to ISO. Furthermore, NOS inhibition resulted in an increase in SR  $\text{Ca}^{2+}$  content in active period (ZT15) myocytes during ISO-stimulation, suggesting

that NO targeted depression in SR function mediates the reduction in responsiveness to ISO in active period (ZT15) myocytes. Although these data suggest that NOS mediates the time-of-day dependent variation in EC-coupling, this data does not confirm which isoform is responsible for the differences we observe, as L-NNA is a non-specific NOS inhibitor capable of inhibiting all isoforms of NOS. Our data reported in chapter three, show that genes encoding sarcolemmal and SR EC-coupling components did not show patterns of diurnal cycling (with the exception of NCX1). The data of the present chapter provides evidence to suggest that NO may be post-translationally modifying these EC-coupling proteins to decrease contractility in active period (ZT15) myocytes. Although historically, NOS3 was thought to be responsible for the NO-dependent modulation of basal and sympathetic induced changes in contraction and  $Ca^{2+}$  homeostasis, in recent years however the role of NOS1 has been established (Casadei, 2006). Therefore, as NO-signalling has been shown to be localised within the cell and NOS1 is restricted to the SR (Xu et al., 1999) it seems likely that post-translational modification occurs as a result of NOS1.

The apparent increase in NOS activity we observe during the active period (ZT15) could reflect either an increase in NOS gene/ protein expression or perhaps modulation of existing NOS which results in an increase in activity. Our data shows that expression of both NOS1 and NOS3 are significantly greater during the active period (ZT15) than the resting period (ZT3). Diurnal variation in endogenous NOS activity has been observed by Ayers *et al* (1996) who have shown that NOS activity and protein levels were greatest during the active period than the resting period in the rat brain, which is supportive of our data and Tunctan *et al* (2002) have also shown circadian variation in NOS activity in mouse brain, aorta, lung, testis and kidney, however, in both these studies the NOS isoform responsible was not identified. However, the magnitude of the increase in NOS3 expression (1.18 fold), although significantly different between time-points, was modest and did not compare to that of NOS1 expression (5.04 fold). Therefore, it seems unlikely that NOS3 is responsible for the diurnal variation we observe as there was only modest variation in NOS3 expression. In addition, NOS3-

signalling is localised to the sarcolemmal membrane and targets the LTCC, which has only a minor role in EC-coupling the rat, suggests that NOS3 contributes far less to the decreased  $\text{Ca}^{2+}$  transient, contraction strength and SR  $\text{Ca}^{2+}$  content we observe in active period (ZT15) myocytes. Whereas, NOS1 is predominately localised to the SR where it targets SR function through the modulation of RyR2, SERCA 2a and PLB (Xu et al., 1999). Therefore, it is likely that NOS1 is responsible for the time-of-day dependent reduction in the responsiveness of active period (ZT15) myocytes to ISO, as SR is responsible for ~90% of  $\text{Ca}^{2+}$  release and uptake during contraction (Bassani et al., 1994, Bers, 2001) and these myocytes exhibit a reduction in SR  $\text{Ca}^{2+}$  content possibly mediated through a reduction in SERCA 2a activity which contributes to the reduced  $\text{Ca}^{2+}$  transient amplitude and contraction strength in these myocytes. In addition, data from this laboratory has shown that the NOS1-specific inhibitor, N-[(4S)-4-amino-5-[(2-aminoethyl)amino]pentyl]-N'-nitroguanidine tris(trifluoroacetate) (4-AAPNT), increases responsiveness of the  $\text{Ca}^{2+}$  transient to ISO in active period (ZT15) myocytes to similar levels as the non-selective NOS inhibitor, L-NNA, supporting the role of NOS1 in the diurnal variation we observe in EC-coupling (Collins and Rodrigo, 2010). Previous genetic studies using both NOS1 and NOS3 gene KO mice have shown different contributions of these isoforms in the responsiveness to  $\beta$ -adrenergic stimulation. Our data suggests that increased NOS1 activity is responsible for the depressed response of the  $\text{Ca}^{2+}$  transient, SR  $\text{Ca}^{2+}$  content and contraction strength to ISO we observe in active period (ZT15) myocytes, rather than an increase in NOS3. In support of our data, Martin *et al* (2006) examined contraction strength in NOS1 and NOS3 KO mice myocytes in response to ISO and found that NOS1 KO mice had an increase in contraction strength to ISO whereas NOS3 KO mice did not differ from wild-type mice, suggesting that NOS1 is responsible for limiting the response to ISO and these NOS1 data were also shown by Ashley *et al* (2002). Conversely, many previously published studies suggest that NOS3 is responsible for a reduction in the responsiveness to  $\beta$ -adrenergic stimulation, as Barouch *et al* (2002) have reported a decreased ISO responsiveness in NOS1 KO mice whereas NOS3 KO mice showed

increased responsiveness to ISO, suggesting that NOS3 may be responsible in limiting the response to ISO. In addition, Varghese *et al* (2000) have shown that both  $\beta_3$ -adrenergic receptor and NOS3 KO mice have a similar increase in the responsiveness to ISO, suggesting that  $\beta_3$ -adrenergic receptor and NOS3 could be responsible for the anti-adrenergic effect we observe in active period (ZT15) myocytes. However, our data does not support the role of NOS3 in reducing the response to  $\beta$ -adrenergic stimulation as NOS1 expression was greater than NOS3 expression in active period (ZT15) myocytes and  $\text{Ca}^{2+}$  transient data obtained in the presence of a specific NOS1 inhibitor indicate NOS1.

Studies using cardiac-specific gene KO or over-expression of NOS isoforms have also reported conflicting data pertaining to the relative involvement of NOS isoforms in basal cardiac contraction and  $\text{Ca}^{2+}$  homeostasis. Using a mouse model of cardiac-specific NOS1 over-expression Burkard *et al* (2007) have shown that the basal  $\text{Ca}^{2+}$  transient amplitude, contraction strength and SERCA 2a activity (decay of the electrically-evoked  $\text{Ca}^{2+}$  transient) were all decreased, which supports our data where we suggest that NOS1 activity increases in active period (ZT15) myocytes. One could speculate that as this NOS1 over-expression model mirrors the time-of-day dependent differences we observe in active period (ZT15) myocytes, that conversely a model of NOS1 KO may mirror the conditions found in the resting period (ZT3) myocytes where NOS1 expression is reduced. Using a mouse model of NOS1 KO, Sears *et al* (2003) reported that these myocytes had increased  $\text{Ca}^{2+}$  transient, contraction strength and SR  $\text{Ca}^{2+}$  content however; the decay of the electrically-evoked  $\text{Ca}^{2+}$  transient was prolonged suggesting that SERCA 2a activity is decreased in these myocytes. Therefore, our data is not fully consistent with the data obtained by Sears and colleagues, as although NOS1 KO data is supportive of the involvement of NOS1 in the depressed response to ISO it does not support this action through an increase in SR activity as we observe in resting period (ZT3) myocytes (Sears et al., 2003). The presence, albeit reduced, of NOS mRNA we observe in our resting period (ZT3) myocytes means that these animals are not similar to the NOS1 KO, which may explain the differences between our data.

Also, this conflict may reflect experimental differences as our data was obtained in myocytes where NOS was inhibited rather than genetically manipulated.

There are many potential drawbacks pertaining to NOS genetic studies as with NOS KO experiments there is the potential for plasticity in the system which may mean that different NOS isoforms are compensating for the lost NOS isoform, which could explain the differences between our data and that of Sears and colleagues (Sears et al., 2003). In addition, although our data were similar to NOS1 over-expression data, genetic over-expression experiments may also have potential drawbacks, as NOS1 over-expression could result in changes in the cellular localisation of NOS isoforms. For example, in addition to increasing SR NOS levels, NOS1 over-expression may result in an increase in the concentration of NOS1 in the sarcolemma/ movement of NOS1 to sarcolemma, where NOS1 is thought to target the LTCC and may explain why LTCC current is altered in active period (ZT15) myocytes (see section 5.3.4).

### **5.3.3 Additional mechanisms for the reduced responsiveness of active period myocytes to isoproterenol**

It is possible that the decreased responsiveness of active period (ZT15) myocytes to ISO may occur indirectly of NOS activation. For example, it has been reported that upon activation of the cardiac  $\beta_3$ -adrenergic receptor, the associated  $G_i$  GTP binding protein will inhibit  $\beta_1$ -adrenergic receptor mediated inotropy through the inhibition of AC and subsequent cAMP production (Taussig et al., 1993). However, data in the present chapter would suggest that this is not the case as the NOS inhibitor, L-NNA increased the responsiveness of active period (ZT15) myocytes to ISO to a similar level as resting period (ZT3) myocytes, suggesting that NOS is responsible for the time-of-day dependent variation we observe in EC-coupling. The decreased responsiveness of active period (ZT15) myocytes we observe in response to ISO may also be due to an increase in the concentration of cGMP in addition to an increase in NOS activity. Our

data suggest that there is an increased  $\beta_3$ -adrenergic receptor density and increased concentration of NOS in active period (ZT15) myocytes, however, we cannot rule out changes in cGMP as these were not investigated as part of this study. It would therefore be ideal to examine cGMP levels in resting period (ZT3) and active period (ZT15) myocytes to determine whether cGMP levels cycle and also whether the time-of-day dependent changes we see are due to an increase in cGMP.

The reduced responsiveness of active period (ZT15) myocytes to ISO could be the result of changes in proteins associated with NOS1. For example, CAPON is physically associated with NOS1 (Beigi et al., 2009) and CAPON may play a role in EC-coupling as its interaction with NOS1 is thought to accelerate repolarisation of the cardiac AP through the inhibition of LTCC (Chang et al., 2008). Our data shows that the expression of CAPON is significantly greater during the resting period (ZT3) than the active period (ZT15), reverse of the expression of NOS1. This is paradoxical as one may expect the NOS1 adaptor protein, CAPON, to show similar patterns of expression to NOS1, as CAPON interacts with NOS1 *in vivo* (Chang et al., 2008, Beigi et al., 2009). However, the magnitude of the increase in CAPON (0.79 fold), although significantly different between time-points, is quite modest and does not compare to that of NOS1 (5.04 fold), therefore, CAPON is likely to have a small contribution (if any) to the decreased responsiveness of active period (ZT15) myocytes we observe. If translated to active protein, the increase in CAPON expression during the resting period (ZT3) may suggest abnormal coupling of NOS1 to CAPON, which may result in a pro-arrhythmic phenotype and may also explain the reduced NOS levels in these myocytes. NOS1 and NOS3 are both  $\text{Ca}^{2+}$  dependent enzymes therefore it is possible that an increase in intracellular  $\text{Ca}^{2+}$  levels could be causing activation of NOS rather than activation of  $\beta_3$ -adrenergic receptor. Therefore, the decreased responsiveness of active period (ZT15) myocytes we observe to ISO stimulation may be due to  $\text{Ca}^{2+}$  dependent activation of NOS. Although  $\text{Ca}^{2+}$  dependent activation of NOS remains a possibility this seems unlikely to have occurred in the present investigation as electrophysiological measurements of LTCC current density (basal and in response to ISO) in resting period

(ZT3) and active period (ZT15) myocytes were obtained in the presence of a high concentration of  $\text{Ca}^{2+}$  chelator, BAPTA (10mM), which buffers intracellular  $\text{Ca}^{2+}$  thereby inhibiting  $\text{Ca}^{2+}$  dependent activation of NOS. This would suggest that the time-of-day dependent variation we observe in the responsiveness of LTCC current of ventricular myocytes to ISO and the effect of NOS on this variation is not likely to be  $\text{Ca}^{2+}$  dependent due to the presence of BAPTA, however, our data does not rule out  $\text{Ca}^{2+}$  dependent activation of NOS and therefore this requires further elucidation.

### **5.3.4 The protective role of NOS in preventing arrhythmogenesis**

An increase in sympathetic activity or ISO stimulation have both been shown to increase the incidence of  $\text{Ca}^{2+}$  dependent after-depolarisations and sympathetic-induced ventricular arrhythmias (Meredith et al., 1991, Barbieri et al., 1994, Veldkamp et al., 2001). These ventricular arrhythmias are associated with either an increase in SR  $\text{Ca}^{2+}$  loading (DAD) or an increase in LTCC current (EAD) (see introduction sections 1.5.1 & 1.5.2 for detail). In the previous chapter, we showed that time-of-day dependent variation exists in the arrhythmic threshold in response to  $\beta$ -adrenergic stimulation with the non-selective  $\beta$ -adrenergic agonist ISO, resulting in a greater percentage of resting period (ZT3) myocytes developing arrhythmic activity in response to ISO than active period (ZT15) myocytes and this increase in arrhythmic activity has since been shown to result from increased incidence of DADs (Collins and Rodrigo, 2010). Taken together with our data showing the depressed responsiveness of  $\text{Ca}^{2+}$ -transient from active period (ZT15) myocytes to stimulation with ISO, is probably due to an increase in NOS1 activity, we suggest that the high levels of NOS1 during the active period protect the animals against stress-induced arrhythmias.

Current literature has shown that NOS-signalling is cardioprotective in terms of reducing  $\text{Ca}^{2+}$  overload, the incidence of ventricular arrhythmias, the  $\beta$ -adrenergic response and preventing adverse ventricular remodelling following MI (Ashley et al.,

2002, Dawson et al., 2005, Sun et al., 2006, Burger et al., 2009). Activation of the negatively inotropic cardiac  $\beta_3$ -adrenergic receptor by ISO acts to limit the positive inotropic response of  $\beta_1/\beta_2$ -adrenergic receptor activation, which may act to reduce sympathetic-induced arrhythmias through the activation of NOS signalling cascade. Therefore, the time-of-day dependent reduction in arrhythmic activity in active period (ZT15) myocytes in response to ISO may indicate the physiological role for the increase in NOS activity/ expression we observe in these myocytes. Indeed, our data show that the percentage of active period (ZT15) myocytes developing arrhythmic activity in response to ISO was increased upon NOS inhibition, with the non-specific NOS-inhibitor L-NNA and more recently by the NOS1 specific inhibitor 4-AAPNT (Collins and Rodrigo, 2010), and this was associated with an increase in SR  $\text{Ca}^{2+}$  content. As the reduction in arrhythmic activity in active period (ZT15) myocytes is due to a decreased SR  $\text{Ca}^{2+}$  content and a decreased incidence of DADs, it may suggest that NOS1 or NOS1-induced NO may target the SR to prevent or reduce spontaneous SR  $\text{Ca}^{2+}$  release. This seems plausible as NOS1 has been shown to target the SR  $\text{Ca}^{2+}$  release channel, RyR2, through direct NO-mediated S-nitrosylation. Indeed, Gonzalez *et al* (2007) have shown there is increased diastolic  $[\text{Ca}^{2+}]$ , incidence of spontaneous  $\text{Ca}^{2+}$  waves and arrhythmic activity in NOS1 KO mice as a result of reduced S-nitrosylation of the RyR2, which may suggest that the reduced incidence of arrhythmic activity we observe in active period (ZT15) is the result of the increased incidence of RyR2 S-nitrosylation. In addition, NO produced by NOS has been shown to also directly target the RyR2 receptor to inactivate SR  $\text{Ca}^{2+}$  release (Zahradnikova et al., 1997). NOS1 has also been shown to target PLB through PKG mediated phosphorylation which impacts on SERCA 2a activity and results in reduced SR  $\text{Ca}^{2+}$  loading, prevents  $\text{Ca}^{2+}$  overload and therefore impacts on the generation of DADs (Raeymaekers et al., 1988). The reduction in the incidence of DADs in active period (ZT15) myocytes could also be due to NOS1 targeting NCX1 to prevent the generation of the transient inward current ( $I_{ti}$ ) in response to ISO which gives rise to DADs and extra-systoles. Our data showed a trend that exponential rate of decay of the caffeine-

induced  $\text{Ca}^{2+}$  transient was increased (an indicator of NCX activity), upon application of the NOS inhibitor, L-NNA during simultaneous ISO stimulation, in active period (ZT15) myocytes, suggesting that NOS1 may reduce NCX1 activity in active period (ZT15) myocytes, thereby reducing the magnitude of  $I_{ti}$ . It is possible that NOS or NOS-induced NO are modulating/ disrupting the signalling process responsible for the generation of  $I_{ti}$  or perhaps NOS or NO are modulating the signalling process in such a way that the outcome is only revealed during sympathetic stimulation, as our data suggests that no diurnal differences exist in NCX1 activity under basal conditions (exponential decay of the caffeine-induced  $\text{Ca}^{2+}$  transient data, see chapter 3 for details). If indeed NOS1 modulates NCX1 activity, this marks a further cardioprotective route for NOS1 whereby in addition to decreasing the incidence of sympathetic-induced ventricular arrhythmias it may also be protective in ischaemia/ reperfusion (I/R) injury. However, Bers and colleagues, amongst others, have previously shown that sympathetic stimulation with ISO does not modulate NCX1 activity (Ginsburg and Bers, 2005, Lin et al., 2006) or modulation by NOS1. In support of this, Gonzalez *et al* (2007) have shown that NCX1 activity is not significantly different between NOS1 KO mice and WT mice, therefore suggesting that NOS1 does not modulate NCX1. Therefore, additional work is required to elucidate whether indeed sympathetic stimulation modulates NCX1 and whether NOS-signalling plays a role in this modulation.

The active period of the rat is associated with a surge of sympathetic activity which is beneficial for the foraging animal to respond to environmental changes and an increase in sympathetic activity has been shown to increase the incidence of ventricular arrhythmias and  $\text{Ca}^{2+}$  dependent after-depolarisations. One may expect to observe an increased incidence of arrhythmic activity during the rat's active period when sympathetic activity is high; however, in our active period (ZT15) myocytes we observe a decreased incidence of arrhythmic activity. Therefore, the increased NOS1 activity and expression we observe during the active period (ZT15) may help to prepare active period (ZT15) myocytes for a sympathetic stimulus through changes in NOS1 expression so that they are protected from sympathetic-induced arrhythmias and may

suggest that NOS1 may act to reduce the incidence of DADs and subsequent ventricular arrhythmias during increased sympathetic activity. However, if there is a delay in the increase of NOS1 during the transition from the resting period to active period, this would render an individual more susceptible to the generation of ventricular arrhythmias in the face of an increase in sympathetic activity, which may explain the morning peak in ventricular arrhythmias and associated SCD.

Although our data suggests that the reduction of arrhythmic activity in active period (ZT15) myocytes is due to a reduction in DADs due to NOS1 targeting SR function, it remains possible that NOS1 may also protect the heart from the generation of EADs during sympathetic stimulation by preventing the reactivation of LTCC, as in addition to its location in the SR can also be located in the sarcolemmal membrane where it may target the LTCC (Bendall et al., 2004). Data from this laboratory has shown that the NOS1 specific inhibitor, 4-AAPNT, increases the responsiveness of the LTCC current to ISO in active period (ZT15) myocytes, suggesting that NOS1 may act to reduce LTCC in response to ISO thereby preventing the generation of EADs in active period (ZT15) myocytes (Collins and Rodrigo, 2010).

### **5.3.5 Limitations of our model and study**

In the present chapter we further validated our quantitative real-time RT-PCR technique. One reason for this was that the Taqman PCR probe used to determine the expression of  $\beta_1$ -adrenergic receptor (*Adrb1*) mRNA is capable of detecting both coding mRNA and contaminating gDNA. To overcome this issue, quantitative real-time RT-PCR was performed on LV free-wall with and without an additional post-extraction DNase step to remove any possible contaminating gDNA. Our data showed that diurnal variation was more pronounced in samples treated with an additional post-extraction DNase, which may suggest that gDNA contamination exists in samples without additional DNase treatment that is perhaps masking the extent of diurnal variation existing in the expression of  $\beta_1$ -adrenergic receptor. In addition, this may also reflect

RNA degradation in samples treated with additional post-extraction DNase, as it has been reported that excessive DNase treatment will cause RNA degradation in addition to gDNA removal (Sambrook and Russell, 2001, Fleige and Pfaffl, 2006). To further validate our quantitative real-time RT-PCR technique and to verify that the isolation of single ventricular myocytes did not have any adverse effects on cell biology (see chapters 3 & 4 for other validation experiments), we examined NOS1 expression in isolated cardiomyocytes and LV free-wall. Our data shows that NOS1 is significantly greater in the active period (ZT15) than the resting period (ZT3) in both instances. This data shows that the circadian clock is not affected by our isolation process, as NOS1 expression has a similar diurnal profile between myocytes and tissue. However, this pattern is more pronounced in left-ventricular tissue (5.04 fold v 2.65 fold) and may be the result of small amounts of RNA degradation in isolated cardiomyocytes samples as LV free-wall is snap frozen immediately after extraction from the rat whereas the heart must first be extracted then undergo isolation process prior to downstream applications like quantitative real-time RT-PCR or could also reflect NOS1 activity in the nerve terminals of the heart. The modest diurnal variation in NOS3 gene expression we observe may be due to NOS3 variation in the myocardium being masked by the presence of endothelial cells in the intact tissue (LV-free wall samples).

We had significant technical issues with the  $\beta_3$ -adrenergic receptor (Adrb3) Taqman probe as it didn't not produce an amplifiable standard curve with standard concentrations of cDNA (see methods section 2.5.9) and also when we increased the starting standard curve cDNA concentration to 400ng. Without an amplifiable standard curve it was difficult to determine the method of analysis (i.e.  $\Delta\Delta CT$  or Pfaffl) to use when determining fold-changes in subsequent PCR reactions. Our analysis of  $\beta_3$ -adrenergic receptor (Adrb3) may therefore have been flawed as we had to use the  $\Delta\Delta CT$  method as we could not calculate probe efficiency without an amplifiable standard curve and by using  $\Delta\Delta CT$  we were assuming efficiencies of *housekeeping gene* and gene of interest were equal, which we could not confirm. In addition, in subsequent PCR reactions we used 400ng of cDNA in each well and similar to the standard curve,

in the majority of cases, we failed to amplify  $\beta_3$ -adrenergic receptor (Adrb3) mRNA within the expectable CT range (CT < 35). We ruled out problems with our cDNA as the *house-keeping gene*,  $\beta$ -actin, was amplifiable in normal ranges (CT ~18) and also this cDNA obtained from adult Wistar was used to determine the expression of all genes of interest in the present investigation. The failure of the  $\beta_3$ -adrenergic receptor (Adrb3) probe to amplify mRNA may suggest that this receptor is of low abundance in the heart which has been confirmed by some previous studies (Barbier et al., 2007b). It would, therefore, be ideal to repeat the quantitative real-time RT-PCR experiments for the  $\beta_3$ -adrenergic receptor (Adrb3) to establish accurate expression levels as it is possible that turnover of the  $\beta_3$ -adrenergic receptor may be slower than  $\beta_{1/2}$ -adrenergic receptor due to the inability of  $\beta$ -ARK to bind to the  $\beta_3$ -adrenergic receptor, therefore, mRNA levels we observe may not reflect protein levels.

Due to time constraints, we were unable to determine SERCA 2a activity (exponential decay of the electrically-evoked  $\text{Ca}^{2+}$  transient) in response to NOS inhibition with L-NNA during simultaneous ISO stimulation. There could be a modulating effect of NOS on SERCA 2a as several reports suggest that NOS1 can affect SR function by modulating the SERCA: PLB ratio (Khan et al., 2003, Sears et al., 2003) which may contribute to the decreased responsiveness of active period (ZT15) myocytes. Therefore, future work will involve the determination of exponential decay of the electrically-evoked  $\text{Ca}^{2+}$  transient in response to NOS inhibition during ISO stimulation to see whether NOS modulates SERCA 2a activity in our myocytes.

In the present chapter we observe a time-of-day dependent increase in NOS levels, in particular, NOS1, in active period (ZT15) myocytes. NOS are responsible for the production of NO; therefore, any changes in NOS expression/ activity may affect the production of NO. However, we unable to quantify NO levels in resting period (ZT3) and active period (ZT15) myocytes in the present investigation and requires further work to determine.

In summary, the data from the present chapter suggest that diurnal variation in the responsiveness of  $\text{Ca}^{2+}$  transient to ISO and the development of sympathetic-induced

arrhythmic activity are due to changes in NOS activity and expression and that increased NOS activity in active period (ZT15) myocytes may highlight a means by which the heart reduces arrhythmic activity in the face of increased sympathetic drive. Sympathetic-induced arrhythmias predominately peak in the early hours of the morning and the incidence of these arrhythmias is further increased in the diseased myocardium (McLenachan et al., 1987, Cleland et al., 2002, Guo and Stein, 2003). The development of several cardiomyopathies, for example, pressure-overload induced hypertrophy and HF, have been associated with abnormal circadian clock gene cycling and depressed cardiac metabolic gene cycling (Young et al., 2001a, Young et al., 2001b) in addition to changes in sympathetic drive (Castellano and Bohm, 1997, Post et al., 1999) and  $Ca^{2+}$  homeostasis (Houser et al., 2000, Bers, 2006). It is therefore possible that if NOS activity/ expression are under the control of the circadian clock, abnormal changes in the clock may disrupt the cycling of NOS1 activity and render the heart more prone to sympathetic-induced arrhythmias and contribute to the increased morning incidence of ventricular arrhythmias in patients with these cardiomyopathies. In the next chapter, using SHR as a model of hypertension-induced hypertrophy, will therefore determine the effects of this cardiomyopathy on diurnal variation in the basal  $Ca^{2+}$  transient, its responsiveness to ISO and mRNA levels we have observed between resting period (ZT3) and active period (ZT15) myocytes.

# **Chapter 6: Effects of hypertension on the diurnal variation in excitation-contraction coupling in left ventricular myocytes**

## ***6.1 Introduction***

Diurnal variation in many cardiovascular haemodynamic parameters is depressed in the hypertensive individual (Pickering, 1990, Verdecchia et al., 1998). For example, in normotensive patients, BP has been shown to exhibit diurnal variation, peaking in the hours after waking and dipping in the evening, however, in hypertensive patients, this diurnal variation in BP is absent and these individuals are referred to as “non-dippers” (Pickering, 1990, Takakuwa et al., 2001, Turfaner et al., 2009). One possible reason for the depressed diurnal variation in haemodynamic parameters in hypertension may be explained by depressed cycling of the endogenous clock genes that result in changes to functional genes. For example, Young *et al* (2001a) have shown that the expression of many carbohydrate, lipid and mitochondrial metabolic genes exhibit diurnal variation, however, in a rat model of pressure-overload induced hypertrophy, produced by aortic banding; they showed that diurnal variation in the expression of these metabolic genes was depressed. It is therefore possible that some of the diurnal variation we observe in the present investigation with respect to the  $\text{Ca}^{2+}$  transient, contraction strength, SR  $\text{Ca}^{2+}$  content and mRNA expression (see chapter 3 for data) may be absent in models of hypertension and pressure-overload.

To determine whether hypertension-induced hypertrophy altered diurnal cycling in EC-coupling, we used the spontaneously hypertensive rat (SHR). The SHR is a popular genetic model of essential hypertension, in which systolic BPs of >150mmHg are routinely observed in adult SHR (Okamoto and Aoki, 1963, Boluyt and Bing, 2000).

SHR do not develop hypertension until 10-15 weeks and therefore, adolescent animals are normotensive (Okamoto and Aoki, 1963). The SHR develops ventricular hypertrophy and reduced CO secondary to hypertension at >24 weeks and this may progress to decompensated re-modelling and HF at 18-24 months (Pfeffer and Pfeffer, 1983, Conrad et al., 1991, Boluyt and Bing, 2000). The initial hypertrophy seen in the SHR is concentric and is a compensatory mechanism in which the ventricular walls thicken to compensate for increased workload/pressure-overload (Lorell and Carabello, 2000, Olson and Schneider, 2003). The SHR develops HF upon progression of compensatory concentric hypertrophy to decompensated eccentric hypertrophy (Lorell and Carabello, 2000, Olson and Schneider, 2003).

In the present investigation, we have shown that significant diurnal variation exists in  $Ca^{2+}$  handling namely in the basal  $Ca^{2+}$  transient and its responsiveness to ISO stimulation. During hypertension and the resulting progression to hypertrophy and HF,  $Ca^{2+}$  handling becomes dysfunctional as a result of changes in the expression and activities of the LTCC, RyR2, NCX1, PLB, SERCA 2a (Houser et al., 2000, Bers, 2006) and the  $\beta$ -adrenergic system (Castellano and Bohm, 1997). The development of hypertrophy and HF is associated with reduced expression and activity of SERCA 2a and a compensatory increase in NCX1 expression and activity (Currie and Smith, 1999, Pogwizd et al., 1999, Houser et al., 2000). PLB hypophosphorylation, which also occurs during hypertrophy, contributes to reduced SERCA 2a activity and during hypertrophy there is an increase in activity of RyR2 and a decrease in the activity of LTCC (Currie and Smith, 1999, Houser et al., 2000). In addition, significant remodelling occurs in the  $\beta$ -adrenergic system, in that positive inotropic  $\beta_1$  and  $\beta_2$ -adrenergic receptors are down-regulated (Hadcock and Malbon, 1988, Bristow et al., 1993) and the negatively inotropic  $\beta_3$ -adrenergic receptor is unregulated (Cheng et al., 2001, Moniotte et al., 2001), contributing to depressed contractility seen in hypertrophy.

We therefore set out to determine whether the diurnal variation in the basal  $Ca^{2+}$  transient and its response to  $\beta$ -adrenergic stimulation with ISO in the adult Wistar was disrupted in hypertension-induced hypertrophy using the SHR, a genetic model of

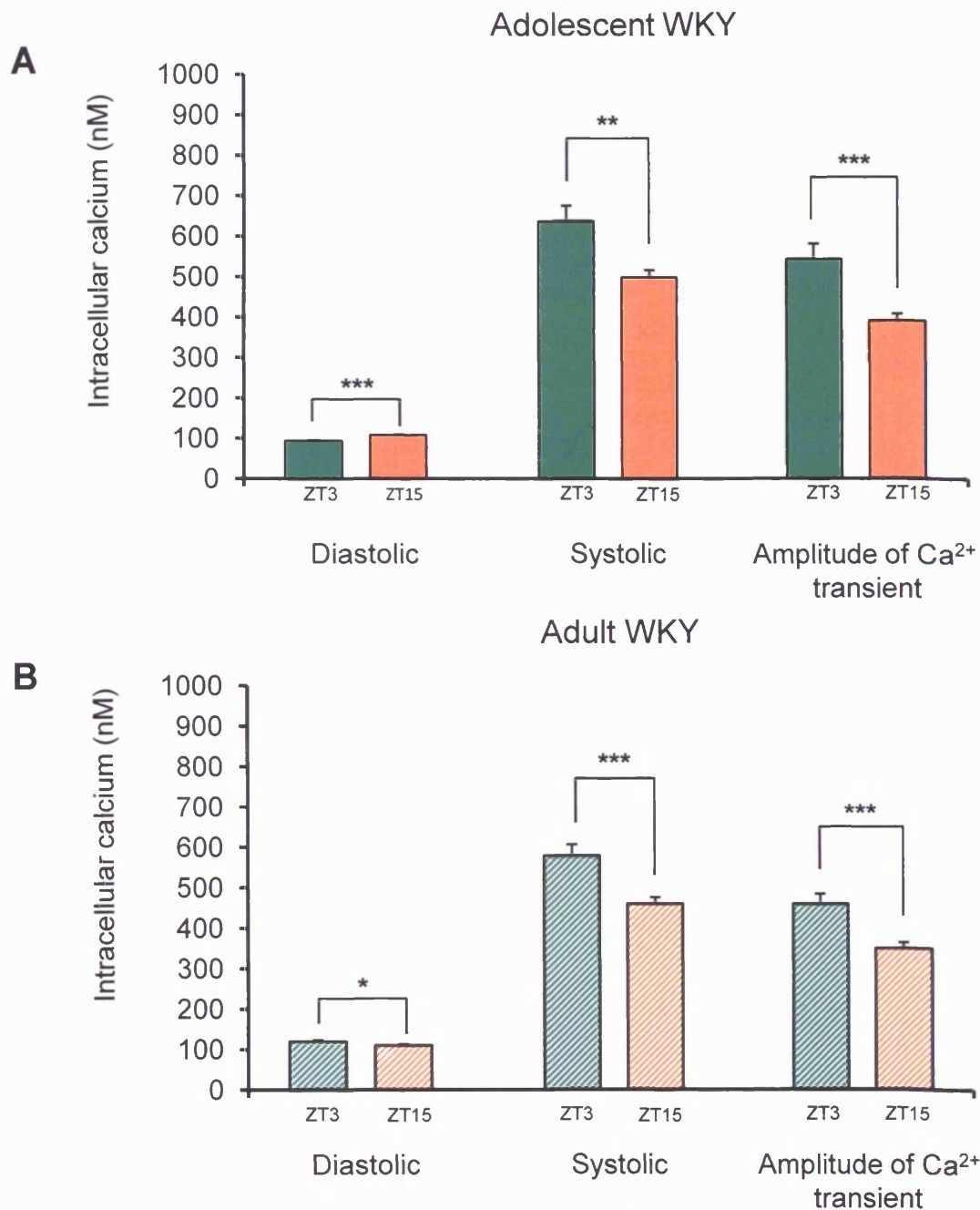
essential hypertension. We looked at the mRNA expression of key circadian clock and mitochondrial metabolic genes in normotensive and hypertensive SHR to ratify our model and to confirm previously published data. We also looked at mRNA expression of key EC-coupling genes and NOS-signalling genes in these SHR, to see whether any disruption to the diurnal variation in the  $\text{Ca}^{2+}$  transient reflects changes in gene expression. We looked at the basal  $\text{Ca}^{2+}$  transient and the response of the  $\text{Ca}^{2+}$  transient to ISO in adolescent and adult WKY myocytes to determine the impact of development on diurnal cycling.

## **6.2 Results**

### **6.2.1 Loss of diurnal variation in the basal $\text{Ca}^{2+}$ transient in adult SHR**

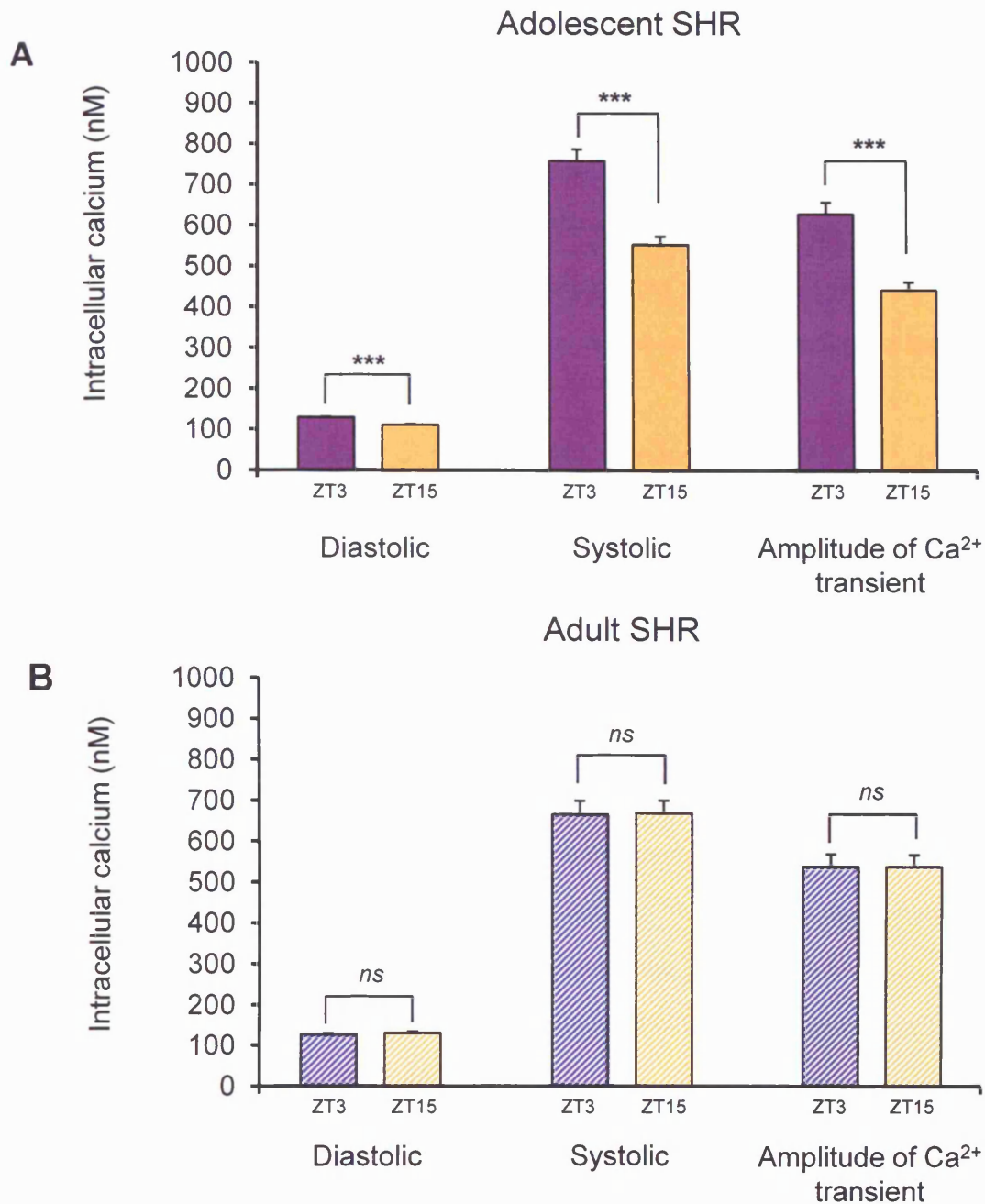
To investigate the effect of hypertension on diurnal variation in the basal  $\text{Ca}^{2+}$  transient, we used age-matched adolescent WKY and SHR at 6 weeks old, which is prior to development of spontaneous hypertension and age-matched adult WKY and SHR at >24 weeks, after which the SHR had developed hypertension-induced hypertrophy, and the WKY rat, was used as a normotensive control. To determine the presence or absence of diurnal variations in the basal  $\text{Ca}^{2+}$  transient, measurements were made from Fura-2 loaded resting period (ZT3) and active period (ZT15) myocytes. Myocytes were superfused with normal Tyrode and stimulated at a rate of 1Hz and measurements of diastolic  $[\text{Ca}^{2+}]$ , systolic  $[\text{Ca}^{2+}]$  and amplitude of  $\text{Ca}^{2+}$  transient were made. As with all Fura-2 measurements in the present study, if the diastolic Fura-2 ratio was >1 (250-300nM) during the superfusion of normal Tyrode, the data was excluded.

Figure 6.1 shows bar charts of the mean data of basal diastolic  $[\text{Ca}^{2+}]$ , systolic  $[\text{Ca}^{2+}]$  and amplitude of the  $\text{Ca}^{2+}$  transient in resting period (ZT3) and active period (ZT15) myocytes isolated from adolescent (A) and adult (B) WKY superfused with normal Tyrode. The profiles of basal systolic  $[\text{Ca}^{2+}]$  and amplitude of the  $\text{Ca}^{2+}$  transient from



**Figure 6.1- The parameters of the Ca<sup>2+</sup> transient of resting period (ZT3) and active period (ZT15) myocytes from adolescent and adult WKY recorded in normal Tyrode.**

- A. Bar chart showing the diastolic [Ca<sup>2+</sup>] (left), systolic [Ca<sup>2+</sup>] (middle) and amplitude of the Ca<sup>2+</sup> transient (right) recorded from resting period (ZT3; green) and active period (ZT15; orange) adolescent WKY myocytes, stimulated at 1Hz and superfused with normal Tyrode. Values are the mean  $\pm$  S.E.M.; number of experiments/ hearts = resting period (ZT3) myocyte,  $n = 18/ 3$  and active period (ZT15) myocyte,  $n = 21/ 3$ ; \*\*  $p < 0.01$ , \*\*\*  $p < 0.001$ , unpaired students  $t$  test.
- B. Bar chart showing the diastolic [Ca<sup>2+</sup>] (left), systolic [Ca<sup>2+</sup>] (middle) and amplitude of the Ca<sup>2+</sup> transient (right) recorded from resting period (ZT3; hatched green) and active period (ZT15; hatched orange) adult WKY myocytes, stimulated at 1Hz and superfused with normal Tyrode. Values are the mean  $\pm$  S.E.M.; number of experiments/ hearts = resting period (ZT3) myocytes,  $n = 20/3$  and active period (ZT15) myocyte,  $n = 22/3$ ; \*  $p < 0.05$ , \*\*\*  $p < 0.001$ , unpaired students  $t$  test.



**Figure 6.2- The parameters of the Ca<sup>2+</sup> transient of resting period (ZT3) and active period (ZT15) myocytes from adolescent and adult SHR recorded in normal Tyrode.**

- A. Bar chart showing the diastolic [Ca<sup>2+</sup>] (left), systolic [Ca<sup>2+</sup>] (middle) and amplitude of the Ca<sup>2+</sup> transient (right) recorded from resting period (ZT3; purple) and active period (ZT15; yellow) adolescent SHR myocytes, stimulated at 1Hz and superfused with normal Tyrode. Values are the mean  $\pm$  S.E.M.; number of experiments/ hearts = resting period (ZT3) myocyte,  $n = 23/ 3$  and active period (ZT15) myocyte,  $n = 19/ 3$ ; \*\*\*  $p < 0.001$ , unpaired students  $t$  test.
- B. Bar chart showing the diastolic [Ca<sup>2+</sup>] (left), systolic [Ca<sup>2+</sup>] (middle) and amplitude of the Ca<sup>2+</sup> transient (right) recorded from resting period (ZT3; hatched purple) and active period (ZT15; hatched yellow) adult SHR myocytes, stimulated at 1Hz and superfused with normal Tyrode. Values are the mean  $\pm$  S.E.M.; number of experiments/ hearts = resting period (ZT3) myocyte,  $n = 21/ 3$  and active period (ZT15) myocyte,  $n = 20/ 3$ ; unpaired students  $t$  test.

adolescent WKY and adult WKY both show significant diurnal variation (see appendix 4 for data) and mirror those seen in adult Wistar (see chapter 3; section 3.2.1). Namely, the systolic  $[Ca^{2+}]$  and amplitude of the  $Ca^{2+}$  transient are significantly greater during the resting period (ZT3) in comparison to the active period (ZT15). The profile of basal diastolic  $[Ca^{2+}]$  from adult WKY shows significant diurnal variation, and mirrors that seen in adult Wistar (see chapter 3 for data) however, this diurnal variation is absent in the adolescent WKY.

Figure 6.2 shows bar charts of the mean data of resting diastolic  $[Ca^{2+}]$ , systolic  $[Ca^{2+}]$  and amplitude of the  $Ca^{2+}$  transient in resting period (ZT3) and active period (ZT15) myocytes isolated from adolescent (A) and adult (B) SHR superfused with normal Tyrode. The profiles of basal systolic  $[Ca^{2+}]$  and amplitude of the  $Ca^{2+}$  transient from normotensive adolescent SHR show significant diurnal variation (see appendix 4 for data), which mirrors the diurnal profiles seen in adolescent and adult WKY, in that the systolic  $[Ca^{2+}]$  and amplitude of the  $Ca^{2+}$  transient are significantly increased during the resting period (ZT3) in comparison to the active period (ZT15). However, the profiles of basal systolic  $[Ca^{2+}]$  and amplitude of the  $Ca^{2+}$  transient in the hypertensive adult SHR do not exhibit significant diurnal variation (see appendix 4 for data). In addition, the profile of basal diastolic  $[Ca^{2+}]$  from adult SHR does not exhibit significant diurnal variation (see appendix 4 for data).

These data show that the diurnal cycling in  $Ca^{2+}$ -handling that we have identified previously (see chapter 3 for data) in the adult Wistar, is also present in adolescent and adult WKY. However, whilst this diurnal variation is still present in the normotensive adolescent SHR, this variation is reduced in hypertensive adult SHR, suggesting that hypertension may modulate the activities of key EC-coupling components in order to blunt diurnal variation in the basal  $Ca^{2+}$  transient.

### **6.2.2 Diurnal variation in the response of the Ca<sup>2+</sup> transient to β-adrenergic stimulation with isoproterenol is lost in the adult SHR**

The previous data show that variation in the basal Ca<sup>2+</sup> transient between resting period (ZT3) and active period (ZT15) myocytes is absent in hypertensive adult SHR. Our previous data (see chapter 4 section 4.2.1) also showed that the response of the Ca<sup>2+</sup> transient to β-adrenergic stimulation with ISO also exhibited a diurnal variation. We therefore sought to determine whether the diurnal variation seen in the responsiveness of the Ca<sup>2+</sup> transient to ISO stimulation was also absent in the hypertensive adult SHR.

To investigate the effect of hypertension on diurnal variation in the responsiveness of the Ca<sup>2+</sup> transient to β-adrenergic stimulation with ISO, we measured [Ca<sup>2+</sup>]<sub>i</sub> in resting period (ZT3) and active period (ZT15) myocytes isolated from hypertensive adult SHR and compared these to normotensive adolescent SHR. As controls, resting period (ZT3) and active period (ZT15) myocytes isolated from normotensive adolescent WKY were compared to normotensive adult WKY (control for age/ development). Fura-2 loaded cells were superfused with normal Tyrode for 5 minutes and then superfused for 5 minutes in succession with normal Tyrode containing ISO in the following concentrations, in nM: 0.1, 0.5, 1, 3, 10, 50, and 100. Myocytes were stimulated at a rate of 1Hz and measurements of diastolic [Ca<sup>2+</sup>], systolic [Ca<sup>2+</sup>] and amplitude of Ca<sup>2+</sup> transient were made.

Figure 6.3 shows the dose-response curves of diastolic [Ca<sup>2+</sup>], systolic [Ca<sup>2+</sup>] and the amplitude of the Ca<sup>2+</sup> transient in response to ISO stimulation recorded in resting period (ZT3; green circles) and active period myocytes (ZT15; orange circles) isolated from adolescent WKY (A) and adult WKY (B) (see appendix 4 for data). The figures show that diastolic [Ca<sup>2+</sup>], systolic [Ca<sup>2+</sup>] and amplitude of Ca<sup>2+</sup> transient all increase in a sigmoidal dose-dependent manner in response to increasing ISO concentrations in both resting period (ZT3) and active period (ZT15) myocytes isolated from adolescent and adult WKY. The data shows that there is no diurnal variation in the responsiveness of

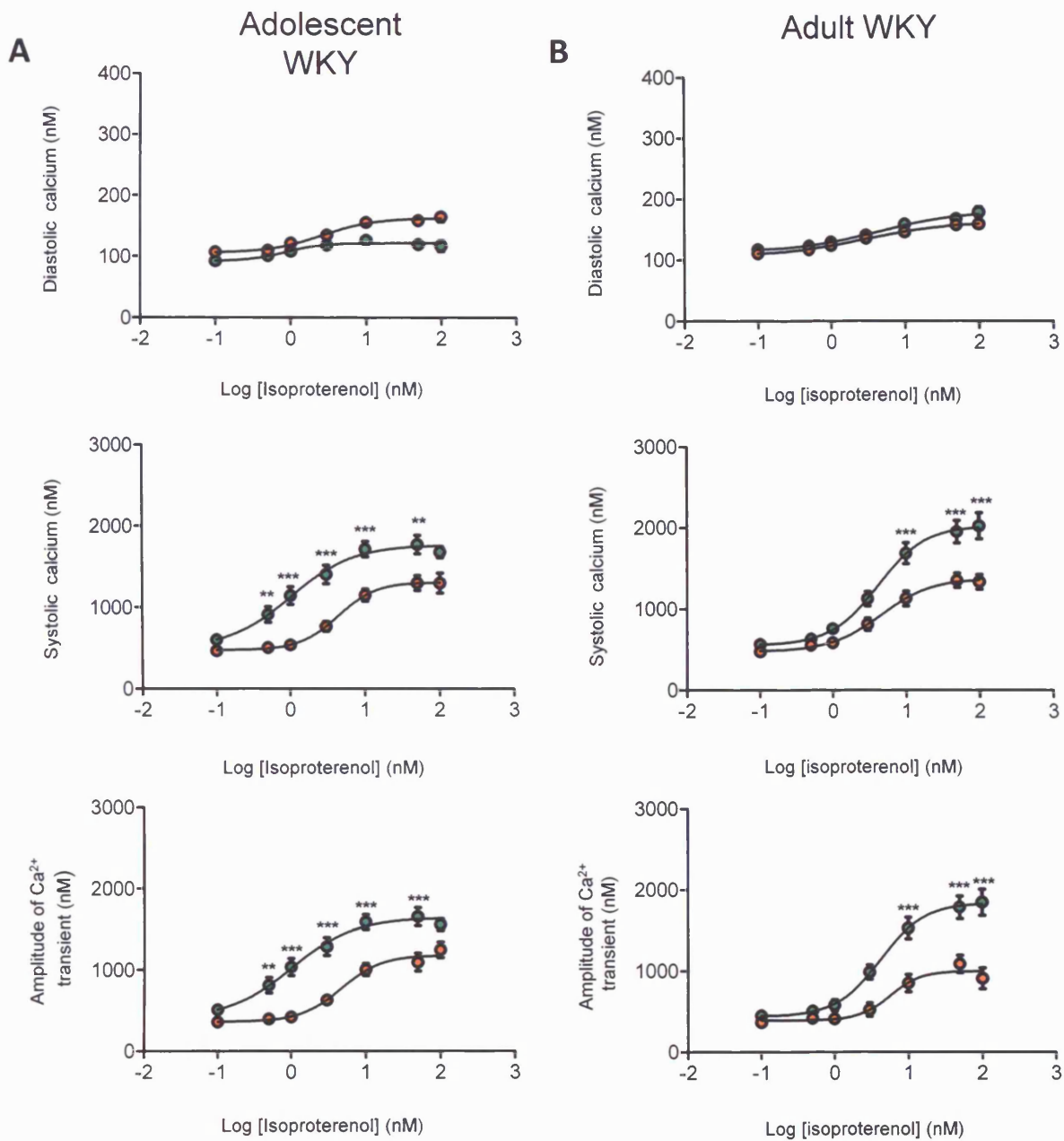


**Figure 6.3- Developmental changes in dose-response curves for diastolic  $[Ca^{2+}]$ , systolic  $[Ca^{2+}]$  and amplitude of  $Ca^{2+}$  transient to  $\beta$ -adrenergic stimulation with isoproterenol (ISO) in adolescent and adult WKY myocytes isolated during the resting period (ZT3) and active period (ZT15).**

- A. Dose-response curve of the effects of ISO on diastolic  $[Ca^{2+}]$  (top), systolic  $[Ca^{2+}]$  (middle) and amplitude of  $Ca^{2+}$  transient (bottom) in adolescent WKY myocytes isolated during the resting period (ZT3; green circles) and the active period (ZT15; orange circles), stimulated at 1Hz. Values are mean  $\pm$  S.E.M.; numbers of experiments/ hearts = resting period (ZT3) myocyte,  $n = 10-23/3$  and active period (ZT15) myocyte,  $n = 14-20/3$ . \*\*  $p < 0.01$ , \*\*\*  $p < 0.001$ , two way ANOVA followed by Bonferroni *post hoc* test.
- B. Dose-response curve of the effects of ISO on diastolic  $[Ca^{2+}]$  (top), systolic  $[Ca^{2+}]$  (middle) and amplitude of  $Ca^{2+}$  transient (bottom) in adult WKY myocytes isolated during the resting period (ZT3; green circles) and the active period (ZT15; orange circles), stimulated at 1Hz. Values are mean  $\pm$  S.E.M.; numbers of experiments/ hearts = Resting period (ZT3) myocyte,  $n = 14-20/3$  and active period (ZT15) myocyte,  $n = 17-20/3$ . \*\*\*  $p < 0.001$ , two way ANOVA followed by Bonferroni *post hoc* test.

diastolic  $[Ca^{2+}]$  to ISO stimulation in both adolescent and adult WKY. However, significant diurnal variation exists in the responsiveness of systolic  $[Ca^{2+}]$  and the amplitude of the  $Ca^{2+}$  transient to ISO stimulation in both adolescent and adult WKY. This profile of diurnal cycling is similar to previous results in chapter 4 section 4.2.1 for Wistar. In adolescent WKY, divergence in the systolic  $[Ca^{2+}]$  and amplitude of  $Ca^{2+}$  transient dose-response relationships between time-points occurs at a lower concentration of ISO at 0.5nM opposed to 10nM in the adult WKY (and adult Wistar), with resting period (ZT3) myocytes having significantly higher systolic  $[Ca^{2+}]$  and amplitude of  $Ca^{2+}$  transient in comparison to active period (ZT15) myocytes. Figure 6.3 also shows that the response of systolic  $[Ca^{2+}]$  and amplitude of  $Ca^{2+}$  transient to the maximal concentration of ISO (100nM) were significantly higher in resting period (ZT3) compared to active period (ZT15) myocytes isolated from adult WKY. However, at very high concentrations of ISO, systolic  $[Ca^{2+}]$  and amplitude of  $Ca^{2+}$  transient were not significantly different between resting period (ZT3) and active period (ZT15) myocytes isolated from adolescent WKY, which may highlight the toxic effects of ISO (see appendix 4 for data).

Figure 6.4 shows the dose-response curves of diastolic  $[Ca^{2+}]$ , systolic  $[Ca^{2+}]$  and the amplitude of the  $Ca^{2+}$  transient in response to ISO stimulation recorded in resting period (ZT3; purple circles) and active period myocytes (ZT15; yellow circles) isolated from adolescent SHR (A) and adult SHR (B). The figures show that diastolic  $[Ca^{2+}]$ , systolic  $[Ca^{2+}]$  and amplitude of  $Ca^{2+}$  transient all increase in a sigmoidal dose-dependent manner in response to increasing ISO concentrations in resting period (ZT3) and active period (ZT15) myocytes isolated from adolescent and adult SHR. In normotensive adolescent SHR there is no diurnal variation in the diastolic  $[Ca^{2+}]$  dose-response relationship, however, the systolic  $[Ca^{2+}]$  and amplitude of  $Ca^{2+}$  transient dose-response relationships significantly diverge at ISO concentrations  $>3nM$  with the effect that significant diurnal variation occurs in systolic  $[Ca^{2+}]$  and amplitude of  $Ca^{2+}$  transient between resting period (ZT3) and active period (ZT15) myocytes isolated from adolescent SHR. This profile of diurnal cycling in the systolic  $[Ca^{2+}]$  and amplitude of

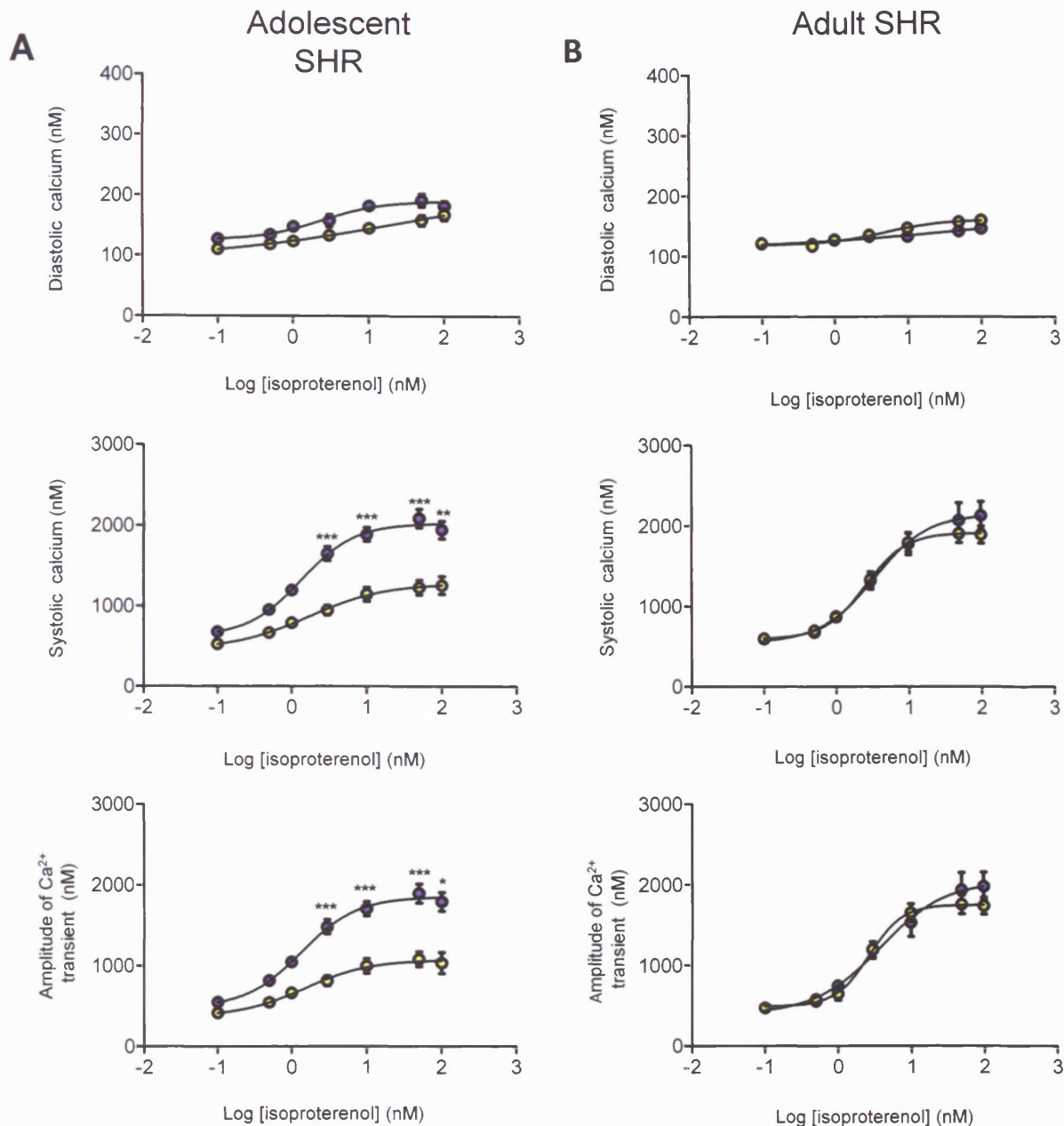


**Figure 6.4- Developmental changes in dose-response curves for diastolic  $[Ca^{2+}]$ , systolic  $[Ca^{2+}]$  and amplitude of  $Ca^{2+}$  transient to  $\beta$ -adrenergic stimulation with isoproterenol (ISO) in adolescent and adult SHR myocytes isolated during the resting period (ZT3) and active period (ZT15).**

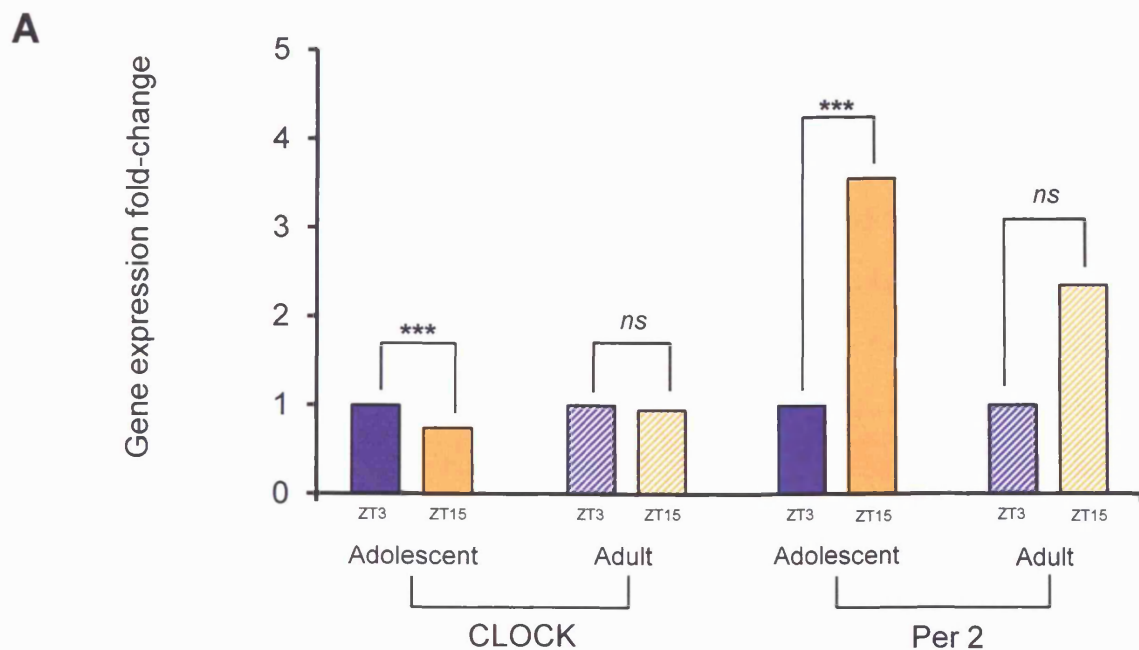
A. Dose-response curve of the effects of ISO on diastolic  $[Ca^{2+}]$  (top), systolic  $[Ca^{2+}]$  (middle) and amplitude of  $Ca^{2+}$  transient (bottom) in adolescent SHR myocytes isolated during the resting period (ZT3; purple circles) and active period (ZT15; yellow circles), stimulated at 1Hz. Values are mean  $\pm$  S.E.M.; numbers of experiments/ hearts = resting period (ZT3) myocyte,  $n = 11-18/3$  and active period (ZT15) myocyte,  $n = 11-21/3$ . \*  $p < 0.05$ , \*\*  $p < 0.01$ , \*\*\*  $p < 0.001$ , two way ANOVA followed by Bonferroni *post hoc* test.

B. Dose-response curve of the effects of ISO on diastolic  $[Ca^{2+}]$  (top), systolic  $[Ca^{2+}]$  (middle) and amplitude of  $Ca^{2+}$  transient (bottom) in adult SHR myocytes isolated during the resting period (ZT3; purple circles) and the active period (ZT15; yellow circles), stimulated at 1Hz. Values are mean  $\pm$  S.E.M.; numbers of experiments/ hearts = resting period (ZT3) myocyte,  $n = 14-21/3$  and active period (ZT15) myocyte,  $n = 19-21/3$ , two way ANOVA followed by Bonferroni *post hoc* test.

$\text{Ca}^{2+}$  transient is similar to previous results for Wistar (chapter 4 section 4.2.1) and also WKY (see figure 6.3). In hypertensive adult SHR there is no diurnal variation in the diastolic  $[\text{Ca}^{2+}]$  dose-response relationship, which is similar to normotensive adolescent SHR. However, the diurnal variation in the systolic  $[\text{Ca}^{2+}]$  and amplitude of  $\text{Ca}^{2+}$  transient dose-response relationships seen in normotensive adolescent SHR are absent in hypertensive adult SHR, suggesting that hypertension may affect this relationship. More specifically, whereas the systolic  $[\text{Ca}^{2+}]$  and amplitude of  $\text{Ca}^{2+}$  transient recorded in the maximal concentration of ISO (100nM) were significantly higher in resting period (ZT3) compared to active period (ZT15) myocytes isolated from normotensive adolescent SHR & WKY (see appendix 4 for data), they were not significantly different between resting period (ZT3) and active period (ZT15) myocytes from the hypertensive adult SHR, which may suggest that hypertension may affect the responsiveness of the  $\text{Ca}^{2+}$  transient to ISO stimulation. The data show that the diurnal variation present in the responsiveness of the  $\text{Ca}^{2+}$  transient (systolic and amplitude) to  $\beta$ -adrenergic stimulation with ISO is present in adolescent and adult WKY and is therefore not a product of adulthood. In addition, this diurnal variation is present in the adolescent SHR but absent in the adult SHR, suggesting a link with the development of hypertension.

### **6.2.3 Diurnal changes in mRNA expression in hypertension**

Young and colleagues have shown that pressure-overload alters the diurnal cycling of circadian clock genes and carbohydrate, fatty acid and mitochondrial metabolic genes (Young et al., 2001a, Young et al., 2001b). The absence of diurnal variation in the basal  $\text{Ca}^{2+}$  transient and the responsiveness of the  $\text{Ca}^{2+}$  transient to  $\beta$ -adrenergic stimulation with ISO we see in the hypertensive adult SHR may therefore, result from the depression of diurnal variation in metabolic gene expression which could impinge on the cycling of EC-coupling genes if they are controlled by the circadian clock.



**B**

| Gene of interest |                | $\Delta$ CT (normalised to $\beta$ -actin) |                      | <i>p</i> -value (from $\Delta$ CT) | Fold change ZT15 (Pfaffl) |
|------------------|----------------|--------------------------------------------|----------------------|------------------------------------|---------------------------|
|                  |                | Resting period (ZT3)                       | Active period (ZT15) |                                    |                           |
| CLOCK            | Adolescent SHR | 5.63 $\pm$ 0.08                            | 6.16 $\pm$ 0.06      | <i>p</i> = 0.0010<br>***           | 0.74<br>#                 |
|                  | Adult SHR      | 5.65 $\pm$ 0.18                            | 5.77 $\pm$ 0.11      | <i>p</i> = 0.6161<br><i>ns</i>     | 0.95<br>#                 |
| Per 2            | Adolescent SHR | 8.95 $\pm$ 0.06                            | 6.85 $\pm$ 0.10      | <i>p</i> < 0.0001<br>***           | 3.56<br>#                 |
|                  | Adult SHR      | 7.84 $\pm$ 0.58                            | 6.43 $\pm$ 0.06      | <i>p</i> = 0.0710<br><i>ns</i>     | 2.35<br>#                 |

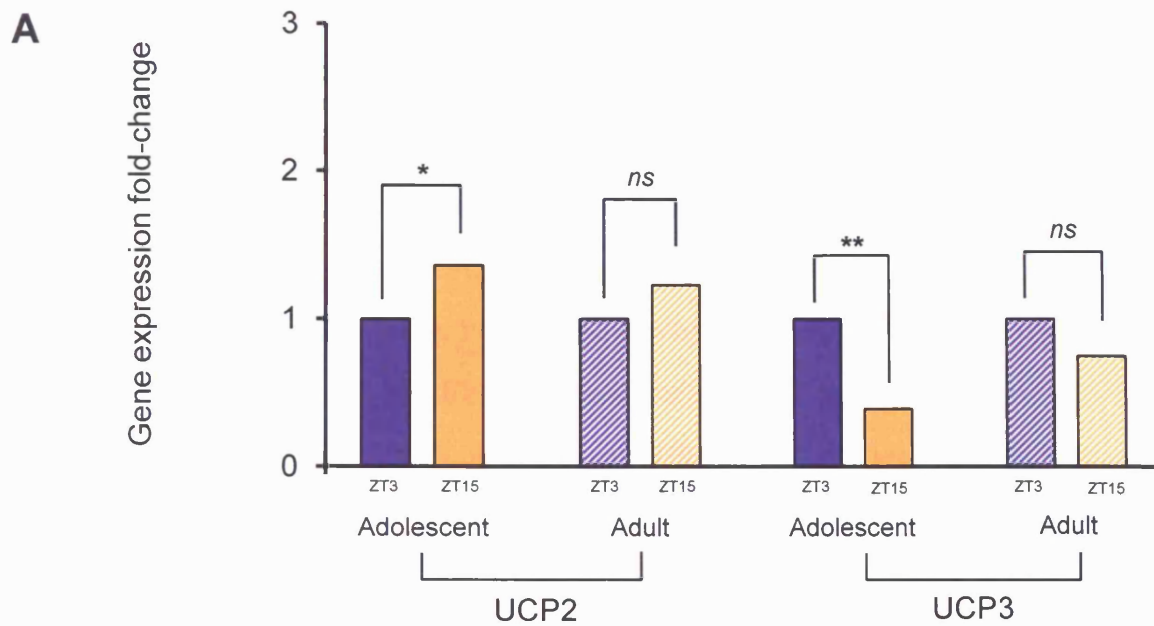
**Figure 6.5- Gene expression levels of the circadian clock genes, CLOCK and Per 2, in adolescent and adult SHR hearts isolated during the resting period (ZT3) and active period (ZT15).**

- A. Bar chart showing the quantitative real-time RT-PCR of CLOCK and Per 2 mRNA expression as fold-changes in left ventricular free-wall isolated during the resting period (ZT3; purple) & active period (ZT15; yellow) of the adolescent SHR and resting period (ZT3; hatched purple) & active period (ZT15; hatched yellow) of the adult SHR. CLOCK and Per 2 mRNA expression was normalised to  $\beta$ -actin mRNA. Fold-changes of CLOCK and Per 2 mRNA were calculated using the Pfaffl method (#, see appendix 4) relative to the control (ZT3; purple bars). The results are mean  $\pm$  S.E.M.; number of samples = resting period (ZT3) adolescent SHR, *n* = 5, resting period (ZT3) adult SHR, *n* = 4, active period (ZT15) adolescent SHR, *n* = 5 & active period (ZT15) adult SHR, *n* = 4. \*\*\* *p* < 0.001 unpaired students *t* test performed on  $\Delta$ CT values.
- B. Table showing the data used to produce the bar chart in figure 6.5 A

To determine whether the absence of diurnal variation in the resting  $\text{Ca}^{2+}$  transient and in response to  $\beta$ -adrenergic stimulation with ISO in adult SHR, are the result of underlying changes in the expression of key EC-coupling and NOS-signalling genes, we performed quantitative real-time Taqman RT-PCR on the left ventricular free-wall isolated from adolescent and adult SHR rat hearts during the resting period (ZT3) and the active period (ZT15) (see section 2.5.9 of methods). In order to verify that the genetic model of hypertension-induced hypertrophy in the SHR had a similar effect on the circadian clock as Young's surgical model of pressure-overload induced hypertrophy, we first looked at the expression of key circadian clock genes and mitochondrial metabolic genes in order to confirm the findings of previously published work (Young et al., 2001a, Young et al., 2001b).

### *Circadian clock genes*

Figure 6.5 is a bar chart showing gene expression as fold-change measurements for the circadian clock genes, CLOCK and Per2, in snap frozen left ventricular tissue isolated during the resting period (ZT3) and active period (ZT15) in adolescent and adult SHR (see figure for data). The gene profiles for CLOCK and Per2 in normotensive adolescent SHR show significant diurnal variation. These diurnal gene expression profiles for CLOCK and Per2 in adolescent SHR mirror those seen in adult Wistar (see chapter 3) and previously published data, as CLOCK expression peaks during the resting period (ZT3) and Per2 expression peaks during the active period (ZT15) (Young et al., 2001a, Naito et al., 2003, Yamamoto et al., 2004). However, unlike normotensive adolescent SHR, the gene expression profiles for CLOCK and Per2 in the hypertensive adult SHR do not exhibit significant diurnal variation. These data also confirm previously published data (Young et al., 2001b) and suggest that hypertension disrupts the diurnal variation in the expression of circadian clock genes.



**B**

| Gene of interest |                | $\Delta$ CT (normalised to $\beta$ -actin) |                      | <i>p</i> -value (from $\Delta$ CT) | Fold change ZT15 ( $\Delta\Delta$ CT/Pfaffl) |
|------------------|----------------|--------------------------------------------|----------------------|------------------------------------|----------------------------------------------|
|                  |                | Resting period (ZT3)                       | Active period (ZT15) |                                    |                                              |
| UCP2             | Adolescent SHR | 1.61 $\pm$ 0.10                            | 1.19 $\pm$ 0.11      | <i>p</i> = 0.0289 *                | 1.36 \$                                      |
|                  | Adult SHR      | 0.87 $\pm$ 0.17                            | 0.62 $\pm$ 0.21      | <i>p</i> = 0.3708 <i>ns</i>        | 1.23 \$                                      |
| UCP3             | Adolescent SHR | 5.67 $\pm$ 0.12                            | 7.25 $\pm$ 0.26      | <i>p</i> = 0.0014 **               | 0.39 #                                       |
|                  | Adult SHR      | 5.95 $\pm$ 0.17                            | 6.45 $\pm$ 0.14      | <i>p</i> = 0.0619 <i>ns</i>        | 0.75 #                                       |

**Figure 6.6- Gene expression levels of the mitochondrial metabolic genes, UCP2 and UCP3, in adolescent and adult SHR hearts isolated during the resting period (ZT3) and active period (ZT15).**

A. Bar chart showing the quantitative real-time RT-PCR of UCP2 and UCP3 mRNA expression as fold-changes in left ventricular free-wall isolated during the resting period (ZT3; purple) & active period (ZT15; yellow) of the adolescent SHR and the resting period (ZT3; hatched purple) & active period (ZT15; hatched yellow) of the adult SHR. UCP2 and UCP3 mRNA expression was normalised to  $\beta$ -actin mRNA. Fold-changes of UCP2 and UCP3 mRNA were calculated using either the  $\Delta\Delta$ CT (\$, UCP2) or the Pfaffl method (#, UCP3, see appendix 4) relative to the control (ZT3; purple bars). The results are mean  $\pm$  S.E.M.; number of samples = resting period (ZT3) adolescent SHR, *n* = 5, resting period (ZT3) adult SHR, *n* = 4, active period (ZT15) adolescent SHR, *n* = 5 & active period (ZT15) adult SHR, *n* = 4. \* *p* < 0.05, \*\* *p* < 0.001 unpaired students *t* test performed on  $\Delta$ CT values.

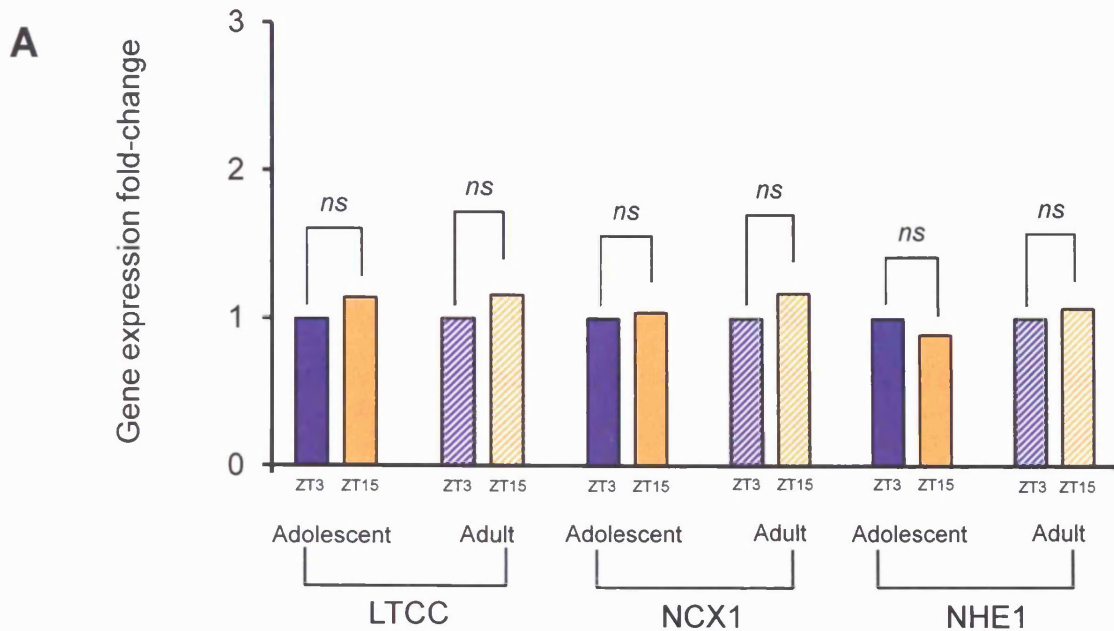
B. Table showing the data used to produce the bar chart in figure 6.6 A

### ***Mitochondrial metabolic genes***

Figure 6.6 is a bar chart showing gene expression as fold-change measurements for the mitochondrial metabolic genes, UCP2 and UCP3, in snap frozen left ventricular tissue isolated during the resting period (ZT3) and active period (ZT15) from adolescent and adult SHR (see figure for data). The gene profiles for UCP2 and UCP3 in normotensive adolescent SHR show significant diurnal variation. These diurnal gene expression profiles for UCP2 and UCP3 in adolescent SHR mirror those seen in adult Wistar (see chapter 3) and previously published data, as UCP2 expression peaks during the active period (ZT15) and UCP3 expression peaks during the resting period (ZT3) (Young et al., 2001a). Although the pattern of diurnal cycling appears to be present in the gene expression profiles for UCP2 and UCP3 in the hypertensive adult SHR, the magnitude of this cycling is greatly depressed so that the expression of UCP2 and UCP3 no longer show significant patterns of diurnal cycling, which confirms previously published data (Young et al., 2001a). These data suggest that hypertension disrupts the diurnal variation in the expression of mitochondrial metabolic genes, possibly reflecting the absence of diurnal cycling in circadian clock genes.

### ***Sarcolemmal excitation-contraction coupling genes***

Our data show that sarcolemmal and SR EC-coupling genes did not show diurnal cycling in the adult Wistar (see chapter 3 for data) and, therefore, did not contribute to the observed diurnal variation in the basal  $Ca^{2+}$  transient and its responsiveness to ISO stimulation. However, as hypertrophy is known to alter the expression of key EC-coupling genes, namely SERCA 2a, NCX1, PLB, RyR2 and LTCC (Houser et al., 2000) we therefore determined whether the absence of diurnal cycling we report in the  $Ca^{2+}$  transient reflects changes in the expression of these key EC-coupling genes



**B**

| Gene of interest |                | $\Delta$ CT (normalised to $\beta$ -actin) |                      | <i>p</i> -value (from $\Delta$ CT) | Fold change ZT15 (Pfaffl) |
|------------------|----------------|--------------------------------------------|----------------------|------------------------------------|---------------------------|
|                  |                | Resting period (ZT3)                       | Active period (ZT15) |                                    |                           |
| LTCC             | Adolescent SHR | 6.13 $\pm$ 0.10                            | 5.94 $\pm$ 0.13      | <i>p</i> = 0.2928<br><i>ns</i>     | 1.14<br>#                 |
|                  | Adult SHR      | 5.46 $\pm$ 0.16                            | 5.32 $\pm$ 0.09      | <i>p</i> = 0.5178<br><i>ns</i>     | 1.16<br>#                 |
| NCX1             | Adolescent SHR | 4.02 $\pm$ 0.14                            | 4.04 $\pm$ 0.14      | <i>p</i> = 0.8987<br><i>ns</i>     | 1.04<br>#                 |
|                  | Adult SHR      | 3.65 $\pm$ 0.13                            | 3.44 $\pm$ 0.03      | <i>p</i> = 0.1936<br><i>ns</i>     | 1.17<br>#                 |
| NHE1             | Adolescent SHR | 6.29 $\pm$ 0.02                            | 6.47 $\pm$ 0.07      | <i>p</i> = 0.0530<br><i>ns</i>     | 0.89<br>#                 |
|                  | Adult SHR      | 6.62 $\pm$ 0.12                            | 6.52 $\pm$ 0.05      | <i>p</i> = 0.4996<br><i>ns</i>     | 1.07<br>#                 |

**Figure 6.7- Gene expression levels of the sarcolemmal proteins, LTCC, NCX1 and NHE1 in adolescent and adult SHR hearts isolated during the resting period (ZT3) and the active period (ZT15).**

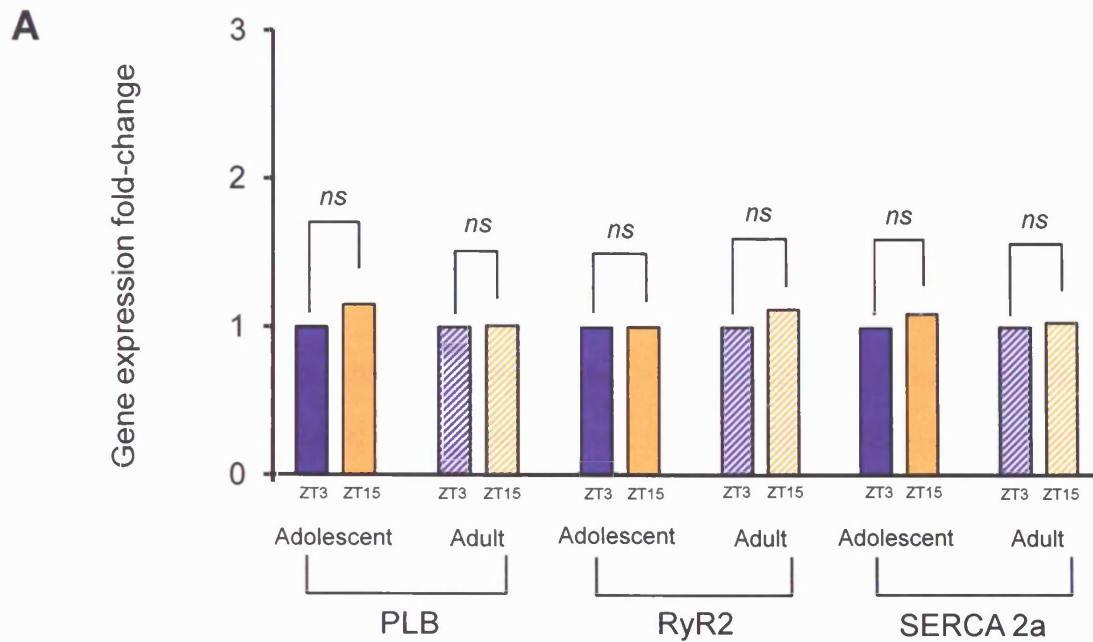
A. Bar chart showing the quantitative real-time RT-PCR of LTCC, NCX1 & NHE1 mRNA expression as fold-changes in left ventricular free-wall isolated during the resting period (ZT3; purple) & active period (ZT15; yellow) of adolescent SHR and the resting period (ZT3; hatched purple) & active period (ZT15; hatched yellow) of the adult SHR. LTCC, NCX1 & NHE1 mRNA expression was normalised to  $\beta$ -actin mRNA. Fold-changes of LTCC, NCX1 & NHE1 mRNA were calculated using the Pfaffl method (#, see appendix 4) relative to the control (ZT3; purple bars). The results are mean  $\pm$  S.E.M.; number of samples = resting period (ZT3) adolescent SHR, *n* = 5, resting period (ZT3) adult SHR, *n* = 4, active period (ZT15) adolescent SHR, *n* = 5 & active period (ZT15) adult SHR, *n* = 4, \* *p* < 0.05, unpaired students *t* test performed on  $\Delta$ CT values.

B. Table showing the data used to produce the bar chart in figure 6.7A

Figure 6.7 is a bar chart showing gene expression as fold-change measurements for the sarcolemmal LTCC ( $\alpha 1c$  subunit), NCX1 and NHE1 in snap frozen left ventricular tissue isolated during the resting period (ZT3) and active period (ZT15) from adolescent and adult SHR (see figure for data). The gene expression profiles for LTCC and NHE1 did not display diurnal variations in adult Wistar (see chapter 3 for data), and this was also found in adolescent and adult SHR ventricular tissue. However, the gene expression profile for NCX1, which did show diurnal variation in adult Wistar (see chapter 3 for data) where NCX1 expression peaked during the active period (ZT15), was not replicated in either adolescent or adult SHR, as NCX1 expression levels were equivalent between ventricular tissue isolated during the resting period (ZT3) and active period (ZT15). These data suggest that hypertension does not alter diurnal cycling in the expression of NCX1, LTCC and NHE1.

#### ***Sarcoplasmic reticulum excitation-contraction coupling genes***

Figure 6.8 is a bar chart showing gene expression as fold-change measurements for the sarcoplasmic reticulum (SR) genes: PLB, RyR2 and SERCA 2a, in snap frozen left ventricular tissue isolated during the resting period (ZT3) and active period (ZT15) from adolescent and adult SHR (see figure for data). The gene expression profiles for PLB, RyR2 and SERCA 2a in normotensive adolescent SHR and in hypertensive adult SHR do not show significant diurnal variation. These gene profiles for PLB, RyR2 and SERCA 2a in adolescent and adult SHR mirror those seen in adult Wistar (see chapter 3 for data). These data suggest that hypertension does not alter diurnal cycling in the expression of the SR EC-coupling genes: PLB, RyR2 and SERCA 2a.



**B**

| Gene of interest |                | $\Delta$ CT (normalised to $\beta$ -actin) |                      | <i>p</i> -value (from $\Delta$ CT) | Fold change ZT15 ( $\Delta\Delta$ CT/ Pfaffl) |
|------------------|----------------|--------------------------------------------|----------------------|------------------------------------|-----------------------------------------------|
|                  |                | Resting period (ZT3)                       | Active period (ZT15) |                                    |                                               |
| PLB              | Adolescent SHR | $-1.52 \pm 0.09$                           | $-1.73 \pm 0.16$     | $p = 0.3374$<br><i>ns</i>          | 1.15<br>#                                     |
|                  | Adult SHR      | $-1.91 \pm 0.13$                           | $-1.91 \pm 0.04$     | $p = 0.9877$<br><i>ns</i>          | 1.01<br>#                                     |
| RyR2             | Adolescent SHR | $1.02 \pm 0.11$                            | $1.04 \pm 0.13$      | $p = 0.9105$<br><i>ns</i>          | 1.00<br>\$                                    |
|                  | Adult SHR      | $0.63 \pm 0.15$                            | $0.48 \pm 0.09$      | $p = 0.4498$<br><i>ns</i>          | 1.12<br>\$                                    |
| SERCA 2a         | Adolescent SHR | $-1.81 \pm 0.10$                           | $-1.96 \pm 0.15$     | $p = 0.4950$<br><i>ns</i>          | 1.09<br>#                                     |
|                  | Adult SHR      | $-2.24 \pm 0.15$                           | $-2.24 \pm 0.12$     | $p = 0.9900$<br><i>ns</i>          | 1.03<br>#                                     |

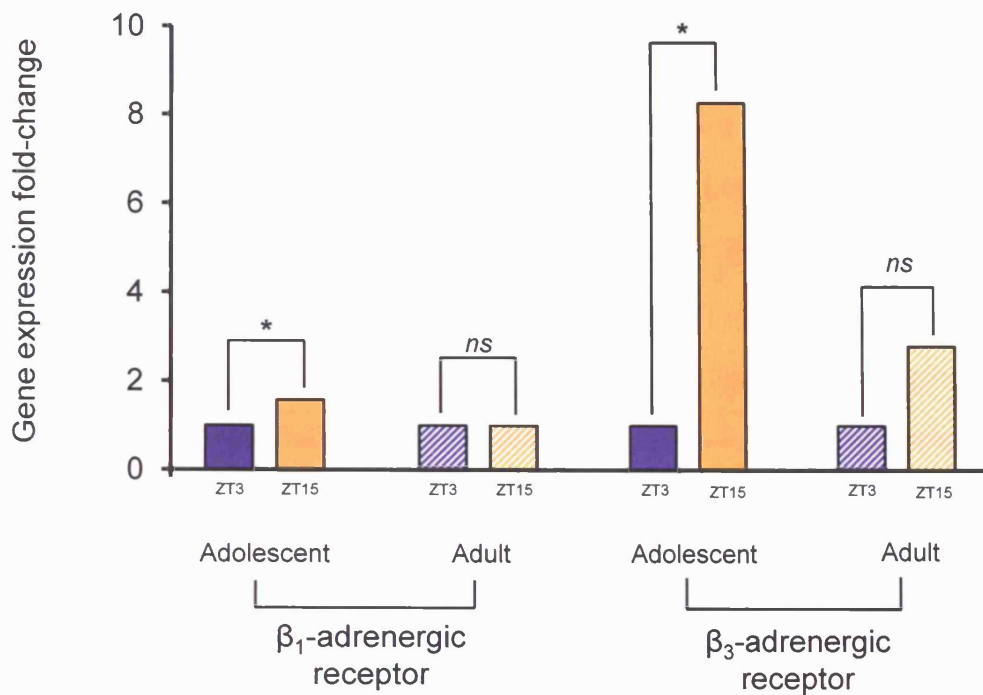
**Figure 6.8- Gene expression levels of the SR proteins, PLB, RyR2 and SERCA 2a in adolescent and adult SHR hearts isolated during the resting period (ZT3) and active period (ZT15).**

- A. Bar chart showing the quantitative real-time RT-PCR of PLB, RyR2 & SERCA 2a mRNA expression as fold-changes in left ventricular free-wall isolated during the resting period (ZT3; purple) & active period (ZT15; yellow) of adolescent SHR and the resting period (ZT3; hatched purple) & active period (ZT15; hatched yellow) of the adult SHR. PLB, RyR2 & SERCA 2a mRNA expression was normalised to  $\beta$ -actin mRNA. Fold-changes of PLB, RyR2 & SERCA 2a mRNA were calculated using either the  $\Delta\Delta$ CT (\$, RyR2) or Pfaffl method (#, PLB & SERCA 2a, see appendix 4) relative to the control (ZT3; purple bars). The results are mean  $\pm$  S.E.M.; number of samples = resting period (ZT3) adolescent SHR,  $n = 5$ , resting period (ZT3) adult SHR,  $n = 4$ , active period (ZT15) adolescent SHR,  $n = 5$  & active period (ZT15) adult SHR,  $n = 4$ , unpaired students *t* test performed on  $\Delta$ CT values.
- B. Table showing the data used to produce the bar chart in figure 6.8 A

### *$\beta$ -adrenergic receptors*

During hypertension and the subsequent development of hypertrophy, significant remodelling occurs in the  $\beta$ -adrenergic receptor system. In particular during hypertrophy, there is substantial down-regulation of  $\beta_1$  and  $\beta_2$ -adrenergic receptors, which limits the quantity of active receptors able to respond to  $\beta$ -adrenergic stimulation, (Hadcock and Malbon, 1988, Bristow et al., 1993) however, the  $\beta_3$ -adrenergic receptor is not down-regulated (Skeberdis, 2004) and is thought to be upregulated in hypertrophy and HF (Cheng et al., 2001, Moniotte et al., 2001). In the present investigation, we identified significant diurnal variation in the responsiveness of the  $\text{Ca}^{2+}$  transient to ISO stimulation (see chapter 4 for data) and in the expression of  $\beta_1$  and  $\beta_3$ -adrenergic receptors (see chapter 5 for data). Therefore, we postulated that the depressed basal  $\text{Ca}^{2+}$  transient and its responsiveness to ISO in adult SHR may be the result of changes or remodelling of the  $\beta$ -adrenergic receptor system in response to hypertension.

Figure 6.9 is a bar chart showing gene expression as fold-change measurements for the  $\beta_1$ -adrenergic receptor (*Adrb1*) and the  $\beta_3$ -adrenergic receptor (*Adrb3*) in snap-frozen LV tissue isolated during the resting period (ZT3) and active period (ZT15) from adolescent and adult SHR (see figure for data). The gene profiles for both the  $\beta_1$ -adrenergic receptor (*Adrb1*) and the  $\beta_3$ -adrenergic receptor (*Adrb3*) in normotensive adolescent SHR show significant diurnal variation. This pattern of diurnal cycling in  $\beta_1$ -adrenergic receptor (*Adrb1*) in adolescent SHR was similar to that seen in adult Wistar (see chapter 3 for data), as in both instances,  $\beta_1$ -adrenergic receptor (*Adrb1*) expression significantly peaks during the active period (ZT15). In addition, the diurnal gene expression profile for  $\beta_3$ -adrenergic receptor (*Adrb3*) in adolescent SHR does not mirror data obtained in adult Wistar (see chapter 3 for data), as in adolescent SHR,  $\beta_3$ -adrenergic receptor (*Adrb3*) expression significantly peaks during the active period (ZT15), whereas, in adult Wistar, this difference was not significant. In hypertensive adult SHR, the gene expression profile for the  $\beta_1$ -adrenergic receptor (*Adrb1*) did not



| Gene of interest                           |                | ΔCT (normalised to β-actin) |                      | p-value (from ΔCT) | Fold change ZT15 (Pfaffl) |
|--------------------------------------------|----------------|-----------------------------|----------------------|--------------------|---------------------------|
|                                            |                | Resting period (ZT3)        | Active period (ZT15) |                    |                           |
| β <sub>1</sub> adrenergic receptor (Adrb1) | Adolescent SHR | 5.41 ± 0.02                 | 4.79 ± 0.16          | p = 0.0119 *       | 1.57 \$                   |
|                                            | Adult SHR      | 4.90 ± 0.14                 | 4.90 ± 0.06          | p = 1.0000 ns      | 1.00 \$                   |
| β <sub>3</sub> adrenergic receptor (Adrb3) | Adolescent SHR | 20.84 ± 0.30                | 17.80 ± 1.07         | p = 0.0492 *       | 8.27 \$                   |
|                                            | Adult SHR      | 21.54 ± 0.40                | 20.06 ± 0.54         | p = 0.0565 ns      | 2.79 \$                   |

**Figure 6.9- Gene expression levels of the β<sub>1</sub>-adrenergic receptor (Adrb1) and β<sub>3</sub>-adrenergic receptor (Adrb3) in adolescent and adult SHR hearts isolated during the resting period (ZT3) and active period (ZT15).**

A. Bar chart showing the quantitative real-time RT-PCR of Adrb1 and Adrb3 mRNA expression as fold-changes in left ventricular free-wall isolated during the resting period (ZT3; purple) & active period (ZT15; yellow) of adolescent SHR and the resting period (ZT3; hatched purple) & active period (ZT15; hatched yellow) of the adult SHR. Adrb1 and Adrb3 mRNA expression were normalised to β-actin mRNA. Fold-changes of Adrb1 and Adrb3 mRNA were calculated using the  $\Delta\Delta$ CT method (\$, see appendix 4) relative to the control (ZT3; purple bars). The results are mean ± S.E.M.; number of samples = resting period (ZT3) adolescent SHR,  $n = 5-6$ , resting period (ZT3) adult SHR,  $n = 4$ , active period (ZT15) adolescent SHR,  $n = 5-10$  & active period (ZT15) adult SHR,  $n = 4-5$ . \*  $p < 0.05$ , unpaired students  $t$  test performed on  $\Delta$ CT values.

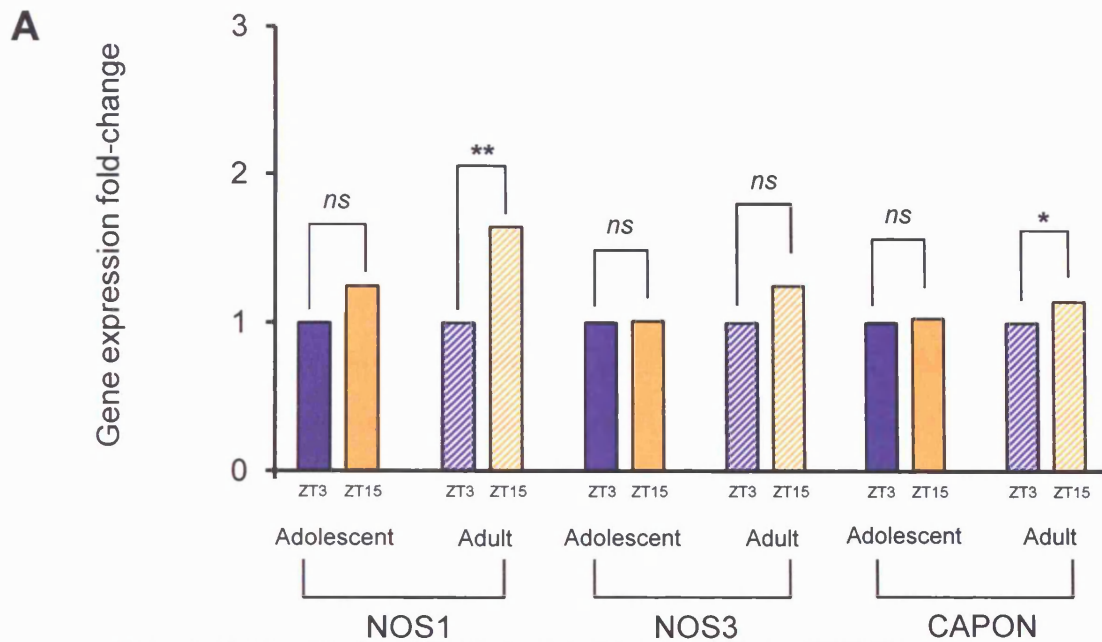
B. Table showing the data used to produce the bar chart in figure 6.9A

exhibit diurnal variation, as diurnal cycling of *Adrb1* expression was absent between time-points. In addition, diurnal cycling in the expression of the  $\beta_3$ -adrenergic receptor (*Adrb3*) was greatly reduced rather than completely absent in the hypertensive adult SHR as expression was no longer significant between time-points. However, some diurnal cycling may still exist in  $\beta_3$ -adrenergic receptor (*Adrb3*) expression as  $\beta_3$ -adrenergic receptor (*Adrb3*) expression was very close to reaching statistical significance between time-points ( $p = 0.056$ ). These data suggest that hypertension also disrupts the diurnal variation in the expression of the  $\beta_1$  and  $\beta_3$ -adrenergic receptor.

### ***Nitric oxide synthase signalling genes***

In hypertension and hypertrophy, the activities and expression of NOS are altered substantially. In particular, NOS1 has been shown to be upregulated and NOS3 has been shown to be downregulated in hypertrophy and HF (Piech et al., 2003, Damy et al., 2004, Loyer et al., 2007, Umar and van der Laarse, 2010). In the present investigation, we strongly believe that NOS1 is responsible for the diurnal variation we see in the basal  $Ca^{2+}$  transient and its responsiveness to ISO stimulation. Therefore, the absence of diurnal variation in the  $Ca^{2+}$  transient in adult SHR would logically suggest the loss of the increase in NOS1 signalling during the animals active period (ZT15). We therefore looked at the expression of the NOS-signalling genes; NOS1, NOS3 and the NOS1 associated anchoring protein, CAPON, in normotensive adolescent and hypertensive adult SHR to determine the effect of hypertension on diurnal cycling.

Figure 6.10 is a bar chart showing gene expression as fold-change measurements for NOS1, NOS3 and CAPON in snap-frozen LV tissue isolated during the resting period (ZT3) and active period (ZT15) from adolescent and adult SHR (see figure for data). The gene profiles for NOS1, NOS3 and CAPON in normotensive adolescent SHR do not show significant diurnal variation. The gene profile for NOS3 in the hypertensive adult SHR mirrors that of normotensive adolescent SHR, as no significant diurnal



**B**

| Gene of interest |                | $\Delta$ CT (normalised to $\beta$ -actin) |                      | <i>p</i> -value (from $\Delta$ CT) | Fold change ZT15 ( $\Delta\Delta$ CT/Pfaffl) |
|------------------|----------------|--------------------------------------------|----------------------|------------------------------------|----------------------------------------------|
|                  |                | Resting period (ZT3)                       | Active period (ZT15) |                                    |                                              |
| NOS1             | Adolescent SHR | 12.43 $\pm$ 0.34                           | 12.06 $\pm$ 0.26     | <i>p</i> = 0.4101<br><i>ns</i>     | 1.25<br>#                                    |
|                  | Adult SHR      | 9.21 $\pm$ 0.05                            | 8.41 $\pm$ 0.18      | <i>p</i> = 0.0058<br>**            | 1.65<br>#                                    |
| NOS3             | Adolescent SHR | 6.33 $\pm$ 0.07                            | 6.36 $\pm$ 0.06      | <i>p</i> = 0.7033<br><i>ns</i>     | 1.01<br>#                                    |
|                  | Adult SHR      | 6.20 $\pm$ 0.12                            | 5.87 $\pm$ 0.10      | <i>p</i> = 0.0949<br><i>ns</i>     | 1.25<br>#                                    |
| CAPON            | Adolescent SHR | 6.92 $\pm$ 0.06                            | 6.91 $\pm$ 0.14      | <i>p</i> = 0.9281<br><i>ns</i>     | 1.03<br>\$                                   |
|                  | Adult SHR      | 6.65 $\pm$ 0.07                            | 6.46 $\pm$ 0.05      | <i>p</i> = 0.0423<br>*             | 1.14<br>\$                                   |

**Figure 6.10- Gene expression levels of neuronal nitric oxide synthase (NOS1), endothelial nitric oxide synthase (NOS3), neuronal nitric oxide synthase adaptor protein 1 (CAPON) in adolescent and adult SHR hearts isolated during the resting period (ZT3) and active period (ZT15).**

A. Bar chart showing the quantitative real-time RT-PCR of NOS1, NOS3 & CAPON mRNA expression as fold-changes in left ventricular free-wall isolated during the resting period (ZT3; purple) & active period (ZT15; yellow) of adolescent SHR and the resting period (ZT3; hatched purple) & active period (ZT15; hatched yellow) of the adult SHR. NOS1, NOS3 & CAPON mRNA expression were normalised to  $\beta$ -actin mRNA. Fold-changes of NOS1, NOS3 & CAPON mRNA were calculated using either the  $\Delta\Delta$ CT (\$, CAPON) or Pfaffl method (#, NOS1 & NOS3, see appendix 4) relative to the control (ZT3; purple bars). The results are mean  $\pm$  S.E.M.; number of samples = resting period (ZT3) adolescent SHR, *n* = 5, resting period (ZT3) adult SHR, *n* = 4, active period (ZT15) adolescent SHR, *n* = 5 & active period (ZT15) adult SHR, *n* = 4. \* *p* < 0.05, \*\* *p* < 0.01, unpaired students *t* test performed on  $\Delta$ CT values.

B. Table showing the data used to produce the bar chart in figure 6.10 A

variation is present. However, unlike normotensive adolescent SHR, the gene expression profiles for NOS1 and CAPON exhibit significant diurnal variation in the hypertensive adult SHR, as NOS1 and CAPON expression both significantly peak during the active period (ZT15), which may suggest that the cellular mechanism for the diurnal variation in adults is different to that in adolescents.

These diurnal gene expression profiles for NOS1, NOS3 and CAPON in adolescent SHR do not mirror those seen in adult Wistar (see chapter 5 for data), as in adult Wistar, NOS1 (fold change of 5.04;  $p < 0.05$ ) and NOS3 expression both significantly peak during the active period (ZT15) and CAPON expression significantly peaks during the resting period (ZT3). However, the diurnal gene expression profile for NOS1 in hypertensive adult SHR is statistically similar to the profile seen in adult Wistar, with NOS1 expression significantly higher during the active period (ZT15) in both instances, although the magnitude of the increase was less pronounced in adult SHR. The diurnal gene expression profile for CAPON was reversed in the hypertensive adult SHR in comparison to adult Wistar (see chapter 5 for data), as in adult SHR, CAPON expression was significantly higher during the active period (ZT15) compared to the peak during the resting period (ZT3) in adult Wistar rats.

These data suggest that hypertension affects the expression of the key circadian clock genes, CLOCK and Per2 and the mitochondrial metabolic genes, UCP2 and UCP3, with the cycling of circadian clock and metabolic genes seen in normotensive adolescent SHR absent in the hypertensive adult SHR. This data confirms that the genetic model of hypertension we have in the SHR produced a similar outcome to Young's surgical model of pressure-overload induced hypertrophy. These data show diurnal cycling in the expression of the  $\beta_1$  &  $\beta_3$ -adrenergic receptors which is present in adult Wistars (See chapter 3) is also present in adolescent and adult WKY but absent in the adult SHR when hypertension develops. Our data also show that hypertension in the adult SHR depresses diurnal cycling of the NOS-signalling genes, NOS1 and CAPON, which may also explain the loss of diurnal variation in the basal  $\text{Ca}^{2+}$  transient and its response to  $\beta$ -adrenergic stimulation with ISO in hypertensive adult SHR.

| WKY                                       |                                       |                                  |                                |
|-------------------------------------------|---------------------------------------|----------------------------------|--------------------------------|
| Resting calcium<br>(normal Tyrode)        | Resting period<br>(ZT3)<br>Adolescent | Resting period<br>(ZT3)<br>Adult | <i>p</i> -value                |
| Diastolic<br>calcium (nM)                 | 94.2 ± 1.7                            | 119.9 ± 3.0                      | <i>p</i> < 0.0001<br>***       |
| Systolic<br>calcium (nM)                  | 636.4 ± 39.9                          | 578.9 ± 27.7                     | <i>p</i> = 0.2374<br><i>ns</i> |
| Amplitude of<br>Calcium<br>transient (nM) | 542.1 ± 38.8                          | 459.0 ± 25.3                     | <i>p</i> = 0.0753<br><i>ns</i> |

**Figure 6.11- Developmental changes in resting Ca<sup>2+</sup> regulation following normal Tyrode superfusion between adolescent and adult WKY myocytes isolated during the resting period (ZT3).**

Table showing diastolic [Ca<sup>2+</sup>], systolic [Ca<sup>2+</sup>] and amplitude of Ca<sup>2+</sup> transient recorded in left ventricular myocytes isolated during the resting period (ZT3) in adolescent and adult WKY rats, superfused with normal Tyrode for 5 minutes and electrically stimulated at 1Hz. Values are the mean ± S.E.M.; number of experiments/ hearts = resting period (ZT3) adolescent WKY, *n* = 18/3, and resting period (ZT3) adult WKY, *n* = 20/3, \*\*\* *p* < 0.0001, unpaired students *t* test.

#### **6.2.4 Developmental differences in the basal $\text{Ca}^{2+}$ transient and the responsiveness of the $\text{Ca}^{2+}$ transient to $\beta$ -adrenergic stimulation with isoproterenol between adolescent and adult WKY.**

In the present chapter, we have shown that diurnal variation in the basal  $\text{Ca}^{2+}$  transient and its responsiveness to  $\beta$ -adrenergic stimulation with ISO is absent in the hypertensive adult SHR. As we used the development of hypertension in the adult SHR as a secondary control for the development of hypertension (primary control was age-matched WKY), we sought to determine whether our data was influenced by the age of the animal. Therefore, we checked whether this disruption to diurnal cycling was the result of the development of hypertension and not the progression from adolescence to adulthood by comparing the parameters of the  $\text{Ca}^{2+}$ -transient between adolescent and adult WKY animals, at one time point (ZT3).

##### ***Developmental differences in the basal $\text{Ca}^{2+}$ transient***

To investigate the developmental differences in the basal  $\text{Ca}^{2+}$  transient, the data obtained previously (see section 6.2.1 for protocol and appendix 4 for data) were re-examined in order to make comparisons between adolescent and adult WKY during the resting period (ZT3). Figure 6.11 is a table showing developmental differences in diastolic  $[\text{Ca}^{2+}]$ , systolic  $[\text{Ca}^{2+}]$  and amplitude of  $\text{Ca}^{2+}$  transient between resting period (ZT3) myocytes isolated from adolescent and adult WKY recorded in normal Tyrode. The data show that variation in the basal  $\text{Ca}^{2+}$  transient was not the result of a developmental change, as systolic  $[\text{Ca}^{2+}]$  and amplitude of  $\text{Ca}^{2+}$  transient were not significantly between adolescent and adult WKY myocytes (see appendix 4 for data).

| WKY                                 |                                 |                            |                                |
|-------------------------------------|---------------------------------|----------------------------|--------------------------------|
| 10nM ISO                            | Resting period (ZT3) Adolescent | Resting period (ZT3) Adult | <i>p</i> -value                |
| Diastolic calcium (nM)              | 126.7 ± 5.7                     | 159.0 ± 5.6                | <i>p</i> < 0.0003<br>***       |
| Systolic calcium (nM)               | 1714.5 ± 94.1                   | 1686.3 ± 130.7             | <i>p</i> = 0.8649<br><i>ns</i> |
| Amplitude of Calcium transient (nM) | 1587.7 ± 91.4                   | 1527.3 ± 131.1             | <i>p</i> = 0.7138<br><i>ns</i> |

**Figure 6.12- Developmental changes in Ca<sup>2+</sup> regulation in response to β-adrenergic stimulation with isoproterenol (ISO) between adolescent and adult WKY myocytes isolated during the resting period (ZT3).**

Table showing diastolic [Ca<sup>2+</sup>], systolic [Ca<sup>2+</sup>] and amplitude of Ca<sup>2+</sup> transient recorded in left ventricular myocytes isolated during the resting period (ZT3) in adolescent and adult WKY rats, superfused with normal Tyrode containing 10nM ISO for 5 minutes and electrically stimulated at 1Hz. Values are the mean ± S.E.M.; number of experiments/ hearts = resting period (ZT3) adolescent WKY, *n* = 17/3, resting period (ZT3) adult WKY, *n* = 19/3, \*\*\* *p* < 0.001, unpaired students *t* test.

### *Developmental differences in the response of Ca<sup>2+</sup> transient to ISO-stimulation*

To investigate the developmental differences in the responsiveness of the Ca<sup>2+</sup> transient to  $\beta$ -adrenergic stimulation with 10nM ISO, the data obtained previously (see section 6.2.2 for protocol and appendix 4 for data) were re-examined in order to make comparisons between adolescent and adult WKY during the resting period (ZT3). Figure 6.12 is a table showing developmental differences in diastolic [Ca<sup>2+</sup>], systolic [Ca<sup>2+</sup>] and amplitude of Ca<sup>2+</sup> transient between resting period (ZT3) myocytes isolated from adolescent and adult WKY recorded in normal Tyrode containing 10nM ISO. The data show that variation in the response of the Ca<sup>2+</sup> transient to ISO was not the result of a developmental change as systolic [Ca<sup>2+</sup>] and amplitude of Ca<sup>2+</sup> transient were not significantly between adolescent and adult WKY myocytes following ISO superfusion (see figure for data).

The data show that the variation in the Ca<sup>2+</sup> transient under resting conditions and in response to  $\beta$ -adrenergic stimulation with ISO in adolescent and adult WKY are not due developmental changes in Ca<sup>2+</sup> regulation.

### **6.3 Discussion**

Diurnal variation in many cardiovascular haemodynamic parameters such as HR, has been shown to be absent or depressed in cases of hypertension (Pickering, 1990, Verdecchia et al., 1998) and associated hypertrophy and is suggested to result from changes in the expression of key metabolic genes. Indeed, the rhythmicity of the circadian clock is altered in the development of many cardiomyopathies and cardiovascular disease (Martino et al., 2007, Shaw and Tofler, 2009). Young and colleagues have shown that in surgical models of pressure-overload induced hypertrophy and MI in the rat there is depressed diurnal cycling of key circadian clock and metabolic genes (Young et al., 2001a, Young et al., 2001b, Kung et al., 2007). We

therefore sought to determine whether the diurnal variation we observed in the basal  $\text{Ca}^{2+}$  transient and its responsiveness to ISO were also depressed in the SHR, a genetic model of hypertension-induced hypertrophy. In the present chapter, we have shown that time-of-day dependent variation in the basal  $\text{Ca}^{2+}$  transient (systolic  $[\text{Ca}^{2+}]$  and amplitude of  $[\text{Ca}^{2+}]$  transient) is absent with the development of hypertension in the adult SHR. This absence of diurnal cycling in the basal  $\text{Ca}^{2+}$  transient was mirrored by absence of variation in the responsiveness of the  $\text{Ca}^{2+}$  transient to ISO in myocytes isolated from the hypertensive adult SHR. The absence of this diurnal cycling was not due to a developmental change from adolescent to adult as the variation was seen in both adolescent and adult normotensive WKY control animals. As predicted from the work of Young *et al* (2001), we found that diurnal cycling in expression of mRNA encoding the circadian clock genes; CLOCK & Per2 and the mitochondrial metabolic genes; UCP2 & UCP3 was depressed in the hypertensive adult SHR (Young et al., 2001a, Young et al., 2001b). However, contrary to our expectation, based on the time-of-day dependent variation in NOS1 expression in adult Wistar rats and its apparent link to the diurnal pattern of responsiveness to ISO-stimulation, NOS1 cycling was not absent in the adult SHR. Paradoxically, we also failed to observe a significant diurnal variation in NOS1 in the adolescent animal. In addition, the absence of diurnal cycling was also observed in the expression of mRNA encoding the  $\beta_1$  and  $\beta_3$ -adrenergic receptors.

### **6.3.1 Why is the time-of-day dependent variation in the $\text{Ca}^{2+}$ transient and its responsiveness to isoproterenol depressed in the hypertensive SHR?**

The depression of diurnal cycling in the  $\text{Ca}^{2+}$  transient and its responsiveness to ISO in the hypertensive adult SHR could reflect disruption to circadian clock gene cycling which may impact on NOS1 activity or any component of the NOS-cGMP-PKG

pathway, for example, the cardiac  $\beta$ -adrenergic receptors, NOS3 and CAPON or other EC-coupling genes. Each of which will be discussed individually below.

### ***Disruption to the circadian clock its impact on neuronal nitric oxide synthase cycling***

The depressed diurnal variation in the basal  $\text{Ca}^{2+}$  transient and its responsiveness to ISO we observe in the adult SHR may be the result of the absence or depression of circadian clock cycling during the development of hypertension and associated hypertrophy in the SHR. In support, abnormal circadian clock gene and myocardial metabolic gene cycling have been previously reported in surgical models of pressure-overload induced hypertrophy (Young et al., 2001b) and MI (Kung et al., 2007), and also in streptozotocin-induced diabetes (Young et al., 2002). Therefore, if cycling of genes including those responsible for EC-coupling are regulated by the peripheral circadian clock rather than external signals (i.e. neuronal or humoral signals), any disruption to the circadian clock in the hypertensive adult SHR may contribute to the depression of diurnal variation we observe in these animals. Our data show that the cycling of circadian clock genes, Per2 and CLOCK, in adolescent (pre-hypertensive) SHR was similar to that shown in adult Wistar, which corroborates previously published data (Young et al., 2001a, Naito et al., 2003, Yamamoto et al., 2004), suggesting that normotensive animals exhibit similar diurnal cycling of circadian clock genes. However, the magnitude of this diurnal cycling in Per2 and CLOCK was depressed in the hypertensive adult SHR. The circadian clock controls the expression of ~10-15% of all rodent myocardial genes (Storch et al., 2002, Martino et al., 2004) therefore, the time-of-day dependent variation in the expression of other myocardial genes controlled by the circadian clock may be likewise affected by hypertension-induced hypertrophy in the SHR and this depression of circadian clock cycling may impact on EC-coupling through changes in genes that control cardiac contraction, which may contribute to the depressed  $\text{Ca}^{2+}$  transient and responsiveness to ISO.

This depression in the magnitude of cycling of the circadian clock genes in the SHR was mirrored by changes in the expression of mitochondrial metabolic genes, UCP2 and UCP3, as expression of both genes was depressed in the hypertensive adult SHR compared with both adolescent SHR and adult Wistar. These data suggest circadian clock cycling appears to be disrupted in hypertensive adult SHR and is consistent with studies by Young *et al* (2001), where a surgical model of pressure-overload induced hypertrophy in the rat disrupted time-of-day dependent variation in the expression of key circadian clock and mitochondrial metabolic genes (Young et al., 2001a, Young et al., 2001b). Our data confirms that a non-surgical, genetic model of hypertension-induced hypertrophy in the adult SHR disrupts the circadian clock cycling in a similar manner as Youngs surgical model and therefore the SHR is an appropriate model to study the effects of hypertension-induced hypertrophy on diurnal cycling of EC-coupling and its modulation by sympathetic stimulation. In the previous chapter we have identified NOS-signalling and in particular NOS1 as being responsible for the reduction of the inotropic response to  $\beta$ -adrenergic stimulation with ISO, and reduction in the development of arrhythmic activity in active period (ZT15) myocytes. Therefore, if NOS1 is under the control of the circadian clock, disruptions to the circadian clock cycling may reduce NOS1 activity and expression which may contribute to the absence of diurnal variation in the basal  $Ca^{2+}$  transient and its responsiveness to ISO in adult SHR. Paradoxically, our data show that there is no time-of-day dependent variation in the expression of NOS1 in adolescent SHR, which does not reflect data obtained in adult Wistar, which exhibit time-of-day dependent increase in NOS1 expression during the active period (ZT15). This may be the result of genetic features specific to the SHR/species variation. In addition, in the hypertensive adult SHR, our data shows that there is a significant increase in NOS1 expression during the active period (ZT15), although the magnitude of this increase was greater in adult Wistar than adult SHR (1.65 fold in adult SHR v 5.04 fold in adult Wistar), as diurnal variation present only in adult SHR and Wistar this may suggest that diurnal variation in NOS may be an adult phenotype, although our data cannot confirm this as we did not perform quantitative real-time RT-

PCR in adolescent WKY/Wistar. These data do not support the idea that the attenuation of the diurnal cycling of the response to ISO in adult SHR animals results from an absence in NOS1 cycling, as we found that diurnal cycling of NOS1 was still present in adult SHR animals. In the previous chapter, we showed that the increase in NOS activity/ expression in active period (ZT15) myocytes was protective against sympathetic overstimulation. Contrary to this, current literature has reported that NOS1 expression is increased in adult SHR (Piech et al., 2003), which would suggest, based on our findings, that SHR may be protected against sympathetic-induced arrhythmias. In support of this, analysis of our NOS1 gene expression data showed that NOS1 expression is significantly greater in adult SHR than adolescent SHR (data not shown) which is supportive of the upregulation of NOS1 expression in hypertension-induced LV hypertrophy (Damy et al., 2003, Damy et al., 2004, Loyer et al., 2007). In addition, Piech *et al* (2003) have shown that NOS1 expression is increased in the aging SHR, however, the SHR used by Piech and colleagues were much older than the ones used in the present investigation. This may mean that the coupling of NOS1 to  $\beta_3$ -adrenergic receptors and/or subsequent coupling of the resulting NO to the SR is disrupted in the adult SHR. Indeed, in hypertension and associated LV hypertrophy, NOS1 is believed to translocate from the SR to the sarcolemmal membrane (Bendall et al., 2004), which will not only reduce the effects of NOS1 on SR function but NOS1 may also target the sarcolemmal LTCC. Our data suggests that NOS1 targeting of the SR was responsible for reduced responsiveness of active period (ZT15) myocytes from Wistar rats to ISO stimulation; therefore, the apparent absence of a diurnal variation in the responsiveness of the  $Ca^{2+}$  transient to ISO in the adult SHR may reflect changes in coupling of the  $\beta_3$ -adrenergic receptors to NOS1-targeting of SR function. The depressed  $Ca^{2+}$  transient and its responsiveness to ISO in adult SHR may be due to uncoupling of NOS1 from  $\beta_3$ -adrenergic receptors; however, our data cannot confirm this. Therefore, based on our data it seems unlikely that depressed cycling of the circadian clock influences NOS1 cycling enough to cause the depressed diurnal cycling we observe in the  $Ca^{2+}$  transient and its responsiveness to ISO in the hypertensive adult SHR. However, as our data does

not confirm changes in the sub-cellular location of NOS1 in adult SHR, changes in the expression of active NOS1 protein nor does it rule out the possibility that uncoupling of  $\beta_3$ -adrenergic receptors to NOS1 activity occurs in the adult SHR and/or the signalling pathways involved in NO-signalling (cGMP and S-nitrosylation), it therefore remains a possibility that NOS1 may somehow directly or indirectly contribute to the depressed diurnal cycling.

### ***$\beta$ -adrenergic receptors***

Significant remodelling occurs in the  $\beta$ -adrenergic receptor system during hypertension and associated LV hypertrophy. Initially, there is a characteristic increase in the  $\beta$ -adrenergic responsiveness of the myocardium due to an increase in sympathetic drive (Post et al., 1999, Greenwood et al., 2001, Schlaich et al., 2003). However, continued exposure to increased sympathetic stimulation leads to desensitisation of positive inotropic  $\beta_1/\beta_2$ -adrenergic receptors through  $\beta$ -ARK phosphorylation and down-regulation through  $\beta$ -arrestin targeting of these receptors for internalisation (Castellano and Bohm, 1997, Post et al., 1999, Rockman et al., 2002), contributing to the decreased abundance of  $\beta_1/\beta_2$ -adrenergic receptors reported in LV hypertrophy (Hadcock and Malbon, 1988, Bristow et al., 1993). In addition, in LV hypertrophy and HF, the negative inotropic  $\beta_3$ -adrenergic receptor is upregulated (Cheng et al., 2001, Moniotte et al., 2001), and does not undergo desensitisation/ down-regulation as it is not targeted by  $\beta$ ARK (Skeberdis, 2004). The combination of a reduction in the abundance of  $\beta_1/\beta_2$ -adrenergic receptors and an increase in abundance  $\beta_3$ -adrenergic receptor makes the diseased myocardium inherently less responsive to sympathetic stimulation. Therefore, the absence of diurnal variation in the basal  $\text{Ca}^{2+}$  transient and its responsiveness to ISO we observe in the adult SHR could be due to  $\beta$ -adrenergic receptor remodelling during the development of hypertension and associated LV hypertrophy in the SHR. The negative inotropic  $\beta_3$ -adrenergic receptors are believed to act against the positive

inotropic effects of  $\beta_1$ -adrenergic receptor; therefore, changes in the ratio of these receptors will impact of the responsiveness to sympathetic stimulation. Recent literature suggests that the  $\beta_3$ -adrenergic receptor is a circadian clock controlled gene (Storch et al., 2002). In addition, diurnal cycling has been reported in  $\beta_3$ -adrenergic receptor expression as Zhou *et al* (2010) have shown that a time-of-day dependent variation exists in the expression of the  $\beta_3$ -adrenergic receptor which they also showed was depressed after induction of MI in the Wistar rat. Therefore, changes in the diurnal cycling in  $\beta_3$ -adrenergic receptor expression may also contribute to the depression of the  $\text{Ca}^{2+}$  transient and responsiveness to ISO in adult SHR. Supportive of this, our data show that there is a time-of-day dependent increase in  $\beta_3$ -adrenergic receptor (Adrb3) expression during the active period (ZT15) in adolescent SHR and adult Wistar, although the increase was far greater in adolescent SHR than adult Wistar. However, this time-of-day dependent variation in  $\beta_3$ -adrenergic receptor (Adrb3) expression was absent in hypertensive adult SHR. This depression of diurnal cycling in  $\beta_3$ -adrenergic receptor expression may contribute to the depression of the responsiveness of the  $\text{Ca}^{2+}$  transient to ISO in adult SHR. Although the gene expression data obtained for the  $\beta_3$ -adrenergic receptor (Adrb3) in this investigation may not have been reliable, due to existence of significant technical issues with the  $\beta_3$ -adrenergic receptor (Adrb3) Taqman probe (see chapter 5 discussion for details) our data supports recently published data (Zhou et al., 2010).

We also proposed that the depressed diurnal variation in the basal  $\text{Ca}^{2+}$  transient and its responsiveness to ISO stimulation could be due to depression of diurnal cycling in  $\beta_1$ -adrenergic receptor expression. Our data shows diurnal cycling with respect to the  $\beta_1$ -adrenergic receptor (Adrb1), with an increase in  $\beta_1$ -adrenergic receptor (Adrb1) expression during the active period (ZT15) in adolescent SHR which is similar to adult Wistar. However, this time-of-day dependent variation in  $\beta_1$ -adrenergic receptor (Adrb1) expression was absent in hypertensive adult SHR. In addition, in previous chapters, changes in the expression of the  $\beta_1$ -adrenergic receptor did not reflect changes in the responsiveness to ISO, although this could suggest changes in  $\beta_1$ -adrenergic

receptor protein and/ or increased receptor desensitisation/ down-regulation associated with LV hypertrophy, it is unlikely that changes in  $\beta_1$ -adrenergic receptor expression contribute to the depressed diurnal cycling in adult SHR.

### ***Endothelial nitric oxide synthase***

Although our data from the previous chapter suggests that NOS1 rather than NOS3 is responsible for the diurnal variation we see in the responsiveness of the  $\text{Ca}^{2+}$  transient to ISO, there is a possibility that the depression of  $\text{Ca}^{2+}$  transient and responsiveness to ISO in hypertensive adult SHR may due to changes in NOS3 expression. Indeed, in hypertension-induced LV hypertrophy, NOS3 has also been shown to be down-regulated (Damy et al., 2004) and through genetic KO experiments decreased NOS3 is believed to be associated with increased arrhythmogenesis (Kubota et al., 2000), increased development of hypertrophy and increased responsiveness to  $\beta$ -adrenergic stimulation (Barouch et al., 2002, Wang et al., 2008b). Therefore, this may suggest more specifically that if NOS3 expression was reduced in hypertensive adult SHR that this may impact on  $\beta$ -adrenergic responsiveness and subsequently contribute to the depressed diurnal cycling in the basal  $\text{Ca}^{2+}$  transient and responsiveness to ISO. However, we did not find a time-of-day dependent variation in the expression of NOS3 in either adolescent or adult SHR, and the variation in adult Wistars was very modest (see chapter 5; figure 5.9). It is possible that at 20+ weeks our animals had not progressed to LV hypertrophy significantly enough to impact on NOS3, and indeed NOS3 expression levels did not differ between adolescent and adult SHR (data not shown). Therefore, these data suggest it is unlikely that changes in NOS3 expression contribute to the depression of diurnal variation in the basal  $\text{Ca}^{2+}$  transient and its responsiveness we observe in hypertensive adult SHR. It is possible that the depressed  $\text{Ca}^{2+}$  transient and responsiveness to ISO are the result of changes in NOS2 expression, which also occur in LV hypertrophy and HF, or changes in additional components of

the NOS signalling pathway, for example, GC, cGMP, NO and the  $\beta_3$ -adrenergic receptor. However, we did not look at NOS2, GC, cGMP, NO levels in the present investigation, therefore, further work is required to elucidate whether these components play a role in the depressed time-of-day dependent variation we observe in adult SHR.

### ***CAPON***

The NOS1 associated protein, NOS1AP (CAPON) is physically associated with NOS1 (Beigi et al., 2009) and has been shown previously to influence the NOS1-mediated modulation of LTCC (Chang et al., 2008). It is therefore possible that changes in CAPON expression could account for the depressed diurnal cycling in hypertensive adult SHR. Our data show that, there was a time-of-day dependent increase in the expression of CAPON during the active period (ZT15) in adult SHR which was absent in adolescent SHR, although the magnitude of this increase was modest. This does not reflect data obtained in adult Wistar, as there was a time-of-day dependent increase in the expression of CAPON during the resting period (ZT3) in adult Wistar, suggesting that CAPON expression is reversed in adult SHR with respect to adult Wistar, which could be due to the differing genetic backgrounds of both species or the effect of hypertension. It is possible that the time-of-day dependent increase in CAPON expression during the active period (ZT15) of adult SHR may contribute to the depressed diurnal variation we observe possibly through changes in its coupling to NOS1, however, due to the low magnitude of CAPON expression it is unlikely that changes in CAPON will significantly impact on the changes we see in diurnal cycling in adult SHR.

### *Excitation-contraction coupling genes*

In previous chapters, we have shown that the basal  $\text{Ca}^{2+}$  transient and its responsiveness to ISO stimulation exhibited time-of-day dependent variation; however, this variation was not reflected by changes in the expression of the key EC-coupling genes; LTCC, NHE1, PLB, SERCA 2a and RyR2. Whilst NCX1 expression was significantly greater during the active period (ZT15) than the resting period (ZT3), the fold changes were modest and therefore, we determined that NCX in addition to LTCC, NHE1, PLB, SERCA 2a and RyR2 were unlikely to play a major roles in this diurnal cycling we observed in the  $\text{Ca}^{2+}$  transient in the Wistar. However, LV hypertrophy and HF are associated with abnormal  $\text{Ca}^{2+}$  regulation and the increased incidence of ventricular arrhythmias namely through changes in the expression of several EC-coupling genes. For example, in these instances expression of NCX1 is increased (Pogwizd et al., 1999) and SERCA 2a expression is decreased (Currie and Smith, 1999), which contributes to greater  $\text{Ca}^{2+}$  extrusion from the myocyte and reduced SR  $\text{Ca}^{2+}$  uptake and content, respectively. SERCA 2a activity is also reduced as there is decreased phosphorylation of PLB (Currie and Smith, 1999). In addition, LTCC current may be reduced which would decrease the  $\text{Ca}^{2+}$  available to trigger SR  $\text{Ca}^{2+}$  release (Houser et al., 2000, Chen et al., 2002) and RyR are hyperphosphorylated which increases channel open probability (Marx et al., 2000) and reduces FKBP12.6 binding, both of which are pro-arrhythmic (Wehrens et al., 2003). Therefore, although we found no diurnal variation in EC-coupling genes in the Wistar, the absence of diurnal variation in the basal  $\text{Ca}^{2+}$  transient and its responsiveness to ISO we observe in the adult SHR could be due to changes in the expression of EC-coupling genes during the development of hypertension and associated hypertrophy in the SHR, which may mask any diurnal influences of NOS1-signalling. However, our data show that there is no time-of-day dependent variation in the expression of the following EC-coupling genes in either adolescent or adult SHR: LTCC, NCX1, NHE1, PLB, SERCA 2a and RyR2 and this

reflected data obtained in adult Wistar, suggesting that the absence of diurnal variation in the  $\text{Ca}^{2+}$  transient and responsiveness to ISO in the adult SHR is not due to changes in the expression of EC-coupling genes.

### 6.3.2 Study limitations

The SHR is an age-related genetic model of essential hypertension and they do not develop hypertension until 10-15 weeks, therefore, adolescent animals (< 6 weeks) are normotensive (Okamoto and Aoki, 1963). In addition, SHR develop ventricular hypertrophy secondary to hypertension at >24 weeks (Okamoto and Aoki, 1963, Conrad et al., 1991, Boluyt and Bing, 2000). As the adult SHR we use may have already developed hypertrophy as a consequence of hypertension, we do not know whether the depression of diurnal variation we see in the basal  $\text{Ca}^{2+}$  transient, its responsiveness of ISO and mRNA levels are the result of hypertension or hypertrophy. Similar to this, although Young and colleagues have reported that pressure-overload induced hypertrophy through aortic banding is responsible for depression of diurnal variation in key circadian clock and metabolic genes; it is unclear whether the differences they observe are due to the initial pressure-overload or the resulting hypertrophy (Young et al., 2001a, Young et al., 2001b). Therefore, in order to establish whether hypertension or the resultant hypertrophy is responsible for the differences we see, in future experiments we could treat SHR with anti-hypertensive drugs to establish the effect of hypertrophy on the  $\text{Ca}^{2+}$  transient and its responsiveness to ISO.

The  $\Delta\text{CT}$  levels obtained for  $\beta_1$ -adrenergic receptor (*Adrb1*) and the  $\beta_3$ -adrenergic receptor (*Adrb3*) indicate that abundance of the  $\beta_1$ -adrenergic receptor is ~4 times greater than the  $\beta_3$ -adrenergic receptor in adolescent and adult SHR. This is supported by previously published data suggesting that ~75% of cardiac  $\beta$ -adrenergic receptors are composed of the  $\beta_1$ -isoform and the remaining ~25% is composed of the  $\beta_2$  and  $\beta_3$ -isoforms (Bristow et al., 1986, Wallukat, 2002), however, this data reflects the non-

diseased myocardium and may suggest that remodelling of these receptors has not yet occurred in our SHR. In support of this notion, a comparison of  $\beta_1$ -adrenergic receptor (*Adrb1*) showed significantly greater expression in the adult SHR than the adolescent SHR, which may mean that the gene expression changes associated with the development of LV hypertrophy may not have occurred, suggesting that the SHRs used in our study had not yet developed LV hypertrophy (data not shown). It may also be the case that the hypertensive adult SHR we have used for analysis have not yet developed adverse changes in  $\text{Ca}^{2+}$  handling. In support of this, upon comparison of these EC-coupling genes (*LTCC*, *NCX1*, *NHE1*, *PLB*, *SERCA 2a* and *RyR2*) between adolescent and adult SHR we found that expression levels did not differ between adolescent and adult SHR, suggesting that the gene expression changes associated with the development of LV hypertrophy have yet to occur, which may indicate that our hypertensive rats have yet to develop LV hypertrophy (data not shown). In addition, Orchard and colleagues have shown that there are no significant changes in  $\text{Ca}^{2+}$  homeostasis in the SHR as Fowler *et al* (2007) have shown that in fact aging contributes more to changes in  $\text{Ca}^{2+}$  homeostasis than LV-hypertrophy in SHR; however, they used older SHR than we have in the present investigation. Future work may therefore comprise of using older SHR that have possibly developed HF or have established LV hypertrophy to repeat RT-PCR experiments to examine the impact on diurnal cycling of EC-coupling genes. Therefore, as diurnal cycling is not present in EC-coupling genes in adult SHR, changes in EC-coupling genes are unlikely to explain the absence of diurnal variation in the  $\text{Ca}^{2+}$  transient and responsiveness to ISO in the adult SHR.

In the present chapter due to time constraints we did not perform quantitative real-time RT-PCR on LV free-wall tissue from normotensive adolescent and adult WKY and as a result relied heavily on comparisons within SHR (between adolescent and adult SHR) and also with Wistar. It would be ideal to repeat the RT-PCR including hearts from both adolescent and adult WKY isolated during the resting period (ZT3) and active period (ZT15). In addition, as we did not look at the adolescent Wistar in the present investigation, future work would involve the study of the basal  $\text{Ca}^{2+}$  transient, its

responsiveness to ISO and mRNA levels of circadian clock, mitochondrial metabolic, EC-coupling and NOS-signalling genes to act as an additional control but to also determine changes in the developmental process of the Wistar.

Due to time constraints, we did not examine contraction strength, SR  $\text{Ca}^{2+}$  content and the development of arrhythmic activity in resting period (ZT3) and active period (ZT15) myocytes from adolescent and adult WKY and SHR. It would seem likely given the depression of diurnal variation in the basal  $\text{Ca}^{2+}$  transient and its responsiveness to ISO we observe in hypertensive adult SHR, that both contraction strength and SR  $\text{Ca}^{2+}$  content would reflect these changes. In addition, it seems likely that due to the increased incidence of ventricular arrhythmias associated with hypertension and associated hypertrophy that the development of arrhythmic activity would be increased in both resting period (ZT3) and active period (ZT15) myocytes from adult SHR. Therefore, future work would involve the determination of SR  $\text{Ca}^{2+}$  content and the incidence of arrhythmic activity in WKY and SHR to examine the effect of hypertension on diurnal variation in these parameters.

The cardiac  $\beta_2$ -adrenergic receptor contributes to a localised positive inotropic effect during  $\beta$ -adrenergic stimulation (Bers, 2002) and in hypertension and LV hypertrophy the  $\beta_2$ -adrenergic receptor is believed to down-regulated in addition to the  $\beta_1$ -adrenergic receptor (Hadcock and Malbon, 1988, Bristow et al., 1993). However, in the present investigation we did not determine whether expression of  $\beta_2$ -adrenergic receptor mRNA (*Adrb2*) was subject to time-of-day dependent variation in either the adult Wistar or adolescent/ adult SHR and therefore future work could investigate this.

In addition, we were unable to examine whether changes in cycling of EC-coupling genes,  $\beta_1$  and  $\beta_3$ -adrenergic receptors and NOS-signalling genes were reflected by similar changes in levels of active protein or more specifically the function of membrane-bound receptors. Therefore, future work would comprise of the determination of the protein levels of the genes investigated and the function of these proteins in adolescent and adult WKY and SHR to establish whether hypertension affects diurnal variation in active protein levels.

In summary, the data from the present chapter suggest that the time-of-day dependent variation in the basal  $\text{Ca}^{2+}$  transient, its responsiveness to ISO and the expression of key circadian clock, mitochondrial metabolic and NOS-signalling genes are depressed in the adult SHR. In the previous chapter, we determined that an increase in NOS1 activity and expression was responsible for reducing the incidence of sympathetic-induced arrhythmias (DADs) during the active period (ZT15), when sympathetic outflow is greatest, through the modulation of SR function. Therefore, the reduction in time-of-day dependent expression of NOS1 during the development of hypertension is likely to contribute to an increased incidence of sympathetic induced arrhythmias during the active period (ZT15) and may therefore contribute to the morning incidence of ventricular arrhythmias and SCD seen in patients with cardiomyopathies. In the next chapter we will discuss the clinical implications of the diurnal variation we have observed NOS1 activity/ expression and the role of NOS1 in reducing arrhythmic activity in terms of potential therapeutic strategies.

## **Chapter 7: Physiological and clinical implications of diurnal cycling in EC-coupling**

Diurnal variation in sympathetic activity is well documented and exhibits a morning peak in man (Hayano et al., 1990, Dodt et al., 1997) and an evening peak in the nocturnal rat (Hashimoto et al., 1999). This morning peak in sympathetic activity may be responsible for diurnal variation in SV and HR and also the increased morning incidence of SCD linked to ventricular arrhythmias (Guo and Stein, 2003).

We have shown a time-of-day dependent variation in EC-coupling and its modulation by sympathetic stimulation with ISO, a non-selective  $\beta$ -adrenergic receptor agonist which activates all cardiac  $\beta$ -adrenergic receptors, with a reduction in responsiveness during the animal's active period. We hypothesised that the reduced responsiveness of active period (ZT15) myocytes reflects increased  $\beta_3$ -adrenergic receptor activation resulting in a negative inotropic effect involving the activation of NOS (Gauthier et al., 2000), which acts to protect the myocardium against  $\text{Ca}^{2+}$ -overload injury induced by sympathetic stimulation.

Cardiomyopathies such as pressure-overload induced hypertrophy and MI are associated with an increased risk of ventricular arrhythmias and associated SCD (McLenachan et al., 1987, Cleland et al., 2002). These cardiomyopathies are also associated with the abnormal diurnal cycling of the circadian clock (Young et al., 2001b, Kung et al., 2007) and dysfunctional  $\text{Ca}^{2+}$  homeostasis (Houser et al., 2000, Bers, 2006). The depressed diurnal variation is the result of hypertension and associated hypertrophy and not due to developmental changes that occur during the aging process in the rat. However, we do not know whether changes in EC-coupling we observe in adult SHR are the result of hypertension or the development of hypertrophy.

## ***7.1 What is the physiological role of diurnal variation in EC-coupling and NOS-signalling in the healthy individual?***

During the transition from the resting period to the active period the heart must increase its output to meet physical demands and one way the heart increases CO (and HR/SV) is through an increase in sympathetic activity. This surge in sympathetic activity is believed to be controlled by the intrinsic central circadian clock located in the SCN and influenced by changes in the light/dark (L/D) cycle and/or transition from the resting period to active period (Durgan et al., 2005, Young, 2006, Young and Bray, 2007). The central circadian clock mechanism anticipates the 24 hour cycle and is reset on a regular basis through light input to the optic nerve. This increase in sympathetic activity is a regulated process and does not occur due to want of the animal and therefore this may be a successful evolutionary adaptation to allow heightened senses of the rat during the active foraging period. Indeed, diurnal variations have been documented in numerous cardiovascular haemodynamic parameters and in the expression of circadian clock and cardiac metabolic genes (Young et al., 2001a, Young et al., 2001b) with all parameters increased during the active period of the rat.

Data from the present investigation shows that diurnal variation in EC-coupling and its response to sympathetic stimulation appears to reflect changes in NOS activity and may reflect a possible physiological advantage. NOS-signalling is central to cell regulation, cell remodelling, cardiac contractility, is important in altering metabolic rates and protects the heart from sympathetic-induced arrhythmic activity and injury (Ashley et al., 2002, Momken et al., 2002, Dawson et al., 2005, Sun et al., 2006, Burger et al., 2009). Indeed studies have shown that pharmacological inhibition/ genetic KO of NOS can increase arrhythmogenesis (Kubota et al., 2000, Burger et al., 2009), and pharmacological activation or gene over-expression of NOS is protective against arrhythmic activity in animal models (Collins and Rodrigo, 2010). In terms of our data we show one of the effects of an increase in NOS during the active period is preventing

SR  $\text{Ca}^{2+}$  loading and the induction of ventricular arrhythmias due to severe sympathetic stimulation. Therefore, diurnal variation in NOS activity could represent a selective advantage/ behavioural adaptation that allows an animal to prepare for environmental changes that occur over a 24 hour period i.e. transition between resting period and active period. During the active period when the animal experiences large surges in sympathetic stimulation, this mechanism exists to depress the responsiveness of the myocardium which impacts on EC-coupling and  $\text{Ca}^{2+}$  regulation. As diurnal variation exists in the incidence of ventricular arrhythmias and associated SCD in man (Muller et al., 1987, Arntz et al., 1993, Tofler et al., 1995) and is thought to reflect the morning increase in sympathetic activity (Guo and Stein, 2003), the animal may be preparing for the increase in sympathetic activity through the increases in NOS affording protection against sympathetic over-stimulation and ventricular arrhythmias. This physiological state, however, will certainly render the animal vulnerable to stressful situations arising during its resting period, when NOS activity has yet to increase, which may explain the increased incidence of SCD in man.

Disruption to sleep pattern is associated with dyssynchrony in the functioning of the circadian clock and the rhythmicity of circadian clock gene expression. Typical situations where the normal sleep pattern and therefore the circadian clock is disturbed include jet lag (Reddy et al., 2002); shift work (Akerstedt, 1990) and also insomnia associated with the elderly (Van Someren, 2000) and these conditions are associated with increased morning incidence of ventricular arrhythmias and SCD. If circadian clock genes regulate NOS expression it is possible that disruption to the sleep pattern could impact on NOS activity resulting in a delay/ phase shift in the increase in NOS activity during the transition between the resting and active period and could possibly further exacerbate the propensity for sympathetic-induced arrhythmias in man.

## ***7.2 What is the physiological role of diurnal variation in EC-coupling and NOS-signalling in the diseased myocardium?***

The increased sensitivity of the myocardium to sympathetic-induced ventricular arrhythmias during the resting period may be further increased in genetic diseases also associated with the increased incidence of arrhythmic activity such as long QT syndrome (Tristani-Firouzi et al., 2001), RyR2 mutation (Priori et al., 2001) and genetic variants of CAPON (Chang et al., 2008, Kao et al., 2009).

The incidence of Ca<sup>2+</sup> dependent after-depolarisations, ventricular arrhythmias and SCD are also increased in cardiomyopathies such as hypertension, pressure-overload induced hypertrophy and MI (McLenachan et al., 1987, Barbieri et al., 1994, Veldkamp et al., 2001). These cardiomyopathies are associated with disruption to normal circadian clock gene cycling, with diurnal cycling in circadian clock and cardiac metabolic gene expression depressed in pressure-overload induced hypertrophy (Young et al., 2001a, Young et al., 2001b) and MI (Kung et al., 2007) and diurnal cycling is also advanced by 2-3 hours in cases of diabetes (Young et al., 2002). In addition, diurnal variation is also depressed in various haemodynamic parameters such as BP (non-dippers) (Turfaner et al., 2009) and also in cardiac electrophysiology namely through depressed diurnal cycling in AV-node conduction (Hayano et al., 1998), and QT interval (Yi et al., 1998), all of which may contribute to the increased incidence of ventricular arrhythmias and SCD in cardiomyopathies. In these cardiomyopathies, in addition to the depressed diurnal cycling in circadian clock and cardiac metabolic genes, there is also a pronounced increase in sympathetic drive and patients appear to have increased sensitivity to this increase in sympathetic drive (Post et al., 1999, Greenwood et al., 2001, Schlaich et al., 2003). Diurnal variation in EC-coupling genes and NOS-signalling genes in hypertension-induced hypertrophy remained unknown until the present investigation. Our data shows that hypertension-induced hypertrophy depresses the diurnal cycling in EC-coupling and its responsiveness to  $\beta$ -adrenergic stimulation; however depression in diurnal cycling does not occur due to changes in the expression

of NOS1 or  $\beta_3$ -adrenergic receptor. However, our data does not rule out changes in protein expression or changes in coupling of the  $\beta_3$ -adrenergic receptor to NOS1 activity.

It is possible that if circadian clock gene cycling or NOS are depressed or phase shifted due to abnormal functioning of the circadian clock, that this will not only alter diurnal variation in EC-coupling but also may render the myocardium more sensitive to sympathetic-induced ventricular arrhythmias. The change in phase between NOS and sympathetic activity may explain why the major cause of death in patients with cardiomyopathies is due to ventricular arrhythmias associated with SCD. If NOS expression is driven by the circadian clock and not by the L/D cycle then NOS activity may be decreased for ~4 hours during the transition from the resting period to the active period, which results in a mismatch between  $\beta_3$ -adrenergic receptor-NOS signalling and sympathetic activity which will continue to be controlled by the L/D cycle, rendering the heart more sensitive to sympathetic-induced arrhythmias.

The effects of hypertrophy on diurnal expression of NOS1 could combine with known changes to diurnal cycling of circadian clock genes, changes in  $\text{Ca}^{2+}$  handling proteins (over-expression of NCX, decreased SERCA 2a expression) and decreases in  $\text{K}^+$  channel expression ( $I_{\text{to}}$  &  $I_{\text{K1}}$ ) to compound the influence of sympathetic activity and promote the generation of ventricular arrhythmias (see introduction section 1.6). Remodelling of the  $\beta$ -adrenergic receptor system occurs during hypertrophy in which  $\beta_3$ -adrenergic receptor expression is increased (Cheng et al., 2001, Moniotte et al., 2001) and  $\beta_1/\beta_2$ -adrenergic receptor expression is downregulated (Hadcock and Malbon, 1988, Bristow et al., 1993), which should work to protect the heart from ventricular arrhythmias, however, NOS1 compartmentalisation is altered which may impact on the incidence of arrhythmias (Barouch et al., 2002, Bendall et al., 2004).

The NOS1 associated protein, NOS1AP (CAPON) is physically associated with NOS1 where it modulates cardiac repolarisation (Arking et al., 2006, Beigi et al., 2009) and has been shown previously to influence the NOS1-mediated modulation of LTCC (Chang et al., 2008), which will impact on APD. Genome wide association studies have

identified genetic variants of the CAPON that are associated with prolonged QT interval and increased risk of SCD (Kao et al., 2009). Our data suggests that diurnal variation exists in the expression of the gene encoding CAPON; therefore it is possible that in addition to the genetic factors impacting on CAPON that diurnal variation in NOS1 may also impact on CAPON, which could then act to compound the effects of diurnal variations in NOS-signalling. However, further work is required to establish the role of CAPON in the diurnal variation we observe in sympathetic-induced arrhythmic activity.

### ***7.3 Is the $\beta_3$ -adrenergic-NOS-cGMP pathway a possible target for the prevention of ventricular arrhythmias that occur in cardiomyopathies?***

A large proportion of people develop HF each year in the UK and it is a leading cause of death in the elderly, and the incidence of SCD is high and one of the major contributors to morbidity (Swedberg et al., 2005). Indeed, the most common cause of death in patients with these cardiomyopathies is the result of ventricular arrhythmias that trigger SCD. The disruption to the circadian clock and coupling of  $\beta_3$ -adrenergic receptors to NOS1-signalling may be responsible for the increased risk of ventricular arrhythmias in patients with hypertension and associated hypertrophy and HF. A major cause of arrhythmias are likely to be  $\text{Ca}^{2+}$  dependent after-depolarisations, which are more pronounced in cardiomyopathies such as MI, LV-hypertrophy and HF (Barbieri et al., 1994, Veldkamp et al., 2001). Therefore, it is essential to not only treat the disease by reducing the symptoms but to also reduce the incidence of ventricular arrhythmia in these patients. Current treatments for LV hypertrophy and HF include angiotensin-converting enzyme (ACE) inhibitors, diuretics, angiotensin II receptor blockers,  $\text{Ca}^{2+}$  channel antagonists,  $\beta$ -blockers, aldosterone antagonists, digoxin and nitrates (Swedberg et al., 2005). More recently,  $\beta_3$ -adrenergic receptors have been suggested as possible pharmacological target to support the failing heart as they promote  $\beta$ -

adrenergic responsiveness contributing to an increase in LV function, and also they cannot be down-regulated (Skeberdis, 2004). However, our data would suggest that  $\beta_3$ -adrenergic receptor antagonists could increase the incidence of arrhythmias.

Our data shows that activation and expression of NOS1, is responsible for diurnal variation we observe in EC-coupling and is cardioprotective against SR  $\text{Ca}^{2+}$  loading and the incidence of sympathetic-induced arrhythmias in active period (ZT15) myocytes. Therefore, activation of the cardiac  $\beta_3$ -adrenergic receptor leading to NOS-signalling could prove an effective therapeutic intervention to reduce the incidence of sympathetic-induced arrhythmias in models of LV hypertrophy and HF. As one arm of the NOS signalling pathway involves the production of cGMP, it should be possible to modulate  $\beta_3$ -adrenergic receptor activation by preventing breakdown of cGMP using phosphodiesterase (PDE) inhibitors. Type V PDE inhibitors are cGMP-dependent phosphodiesterases and therefore prevent the breakdown of cGMP, thereby potentiating the cardioprotective effects of NO-cGMP dependent pathway. Sildenafil (Viagra) is a type V PDE inhibitor currently used for the treatment of erectile dysfunction (Boolell et al., 1996). Some studies have indicated that Sildenafil is also cardioprotective as it has been shown to reduce I/R injury in rabbits (Bremer et al., 2005) and rats (Rosanio et al., 2006) and reduces the incidence of arrhythmic activity induced by ischaemia in canine models (Nagy et al., 2004). In addition, Sildenafil can induce protection similar to preconditioning in the rabbit heart (Kukreja et al., 2003) and some studies have shown that it produces cardioprotection through the opening of ATP-sensitive  $\text{K}^+$  ( $\text{K}_{\text{ATP}}$ ) channels (Ockaili et al., 2002). Moreover, Sildenafil has also been shown to reduce the ISO sensitivity of the rat heart in hypertrophy (Hassan and Ketat, 2005).

Some studies have suggested that selective type III PDE inhibitors could also increase mortality in HF. Type III PDE inhibitors prevent the breakdown of cAMP thereby increasing cAMP concentration and PKA activation which promote positive inotropism. This is beneficial as there is substantial downregulation of the positive inotropic  $\beta_1/\beta_2$ -adrenergic receptors (Hadcock and Malbon, 1988, Bristow et al., 1993) and therefore type III PDE inhibitors could potentially act to increase inotropy and LV function in the

failing heart. Therefore, further work is required to determine whether PDE inhibitors could be used in the treatment of HF. Currently PDE inhibitors are not regularly prescribed for the treatment of HF and clinical trials are ongoing.

Activation of the “anti-adrenergic” cardiac  $\beta_3$ -adrenergic receptors are linked to NOS activation and have also been suggested to protect the rat heart from  $\text{Ca}^{2+}$  overload, sympathetic induced stress and arrhythmic activity, through activation NO/cGMP pathway (Sun et al., 2006, Zhou et al., 2008). The activation of cardiac  $\beta_3$ -adrenergic receptors and subsequent activation of NOS produces negative inotropic effects in the heart, through cGMP-dependent (PKG activation) and cGMP-independent (S-nitrosylation by NO) modulation of  $\text{Ca}^{2+}$  current (LTCC) and SR function (RyR2 and SERCA 2a/PLB) which reduce cardiac contractility (Gauthier et al., 1998, Ziolo, 2008). Therefore, activation of cardiac  $\beta_3$ -adrenergic receptors and activation of NOS may therefore represent a pharmacological intervention in the prevention of sympathetic-induced arrhythmias. A decrease in  $\beta_3$ -adrenergic receptor activity during the resting period will result in the decreased activation and activity of NOS1 which in itself may be pro-arrhythmic.

#### ***7.4 Possible future work arising from present investigation***

We studied the responsiveness of resting period (ZT3) and active period (ZT15) myocytes to sympathetic stimulation with the non-specific  $\beta$ -adrenergic receptor agonist ISO. However, as sympathetic stimulation involves both circulating catecholamines and the release of norepinephrine from nerve terminals and there may also be additional effects on conduction velocities and regional APD variation, therefore, further work is required to establish whether our data translates in *in-vivo*, for example, by inducing a stressful stimulus like foot-shock treatment (Penna and Bassani, 2010)/ cold-water stress (Johnson et al., 1977) or administration of ISO to the animals through injection.

In addition, we identified that NOS was responsible for the diurnal variation we observed in the responsiveness of resting period (ZT3) and active period (ZT15) myocytes to sympathetic stimulation with ISO using the non-specific NOS inhibitor, L-NNA. However, as part of the present investigation we did not examine whether NOS was responsible for the diurnal variation we observed in resting period (ZT3) and active period (ZT15) myocytes under basal conditions, therefore, future work would involve the application of L-NNA under these conditions to determine the role of NOS.

As little is known whether diurnal variation in EC-coupling and NOS activity is present in humans, it would therefore be ideal to determine NOS/ NO levels through the examination of the levels of nitrite products of NO metabolism in the blood to establish whether the diurnal variation present in NOS is present in man. It would also be beneficial to determine endogenous NOS activity levels in resting period (ZT3) and active period (ZT15) myocytes from Wistar, WKY and SHR to support our NOS data.

As our data from chapter 6 suggests that NOS levels still cycle in the hypertensive adult SHR, it would also be interesting to determine what is happening to NOS-signalling after the  $\beta_3$ -adrenergic receptor, as it is possible that  $\beta_3$ -adrenergic receptor-NOS signalling has become uncoupled in hypertension-induced hypertrophy possibly through the documented translocation of NOS1 to the sarcolemmal membrane from the SR (Bendall et al., 2004) (see discussion 6 section 6.3.1). It would therefore be ideal to perform receptor density studies to establish whether there are any changes in the population of  $\beta_3$ -adrenergic receptors.

It would also be interesting to repeat the experiments in which we have determined the percentage of myocytes developing arrhythmic activity in response to ISO using  $\beta_3$ -adrenergic receptor agonists like SR59230A and BRL37344 to establish whether these  $\beta_3$ -adrenergic receptor agonists, like NOS inhibitors, are protective against sympathetic-induced arrhythmic activity.

As we have shown that NOS1 is protective against sympathetic-induced ventricular arrhythmias it would also be of particular benefit to look the effectiveness of drugs that enhance the cardioprotective  $\beta_3$ -adrenergic/NOS/cGMP signalling pathway for

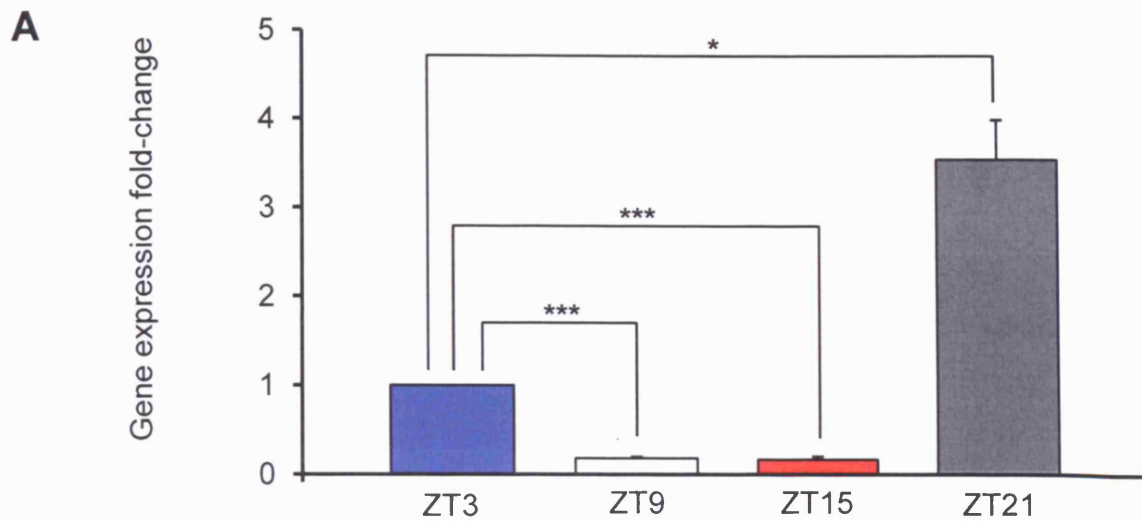
example,  $\beta_3$ -adrenergic receptor agonists, NO donors, Type V PDE inhibitors in preventing sympathetic-induced arrhythmic activity in resting period (ZT3) and active period (ZT15) myocytes in the Wistar, WKY and SHR. If these pharmacological interventions were successful then they could possibly be used for treating cardiomyopathies like HF to decrease the incidence of arrhythmias occurring due to abnormal cycling of the circadian clock.

## **Appendix 1**

|                                          | Gene of interest | Gene symbol | Standard curve slope value | Calculated gene efficiency (%) | $\Delta\Delta$ CT or Pfaffl method of analysis |
|------------------------------------------|------------------|-------------|----------------------------|--------------------------------|------------------------------------------------|
| <i>House keeping gene</i>                | $\beta$ -actin   | Actb        | -3.4                       | 95.0                           | N/A                                            |
| Circadian clock genes                    | CLOCK            | CLOCK       | -3.7                       | 86.2                           | Pfaffl                                         |
|                                          | Per 2            | Per 2       | -3.6                       | 89.5                           | Pfaffl                                         |
| Mitochondrial metabolic genes            | UCP2             | UCP2        | -3.4                       | 95.0                           | $\Delta\Delta$ CT                              |
|                                          | UCP3             | UCP3        | -3.5                       | 93.1                           | $\Delta\Delta$ CT                              |
| Sarcolemmal EC-coupling genes            | NCX1             | Slc8a1      | -3.9                       | 80.3                           | Pfaffl                                         |
|                                          | NHE              | Slc9a1      | -3.6                       | 89.5                           | Pfaffl                                         |
|                                          | LTCC             | Cacna1c     | -3.4                       | 95.0                           | $\Delta\Delta$ CT                              |
| Sarcoplasmic reticulum EC-coupling genes | PLB              | Pln         | -3.4                       | 95.0                           | $\Delta\Delta$ CT                              |
|                                          | SERCA 2a         | Atp2a2      | -3.1                       | 109.0                          | Pfaffl                                         |
|                                          | RyR2             | RyR2        | -3.5                       | 93.1                           | $\Delta\Delta$ CT                              |

**Appendix 1 figure 1- Standard curve data and mRNA analysis in left ventricular free-wall tissue isolated from adult Wistar rats during the resting period (ZT3) and active period (ZT15).**

Table showing the standard curve values obtained for each Taqman gene expression probe based assay investigated in chapter 3 of the results section using a 2-fold dilution. All Taqman probes shown produced a linear standard curve with PCR efficiency values between 80-110%. If the PCR efficiency of the gene of interest was within  $\pm 5\%$  from the efficiency of the housekeeping control gene,  $\beta$ -actin, then the mRNA were analysed using the  $\Delta\Delta$ CT method, however, if the PCR efficiency of the gene of interest differed from the efficiency of  $\beta$ -actin, then the Pfaffl method of mRNA analysis was preferred (see section 2.5.9 of materials and methods for details).



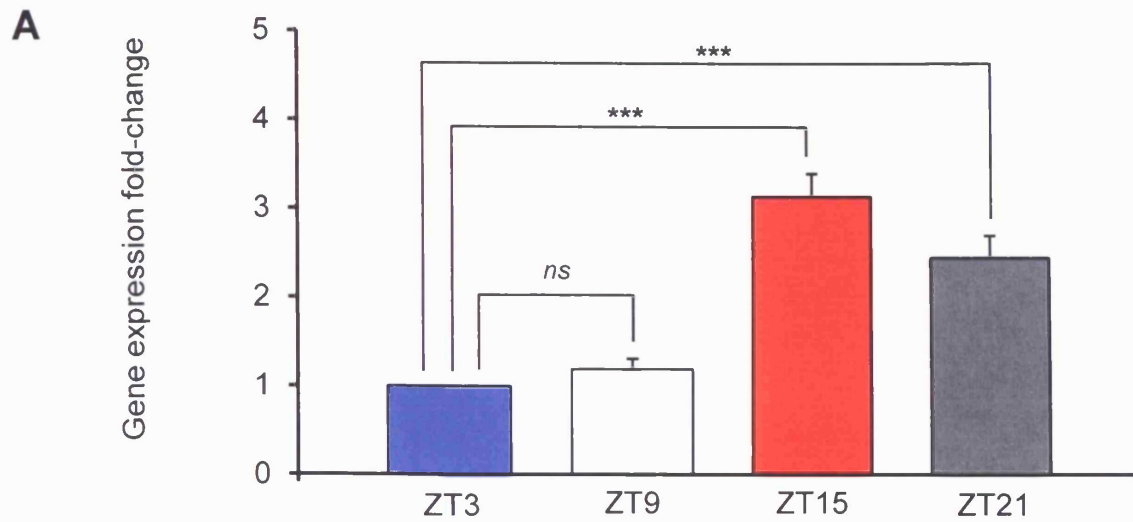
**B**

| Gene of interest |                                                     | ZT3 Wistar  | ZT9 Wistar               | ZT15 Wistar              | ZT21 Wistar            |
|------------------|-----------------------------------------------------|-------------|--------------------------|--------------------------|------------------------|
| CLOCK            | $\Delta$ CT (normalised to Beta-actin)              | 9.19 ± 0.28 | 12.28 ± 0.14             | 13.48 ± 0.24             | 8.16 ± 0.19            |
|                  | Fold change ( $\Delta\Delta$ CT)                    | 1.00 ± 0.00 | 0.18 ± 0.02              | 0.17 ± 0.04              | 3.54 ± 0.45            |
|                  | <i>p</i> -value (from $\Delta$ CT, compared to ZT3) | N/A         | <i>p</i> < 0.0001<br>*** | <i>p</i> < 0.0001<br>*** | <i>p</i> = 0.0294<br>* |

**Appendix 1 figure 2- Gene expression fold-change levels of the circadian clock gene, CLOCK, in adult Wistar hearts isolated at ZT3, ZT9, ZT15 and ZT21.**

A. Bar chart showing the real-time quantitative RT-PCR of CLOCK mRNA expression as fold-changes in left ventricular free-wall of ZT3 (Blue), ZT9 (White), ZT15 (Red) and ZT21 adult Wistar (Grey). CLOCK mRNA expression was normalised to  $\beta$ -actin mRNA. Fold-changes of CLOCK mRNA was calculated relative to the control (ZT3; Blue bars). The results are mean  $\pm$  S.E.M.; number of samples = ZT3 Wistar *n* = 4, ZT9 Wistar *n* = 5, ZT15 Wistar *n* = 8 and ZT21 Wistar *n* = 6. \* *p* < 0.05, \*\*\* *p* < 0.0001, unpaired students *t* test performed on  $\Delta$ CT values.

B. Table showing the data used to produce figure in A



**B**

| Gene of interest |                                                     | ZT3 Wistar  | ZT9 Wistar                     | ZT15 Wistar              | ZT21 Wistar              |
|------------------|-----------------------------------------------------|-------------|--------------------------------|--------------------------|--------------------------|
| Per2             | $\Delta$ CT (normalised to Beta-actin)              | 9.86 ± 0.23 | 9.66 ± 0.15                    | 8.24 ± 0.13              | 8.44 ± 0.14              |
|                  | Fold change ( $\Delta\Delta$ CT)                    | 1.00 ± 0.00 | 1.19 ± 0.12                    | 3.14 ± 0.26              | 2.72 ± 0.28              |
|                  | <i>p</i> -value (from $\Delta$ CT, compared to ZT3) | N/A         | <i>p</i> = 0.4687<br><i>ns</i> | <i>p</i> < 0.0001<br>*** | <i>p</i> = 0.0008<br>*** |

**Appendix 1 figure 3- Gene expression fold-change levels of the circadian clock gene, Per2, in adult Wistar hearts isolated at ZT3, ZT9, ZT15 and ZT21.**

A. Bar chart showing the real-time quantitative RT-PCR of Per2 mRNA expression as fold-changes in left ventricular free-wall of ZT3 (Blue), ZT9 (White), ZT15 (Red) and ZT21 adult Wistar (Grey). Per2 mRNA expression was normalised to  $\beta$ -actin mRNA. Fold-changes of Per2 mRNA were calculated relative to the control (ZT3; Blue bars). The results are mean  $\pm$  S.E.M.; number of samples = ZT3 Wistar *n* = 7, ZT9 Wistar *n* = 8, ZT15 Wistar *n* = 7 and ZT21 Wistar *n* = 6. \*\*\* *p* < 0.0001, unpaired students *t* test performed on  $\Delta$ CT values.

B. Table showing the data used to produce figure in A

## **Appendix 2**

| EC <sub>50</sub>           |       |                      |                               |                               |                                     |
|----------------------------|-------|----------------------|-------------------------------|-------------------------------|-------------------------------------|
| Dose-response curve to ISO |       |                      | Diastolic Calcium (nM)        | Systolic calcium (nM)         | Amplitude of calcium transient (nM) |
| Wistar                     | 0.5Hz | Resting period (ZT3) | 4.41 ± 0.80                   | 3.44 ± 1.04                   | 3.73 ± 1.29                         |
|                            |       | Active period (ZT15) | 2.53 ± 0.77                   | 2.42 ± 0.33                   | 2.93 ± 0.71                         |
|                            |       | <i>p</i> -value      | <i>p</i> > 0.05 ( <i>ns</i> ) | <i>p</i> > 0.05 ( <i>ns</i> ) | <i>p</i> > 0.05 ( <i>ns</i> )       |
|                            | 2Hz   | Resting period (ZT3) | 2.19 ± 0.67                   | 2.89 ± 0.85                   | 2.03 ± 0.36                         |
|                            |       | Active period (ZT15) | 0.94 ± 0.45                   | 1.48 ± 0.23                   | 1.51 ± 0.22                         |
|                            |       | <i>p</i> -value      | <i>p</i> > 0.05 ( <i>ns</i> ) | <i>p</i> > 0.05 ( <i>ns</i> ) | <i>p</i> > 0.05 ( <i>ns</i> )       |

**Appendix 2 figure 1- The EC<sub>50</sub> obtained during  $\beta$ -adrenergic stimulation with isoproterenol in response to changes in stimulation frequency in resting period (ZT3) and active period (ZT15) myocytes.** Table showing the EC<sub>50</sub> for diastolic [Ca<sup>2+</sup>], systolic [Ca<sup>2+</sup>] and amplitude of the Ca<sup>2+</sup> transient during ISO stimulation and electrical field stimulation at 0.5Hz and 2Hz in resting period (ZT3) myocytes and active period (ZT15) myocytes, obtained from experiments graphically represented in results chapter 4 (figure 4.5). Values are the mean  $\pm$  S.E.M.; number of experiments/ hearts = resting period (ZT3) myocyte (0.5Hz *n* =12-26/6; 2Hz = 4-15/3) and active period (ZT15) myocyte (0.5Hz *n* = 16-22/6; 2Hz = 5-9/2); unpaired students *t* test.

| Maximal response to 100nM ISO |       |                      |                               |                               |                                     |
|-------------------------------|-------|----------------------|-------------------------------|-------------------------------|-------------------------------------|
|                               |       |                      | Diastolic Calcium (nM)        | Systolic calcium (nM)         | Amplitude of calcium transient (nM) |
| Wistar                        | 0.5Hz | Resting period (ZT3) | 254 ± 18                      | 1540 ± 165                    | 1286 ± 169                          |
|                               |       | Active period (ZT15) | 244 ± 25                      | 1036 ± 43                     | 791 ± 46                            |
|                               |       | <i>p</i> -value      | <i>p</i> > 0.05 ( <i>ns</i> ) | <i>p</i> < 0.01               | <i>p</i> < 0.01                     |
|                               | 2Hz   | Resting period (ZT3) | 476 ± 21                      | 3599 ± 1221                   | 3123 ± 1233                         |
|                               |       | Active period (ZT15) | 342 ± 36                      | 3287 ± 819                    | 2946 ± 811                          |
|                               |       | <i>p</i> -value      | <i>p</i> < 0.05               | <i>p</i> > 0.05 ( <i>ns</i> ) | <i>p</i> > 0.05 ( <i>ns</i> )       |

**Appendix 2 figure 2- The parameters of the Ca<sup>2+</sup> transient obtained during maximal isoproterenol stimulation in response to changes in stimulation frequency in resting period (ZT3) and active period (ZT15) myocytes.**

Table showing the diastolic [Ca<sup>2+</sup>], systolic [Ca<sup>2+</sup>] and amplitude of the Ca<sup>2+</sup> transient during maximal ISO stimulation (100nM) and electrical field stimulation at 0.5Hz and 2Hz in resting period (ZT3) myocytes and active period (ZT15) myocytes, obtained from experiments graphically represented in results chapter 4 (figure 4.5). Values are the mean ± S.E.M.; number of experiments/ hearts = resting period (ZT3) myocyte (0.5Hz *n* = 12-26/6; 2Hz = 4-15/3) and active period (ZT15) myocyte (0.5Hz *n* = 16-22/6; 2Hz = 5-9/2); \* *p* < 0.05, \*\* *p* < 0.01, unpaired students *t* test.

| Response to 10nM ISO |                       |                      |                               |                               |                                     |
|----------------------|-----------------------|----------------------|-------------------------------|-------------------------------|-------------------------------------|
|                      | Stimulation frequency |                      | Diastolic Calcium (nM)        | Systolic calcium (nM)         | Amplitude of calcium transient (nM) |
| Wistar               | 0.5Hz                 | Resting period (ZT3) | 228 ± 14                      | 1473 ± 156                    | 1246 ± 154                          |
|                      |                       | Active period (ZT15) | 231 ± 19                      | 1014 ± 44                     | 738 ± 51                            |
|                      |                       | <i>p</i> -value      | <i>p</i> > 0.05 ( <i>ns</i> ) | <i>p</i> < 0.01               | <i>p</i> < 0.01                     |
|                      | 1Hz                   | Resting period (ZT3) | 246 ± 17                      | 1921 ± 192                    | 1667 ± 188                          |
|                      |                       | Active period (ZT15) | 268 ± 18                      | 1234 ± 82                     | 966 ± 82                            |
|                      |                       | <i>p</i> -value      | <i>p</i> > 0.05 ( <i>ns</i> ) | <i>p</i> < 0.01               | <i>p</i> < 0.001                    |
|                      | 2Hz                   | Resting period (ZT3) | 438 ± 36                      | 4038 ± 1067                   | 3606 ± 1068                         |
|                      |                       | Active period (ZT15) | 426 ± 79                      | 2874 ± 1132                   | 2397 ± 846                          |
|                      |                       | <i>p</i> -value      | <i>p</i> > 0.05 ( <i>ns</i> ) | <i>p</i> > 0.05 ( <i>ns</i> ) | <i>p</i> > 0.05 ( <i>ns</i> )       |

**Appendix 2 figure 3- The effect of stimulation frequency on the parameters of the Ca<sup>2+</sup> transient in response to β-adrenergic stimulation with 10nM isoproterenol in resting period (ZT3) and active period (ZT15) myocytes.**

Table showing the diastolic [Ca<sup>2+</sup>], systolic [Ca<sup>2+</sup>] and amplitude of the Ca<sup>2+</sup> transient during superfusion of 10nM ISO and electrical field stimulation at 0.5Hz, 1Hz and 2Hz in resting period (ZT3) myocytes and active period (ZT15) myocytes, obtained from experiments graphically represented in results chapter 4 (figure 4.6). Values are the mean ± S.E.M.; number of experiments/ hearts = resting period (ZT3) myocyte (0.5Hz *n* = 16/6 ; 1Hz *n* = 47/10; 2Hz = 4/3) and active period (ZT15) myocyte (0.5Hz *n* = 20/6 ; 1Hz *n* = 49/11; 2Hz = 7/2); \*\* *p* < 0.01, \*\*\* *p* < 0.001, unpaired students *t* test.

## **Appendix 3**

|                               | Gene of interest                                 | Gene symbol | Standard curve slope value | Calculated gene efficiency (%) | $\Delta\Delta$ CT or Pfaffl method of analysis |
|-------------------------------|--------------------------------------------------|-------------|----------------------------|--------------------------------|------------------------------------------------|
| <i>House keeping gene</i>     | $\beta$ -actin                                   | actb        | -3.4                       | 95.0                           | N/A                                            |
| $\beta$ -adrenergic receptors | $\beta_1$ -adrenergic receptor                   | Adrb1       | -3.4                       | 95.0                           | $\Delta\Delta$ CT                              |
|                               | $\beta_3$ -adrenergic receptor                   | Adrb3       | N/A                        | N/A                            | $\Delta\Delta$ CT**                            |
| NOS signalling genes          | Neuronal nitric oxide synthase (nNOS)            | Nos1        | -3.8                       | 82.0                           | Pfaffl                                         |
|                               | Endothelial nitric oxide synthase (eNOS)         | Nos3        | -3.6                       | 89.5                           | Pfaffl                                         |
|                               | Nitric oxide synthase 1 adaptor protein (NOS1AP) | CAPON       | -3.4                       | 95.0                           | $\Delta\Delta$ CT                              |

**Appendix 3 figure 1- Standard curve data and mRNA analysis in left ventricular free-wall tissue isolated from resting period (ZT3) and active period (ZT15) adult Wistar rats**

Table showing the standard curve values obtained for each Taqman gene expression probe based assay investigated in chapter 5 of the results section using a 2-fold dilution. All Taqman probes shown produced a linear standard curve with PCR efficiency values between 80-110%. If the PCR efficiency of the gene of interest was within  $\pm 5\%$  from the efficiency of the housekeeping control gene,  $\beta$ -actin, then the mRNA were analysed using the  $\Delta\Delta$ CT method, however, if the PCR efficiency of the gene of interest differed from the efficiency of  $\beta$ -actin, then the Pfaffl method of mRNA analysis was preferred (see section 2.5.9 of materials and methods for details). \*\* The probe encoding  $\beta_3$ -adrenergic receptor did not produce an amplifiable standard curve and therefore, data using this probe were analysed with caution using the  $\Delta\Delta$ CT method.

## **Appendix 4**

**A**

| Resting calcium (normal Tyrode) |            |                      | Diastolic Calcium (nM) | Systolic calcium (nM) | Amplitude of calcium transient (nM) |
|---------------------------------|------------|----------------------|------------------------|-----------------------|-------------------------------------|
| WKY                             | Adolescent | Resting period (ZT3) | 94.2 ± 1.7             | 636.4 ± 39.9          | 542.1 ± 38.8                        |
|                                 |            | Active period (ZT15) | 107.8 ± 2.1            | 497.8 ± 19.0          | 390.0 ± 17.7                        |
|                                 |            | <i>p</i> -value      | <i>p</i> < 0.0001 ***  | <i>p</i> = 0.0023 **  | <i>p</i> = 0.0006 ***               |
|                                 | Adult      | Resting period (ZT3) | 119.9 ± 3.0            | 578.9 ± 27.7          | 459.0 ± 25.3                        |
|                                 |            | Active period (ZT15) | 110.1 ± 2.4            | 459.6 ± 16.6          | 349.6 ± 14.7                        |
|                                 |            | <i>p</i> -value      | <i>p</i> = 0.0128 *    | <i>p</i> = 0.0005 *** | <i>p</i> = 0.0004 ***               |

**B**

| Resting calcium (normal Tyrode) |            |                      | Diastolic Calcium (nM) | Systolic calcium (nM) | Amplitude of calcium transient (nM) |
|---------------------------------|------------|----------------------|------------------------|-----------------------|-------------------------------------|
| SHR                             | Adolescent | Resting period (ZT3) | 129.6 ± 1.8            | 759.2 ± 29.5          | 629.6 ± 28.7                        |
|                                 |            | Active period (ZT15) | 111.2 ± 1.4            | 554.1 ± 20.3          | 442.9 ± 20.4                        |
|                                 |            | <i>p</i> -value      | <i>p</i> < 0.0001 ***  | <i>p</i> < 0.0001 *** | <i>p</i> < 0.0001 ***               |
|                                 | Adult      | Resting period (ZT3) | 127.3 ± 3.8            | 666.1 ± 33.3          | 538.7 ± 30.7                        |
|                                 |            | Active period (ZT15) | 130.5 ± 4.3            | 669.2 ± 31.2          | 538.7 ± 29.0                        |
|                                 |            | <i>p</i> -value      | <i>p</i> = 0.5794      | <i>p</i> = 0.9449     | <i>p</i> = 0.9997                   |

**Appendix 4 figure 1- The parameters of the Ca<sup>2+</sup> transient of resting period (ZT3) and active period (ZT15) myocytes isolated from adolescent and adult WKY and SHR recorded in normal Tyrode**

A. Table showing the diastolic [Ca<sup>2+</sup>], systolic [Ca<sup>2+</sup>] and amplitude of the Ca<sup>2+</sup> transient recorded from resting period (ZT3) and active period (ZT15) myocytes from adolescent and adult WKY, stimulated at 1Hz and superfused with normal Tyrode. Values are the mean ± S.E.M.; number of experiments/ hearts = resting period (ZT3) myocyte (adolescent *n* = 18/ 3; adult *n* = 20/3) and active period (ZT15) myocyte (adolescent *n* = 21/ 3; adult *n* = 22/3); \* *p* < 0.05, \*\* *p* < 0.01, \*\*\* *p* < 0.001, unpaired students *t* test.

B. Table showing the diastolic [Ca<sup>2+</sup>], systolic [Ca<sup>2+</sup>] and amplitude of the Ca<sup>2+</sup> transient recorded from resting period (ZT3) and active period (ZT15) myocytes from adolescent and adult SHR, stimulated at 1Hz and superfused with normal Tyrode. Values are the mean ± S.E.M.; number of experiments/ hearts = resting period (ZT3) myocyte (adolescent *n* = 23/ 3; adult *n* = 21/3) and active period (ZT15) myocyte (adolescent *n* = 19/ 3; adult *n* = 20/3); \*\*\* *p* < 0.001, unpaired students *t* test.

A

| Maximal response to 100nM ISO |            |                      |                        |                       |                                     |
|-------------------------------|------------|----------------------|------------------------|-----------------------|-------------------------------------|
|                               |            |                      | Diastolic Calcium (nM) | Systolic calcium (nM) | Amplitude of calcium transient (nM) |
| WKY                           | Adolescent | Resting period (ZT3) | 117.3 ± 8.6            | 1678.8 ± 70.6         | 1555.5 ± 71.5                       |
|                               |            | Active period (ZT15) | 165.1 ± 7.8            | 1299.8 ± 122.6        | 1247.3 ± 95.7                       |
|                               |            | <i>p</i> -value      | <i>ns</i>              | <i>ns</i>             | <i>ns</i>                           |
|                               | Adult      | Resting period (ZT3) | 178.7 ± 8.4            | 2024.4 ± 162.9        | 1845.7 ± 161.4                      |
|                               |            | Active period (ZT15) | 159.1 ± 6.9            | 1334.0 ± 90.2         | 1174.9 ± 89.6                       |
|                               |            | <i>p</i> -value      | <i>ns</i>              | <i>p</i> = 0.001 ***  | <i>p</i> < 0.001 ***                |

B

| Maximal response to 100nM ISO |            |                      |                        |                       |                                     |
|-------------------------------|------------|----------------------|------------------------|-----------------------|-------------------------------------|
|                               |            |                      | Diastolic Calcium (nM) | Systolic calcium (nM) | Amplitude of calcium transient (nM) |
| SHR                           | Adolescent | Resting period (ZT3) | 183.0 ± 8.0            | 1945.2 ± 107.9        | 1792.7 ± 114.9                      |
|                               |            | Active period (ZT15) | 168.9 ± 9.6            | 1256.9 ± 110.5        | 1033.9 ± 129.7                      |
|                               |            | <i>p</i> -value      | <i>ns</i>              | <i>p</i> < 0.01 **    | <i>p</i> < 0.05 *                   |
|                               | Adult      | Resting period (ZT3) | 233.7 ± 16.3           | 3961.6 ± 363.1        | 3727.9 ± 364.3                      |
|                               |            | Active period (ZT15) | 268.6 ± 19.0           | 3461.4 ± 218.5        | 3172.0 ± 224.0                      |
|                               |            | <i>p</i> -value      | <i>ns</i>              | <i>ns</i>             | <i>ns</i>                           |

**Appendix 4 figure 2- The parameters of the Ca<sup>2+</sup> transient obtained during maximal isoproterenol stimulation (100nM) in resting period (ZT3) and active period (ZT15) myocytes isolated from adolescent and adult WKY and SHR.**

A. Table showing the diastolic [Ca<sup>2+</sup>], systolic [Ca<sup>2+</sup>] and amplitude of the Ca<sup>2+</sup> transient recorded from resting period (ZT3) and active period (ZT15) myocytes from adolescent and adult WKY, stimulated at 1Hz and superfused with normal Tyrode containing 100nM ISO. Values are mean ± S.E.M.; numbers of experiments/ hearts = resting period (ZT3) myocyte (adolescent *n* = 10-23/3; adult *n* = 14-20/3) and active period (ZT15) myocyte (adolescent *n* = 14-20/3; adult *n* = 17-20/3). \*\*\* *p* < 0.001, two way ANOVA followed by Bonferroni *post hoc* test.

B. Table showing the diastolic [Ca<sup>2+</sup>], systolic [Ca<sup>2+</sup>] and amplitude of the Ca<sup>2+</sup> transient recorded from resting period (ZT3) and active period (ZT15) myocytes from adolescent and adult SHR, stimulated at 1Hz and superfused with normal Tyrode containing 100nM ISO. Values are mean ± S.E.M.; numbers of experiments/ hearts = resting period (ZT3) myocyte (adolescent *n* = 11-18/3; adult *n* = 14-21/3) and active period (ZT15) myocyte (adolescent *n* = 11-21/3; adult *n* = 19-21/3). \* *p* < 0.05, \*\* *p* < 0.01, two way ANOVA followed by Bonferroni *post hoc* test.

# Bibliography

- ABI-GERGES, N., FISCHMEISTER, R. & MERY, P. F. (2001) G protein-mediated inhibitory effect of a nitric oxide donor on the L-type  $\text{Ca}^{2+}$  current in rat ventricular myocytes. *J Physiol*, 531, 117-30.
- ADACHI-AKAHANE, S., CLEEMANN, L. & MORAD, M. (1996) Cross-signaling between L-type  $\text{Ca}^{2+}$  channels and ryanodine receptors in rat ventricular myocytes. *J Gen Physiol*, 108, 435-54.
- AKERSTEDT, T. (1990) Psychological and psychophysiological effects of shift work. *Scand J Work Environ Health*, 16 Suppl 1, 67-73.
- AKHTAR, R. A., REDDY, A. B., MAYWOOD, E. S., CLAYTON, J. D., KING, V. M., SMITH, A. G., GANT, T. W., HASTINGS, M. H. & KYRIACOU, C. P. (2002) Circadian cycling of the mouse liver transcriptome, as revealed by cDNA microarray, is driven by the suprachiasmatic nucleus. *Curr Biol*, 12, 540-50.
- AKITA, M., ISHII, K., KUWAHARA, M. & TSUBONE, H. (2002) Power spectral analysis of heart rate variability for assessment of diurnal variation of autonomic nervous activity in guinea pigs. *Exp Anim*, 51, 1-7.
- ALTAMIRANO, J. & BERS, D. M. (2007) Effect of intracellular  $\text{Ca}^{2+}$  and action potential duration on L-type  $\text{Ca}^{2+}$  channel inactivation and recovery from inactivation in rabbit cardiac myocytes. *Am J Physiol Heart Circ Physiol*, 293, H563-73.
- ANDERSON, K. P. (2003) Sympathetic nervous system activity and ventricular tachyarrhythmias: recent advances. *Ann Noninvasive Electrocardiol*, 8, 75-89.
- ARKING, D. E., PFEUFER, A., POST, W., KAO, W. H., NEWTON-CHEH, C., IKEDA, M., WEST, K., KASHUK, C., AKYOL, M., PERZ, S., JALILZADEH, S., ILLIG, T., GIEGER, C., GUO, C. Y., LARSON, M. G., WICHMANN, H. E., MARBAN, E., O'DONNELL, C. J., HIRSCHHORN, J. N., KAAB, S., SPOONER, P. M., MEITINGER, T. & CHAKRAVARTI, A. (2006) A common genetic variant in the NOS1 regulator NOS1AP modulates cardiac repolarization. *Nat Genet*, 38, 644-51.
- ARMOUNDAS, A. A., HOBAL, I. A., TOMASELLI, G. F., WINSLOW, R. L. & O'ROURKE, B. (2003) Role of sodium-calcium exchanger in modulating the action potential of ventricular myocytes from normal and failing hearts. *Circ Res*, 93, 46-53.
- ARNTZ, H. R., WILLICH, S. N., OEFF, M., BRUGGEMANN, T., STERN, R., HEINZMANN, A., MATENAER, B. & SCHRODER, R. (1993) Circadian variation of sudden cardiac death reflects age-related variability in ventricular fibrillation. *Circulation*, 88, 2284-9.
- ARONOW, W. S. & AHN, C. (2003) Circadian variation of death from congestive heart failure after prior myocardial infarction in patients >60 years of age. *Am J Cardiol*, 92, 1354-5.
- ASHLEY, E. A., SEARS, C. E., BRYANT, S. M., WATKINS, H. C. & CASADEI, B. (2002) Cardiac nitric oxide synthase 1 regulates basal and beta-adrenergic contractility in murine ventricular myocytes. *Circulation*, 105, 3011-6.
- AUDIGANE, L., KERFANT, B. G., EL HARCHI, A., LORENZEN-SCHMIDT, I., TOUMANIANTZ, G., CANTEREAU, A., POTREAU, D., CHARPENTIER, F., NOIREAUD, J. & GAUTHIER, C. (2009) Rabbit, a relevant model for the study of cardiac beta 3-adrenoceptors. *Exp Physiol*, 94, 400-11.
- AYERS, N. A., KAPAS, L. & KRUEGER, J. M. (1996) Circadian variation of nitric oxide synthase activity and cytosolic protein levels in rat brain. *Brain Res*, 707, 127-30.
- BAARTSCHEER, A. (2001) Adenovirus gene transfer of SERCA in heart failure. A promising therapeutic approach? *Cardiovasc Res*, 49, 249-52.
- BALIJEPALLI, R. C., FOELL, J. D., HALL, D. D., HELL, J. W. & KAMP, T. J. (2006) Localization of cardiac L-type  $\text{Ca}^{2+}$  channels to a caveolar macromolecular signaling complex is required for beta(2)-adrenergic regulation. *Proc Natl Acad Sci USA*, 103, 7500-5.
- BALLIGAND, J. L. & CANNON, P. J. (1997) Nitric oxide synthases and cardiac muscle. Autocrine and paracrine influences. *Arterioscler Thromb Vasc Biol*, 17, 1846-58.
- BALSALOBRE, A., BROWN, S. A., MARCACCI, L., TRONCHE, F., KELLENDONK, C., REICHARDT, H. M., SCHUTZ, G. & SCHIBLER, U. (2000) Resetting of circadian time in peripheral tissues by glucocorticoid signaling. *Science*, 289, 2344-7.

- BALSALOBRE, A., DAMIOLA, F. & SCHIBLER, U. (1998) A serum shock induces circadian gene expression in mammalian tissue culture cells. *Cell*, 93, 929-37.
- BARBIER, J., MOUAS, C., RANNOU-BEKONO, F. & CARRE, F. (2007a) Existence of beta(3)-adrenoceptors in rat heart: functional implications. *Clin Exp Pharmacol Physiol*, 34, 796-8.
- BARBIER, J., RANNOU-BEKONO, F., MARCHAIS, J., TANGUY, S. & CARRE, F. (2007b) Alterations of beta3-adrenoceptors expression and their myocardial functional effects in physiological model of chronic exercise-induced cardiac hypertrophy. *Mol Cell Biochem*, 300, 69-75.
- BARBIERI, M., VARANI, K., CERBAI, E., GUERRA, L., LI, Q., BOREA, P. A. & MUGELLI, A. (1994) Electrophysiological basis for the enhanced cardiac arrhythmogenic effect of isoprenaline in aged spontaneously hypertensive rats. *J Mol Cell Cardiol*, 26, 849-60.
- BAROUCH, L. A., HARRISON, R. W., SKAF, M. W., ROSAS, G. O., CAPPOLA, T. P., KOBEISSI, Z. A., HOBBI, I. A., LEMMON, C. A., BURNETT, A. L., O'ROURKE, B., RODRIGUEZ, E. R., HUANG, P. L., LIMA, J. A., BERKOWITZ, D. E. & HARE, J. M. (2002) Nitric oxide regulates the heart by spatial confinement of nitric oxide synthase isoforms. *Nature*, 416, 337-9.
- BASSANI, J. W., BASSANI, R. A. & BERS, D. M. (1994) Relaxation in rabbit and rat cardiac cells: species-dependent differences in cellular mechanisms. *J Physiol*, 476, 279-93.
- BASSANI, J. W., YUAN, W. & BERS, D. M. (1995) Fractional SR Ca release is regulated by trigger Ca and SR Ca content in cardiac myocytes. *Am J Physiol*, 268, C1313-9.
- BEARD, N. A., WEI, L. & DULHUNTY, A. F. (2009) Ca(2+) signaling in striated muscle: the elusive roles of triadin, junctin, and calsequestrin. *Eur Biophys J*, 39, 27-36.
- BEIGI, F., OSKOUEI, B. N., ZHENG, M., COOKE, C. A., LAMIRAULT, G. & HARE, J. M. (2009) Cardiac nitric oxide synthase-1 localization within the cardiomyocyte is accompanied by the adaptor protein, CAPON. *Nitric Oxide*, 21, 226-33.
- BENDALL, J. K., DAMY, T., RATAJCZAK, P., LOYER, X., MONCEAU, V., MARTY, I., MILLIEZ, P., ROBIDEL, E., MAROTTE, F., SAMUEL, J. L. & HEYMES, C. (2004) Role of myocardial neuronal nitric oxide synthase-derived nitric oxide in beta-adrenergic hyporesponsiveness after myocardial infarction-induced heart failure in rat. *Circulation*, 110, 2368-75.
- BENGEL, F. M., UEBERFUHR, P., SCHIEPEL, N., NEKOLLA, S. G., REICHART, B. & SCHWAIGER, M. (2001) Effect of sympathetic reinnervation on cardiac performance after heart transplantation. *N Engl J Med*, 345, 731-8.
- BERS, D. M. (2001) *Excitation-contraction coupling and cardiac contractile force*, Dordrecht ; London, Kluwer Academic.
- BERS, D. M. (2002) Cardiac excitation-contraction coupling. *Nature*, 415, 198-205.
- BERS, D. M. (2006) Altered cardiac myocyte Ca regulation in heart failure. *Physiology (Bethesda)*, 21, 380-7.
- BETZENHAUSER, M. J., FIKE, J. L., WAGNER, L. E., 2ND & YULE, D. I. (2009) Protein kinase A increases type-2 inositol 1,4,5-trisphosphate receptor activity by phosphorylation of serine 937. *J Biol Chem*, 284, 25116-25.
- BEXTON, R. S., VALLIN, H. O. & CAMM, A. J. (1986) Diurnal variation of the QT interval--influence of the autonomic nervous system. *Br Heart J*, 55, 253-8.
- BIEL, M., SCHNEIDER, A. & WAHL, C. (2002) Cardiac HCN channels: structure, function, and modulation. *Trends Cardiovasc Med*, 12, 206-12.
- BOLUYT, M. O. & BING, O. H. (2000) Matrix gene expression and decompensated heart failure: the aged SHR model. *Cardiovasc Res*, 46, 239-49.
- BOOLELL, M., ALLEN, M. J., BALLARD, S. A., GEPI-ATTEE, S., MUIRHEAD, G. J., NAYLOR, A. M., OSTERLOH, I. H. & GINGELL, C. (1996) Sildenafil: an orally active type 5 cyclic GMP-specific phosphodiesterase inhibitor for the treatment of penile erectile dysfunction. *Int J Impot Res*, 8, 47-52.
- BOUCHARD, R. A., CLARK, R. B. & GILES, W. R. (1995) Effects of action potential duration on excitation-contraction coupling in rat ventricular myocytes. Action potential voltage-clamp measurements. *Circ Res*, 76, 790-801.
- BRAY, M. S., SHAW, C. A., MOORE, M. W., GARCIA, R. A., ZANQUETTA, M. M., DURGAN, D. J., JEONG, W. J., TSAI, J. Y., BUGGER, H., ZHANG, D., ROHRWASSER, A., RENNISON, J. H., DYCK, J. R., LITWIN, S. E., HARDIN, P. E., CHOW, C. W., CHANDLER, M. P., ABEL, E. D. & YOUNG, M. E. (2008) Disruption of the circadian clock within the cardiomyocyte influences myocardial contractile function, metabolism, and gene expression. *Am J Physiol Heart Circ Physiol*, 294, H1036-47.

- BREDOW, S., GUHA-THAKURTA, N., TAISHI, P., OBAL, F., JR. & KRUEGER, J. M. (1997) Diurnal variations of tumor necrosis factor alpha mRNA and alpha-tubulin mRNA in rat brain. *Neuroimmunomodulation*, 4, 84-90.
- BREMER, Y. A., SALLOUM, F., OCKAILI, R., CHOU, E., MOSKOWITZ, W. B. & KUKREJA, R. C. (2005) Sildenafil citrate (viagra) induces cardioprotective effects after ischemia/reperfusion injury in infant rabbits. *Pediatr Res*, 57, 22-7.
- BRISTOW, M. R., GINSBURG, R., UMANS, V., FOWLER, M., MINOBE, W., RASMUSSEN, R., ZERA, P., MENLOVE, R., SHAH, P., JAMIESON, S. & ET AL. (1986) Beta 1- and beta 2-adrenergic-receptor subpopulations in nonfailing and failing human ventricular myocardium: coupling of both receptor subtypes to muscle contraction and selective beta 1-receptor down-regulation in heart failure. *Circ Res*, 59, 297-309.
- BRISTOW, M. R., MINOBE, W. A., RAYNOLDS, M. V., PORT, J. D., RASMUSSEN, R., RAY, P. E. & FELDMAN, A. M. (1993) Reduced beta 1 receptor messenger RNA abundance in the failing human heart. *J Clin Invest*, 92, 2737-45.
- BRODDE, O. E. (1993) Beta-adrenoceptors in cardiac disease. *Pharmacol Ther*, 60, 405-30.
- BRUNNER, F., ANDREW, P., WOLKART, G., ZECHNER, R. & MAYER, B. (2001) Myocardial contractile function and heart rate in mice with myocyte-specific overexpression of endothelial nitric oxide synthase. *Circulation*, 104, 3097-102.
- BRUNNER, M., KODIROV, S. A., MITCHELL, G. F., BUCKETT, P. D., SHIBATA, K., FOLCO, E. J., BAKER, L., SALAMA, G., CHAN, D. P., ZHOU, J. & KOREN, G. (2003) In vivo gene transfer of Kv1.5 normalizes action potential duration and shortens QT interval in mice with long QT phenotype. *Am J Physiol Heart Circ Physiol*, 285, H194-203.
- BUHLER, H. U., DA PRADA, M., HAEFELY, W. & PICOTTI, G. B. (1978) Plasma adrenaline, noradrenaline and dopamine in man and different animal species. *J Physiol*, 276, 311-20.
- BURGER, D. E., LU, X., LEI, M., XIANG, F. L., HAMMOUD, L., JIANG, M., WANG, H., JONES, D. L., SIMS, S. M. & FENG, Q. (2009) Neuronal nitric oxide synthase protects against myocardial infarction-induced ventricular arrhythmia and mortality in mice. *Circulation*, 120, 1345-54.
- BURKARD, N., ROKITA, A. G., KAUFMANN, S. G., HALLHUBER, M., WU, R., HU, K., HOFMANN, U., BONZ, A., FRANTZ, S., CARTWRIGHT, E. J., NEYSES, L., MAIER, L. S., MAIER, S. K., RENNE, T., SCHUH, K. & RITTER, O. (2007) Conditional neuronal nitric oxide synthase overexpression impairs myocardial contractility. *Circ Res*, 100, e32-44.
- BUSTIN, S. A. (2000) Absolute quantification of mRNA using real-time reverse transcription polymerase chain reaction assays. *J Mol Endocrinol*, 25, 169-93.
- BUSTIN, S. A. & NOLAN, T. (2004) Pitfalls of quantitative real-time reverse-transcription polymerase chain reaction. *J Biomol Tech*, 15, 155-66.
- CALAGHAN, S., KOZERA, L. & WHITE, E. (2008) Compartmentalisation of cAMP-dependent signalling by caveolae in the adult cardiac myocyte. *J Mol Cell Cardiol*, 45, 88-92.
- CALAGHAN, S. & WHITE, E. (2006) Caveolae modulate excitation-contraction coupling and beta2-adrenergic signalling in adult rat ventricular myocytes. *Cardiovasc Res*, 69, 816-24.
- CASADEI, B. (2006) The emerging role of neuronal nitric oxide synthase in the regulation of myocardial function. *Exp Physiol*, 91, 943-55.
- CASTELLANO, M. & BOHM, M. (1997) The cardiac beta-adrenoceptor-mediated signaling pathway and its alterations in hypertensive heart disease. *Hypertension*, 29, 715-22.
- CHA, R. S. & THILLY, W. G. (1993) Specificity, efficiency, and fidelity of PCR. *PCR Methods Appl*, 3, S18-29.
- CHANG, K. C., BARTH, A. S., SASANO, T., KIZANA, E., KASHIWAKURA, Y., ZHANG, Y., FOSTER, D. B. & MARBAN, E. (2008) CAPON modulates cardiac repolarization via neuronal nitric oxide synthase signaling in the heart. *Proc Natl Acad Sci US A*, 105, 4477-82.
- CHARPENTIER, F., DROUIN, E., GAUTHIER, C. & LE MAREC, H. (1993) Early after/depolarizations and triggered activity: mechanisms and autonomic regulation. *Fundam Clin Pharmacol*, 7, 39-49.
- CHEN-IZU, Y., XIAO, R. P., IZU, L. T., CHENG, H., KUSCHEL, M., SPURGEON, H. & LAKATTA, E. G. (2000) G(i)-dependent localization of beta(2)-adrenergic receptor signaling to L-type Ca(2+) channels. *Biophys J*, 79, 2547-56.
- CHEN, X., PIACENTINO, V., 3RD, FURUKAWA, S., GOLDMAN, B., MARGULIES, K. B. & HOUSER, S. R. (2002) L-type Ca<sup>2+</sup> channel density and regulation are altered in failing human ventricular myocytes and recover after support with mechanical assist devices. *Circ Res*, 91, 517-24.
- CHENG, H., LEDERER, W. J. & CANNELL, M. B. (1993) Calcium sparks: elementary events underlying excitation-contraction coupling in heart muscle. *Science*, 262, 740-4.

- CHENG, H. J., ZHANG, Z. S., ONISHI, K., UKAI, T., SANE, D. C. & CHENG, C. P. (2001) Upregulation of functional beta(3)-adrenergic receptor in the failing canine myocardium. *Circ Res*, 89, 599-606.
- CHOMCZYNSKI, P. (1992) Solubilization in formamide protects RNA from degradation. *Nucleic Acids Res*, 20, 3791-2.
- CHOMCZYNSKI, P. & SACCHI, N. (2006) The single-step method of RNA isolation by acid guanidinium thiocyanate-phenol-chloroform extraction: twenty-something years on. *Nat Protoc*, 1, 581-5.
- CHOPRA, N., YANG, T., ASGHARI, P., MOORE, E. D., HUKU, S., AKIN, B., CATTOLICA, R. A., PEREZ, C. F., HLAING, T., KNOLLMANN-RITSCHER, B. E., JONES, L. R., PESSAH, I. N., ALLEN, P. D., FRANZINI-ARMSTRONG, C. & KNOLLMANN, B. C. (2009) Ablation of triadin causes loss of cardiac Ca<sup>2+</sup> release units, impaired excitation-contraction coupling, and cardiac arrhythmias. *Proc Natl Acad Sci U S A*, 106, 7636-41.
- CINCA, J., MOYA, A., FIGUERAS, J., ROMA, F. & RIUS, J. (1986) Circadian variations in the electrical properties of the human heart assessed by sequential bedside electrophysiologic testing. *Am Heart J*, 112, 315-21.
- CLELAND, J. G., CHATTOPADHYAY, S., KHAND, A., HOUGHTON, T. & KAYE, G. C. (2002) Prevalence and incidence of arrhythmias and sudden death in heart failure. *Heart Fail Rev*, 7, 229-42.
- COKER, R. H., KRISHNA, M. G., LACY, D. B., ALLEN, E. J. & WASSERMAN, D. H. (1997) Sympathetic drive to liver and nonhepatic splanchnic tissue during heavy exercise. *J Appl Physiol*, 82, 1244-9.
- COLLINS, H. E. & RODRIGO, G. C. (2010) Inotropic response of cardiac ventricular myocytes to beta-adrenergic stimulation with isoproterenol exhibits diurnal variation: involvement of nitric oxide. *Circ Res*, 106, 1244-52.
- COLWELL, C. S. (2000) Circadian modulation of calcium levels in cells in the suprachiasmatic nucleus. *Eur J Neurosci*, 12, 571-6.
- CONRAD, C. H., BROOKS, W. W., ROBINSON, K. G. & BING, O. H. (1991) Impaired myocardial function in spontaneously hypertensive rats with heart failure. *Am J Physiol*, 260, H136-45.
- CURRIE, S. & SMITH, G. L. (1999) Enhanced phosphorylation of phospholamban and downregulation of sarco/endoplasmic reticulum Ca<sup>2+</sup> ATPase type 2 (SERCA 2) in cardiac sarcoplasmic reticulum from rabbits with heart failure. *Cardiovasc Res*, 41, 135-46.
- DAMY, T., RATAJCZAK, P., ROBIDEL, E., BENDALL, J. K., OLIVIERO, P., BOCZKOWSKI, J., EBRAHIMIAN, T., MAROTTE, F., SAMUEL, J. L. & HEYMES, C. (2003) Up-regulation of cardiac nitric oxide synthase 1-derived nitric oxide after myocardial infarction in senescent rats. *FASEB J*, 17, 1934-6.
- DAMY, T., RATAJCZAK, P., SHAH, A. M., CAMORS, E., MARTY, I., HASENFUSS, G., MAROTTE, F., SAMUEL, J. L. & HEYMES, C. (2004) Increased neuronal nitric oxide synthase-derived NO production in the failing human heart. *Lancet*, 363, 1365-7.
- DAVIA, K., BERNOBICH, E., RANU, H. K., DEL MONTE, F., TERRACCIANO, C. M., MACLEOD, K. T., ADAMSON, D. L., CHAUDHRI, B., HAJJAR, R. J. & HARDING, S. E. (2001) SERCA2A overexpression decreases the incidence of aftercontractions in adult rabbit ventricular myocytes. *J Mol Cell Cardiol*, 33, 1005-15.
- DAVIDSON, A. J., LONDON, B., BLOCK, G. D. & MENAKER, M. (2005) Cardiovascular tissues contain independent circadian clocks. *Clin Exp Hypertens*, 27, 307-11.
- DAWSON, D., LYGATE, C. A., ZHANG, M. H., HULBERT, K., NEUBAUER, S. & CASADEI, B. (2005) nNOS gene deletion exacerbates pathological left ventricular remodeling and functional deterioration after myocardial infarction. *Circulation*, 112, 3729-37.
- DAY, C. P., MCCOMB, J. M. & CAMPBELL, R. W. (1990) QT dispersion: an indication of arrhythmia risk in patients with long QT intervals. *Br Heart J*, 63, 342-4.
- DE FERRARI, G. M., VIOLA, M. C., D'AMATO, E., ANTOLINI, R. & FORTI, S. (1995) Distinct patterns of calcium transients during early and delayed afterdepolarizations induced by isoproterenol in ventricular myocytes. *Circulation*, 91, 2510-5.
- DE LUCA, G., SURYAPRANATA, H., OTTERVANGER, J. P., VAN 'T HOF, A. W., HOORNTJE, J. C., GOSSELINK, A. T., DAMBRINK, J. H., ZIJLSTRA, F. & DE BOER, M. J. (2005) Circadian variation in myocardial perfusion and mortality in patients with ST-segment elevation myocardial infarction treated by primary angioplasty. *Am Heart J*, 150, 1185-9.
- DEGAUTE, J. P., VAN DE BORNE, P., LINKOWSKI, P. & VAN CAUTER, E. (1991) Quantitative analysis of the 24-hour blood pressure and heart rate patterns in young men. *Hypertension*, 18, 199-210.

- DELGADO, C., ARTILES, A., GOMEZ, A. M. & VASSORT, G. (1999) Frequency-dependent increase in cardiac  $Ca^{2+}$  current is due to reduced  $Ca^{2+}$  release by the sarcoplasmic reticulum. *J Mol Cell Cardiol*, 31, 1783-93.
- DEY, A., SACHAN, N., OH, M., HILL, J. A. & ROTHERMEL, B. A. (2008) Normal Circadian Rhythms In Calcineurin-dependent Signaling And Protein Phosphorylation Are Disrupted In Heart Failure. *Circulation*, 118, S\_425.
- DHEDA, K., HUGGETT, J. F., BUSTIN, S. A., JOHNSON, M. A., ROOK, G. & ZUMLA, A. (2004) Validation of housekeeping genes for normalizing RNA expression in real-time PCR. *Biotechniques*, 37, 112-4, 116, 118-9.
- DIFRANCESCO, D. (1995) The onset and autonomic regulation of cardiac pacemaker activity: relevance of the f current. *Cardiovasc Res*, 29, 449-56.
- DODT, C., BRECKLING, U., DERAD, I., FEHM, H. L. & BORN, J. (1997) Plasma epinephrine and norepinephrine concentrations of healthy humans associated with nighttime sleep and morning arousal. *Hypertension*, 30, 71-6.
- DORIAN, P. (2005) Antiarrhythmic action of beta-blockers: potential mechanisms. *J Cardiovasc Pharmacol Ther*, 10 Suppl 1, S15-22.
- DURGAN, D. J., HOTZE, M. A., TOMLIN, T. M., EGBEJIMI, O., GRAVELEAU, C., ABEL, E. D., SHAW, C. A., BRAY, M. S., HARDIN, P. E. & YOUNG, M. E. (2005) The intrinsic circadian clock within the cardiomyocyte. *Am J Physiol Heart Circ Physiol*, 289, H1530-41.
- DURGAN, D. J., PULINILKUNNIL, T., VILLEGAS-MONTOYA, C., GARVEY, M. E., FRANGOIANNIS, N. G., MICHAEL, L. H., CHOW, C. W., DYCK, J. R. & YOUNG, M. E. (2010) Short communication: ischemia/reperfusion tolerance is time-of-day-dependent: mediation by the cardiomyocyte circadian clock. *Circ Res*, 106, 546-50.
- DURGAN, D. J. & YOUNG, M. E. (2010) The cardiomyocyte circadian clock: emerging roles in health and disease. *Circ Res*, 106, 647-58.
- EDERY, I. (2000) Circadian rhythms in a nutshell. *Physiol Genomics*, 3, 59-74.
- ENDO, M. & BLINKS, J. R. (1988) Actions of sympathomimetic amines on the  $Ca^{2+}$  transients and contractions of rabbit myocardium: reciprocal changes in myofibrillar responsiveness to  $Ca^{2+}$  mediated through alpha- and beta-adrenoceptors. *Circ Res*, 62, 247-65.
- ENDO, M., SCHUMANN, H. J., KRAPPITZ, N. & HILLEN, B. (1976) alpha-Adrenoceptors mediating positive inotropic effects on the ventricular myocardium: some aspects of structure-activity relationship of sympathomimetic amines. *Jpn J Pharmacol*, 26, 179-90.
- ENGEL, B. T. & TALAN, M. I. (1991) Diurnal variations in central venous pressure. *Acta Physiol Scand*, 141, 273-8.
- FAGARD, R., MACOR, F. & VANHAECKE, J. (1995) Signs of functional efferent reinnervation of the heart in patients after cardiac transplantation. *Acta Cardiol*, 50, 369-80.
- FAUCONNIER, J., LACAMPAGNE, A., RAUZIER, J. M., VASSORT, G. & RICHARD, S. (2005)  $Ca^{2+}$ -dependent reduction of IK1 in rat ventricular cells: a novel paradigm for arrhythmia in heart failure? *Cardiovasc Res*, 68, 204-12.
- FINK, M. A., ZAKHARY, D. R., MACKAY, J. A., DESNOYER, R. W., APPERSON-HANSEN, C., DAMRON, D. S. & BOND, M. (2001) AKAP-mediated targeting of protein kinase a regulates contractility in cardiac myocytes. *Circ Res*, 88, 291-7.
- FISSET, C., CLARK, R. B., LARSEN, T. S. & GILES, W. R. (1997) A rapidly activating sustained  $K^{+}$  current modulates repolarization and excitation-contraction coupling in adult mouse ventricle. *J Physiol*, 504 ( Pt 3), 557-63.
- FLEIGE, S. & PFAFFL, M. W. (2006) RNA integrity and the effect on the real-time qRT-PCR performance. *Mol Aspects Med*, 27, 126-39.
- FOWLER, M. R., NAZ, J. R., GRAHAM, M. D., ORCHARD, C. H. & HARRISON, S. M. (2007) Age and hypertrophy alter the contribution of sarcoplasmic reticulum and  $Na^{+}/Ca^{2+}$  exchange to  $Ca^{2+}$  removal in rat left ventricular myocytes. *J Mol Cell Cardiol*, 42, 582-9.
- FOZZARD, H. A. (1992) Afterdepolarizations and triggered activity. *Basic Res Cardiol*, 87 Suppl 2, 105-13.
- FRAMPTON, J. E., HARRISON, S. M., BOYETT, M. R. & ORCHARD, C. H. (1991)  $Ca^{2+}$  and  $Na^{+}$  in rat myocytes showing different force-frequency relationships. *Am J Physiol*, 261, C739-50.
- GAROFALO, F., PARISELLA, M. L., AMELIO, D., TOTA, B. & IMBROGNO, S. (2009) Phospholamban S-nitrosylation modulates Starling response in fish heart. *Proc Biol Sci*, 276, 4043-52.
- GAUTHIER, C., LEBLAIS, V., KOBZIK, L., TROCHU, J. N., KHANDOUDI, N., BRIL, A., BALLIGAND, J. L. & LE MAREC, H. (1998) The negative inotropic effect of beta3-

- adrenoceptor stimulation is mediated by activation of a nitric oxide synthase pathway in human ventricle. *J Clin Invest*, 102, 1377-84.
- GAUTHIER, C., LEBLAIS, V., MONIOTTE, S., LANGIN, D. & BALLIGAND, J. L. (2000) The negative inotropic action of catecholamines: role of beta3-adrenoceptors. *Can J Physiol Pharmacol*, 78, 681-90.
- GAUTHIER, C., TAVERNIER, G., CHARPENTIER, F., LANGIN, D. & LE MAREC, H. (1996) Functional beta3-adrenoceptor in the human heart. *J Clin Invest*, 98, 556-62.
- GELLEN, B., FERNANDEZ-VELASCO, M., BRIEC, F., VINET, L., LEQUANG, K., ROUET-BENZINEB, P., BENITAH, J. P., PEZET, M., PALAIS, G., PELLEGRIN, N., ZHANG, A., PERRIER, R., ESCOUBET, B., MARNIQUET, X., RICHARD, S., JAISSE, F., GOMEZ, A. M., CHARPENTIER, F. & MERCADIER, J. J. (2008) Conditional FKBP12.6 overexpression in mouse cardiac myocytes prevents triggered ventricular tachycardia through specific alterations in excitation-contraction coupling. *Circulation*, 117, 1778-86.
- GINSBURG, K. S. & BERS, D. M. (2005) Isoproterenol does not enhance Ca-dependent Na/Ca exchange current in intact rabbit ventricular myocytes. *J Mol Cell Cardiol*, 39, 972-81.
- GODA, S. K. & MINTON, N. P. (1995) A simple procedure for gel electrophoresis and northern blotting of RNA. *Nucleic Acids Res*, 23, 3357-8.
- GOLDSTEIN, S., ZOBLE, R. G., AKIYAMA, T., COHEN, J. D., LANCASTER, S., LIEBSON, P. R., RAPAPORT, E., GOLDBERG, A. D., PETERS, R. W. & GILLIS, A. M. (1996) Relation of circadian ventricular ectopic activity to cardiac mortality. CAST Investigators. *Am J Cardiol*, 78, 881-5.
- GONZALEZ, D. R., BEIGI, F., TREUER, A. V. & HARE, J. M. (2007) Deficient ryanodine receptor S-nitrosylation increases sarcoplasmic reticulum calcium leak and arrhythmogenesis in cardiomyocytes. *Proc Natl Acad Sci U S A*, 104, 20612-7.
- GRANT, A. O. (2009) Cardiac ion channels. *Circ Arrhythm Electrophysiol*, 2, 185-94.
- GREENWOOD, J. P., SCOTT, E. M., STOKER, J. B. & MARY, D. A. (2001) Hypertensive left ventricular hypertrophy: relation to peripheral sympathetic drive. *J Am Coll Cardiol*, 38, 1711-7.
- GRODEN, D. L., GUAN, Z. & STOKES, B. T. (1991) Determination of Fura-2 dissociation constants following adjustment of the apparent Ca-EGTA association constant for temperature and ionic strength. *Cell Calcium*, 12, 279-87.
- GUO, Y. F. & STEIN, P. K. (2003) Circadian rhythm in the cardiovascular system: chronocardiology. *Am Heart J*, 145, 779-86.
- HADCOCK, J. R. & MALBON, C. C. (1988) Down-regulation of beta-adrenergic receptors: agonist-induced reduction in receptor mRNA levels. *Proc Natl Acad Sci U S A*, 85, 5021-5.
- HARE, J. M. (2003) Nitric oxide and excitation-contraction coupling. *J Mol Cell Cardiol*, 35, 719-29.
- HARZHEIM, D., MOVASSAGH, M., FOO, R. S., RITTER, O., TASHFEEN, A., CONWAY, S. J., BOOTMAN, M. D. & RODERICK, H. L. (2009) Increased InsP3Rs in the junctional sarcoplasmic reticulum augment Ca<sup>2+</sup> transients and arrhythmias associated with cardiac hypertrophy. *Proc Natl Acad Sci U S A*, 106, 11406-11.
- HASHIMOTO, M., KUWAHARA, M., TSUBONE, H. & SUGANO, S. (1999) Diurnal variation of autonomic nervous activity in the rat: investigation by power spectral analysis of heart rate variability. *J Electrocardiol*, 32, 167-71.
- HASSAN, M. A. & KETAT, A. F. (2005) Sildenafil citrate increases myocardial cGMP content in rat heart, decreases its hypertrophic response to isoproterenol and decreases myocardial leak of creatine kinase and troponin T. *BMC Pharmacol*, 5, 10.
- HASTINGS, M. H., REDDY, A. B. & MAYWOOD, E. S. (2003) A clockwork web: circadian timing in brain and periphery, in health and disease. *Nat Rev Neurosci*, 4, 649-61.
- HAWTHORN, M. H. & BROADLEY, K. J. (1982) Evidence from use of neuronal uptake inhibition that beta 1-adrenoceptors, but not beta 2-adrenoceptors, are innervated. *J Pharm Pharmacol*, 34, 664-6.
- HAYANO, J., SAKAKIBARA, Y., YAMADA, M., KAMIYA, T., FUJINAMI, T., YOKOYAMA, K., WATANABE, Y. & TAKATA, K. (1990) Diurnal variations in vagal and sympathetic cardiac control. *Am J Physiol*, 258, H642-6.
- HAYANO, J., SAKATA, S., OKADA, A., MUKAI, S. & FUJINAMI, T. (1998) Circadian rhythms of atrioventricular conduction properties in chronic atrial fibrillation with and without heart failure. *J Am Coll Cardiol*, 31, 158-66.
- HENKE, W., CETINSOY, C., JUNG, K. & LOENING, S. (1996) Non-hyperbolic calcium calibration curve of Fura-2: implications for the reliability of quantitative Ca<sup>2+</sup> measurements. *Cell Calcium*, 20, 287-92.

- HENRY, R., CASTO, R. & PRINTZ, M. P. (1990) Diurnal cardiovascular patterns in spontaneously hypertensive and Wistar-Kyoto rats. *Hypertension*, 16, 422-8.
- HILLE, B. (2001) *Ion channels of excitable membranes*, Sunderland, Mass., Sinauer Associates.
- HIRAOKA, M., SUNAMI, A., FAN, Z. & SAWANOBORI, T. (1992) Multiple ionic mechanisms of early afterdepolarizations in isolated ventricular myocytes from guinea-pig hearts. *Ann N Y Acad Sci*, 644, 33-47.
- HOFFMANN, C., LEITZ, M. R., OBERDORF-MAASS, S., LOHSE, M. J. & KLOTZ, K. N. (2004) Comparative pharmacology of human beta-adrenergic receptor subtypes--characterization of stably transfected receptors in CHO cells. *Naunyn Schmiedebergs Arch Pharmacol*, 369, 151-9.
- HOUSER, S. R., PIACENTINO, V., 3RD & WEISSER, J. (2000) Abnormalities of calcium cycling in the hypertrophied and failing heart. *J Mol Cell Cardiol*, 32, 1595-607.
- IDEMA, R. N., VAN DEN MEIRACKER, A. H., BALK, A. H., BOS, E., SCHALEKAMP, M. A. & MAN IN 'T VELD, A. J. (1994) Abnormal diurnal variation of blood pressure, cardiac output, and vascular resistance in cardiac transplant recipients. *Circulation*, 90, 2797-803.
- INUI, M., CHAMBERLAIN, B. K., SAITO, A. & FLEISCHER, S. (1986) The nature of the modulation of Ca<sup>2+</sup> transport as studied by reconstitution of cardiac sarcoplasmic reticulum. *J Biol Chem*, 261, 1794-800.
- ISHIKAWA, Y., SOROTA, S., KIUCHI, K., SHANNON, R. P., KOMAMURA, K., KATSUSHIKA, S., VATNER, D. E., VATNER, S. F. & HOMCY, C. J. (1994) Downregulation of adenylylcyclase types V and VI mRNA levels in pacing-induced heart failure in dogs. *J Clin Invest*, 93, 2224-9.
- JANSE, M. J. (2004) Electrophysiological changes in heart failure and their relationship to arrhythmogenesis. *Cardiovasc Res*, 61, 208-17.
- JANUARY, C. T., CHAU, V. & MAKIELSKI, J. C. (1991) Triggered activity in the heart: cellular mechanisms of early after-depolarizations. *Eur Heart J*, 12 Suppl F, 4-9.
- JANUARY, C. T. & RIDDLE, J. M. (1989) Early afterdepolarizations: mechanism of induction and block. A role for L-type Ca<sup>2+</sup> current. *Circ Res*, 64, 977-90.
- JOHNSON, D. G., HAYWARD, J. S., JACOBS, T. P., COLLIS, M. L., ECKERSON, J. D. & WILLIAMS, R. H. (1977) Plasma norepinephrine responses of man in cold water. *J Appl Physiol*, 43, 216-20.
- JUREVICIUS, J. & FISCHMEISTER, R. (1996) cAMP compartmentation is responsible for a local activation of cardiac Ca<sup>2+</sup> channels by beta-adrenergic agonists. *Proc Natl Acad Sci U S A*, 93, 295-9.
- KAAB, S., DIXON, J., DUC, J., ASHEN, D., NABAUER, M., BEUCKELMANN, D. J., STEINBECK, G., MCKINNON, D. & TOMASELLI, G. F. (1998) Molecular basis of transient outward potassium current downregulation in human heart failure: a decrease in Kv4.3 mRNA correlates with a reduction in current density. *Circulation*, 98, 1383-93.
- KANAI, A. J., PEARCE, L. L., CLEMENS, P. R., BIRDER, L. A., VANBIBBER, M. M., CHOI, S. Y., DE GROAT, W. C. & PETERSON, J. (2001) Identification of a neuronal nitric oxide synthase in isolated cardiac mitochondria using electrochemical detection. *Proc Natl Acad Sci U S A*, 98, 14126-31.
- KAO, W. H., ARKING, D. E., POST, W., REA, T. D., SOTOODEHNIA, N., PRINEAS, R. J., BISHE, B., DOAN, B. Q., BOERWINKLE, E., PSATY, B. M., TOMASELLI, G. F., CORESH, J., SISCOVICK, D. S., MARBAN, E., SPOONER, P. M., BURKE, G. L. & CHAKRAVARTI, A. (2009) Genetic variations in nitric oxide synthase 1 adaptor protein are associated with sudden cardiac death in US white community-based populations. *Circulation*, 119, 940-51.
- KARIO, K., SCHWARTZ, J. E. & PICKERING, T. G. (1999) Ambulatory physical activity as a determinant of diurnal blood pressure variation. *Hypertension*, 34, 685-91.
- KASS, R. S. & SANGUINETTI, M. C. (1984) Inactivation of calcium channel current in the calf cardiac Purkinje fiber. Evidence for voltage- and calcium-mediated mechanisms. *J Gen Physiol*, 84, 705-26.
- KAWAI, T. & KIN, K. (1975) Letter: Diurnal variation of serum beta 2 microglobulin in normal subjects. *N Engl J Med*, 293, 879-80.
- KELLY, R. A., BALLIGAND, J. L. & SMITH, T. W. (1996) Nitric oxide and cardiac function. *Circ Res*, 79, 363-80.
- KENTISH, J. C., MCCLOSKEY, D. T., LAYLAND, J., PALMER, S., LEIDEN, J. M., MARTIN, A. F. & SOLARO, R. J. (2001) Phosphorylation of troponin I by protein kinase A accelerates relaxation and crossbridge cycle kinetics in mouse ventricular muscle. *Circ Res*, 88, 1059-65.
- KHAN, S. A., LEE, K., MINHAS, K. M., GONZALEZ, D. R., RAJU, S. V., TEJANI, A. D., LI, D., BERKOWITZ, D. E. & HARE, J. M. (2004) Neuronal nitric oxide synthase negatively regulates

- xanthine oxidoreductase inhibition of cardiac excitation-contraction coupling. *Proc Natl Acad Sci U S A*, 101, 15944-8.
- KHAN, S. A., SKAF, M. W., HARRISON, R. W., LEE, K., MINHAS, K. M., KUMAR, A., FRADLEY, M., SHOUKAS, A. A., BERKOWITZ, D. E. & HARE, J. M. (2003) Nitric oxide regulation of myocardial contractility and calcium cycling: independent impact of neuronal and endothelial nitric oxide synthases. *Circ Res*, 92, 1322-9.
- KITAMURA, T., ONISHI, K., DOHI, K., OKINAKA, T., ISAKA, N. & NAKANO, T. (2000) The negative inotropic effect of beta3-adrenoceptor stimulation in the beating guinea pig heart. *J Cardiovasc Pharmacol*, 35, 786-90.
- KLABUNDE, R. E. (2005) *Cardiovascular physiology concepts*, Philadelphia, Pa. ; London, Lippincott Williams & Wilkins.
- KONG, T. Q., JR., GOLDBERGER, J. J., PARKER, M., WANG, T. & KADISH, A. H. (1995) Circadian variation in human ventricular refractoriness. *Circulation*, 92, 1507-16.
- KUBOTA, I., HAN, X., OPEL, D. J., ZHAO, Y. Y., BALIGA, R., HUANG, P., FISHMAN, M. C., SHANNON, R. P., MICHEL, T. & KELLY, R. A. (2000) Increased susceptibility to development of triggered activity in myocytes from mice with targeted disruption of endothelial nitric oxide synthase. *J Mol Cell Cardiol*, 32, 1239-48.
- KUKREJA, R. C., OCKAILI, R., SALLOUM, F. & XI, L. (2003) Sildenafil-induced cardioprotection in rabbits. *Cardiovasc Res*, 60, 700-1; author reply 702-3.
- KUNG, T. A., EGBEJIMI, O., CUI, J., HA, N. P., DURGAN, D. J., ESSOP, M. F., BRAY, M. S., SHAW, C. A., HARDIN, P. E., STANLEY, W. C. & YOUNG, M. E. (2007) Rapid attenuation of circadian clock gene oscillations in the rat heart following ischemia-reperfusion. *J Mol Cell Cardiol*, 43, 744-53.
- KUWAHARA, M., SUZUKI, A., TSUTSUMI, H., TANIGAWA, M., TSUBONE, H. & SUGANO, S. (1999) Power spectral analysis of heart rate variability for assessment of diurnal variation of autonomic nervous activity in miniature swine. *Lab Anim Sci*, 49, 202-8.
- LAWRENCE, C. & RODRIGO, G. C. (1999) A Na<sup>+</sup>-activated K<sup>+</sup> current (IK,Na) is present in guinea-pig but not rat ventricular myocytes. *Pflugers Arch*, 437, 831-8.
- LAYLAND, J., LI, J. M. & SHAH, A. M. (2002) Role of cyclic GMP-dependent protein kinase in the contractile response to exogenous nitric oxide in rat cardiac myocytes. *J Physiol*, 540, 457-67.
- LEE, J. K., JOHN, S. A. & WEISS, J. N. (1999) Novel gating mechanism of polyamine block in the strong inward rectifier K channel Kir2.1. *J Gen Physiol*, 113, 555-64.
- LEMMER, B. (2006) The importance of circadian rhythms on drug response in hypertension and coronary heart disease--from mice and man. *Pharmacol Ther*, 111, 629-51.
- LEVESQUE, P. C., LEBLANC, N. & HUME, J. R. (1994) Release of calcium from guinea pig cardiac sarcoplasmic reticulum induced by sodium-calcium exchange. *Cardiovasc Res*, 28, 370-8.
- LEVICK, J. R. (2003) *An introduction to cardiovascular physiology*, London, Arnold.
- LI, L., DESANTIAGO, J., CHU, G., KRANIAS, E. G. & BERS, D. M. (2000) Phosphorylation of phospholamban and troponin I in beta-adrenergic-induced acceleration of cardiac relaxation. *Am J Physiol Heart Circ Physiol*, 278, H769-79.
- LIM, G., VENETUCCI, L., EISNER, D. A. & CASADEI, B. (2008) Does nitric oxide modulate cardiac ryanodine receptor function? Implications for excitation-contraction coupling. *Cardiovasc Res*, 77, 256-64.
- LIN, X., JO, H., SAKAKIBARA, Y., TAMBARA, K., KIM, B., KOMEDA, M. & MATSUOKA, S. (2006) Beta-adrenergic stimulation does not activate Na<sup>+</sup>/Ca<sup>2+</sup> exchange current in guinea pig, mouse, and rat ventricular myocytes. *Am J Physiol Cell Physiol*, 290, C601-8.
- LINSELL, C. R., LIGHTMAN, S. L., MULLEN, P. E., BROWN, M. J. & CAUSON, R. C. (1985) Circadian rhythms of epinephrine and norepinephrine in man. *J Clin Endocrinol Metab*, 60, 1210-5.
- LIVAK, K. J. & SCHMITTGEN, T. D. (2001) Analysis of relative gene expression data using real-time quantitative PCR and the 2(-Delta Delta C(T)) Method. *Methods*, 25, 402-8.
- LOMBARDI, F., SANDRONE, G., MORTARA, A., LA ROVERE, M. T., COLOMBO, E., GUZZETTI, S. & MALLIANI, A. (1992) Circadian variation of spectral indices of heart rate variability after myocardial infarction. *Am Heart J*, 123, 1521-9.
- LORELL, B. H. & CARABELLO, B. A. (2000) Left ventricular hypertrophy: pathogenesis, detection, and prognosis. *Circulation*, 102, 470-9.
- LOYER, X., OLIVIERO, P., DAMY, T., ROBIDEL, E., MAROTTE, F., HEYMES, C. & SAMUEL, J. L. (2007) Effects of sex differences on constitutive nitric oxide synthase expression and activity in response to pressure overload in rats. *Am J Physiol Heart Circ Physiol*, 293, H2650-8.

- LUKYANENKO, V., GYORKE, I. & GYORKE, S. (1996) Regulation of calcium release by calcium inside the sarcoplasmic reticulum in ventricular myocytes. *Pflugers Arch*, 432, 1047-54.
- MALBON, C. C., TAO, J. & WANG, H. Y. (2004) AKAPs (A-kinase anchoring proteins) and molecules that compose their G-protein-coupled receptor signalling complexes. *Biochem J*, 379, 1-9.
- MALLAVARAPU, C., PANCHOLY, S., SCHWARTZMAN, D., CALLANS, D. J., HEO, J., GOTTLIEB, C. D. & MARCHLINSKI, F. E. (1995) Circadian variation of ventricular arrhythmia recurrences after cardioverter-defibrillator implantation in patients with healed myocardial infarcts. *Am J Cardiol*, 75, 1140-4.
- MARON, B. J., KOGAN, J., PROSCHAN, M. A., HECHT, G. M. & ROBERTS, W. C. (1994) Circadian variability in the occurrence of sudden cardiac death in patients with hypertrophic cardiomyopathy. *J Am Coll Cardiol*, 23, 1405-9.
- MARTIN, S. R., EMANUEL, K., SEARS, C. E., ZHANG, Y. H. & CASADEI, B. (2006) Are myocardial eNOS and nNOS involved in the beta-adrenergic and muscarinic regulation of inotropy? A systematic investigation. *Cardiovasc Res*, 70, 97-106.
- MARTINO, T., ARAB, S., STRAUME, M., BELSHAM, D. D., TATA, N., CAI, F., LIU, P., TRIVIERI, M., RALPH, M. & SOLE, M. J. (2004) Day/night rhythms in gene expression of the normal murine heart. *J Mol Med*, 82, 256-64.
- MARTINO, T. A., TATA, N., BELSHAM, D. D., CHALMERS, J., STRAUME, M., LEE, P., PRIBIAG, H., KHAPER, N., LIU, P. P., DAWOOD, F., BACKX, P. H., RALPH, M. R. & SOLE, M. J. (2007) Disturbed diurnal rhythm alters gene expression and exacerbates cardiovascular disease with rescue by resynchronization. *Hypertension*, 49, 1104-13.
- MARX, S. O., REIKEN, S., HISAMATSU, Y., JAYARAMAN, T., BURKHOFF, D., ROSEMBLIT, N. & MARKS, A. R. (2000) PKA phosphorylation dissociates FKBP12.6 from the calcium release channel (ryanodine receptor): defective regulation in failing hearts. *Cell*, 101, 365-76.
- MASSION, P. B. & BALLIGAND, J. L. (2003) Modulation of cardiac contraction, relaxation and rate by the endothelial nitric oxide synthase (eNOS): lessons from genetically modified mice. *J Physiol*, 546, 63-75.
- MATSUDA, J. J., LEE, H. & SHIBATA, E. F. (1992) Enhancement of rabbit cardiac sodium channels by beta-adrenergic stimulation. *Circ Res*, 70, 199-207.
- MCLLENACHAN, J. M., HENDERSON, E., MORRIS, K. I. & DARGIE, H. J. (1987) Ventricular arrhythmias in patients with hypertensive left ventricular hypertrophy. *N Engl J Med*, 317, 787-92.
- MCNAMARA, P., SEO, S. B., RUDIC, R. D., SEHGAL, A., CHAKRAVARTI, D. & FITZGERALD, G. A. (2001) Regulation of CLOCK and MOP4 by nuclear hormone receptors in the vasculature: a humoral mechanism to reset a peripheral clock. *Cell*, 105, 877-89.
- MEREDITH, I. T., BROUGHTON, A., JENNINGS, G. L. & ESLER, M. D. (1991) Evidence of a selective increase in cardiac sympathetic activity in patients with sustained ventricular arrhythmias. *N Engl J Med*, 325, 618-24.
- MEYER, M., BLUHM, W. F., HE, H., POST, S. R., GIORDANO, F. J., LEW, W. Y. & DILLMANN, W. H. (1999) Phospholamban-to-SERCA2 ratio controls the force-frequency relationship. *Am J Physiol*, 276, H779-85.
- MILHAUD, G., PERAULT-STAU, A. M. & STAU, J. F. (1972) Diurnal variation of plasma calcium and calcitonin function in the rat. *J Physiol*, 222, 559-67.
- MITRA, R. & MORAD, M. (1985) A uniform enzymatic method for dissociation of myocytes from hearts and stomachs of vertebrates. *Am J Physiol*, 249, H1056-60.
- MOMKEN, I., FORTIN, D., SERRURIER, B., BIGARD, X., VENTURA-CLAPIER, R. & VEKSLER, V. (2002) Endothelial nitric oxide synthase (NOS) deficiency affects energy metabolism pattern in murine oxidative skeletal muscle. *Biochem J*, 368, 341-7.
- MONIOTTE, S., KOBZIK, L., FERON, O., TROCHU, J. N., GAUTHIER, C. & BALLIGAND, J. L. (2001) Upregulation of beta(3)-adrenoceptors and altered contractile response to inotropic amines in human failing myocardium. *Circulation*, 103, 1649-55.
- MUKAMAL, K. J., MULLER, J. E., MACLURE, M., SHERWOOD, J. B. & MITTLEMAN, M. A. (2000) Increased risk of congestive heart failure among infarctions with nighttime onset. *Am Heart J*, 140, 438-42.
- MULLER, J. E., LUDMER, P. L., WILLICH, S. N., TOFLER, G. H., AYLNER, G., KLANGOS, I. & STONE, P. H. (1987) Circadian variation in the frequency of sudden cardiac death. *Circulation*, 75, 131-8.
- MULLINS, L. J. & NODA, K. (1963) The Influence of Sodium-Free Solutions on the Membrane Potential of Frog Muscle Fibers. *J Gen Physiol*, 47, 117-32.

- MURPHY, D. A., THOMPSON, G. W., ARDELL, J. L., MCCRATY, R., STEVENSON, R. S., SANGALANG, V. E., CARDINAL, R., WILKINSON, M., CRAIG, S., SMITH, F. M., KINGMA, J. G. & ARMOUR, J. A. (2000) The heart reinnervates after transplantation. *Ann Thorac Surg*, 69, 1769-81.
- NABAUER, M. & KAAB, S. (1998) Potassium channel down-regulation in heart failure. *Cardiovasc Res*, 37, 324-34.
- NAGY, O., HAJNAL, A., PARRATT, J. R. & VEGH, A. (2004) Sildenafil (Viagra) reduces arrhythmia severity during ischaemia 24 h after oral administration in dogs. *Br J Pharmacol*, 141, 549-51.
- NAITO, Y., TSUJINO, T., KAWASAKI, D., OKUMURA, T., MORIMOTO, S., MASAI, M., SAKODA, T., FUJIOKA, Y., OHYANAGI, M. & IWASAKI, T. (2003) Circadian gene expression of clock genes and plasminogen activator inhibitor-1 in heart and aorta of spontaneously hypertensive and Wistar-Kyoto rats. *J Hypertens*, 21, 1107-15.
- NARKIEWICZ, K., WINNICKI, M., SCHROEDER, K., PHILLIPS, B. G., KATO, M., CWALINA, E. & SOMERS, V. K. (2002) Relationship between muscle sympathetic nerve activity and diurnal blood pressure profile. *Hypertension*, 39, 168-72.
- NERBONNE, J. M. & KASS, R. S. (2005) Molecular physiology of cardiac repolarization. *Physiol Rev*, 85, 1205-53.
- NEUMANN, F. J., OTT, I., GAWAZ, M., RICHARDT, G., HOLZAPFEL, H., JOCHUM, M. & SCHOMIG, A. (1995) Cardiac release of cytokines and inflammatory responses in acute myocardial infarction. *Circulation*, 92, 748-55.
- NICHOLLS, J. G. (2001) *From neuron to brain*, Sunderland, Mass., Sinauer Associates.
- NIELSEN, H. K., LAURBERG, P., BRIKEN, K. & MOSEKILDE, L. (1991) Relations between diurnal variations in serum osteocalcin, cortisol, parathyroid hormone, and ionized calcium in normal individuals. *Acta Endocrinol (Copenh)*, 124, 391-8.
- NOLAN, T., HANDS, R. E. & BUSTIN, S. A. (2006) Quantification of mRNA using real-time RT-PCR. *Nat Protoc*, 1, 1559-82.
- NORDSKOG, B. K., HAMMARBACK, J. A. & GODWIN, D. W. (2006) Diurnal gene expression patterns of T-type calcium channels and their modulation by ethanol. *Neuroscience*, 141, 1365-73.
- O'SHEA, J. C. & MURPHY, M. B. (2000) Nocturnal blood pressure dipping: a consequence of diurnal physical activity blipping? *Am J Hypertens*, 13, 601-6.
- OCKAILI, R., SALLOUM, F., HAWKINS, J. & KUKREJA, R. C. (2002) Sildenafil (Viagra) induces powerful cardioprotective effect via opening of mitochondrial K(ATP) channels in rabbits. *Am J Physiol Heart Circ Physiol*, 283, H1263-9.
- OHYA, Y., OHTSUBO, T., TSUCHIHASHI, T., ETO, K., SADANAGA, T., NAGAO, T., ABE, I. & FUJISHIMA, M. (2001) Altered diurnal variation of blood pressure in elderly subjects with decreased activity of daily living and impaired cognitive function. *Hypertens Res*, 24, 655-61.
- OKAMOTO, K. & AOKI, K. (1963) Development of a strain of spontaneously hypertensive rats. *Jpn Circ J*, 27, 282-93.
- OKAZAKI, O., SUDA, N., HONGO, K., KONISHI, M. & KURIHARA, S. (1990) Modulation of Ca<sup>2+</sup> transients and contractile properties by beta-adrenoceptor stimulation in ferret ventricular muscles. *J Physiol*, 423, 221-40.
- OLSON, E. N. & SCHNEIDER, M. D. (2003) Sizing up the heart: development redux in disease. *Genes Dev*, 17, 1937-56.
- ONO, K. & IJIMA, T. (2010) Cardiac T-type Ca(2+) channels in the heart. *J Mol Cell Cardiol*, 48, 65-70.
- PECKOVA, M., FAHRENBRUCH, C. E., COBB, L. A. & HALLSTROM, A. P. (1998) Circadian variations in the occurrence of cardiac arrests: initial and repeat episodes. *Circulation*, 98, 31-9.
- PENNA, L. B. & BASSANI, R. A. (2010) Increased spontaneous activity and reduced inotropic response to catecholamines in ventricular myocytes from footshock-stressed rats. *Stress*, 13, 73-82.
- PENNARTZ, C. M., DE JEU, M. T., BOS, N. P., SCHAAP, J. & GEURTSSEN, A. M. (2002) Diurnal modulation of pacemaker potentials and calcium current in the mammalian circadian clock. *Nature*, 416, 286-90.
- PFAFFL, M. W. (2001) A new mathematical model for relative quantification in real-time RT-PCR. *Nucleic Acids Res*, 29, e45.
- PFEFFER, M. A. & PFEFFER, J. M. (1983) Blood pressure and left ventricular dysfunction in the spontaneously hypertensive rat. *Fed Proc*, 42, 2698-702.
- PICKERING, T. G. (1990) The clinical significance of diurnal blood pressure variations. Dippers and nondippers. *Circulation*, 81, 700-2.

- PIECH, A., DESSY, C., HAVAUX, X., FERON, O. & BALLIGAND, J. L. (2003) Differential regulation of nitric oxide synthases and their allosteric regulators in heart and vessels of hypertensive rats. *Cardiovasc Res*, 57, 456-67.
- PIEPOLI, M. F. & CAPUCCI, A. (2007) Autonomic nervous system in the genesis of arrhythmias in chronic heart failure: implication for risk stratification. *Minerva Cardioangiol*, 55, 325-33.
- POGWIZD, S. M., QI, M., YUAN, W., SAMAREL, A. M. & BERS, D. M. (1999) Upregulation of Na(+)/Ca(2+) exchanger expression and function in an arrhythmogenic rabbit model of heart failure. *Circ Res*, 85, 1009-19.
- POST, S. R., HAMMOND, H. K. & INSEL, P. A. (1999) Beta-adrenergic receptors and receptor signaling in heart failure. *Annu Rev Pharmacol Toxicol*, 39, 343-60.
- POTT, C., YIP, M., GOLDBERGER, J. I. & PHILIPSON, K. D. (2007) Regulation of cardiac L-type Ca<sup>2+</sup> current in Na<sup>+</sup>-Ca<sup>2+</sup> exchanger knockout mice: functional coupling of the Ca<sup>2+</sup> channel and the Na<sup>+</sup>-Ca<sup>2+</sup> exchanger. *Biophys J*, 92, 1431-7.
- PRINZ, P. N., HALTER, J., BENEDETTI, C. & RASKIND, M. (1979) Circadian variation of plasma catecholamines in young and old men: relation to rapid eye movement and slow wave sleep. *J Clin Endocrinol Metab*, 49, 300-4.
- PRIORI, S. G. & CORR, P. B. (1990) Mechanisms underlying early and delayed afterdepolarizations induced by catecholamines. *Am J Physiol*, 258, H1796-805.
- PRIORI, S. G., NAPOLITANO, C., TISO, N., MEMMI, M., VIGNATI, G., BLOISE, R., SORRENTINO, V. & DANIELI, G. A. (2001) Mutations in the cardiac ryanodine receptor gene (hRyR2) underlie catecholaminergic polymorphic ventricular tachycardia. *Circulation*, 103, 196-200.
- PUGLISI, J. L., YUAN, W., BASSANI, J. W. & BERS, D. M. (1999) Ca(2+) influx through Ca(2+) channels in rabbit ventricular myocytes during action potential clamp: influence of temperature. *Circ Res*, 85, e7-e16.
- QUYYUMI, A. A. (1990) Circadian rhythms in cardiovascular disease. *Am Heart J*, 120, 726-33.
- RACHMANI, R., SHENHAV, G., SLAVACHEVSKY, I., LEVY, Z. & RAVID, M. (2004) Use of a mild sedative helps to identify true non-dippers by ABPM: a study in patients with diabetes mellitus and hypertension. *Blood Press Monit*, 9, 65-9.
- RADI, R., BECKMAN, J. S., BUSH, K. M. & FREEMAN, B. A. (1991) Peroxynitrite-induced membrane lipid peroxidation: the cytotoxic potential of superoxide and nitric oxide. *Arch Biochem Biophys*, 288, 481-7.
- RAEYMAEKERS, L., HOFMANN, F. & CASTEELS, R. (1988) Cyclic GMP-dependent protein kinase phosphorylates phospholamban in isolated sarcoplasmic reticulum from cardiac and smooth muscle. *Biochem J*, 252, 269-73.
- RANU, H. K., TERRACCIANO, C. M., DAVIA, K., BERNOBICH, E., CHAUDHRI, B., ROBINSON, S. E., BIN KANG, Z., HAJJAR, R. J., MACLEOD, K. T. & HARDING, S. E. (2002) Effects of Na(+)/Ca(2+)-exchanger overexpression on excitation-contraction coupling in adult rabbit ventricular myocytes. *J Mol Cell Cardiol*, 34, 389-400.
- RAU, E. & MEYER, D. K. (1975) A diurnal rhythm of incorporation of L-[3H] leucine in myocardium of the rat. *Recent Adv Stud Cardiac Struct Metab*, 7, 105-10.
- RAY, K. P. & ENGLAND, P. J. (1976) Phosphorylation of the inhibitory subunit of troponin and its effect on the calcium dependence of cardiac myofibril adenosine triphosphatase. *FEBS Lett*, 70, 11-6.
- REDDY, A. B., FIELD, M. D., MAYWOOD, E. S. & HASTINGS, M. H. (2002) Differential resynchronization of circadian clock gene expression within the suprachiasmatic nuclei of mice subjected to experimental jet lag. *J Neurosci*, 22, 7326-30.
- REEVES, J. P. & HALE, C. C. (1984) The stoichiometry of the cardiac sodium-calcium exchange system. *J Biol Chem*, 259, 7733-9.
- RESUEHR, D. & SPIESS, A. N. (2003) A real-time polymerase chain reaction-based evaluation of cDNA synthesis priming methods. *Anal Biochem*, 322, 287-91.
- RICHARDS, A. M., NICHOLLS, M. G., ESPINER, E. A., IKRAM, H., CULLENS, M. & HINTON, D. (1986) Diurnal patterns of blood pressure, heart rate and vasoactive hormones in normal man. *Clin Exp Hypertens A*, 8, 153-66.
- ROBINSON, J. (1975) *A prelude to physiology*. London, Blackwell Scientific Publication.
- ROCKMAN, H. A., KOCH, W. J. & LEFKOWITZ, R. J. (2002) Seven-transmembrane-spanning receptors and heart function. *Nature*, 415, 206-12.
- RODEFELD, M. D., BEAU, S. L., SCHUESSLER, R. B., BOINEAU, J. P. & SAFFITZ, J. E. (1996) Beta-adrenergic and muscarinic cholinergic receptor densities in the human sinoatrial node:

- identification of a high beta 2-adrenergic receptor density. *J Cardiovasc Electrophysiol*, 7, 1039-49.
- RODRIGO, G. C., DAVIES, N. W. & STANDEN, N. B. (2004) Diazoxide causes early activation of cardiac sarcolemmal KATP channels during metabolic inhibition by an indirect mechanism. *Cardiovasc Res*, 61, 570-9.
- RODRIGO, G. C., LAWRENCE, C. L. & STANDEN, N. B. (2002) Dinitrophenol pretreatment of rat ventricular myocytes protects against damage by metabolic inhibition and reperfusion. *J Mol Cell Cardiol*, 34, 555-69.
- RODRIGO, G. C. & SAMANI, N. J. (2008) Ischemic preconditioning of the whole heart confers protection on subsequently isolated ventricular myocytes. *Am J Physiol Heart Circ Physiol*, 294, H524-31.
- RODRIGO, G. C. & STANDEN, N. B. (2005a) ATP-sensitive potassium channels. *Curr Pharm Des*, 11, 1915-40.
- RODRIGO, G. C. & STANDEN, N. B. (2005b) Role of mitochondrial re-energization and Ca<sup>2+</sup> influx in reperfusion injury of metabolically inhibited cardiac myocytes. *Cardiovasc Res*, 67, 291-300.
- ROSANIO, S., YE, Y., ATAR, S., RAHMAN, A. M., FREEBERG, S. Y., HUANG, M. H., URETSKY, B. F. & BIRNBAUM, Y. (2006) Enhanced cardioprotection against ischemia-reperfusion injury with combining sildenafil with low-dose atorvastatin. *Cardiovasc Drugs Ther*, 20, 27-36.
- RUBIN, S. A., FISHBEIN, M. C. & SWAN, H. J. (1983) Compensatory hypertrophy in the heart after myocardial infarction in the rat. *J Am Coll Cardiol*, 1, 1435-41.
- SAMBROOK, J. & RUSSELL, D. W. (2001) *Molecular cloning : a laboratory manual*, Cold Spring Harbor, N.Y., Cold Spring Harbor Laboratory Press.
- SARAIVA, R. M., MINHAS, K. M., RAJU, S. V., BAROUCH, L. A., PITZ, E., SCHULERI, K. H., VANDEGAER, K., LI, D. & HARE, J. M. (2005) Deficiency of neuronal nitric oxide synthase increases mortality and cardiac remodeling after myocardial infarction: role of nitroso-redox equilibrium. *Circulation*, 112, 3415-22.
- SATO, M., GONG, H., TERRACCIANO, C. M., RANU, H. & HARDING, S. E. (2004) Loss of beta-adrenoceptor response in myocytes overexpressing the Na<sup>+</sup>/Ca<sup>2+</sup>-exchanger. *J Mol Cell Cardiol*, 36, 43-8.
- SCHEER, F. A., VAN DOORNEN, L. J. & BUIJS, R. M. (2004) Light and diurnal cycle affect autonomic cardiac balance in human; possible role for the biological clock. *Auton Neurosci*, 110, 44-8.
- SCHLAICH, M. P., KAYE, D. M., LAMBERT, E., SOMMERVILLE, M., SOCRATOUS, F. & ESLER, M. D. (2003) Relation between cardiac sympathetic activity and hypertensive left ventricular hypertrophy. *Circulation*, 108, 560-5.
- SCHLOTTHAUER, K. & BERS, D. M. (2000) Sarcoplasmic reticulum Ca<sup>2+</sup> release causes myocyte depolarization. Underlying mechanism and threshold for triggered action potentials. *Circ Res*, 87, 774-80.
- SCHMITTGEN, T. D. & LIVAK, K. J. (2008) Analyzing real-time PCR data by the comparative C(T) method. *Nat Protoc*, 3, 1101-8.
- SCHOUTEN, V. J. & TER KEURS, H. E. (1986) The force-frequency relationship in rat myocardium. The influence of muscle dimensions. *Pflugers Arch*, 407, 14-7.
- SCRIVEN, D. R., DAN, P. & MOORE, E. D. (2000) Distribution of proteins implicated in excitation-contraction coupling in rat ventricular myocytes. *Biophys J*, 79, 2682-91.
- SEARS, C. E., BRYANT, S. M., ASHLEY, E. A., LYGATE, C. A., RAKOVIC, S., WALLIS, H. L., NEUBAUER, S., TERRAR, D. A. & CASADEI, B. (2003) Cardiac neuronal nitric oxide synthase isoform regulates myocardial contraction and calcium handling. *Circ Res*, 92, e52-9.
- SEI, H., OISHI, K., CHIKAHISA, S., KITAOKA, K., TAKEDA, E. & ISHIDA, N. (2008) Diurnal amplitudes of arterial pressure and heart rate are dampened in Clock mutant mice and adrenalectomized mice. *Endocrinology*, 149, 3576-80.
- SEINO, S. & MIKI, T. (2003) Physiological and pathophysiological roles of ATP-sensitive K<sup>+</sup> channels. *Prog Biophys Mol Biol*, 81, 133-76.
- SHAM, J. S., SONG, L. S., CHEN, Y., DENG, L. H., STERN, M. D., LAKATTA, E. G. & CHENG, H. (1998) Termination of Ca<sup>2+</sup> release by a local inactivation of ryanodine receptors in cardiac myocytes. *Proc Natl Acad Sci U S A*, 95, 15096-101.
- SHAW, E. & TOFLER, G. H. (2009) Circadian rhythm and cardiovascular disease. *Curr Atheroscler Rep*, 11, 289-95.
- SHEN, C., LIN, M. J., YARADANAKUL, A., LARICCIA, V., HILL, J. A. & HILGEMANN, D. W. (2007) Dual control of cardiac Na<sup>+</sup> Ca<sup>2+</sup> exchange by PIP(2): analysis of the surface membrane fraction by extracellular cysteine PEGylation. *J Physiol*, 582, 1011-26.

- SHER, A. A., NOBLE, P. J., HINCH, R., GAVAGHAN, D. J. & NOBLE, D. (2008) The role of the  $\text{Na}^+/\text{Ca}^{2+}$  exchangers in  $\text{Ca}^{2+}$  dynamics in ventricular myocytes. *Prog Biophys Mol Biol*, 96, 377-98.
- SHERWOOD, A., STEFFEN, P. R., BLUMENTHAL, J. A., KUHN, C. & HINDERLITER, A. L. (2002) Nighttime blood pressure dipping: the role of the sympathetic nervous system. *Am J Hypertens*, 15, 111-8.
- SHINOHARA, M. L., LOROS, J. J. & DUNLAP, J. C. (1998) Glyceraldehyde-3-phosphate dehydrogenase is regulated on a daily basis by the circadian clock. *J Biol Chem*, 273, 446-52.
- SIEBERT, P. D. & CHENCHIK, A. (1993) Modified acid guanidinium thiocyanate-phenol-chloroform RNA extraction method which greatly reduces DNA contamination. *Nucleic Acids Res*, 21, 2019-20.
- SIPIDO, K. R., CARMELIET, E. & VAN DE WERF, F. (1998) T-type  $\text{Ca}^{2+}$  current as a trigger for  $\text{Ca}^{2+}$  release from the sarcoplasmic reticulum in guinea-pig ventricular myocytes. *J Physiol*, 508 ( Pt 2), 439-51.
- SKEBERDIS, V. A. (2004) Structure and function of beta3-adrenergic receptors. *Medicina (Kaunas)*, 40, 407-13.
- SMITH, T. L., COLEMAN, T. G., STANEK, K. A. & MURPHY, W. R. (1987) Hemodynamic monitoring for 24 h in unanesthetized rats. *Am J Physiol*, 253, H1335-41.
- SOLARO, R. J. & RARICK, H. M. (1998) Troponin and tropomyosin: proteins that switch on and tune in the activity of cardiac myofilaments. *Circ Res*, 83, 471-80.
- SONG, Y., SHRYOCK, J. C., KNOT, H. J. & BELARDINELLI, L. (2001) Selective attenuation by adenosine of arrhythmogenic action of isoproterenol on ventricular myocytes. *Am J Physiol Heart Circ Physiol*, 280, H2789-95.
- STORCH, K. F., LIPAN, O., LEYKIN, I., VISWANATHAN, N., DAVIS, F. C., WONG, W. H. & WEITZ, C. J. (2002) Extensive and divergent circadian gene expression in liver and heart. *Nature*, 417, 78-83.
- STOYANOVSKY, D., MURPHY, T., ANNO, P. R., KIM, Y. M. & SALAMA, G. (1997) Nitric oxide activates skeletal and cardiac ryanodine receptors. *Cell Calcium*, 21, 19-29.
- SUN, J., DRUHAN, L. J. & ZWEIER, J. L. (2008) Dose dependent effects of reactive oxygen and nitrogen species on the function of neuronal nitric oxide synthase. *Arch Biochem Biophys*, 471, 126-33.
- SUN, J., MORGAN, M., SHEN, R. F., STEENBERGEN, C. & MURPHY, E. (2007) Preconditioning results in S-nitrosylation of proteins involved in regulation of mitochondrial energetics and calcium transport. *Circ Res*, 101, 1155-63.
- SUN, J., PICHT, E., GINSBURG, K. S., BERS, D. M., STEENBERGEN, C. & MURPHY, E. (2006) Hypercontractile female hearts exhibit increased S-nitrosylation of the L-type  $\text{Ca}^{2+}$  channel alpha1 subunit and reduced ischemia/reperfusion injury. *Circ Res*, 98, 403-11.
- SVORC, P., WILK, P., MURAR, J., PODLUBNY, I., KUJANIK, S., BRACOKOVA, I. & MURIN, M. (1994) Circadian rhythm of the ventricular fibrillation threshold in female Wistar rats. *Physiol Res*, 43, 355-8.
- SWEDBERG, K., CLELAND, J., DARGIE, H., DREXLER, H., FOLLATH, F., KOMAJDA, M., TAVAZZI, L., SMISETH, O. A., GAVAZZI, A., HAVERICH, A., HOES, A., JAARSMA, T., KOREWICKI, J., LEVY, S., LINDE, C., LOPEZ-SENDON, J. L., NIEMINEN, M. S., PIERARD, L. & REMME, W. J. (2005) [Guidelines for the Diagnosis and Treatment of Chronic Heart Failure: executive summary (update 2005)]. *Rev Esp Cardiol*, 58, 1062-92.
- TAKAHASHI, A., CAMACHO, P., LECHLEITER, J. D. & HERMAN, B. (1999) Measurement of intracellular calcium. *Physiol Rev*, 79, 1089-125.
- TAKAKUWA, H., ISE, T., KATO, T., IZUMIYA, Y., SHIMIZU, K., YOKOYAMA, H. & KOBAYASHI, K. I. (2001) Diurnal variation of hemodynamic indices in non-dipper hypertensive patients. *Hypertens Res*, 24, 195-201.
- TAKAMATSU, H., NAGAO, T., ICHIJO, H. & ADACHI-AKAHANE, S. (2003) L-type  $\text{Ca}^{2+}$  channels serve as a sensor of the SR  $\text{Ca}^{2+}$  for tuning the efficacy of  $\text{Ca}^{2+}$ -induced  $\text{Ca}^{2+}$  release in rat ventricular myocytes. *J Physiol*, 552, 415-24.
- TAKASAGO, T., IMAGAWA, T., FURUKAWA, K., OGURUSU, T. & SHIGEKAWA, M. (1991) Regulation of the cardiac ryanodine receptor by protein kinase-dependent phosphorylation. *J Biochem*, 109, 163-70.
- TAMARGO, J., CABALLERO, R., GOMEZ, R., VALENZUELA, C. & DELPON, E. (2004) Pharmacology of cardiac potassium channels. *Cardiovasc Res*, 62, 9-33.

- TANABE, Y., HATADA, K., NAITO, N., AIZAWA, Y., CHINUSHI, M. & NAWA, H. (2006) Over-expression of Kv1.5 in rat cardiomyocytes extremely shortens the duration of the action potential and causes rapid excitation. *Biochem Biophys Res Commun*, 345, 1116-21.
- TAUSSIG, R., INIGUEZ-LLUHI, J. A. & GILMAN, A. G. (1993) Inhibition of adenylyl cyclase by Gi alpha. *Science*, 261, 218-21.
- TERENTYEV, D., CALA, S. E., HOULE, T. D., VIATCHENKO-KARPINSKI, S., GYORKE, I., TERENTYEVA, R., WILLIAMS, S. C. & GYORKE, S. (2005) Triadin overexpression stimulates excitation-contraction coupling and increases predisposition to cellular arrhythmia in cardiac myocytes. *Circ Res*, 96, 651-8.
- TERRENOIRE, C., CLANCY, C. E., CORMIER, J. W., SAMPSON, K. J. & KASS, R. S. (2005) Autonomic control of cardiac action potentials: role of potassium channel kinetics in response to sympathetic stimulation. *Circ Res*, 96, e25-34.
- THELLIN, O., ZORZI, W., LAKAYE, B., DE BORMAN, B., COUMANS, B., HENNEN, G., GRISAR, T., IGOUT, A. & HEINEN, E. (1999) Housekeeping genes as internal standards: use and limits. *J Biotechnol*, 75, 291-5.
- TOFLER, G. H., GEBARA, O. C., MITTLEMAN, M. A., TAYLOR, P., SIEGEL, W., VENDITTI, F. J., JR., RASMUSSEN, C. A. & MULLER, J. E. (1995) Morning peak in ventricular tachyarrhythmias detected by time of implantable cardioverter/defibrillator therapy. The CPI Investigators. *Circulation*, 92, 1203-8.
- TOSAKI, A., BEHJET, N. S., ENGELMAN, D. T., ENGELMAN, R. M. & DAS, D. K. (1995) Alpha-1 adrenergic receptor agonist-induced preconditioning in isolated working rat hearts. *J Pharmacol Exp Ther*, 273, 689-94.
- TRISTANI-FIROUZI, M., CHEN, J., MITCHESON, J. S. & SANGUINETTI, M. C. (2001) Molecular biology of K(+) channels and their role in cardiac arrhythmias. *Am J Med*, 110, 50-9.
- TSIEN, R. W., BEAN, B. P., HESS, P., LANSMAN, J. B., NILIUS, B. & NOWYCKY, M. C. (1986) Mechanisms of calcium channel modulation by beta-adrenergic agents and dihydropyridine calcium agonists. *J Mol Cell Cardiol*, 18, 691-710.
- TUNCTAN, B., WEIGL, Y., DOTAN, A., PELEG, L., ZENGIL, H., ASHKENAZI, I. & ABACIOGLU, N. (2002) Circadian variation of nitric oxide synthase activity in mouse tissue. *Chronobiol Int*, 19, 393-404.
- TURFANER, N., KARTER, Y., CURGUNLU, A., AYAN, F., MIHMANLI, I. & SIPAHIOGLU, F. (2009) Blunted nocturnal fall of blood pressure in isolated clinical hypertension. *Swiss Med Wkly*, 139, 251-5.
- UMAR, S. & VAN DER LAARSE, (2010) A. Nitric oxide and nitric oxide synthase isoforms in the normal, hypertrophic, and failing heart. *Mol Cell Biochem*, 333, 191-201.
- VAN DEN BUUSE, M. (1999) Circadian rhythms of blood pressure and heart rate in conscious rats: effects of light cycle shift and timed feeding. *Physiol Behav*, 68, 9-15.
- VAN SOMEREN, E. J. (2000) Circadian and sleep disturbances in the elderly. *Exp Gerontol*, 35, 1229-37.
- VANDEBERG, C. A. (1987) Inward rectification of a potassium channel in cardiac ventricular cells depends on internal magnesium ions. *Proc Natl Acad Sci USA*, 84, 2560-4.
- VANDESOMPELE, J., DE PRETER, K., PATTYN, F., POPPE, B., VAN ROY, N., DE PAEPE, A. & SPELEMAN, F. (2002) Accurate normalization of real-time quantitative RT-PCR data by geometric averaging of multiple internal control genes. *Genome Biol*, 3, RESEARCH0034.
- VARGHESE, P., HARRISON, R. W., LOFTHOUSE, R. A., GEORGAKOPOULOS, D., BERKOWITZ, D. E. & HARE, J. M. (2000) beta(3)-adrenoceptor deficiency blocks nitric oxide-dependent inhibition of myocardial contractility. *J Clin Invest*, 106, 697-703.
- VEERMAN, D. P., IMHOLZ, B. P., WIELING, W., WESSELING, K. H. & VAN MONTFRANS, G. A. (1995) Circadian profile of systemic hemodynamics. *Hypertension*, 26, 55-9.
- VELDKAMP, M. W., VERKERK, A. O., VAN GINNEKEN, A. C., BAARTSCHEER, A., SCHUMACHER, C., DE JONGE, N., DE BAKKER, J. M. & OPTHOF, T. (2001) Norepinephrine induces action potential prolongation and early afterdepolarizations in ventricular myocytes isolated from human end-stage failing hearts. *Eur Heart J*, 22, 955-63.
- VERDECCHIA, P., SCHILLACI, G., BORGIONI, C., CIUCCI, A., TELERA, M. P., PEDE, S., GATTOBIGIO, R. & PORCELLATI, C. (1998) Adverse prognostic value of a blunted circadian rhythm of heart rate in essential hypertension. *J Hypertens*, 16, 1335-43.
- VINCENT, G. M., TIMOTHY, K. W., LEPPERT, M. & KEATING, M. (1992) The spectrum of symptoms and QT intervals in carriers of the gene for the long-QT syndrome. *N Engl J Med*, 327, 846-52.
- WALLUKAT, G. (2002) The beta-adrenergic receptors. *Herz*, 27, 683-90.

- WALSH, K. B., BEGENISICH, T. B. & KASS, R. S. (1989) Beta-adrenergic modulation of cardiac ion channels. Differential temperature sensitivity of potassium and calcium currents. *J Gen Physiol*, 93, 841-54.
- WANG, H., KOHR, M. J., TRAYNHAM, C. J., WHEELER, D. G., JANSSEN, P. M. & ZIOLO, M. T. (2008a) Neuronal nitric oxide synthase signaling within cardiac myocytes targets phospholamban. *Am J Physiol Cell Physiol*, 294, C1566-75.
- WANG, H., KOHR, M. J., TRAYNHAM, C. J. & ZIOLO, M. T. (2009) Phosphodiesterase 5 restricts NOS3/Soluble guanylate cyclase signaling to L-type  $Ca^{2+}$  current in cardiac myocytes. *J Mol Cell Cardiol*, 47, 304-14.
- WANG, H., KOHR, M. J., WHEELER, D. G. & ZIOLO, M. T. (2008b) Endothelial nitric oxide synthase decreases beta-adrenergic responsiveness via inhibition of the L-type  $Ca^{2+}$  current. *Am J Physiol Heart Circ Physiol*, 294, H1473-80.
- WANG, H., VIATCHENKO-KARPINSKI, S., SUN, J., GYORKE, I., BENKUSKY, N. A., KOHR, M. J., VALDIVIA, H. H., MURPHY, E., GYORKE, S. & ZIOLO, M. T. Regulation of myocyte contraction via neuronal nitric oxide synthase: role of ryanodine receptor S-nitrosylation. *J Physiol*, 588, 2905-17.
- WANG, Z. R., WANG, L., WAN, C. M., CORNELISSEN, G., ANAND, I. & HALBERG, F. (1999) Circadian rhythm of gene expression of myocardial contractile protein, left ventricular pressure and contractility. *Space Med Med Eng (Beijing)*, 12, 391-6.
- WEBER, C. R., PIACENTINO, V., 3RD, GINSBURG, K. S., HOUSER, S. R. & BERS, D. M. (2002)  $Na^{+}$ - $Ca^{2+}$  exchange current and submembrane  $[Ca^{2+}]$  during the cardiac action potential. *Circ Res*, 90, 182-9.
- WEHRENS, X. H., LEHNART, S. E., HUANG, F., VEST, J. A., REIKEN, S. R., MOHLER, P. J., SUN, J., GUATIMOSIM, S., SONG, L. S., ROSEMBLIT, N., D'ARMIENTO, J. M., NAPOLITANO, C., MEMMI, M., PRIORI, S. G., LEDERER, W. J. & MARKS, A. R. (2003) FKBP12.6 deficiency and defective calcium release channel (ryanodine receptor) function linked to exercise-induced sudden cardiac death. *Cell*, 113, 829-40.
- WEI, S. K., HANLON, S. U. & HAIGNEY, M. C. (2002) Beta-adrenergic stimulation of pig myocytes with decreased cytosolic free magnesium prolongs the action potential and enhances triggered activity. *J Cardiovasc Electrophysiol*, 13, 587-92.
- WIER, W. G. & BALKE, C. W. (1999)  $Ca^{2+}$  release mechanisms,  $Ca^{2+}$  sparks, and local control of excitation-contraction coupling in normal heart muscle. *Circ Res*, 85, 770-6.
- WILDHIRT, S. M., WEISMUELLER, S., SCHULZE, C., CONRAD, N., KORNBERG, A. & REICHHART, B. (1999) Inducible nitric oxide synthase activation after ischemia/reperfusion contributes to myocardial dysfunction and extent of infarct size in rabbits: evidence for a late phase of nitric oxide-mediated reperfusion injury. *Cardiovasc Res*, 43, 698-711.
- WILLIAMS, D. A. & FAY, F. S. (1990) Intracellular calibration of the fluorescent calcium indicator Fura-2. *Cell Calcium*, 11, 75-83.
- WILLICH, S. N., LEVY, D., ROCCO, M. B., TOFLER, G. H., STONE, P. H. & MULLER, J. E. (1987) Circadian variation in the incidence of sudden cardiac death in the Framingham Heart Study population. *Am J Cardiol*, 60, 801-6.
- WILLS, M. R. (1970) The effect of diurnal variation on total plasma calcium concentration in normal subjects. *J Clin Pathol*, 23, 772-7.
- WROBEL, J. & NAGEL, G. (1979) Diurnal rhythm of active calcium transport in rat intestine. *Experientia*, 35, 1581-2.
- WU, M. & TINOCO, I., JR. (1998) RNA folding causes secondary structure rearrangement. *Proc Natl Acad Sci U S A*, 95, 11555-60.
- XIAO, R. P. (2001) Beta-adrenergic signaling in the heart: dual coupling of the beta2-adrenergic receptor to G(s) and G(i) proteins. *Sci STKE*, 2001, re15.
- XIAO, R. P., HOHL, C., ALTSCHULD, R., JONES, L., LIVINGSTON, B., ZIMAN, B., TANTINI, B. & LAKATTA, E. G. (1994) Beta 2-adrenergic receptor-stimulated increase in cAMP in rat heart cells is not coupled to changes in  $Ca^{2+}$  dynamics, contractility, or phospholamban phosphorylation. *J Biol Chem*, 269, 19151-6.
- XU, K. Y., HUSO, D. L., DAWSON, T. M., BREDDT, D. S. & BECKER, L. C. (1999) Nitric oxide synthase in cardiac sarcoplasmic reticulum. *Proc Natl Acad Sci U S A*, 96, 657-62.
- XU, L., EU, J. P., MEISSNER, G. & STAMLER, J. S. (1998) Activation of the cardiac calcium release channel (ryanodine receptor) by poly-S-nitrosylation. *Science*, 279, 234-7.
- YAMAMOTO, T., NAKAHATA, Y., SOMA, H., AKASHI, M., MAMINE, T. & TAKUMI, T. (2004) Transcriptional oscillation of canonical clock genes in mouse peripheral tissues. *BMC Mol Biol*, 5, 18.

- YAMASAKI, Y., KODAMA, M., MATSUHISA, M., KISHIMOTO, M., OZAKI, H., TANI, A., UEDA, N., ISHIDA, Y. & KAMADA, T. (1996) Diurnal heart rate variability in healthy subjects: effects of aging and sex difference. *Am J Physiol*, 271, H303-10.
- YAMASHITA, T., SEKIGUCHI, A., IWASAKI, Y. K., SAGARA, K., IINUMA, H., HATANNO, S., FU, L. T. & WATANABE, H. (2003) Circadian variation of cardiac K<sup>+</sup> channel gene expression. *Circulation*, 107, 1917-22.
- YANG, L., LIU, G., ZAKHAROV, S. I., BELLINGER, A. M., MONGILLO, M. & MARX, S. O. (2007) Protein kinase G phosphorylates Cav1.2 alpha1c and beta2 subunits. *Circ Res*, 101, 465-74.
- YI, G., GUO, X. H., REARDON, M., GALLAGHER, M. M., HNATKOVA, K., CAMM, A. J. & MALIK, M. (1998) Circadian variation of the QT interval in patients with sudden cardiac death after myocardial infarction. *Am J Cardiol*, 81, 950-6.
- YOUNG, M. E. (2006) The circadian clock within the heart: potential influence on myocardial gene expression, metabolism, and function. *Am J Physiol Heart Circ Physiol*, 290, H1-16.
- YOUNG, M. E. & BRAY, M. S. (2007) Potential role for peripheral circadian clock dyssynchrony in the pathogenesis of cardiovascular dysfunction. *Sleep Med*, 8, 656-67.
- YOUNG, M. E., RAZEGHI, P., CEDARS, A. M., GUTHRIE, P. H. & TAEGTMEYER, H. (2001a) Intrinsic diurnal variations in cardiac metabolism and contractile function. *Circ Res*, 89, 1199-208.
- YOUNG, M. E., RAZEGHI, P. & TAEGTMEYER, H. (2001b) Clock genes in the heart: characterization and attenuation with hypertrophy. *Circ Res*, 88, 1142-50.
- YOUNG, M. E., WILSON, C. R., RAZEGHI, P., GUTHRIE, P. H. & TAEGTMEYER, H. (2002) Alterations of the circadian clock in the heart by streptozotocin-induced diabetes. *J Mol Cell Cardiol*, 34, 223-31.
- ZAHRADNIKOVA, A., MINAROVIC, I., VENEMA, R. C. & MESZAROS, L. G. (1997) Inactivation of the cardiac ryanodine receptor calcium release channel by nitric oxide. *Cell Calcium*, 22, 447-54.
- ZHANG, Y. H., ZHANG, M. H., SEARS, C. E., EMANUEL, K., REDWOOD, C., EL-ARMOUCHE, A., KRANIAS, E. G. & CASADEI, B. (2008) Reduced phospholamban phosphorylation is associated with impaired relaxation in left ventricular myocytes from neuronal NO synthase-deficient mice. *Circ Res*, 102, 242-9.
- ZHOU, L., ZHANG, P., CHENG, Z., HAO, W., WANG, R., FANG, Q. & CAO, J. M. (2010) Altered circadian rhythm of cardiac beta3-adrenoceptor activity following myocardial infarction in the rat. *Basic Res Cardiol*.
- ZHOU, S., TAN, A. Y., PAZ, O., OGAWA, M., CHOU, C. C., HAYASHI, H., NIHEI, M., FISHBEIN, M. C., CHEN, L. S., LIN, S. F. & CHEN, P. S. (2008) Antiarrhythmic effects of beta3-adrenergic receptor stimulation in a canine model of ventricular tachycardia. *Heart Rhythm*, 5, 289-97.
- ZIOLO, M. T. (2008) The fork in the nitric oxide road: cyclic GMP or nitrosylation? *Nitric Oxide*, 18, 153-6.
- ZIOLO, M. T., KOHR, M. J. & WANG, H. (2008) Nitric oxide signaling and the regulation of myocardial function. *J Mol Cell Cardiol*, 45, 625-32.